Technische Universität München

Max-Planck-Institut für Physik
(Werner-Heisenberg-Institut)

Precision Calculations for the Decay of Higgs Bosons in the MSSM

Jianhui Zhang

Vollständiger Abdruck der von der Fakultät für Physik
der Technischen Universität München
zur Erlangung des akademischen Grades eines
Doktors der Naturwissenschaften (Dr. rer. nat.)
genehmigten Dissertation.

Vorsitzender:		Univ.-Prof. Dr. L. Oberauer
Prüfer der Dissertation:	1.	Hon.-Prof. Dr. W. F. L. Hollik
	2.	Univ.-Prof. Dr. A. J. Buras

Die Dissertation wurde am 22.10.2008
bei der Technischen Universität München eingereicht und
durch die Fakultät für Physik am 21.01.2009 angenommen.

Abstract

Precision calculations are required for the verification of the standard model (SM) and serve as a useful tool for probing and disentangling new physics beyond the SM. In this thesis we concentrate on the extension of the SM with supersymmetry, i.e. the minimal supersymmetric extension of the standard model (MSSM) and investigate the decay processes of Higgs bosons within this model. At tree-level, the light CP-even MSSM Higgs boson, h^0, becomes SM-like when the other Higgs bosons get heavy. Thus it is of particular interest to investigate the impact of higher order corrections. We present the complete one-loop electroweak radiative corrections to the decay of h^0 to four fermions via gauge boson pair, the results are further improved by currently available two-loop corrections to the Higgs boson self energies. The gauge boson in the photonic one-loop diagrams can become resonant and lead to singularities that have to be regularized by its finite width. To incorporation the gauge boson width, the one-loop integrals that involve such singularities are evaluated analytically. While the one-loop electroweak corrections yield visible effects for a relatively light MSSM Higgs sector, they only give rise to negligible effects when the Higgs bosons other than h^0 become heavy, even if the genuine supersymmetric particle spectrum is relatively light. Consequently it is rather difficult to distinguish the light CP-even MSSM Higgs boson from the SM one if all other MSSM Higgs bosons are heavy, even though the one-loop corrections are included. We also consider the decay of the heavy CP-even MSSM Higgs boson, H^0, to off-/on-shell gauge boson pair. The one-loop corrections turn out to be significant as the tree-level coupling of H^0 to gauge bosons is usually suppressed.

Contents

Chapter 1

Introduction

The main goal of theoretical physics is to provide an explanation for as many phenomena in nature as possible in an as simple as possible manner, or in other words, with as few physical principles as possible. Currently our best description of nature is given by the standard model of elementary particles [1, 2], in which the conceptual ideas of quantum mechanics and special relativity, the two cornerstones of the twentieth-century physics, are successfully combined. The standard model incorporates all elementary particles observed so far, and can describe their electromagnetic, weak and strong interactions. Its predictions have been tested by a large variety of experiments to an unprecedented accuracy. The only ingredient of the standard model that is still missing is the Higgs boson, a hypothetical fundamental scalar particle that generates the masses of fermions and gauge bosons in an acceptable way. The electroweak precision data accumulated at LEP, SLC and Tevatron in the last decade strongly favors a light Higgs boson, which is widely hoped to be discovered soon with the startup of the Large Hadron Collider (LHC) at CERN this year.

The existence of a fundamental scalar particle in the standard model is somewhat puzzling. Understanding this fact points to new physics beyond the standard model, which is supposed to come into play at the TeV energy scale that will be probed by the LHC. Among the proposals for new physics, supersymmetry is one of the most promising candidates. It is the only possible non-trivial extension of the Poincaré symmetry and relates particles of different spins. Besides that supersymmetry can provide solutions for a number of phenomenological problems, as we will see in the next chapters. It even has the potential to incorporate the other fundamental interaction, the gravitational interaction.

In contrast to the standard model, which contains only one Higgs boson, its supersymmetric extensions usually introduce more Higgs boson, with one of them is relatively light. At the LHC, the neutral supersymmetric Higgs bosons are mainly produced in the same way as the standard model Higgs boson, i.e. via gluon fusion, vector boson fusion etc. A detailed analysis of their subsequent decay processes is then required for the kinematic reconstruction of them. The extensions of the standard model in general resemble the standard model at the electroweak scale. Therefore to disentangle between them, precise predictions of both the standard model and its extensions are required.

In this thesis we consider the decay processes of the Higgs bosons in the minimal supersymmetric extension of the standard model [3,4]. The one-loop corrections to these processes are presented, improved by the two-loop corrections implemented in the program package FeynHiggs [5].

The outline of this thesis is as follows. In chapter 2 a brief review of the standard model is given, where we present all essential ingredients of the standard model, and put special emphasis on the Higgs mechanism. Also some deficiencies of the standard model are mentioned at the end of this chapter, which motivate the physics beyond the standard model.

In chapter 3 we concentrate on supersymmetry. After presenting the necessary ingredients for the construction of supersymmetric Lagrangians, we briefly discuss the elegant non-renormalization theorem, as well as the drawback of theories with extended supersymmetries for the construction of phenomenologically viable models.

Chapter 4 is devoted to the minimal supersymmetric extension of the standard model (MSSM). The MSSM Lagrangian with soft supersymmetry breaking terms is given. Then a counting of independent parameters involved in the Lagrangian is sketched. When introducing the particle content of the model, we put special emphasis on the Higgs sector, which is the most relevant sector for the computation in this thesis. We also describe the basic strategies of the regularization and renormalization procedure and discuss different regularization and renormalization schemes. Finally we present in detail the renormalization of the MSSM Higgs sector.

In chapter 5 the relative $\mathcal{O}(\alpha)$ electroweak corrections to the decay of the lightest CP-even Higgs boson in the MSSM to four fermions via gauge boson pair are presented. The mass of the lightest MSSM Higgs boson has an upper bound of about 135 GeV, including radiative corrections up to two-loop order. The dominant decay channel of such a light Higgs boson will be the decay into bottom and anti-bottom quark pair. This channel is not very promising for the discovery of Higgs boson at hadron colliders due to the large QCD background [6]. Therefore it is necessary to investigate other more rare decay modes. In the case that only one light Higgs boson is observable at the LHC, the detailed investigation of the decay properties of the lightest MSSM Higgs boson can help to distinguish it from a standard model Higgs boson. For the process under consideration, the intermediate gauge boson can become resonant, a proper treatment of its width effects is thus required in order to avoid the occurrence of singularities. At the one-loop level, we compute analytically the integrals that become singular when the gauge boson approaches on-shell and insert the gauge boson width afterwards. Two different methods are used to compute the real Bremsstrahlung corrections. We then evaluate the partial decay width as well as the distributions, and make a comparison of our results with the standard model predictions.

Chapter 6 deals with the decay of the heavy MSSM CP-even Higgs boson to gauge boson pair. In contrast to the discovery of a light Higgs boson, which may be compatible with both the standard model and the MSSM, the discovery of such a heavy Higgs boson is a clear signature for physics beyond the standard model. Although the tree-level coupling of this heavy CP-even Higgs boson to gauge bosons is usually suppressed compared to the corresponding standard model coupling, the one-loop corrections, especially those from the

fermionic and sfermionic sector, can play a significant role, since they involve potentially large Yukawa couplings. We give the analytical results for the fermionic and sfermionic corrections, which can be applied to more complicated processes involving the coupling of the heavy CP-even Higgs boson to gauge bosons. For comparison purposes, we also present the complete one-loop corrections.

In Appendix A we briefly summarize the properties of spinors, starting from their defining algebra in arbitrary space-time dimensions.

Appendix B defines the one-loop integrals used throughout this thesis. The basic strategies of the reduction of tensor integrals into scalar integrals are also given there. At the end of this Appendix we collect the analytical results of the integrals that are revelant for the computation in chapter 5.

A short discussion on unstable particles is given in Appendix C, where we also discuss the gauge invariant definition of the mass of unstable particles.

Chapter 2

The Standard Model

2.1 Structure of the standard model

The standard model of elementary particles [1,2] provides a spectacularly successful description of the non-gravitational physical phenomena at energies currently accessible at accelerators. It is a non-abelian gauge theory based on the gauge group $SU(3)_C \times SU(2)_L \times U(1)_Y$. To each of the generators of the gauge groups, there corresponds a gauge vector boson, which is the force mediator. The number of gauge vector bosons is 8 (gluons) for $SU(3)_C$, 3 (W bosons) and 1 (B boson) for $SU(2)_L$ and $U(1)_Y$ respectively, in accordance with the dimension of each gauge group. The gauge bosons transform in the adjoint representation of the gauge group.

The fermionic matter content consists of three generations of quarks and leptons, whose left- and right-handed components are assigned into different representations of the gauge group (there are no right-handed neutrinos in the framework of the standard model), thereby allowing for the chiral structure of weak interactions. Experimentally there exist gauge vector bosons and fermions that are massive. However, introducing an explicit mass term for the gauge boson or fermion into the Lagrangian is forbidden by gauge invariance, which is a crucial symmetry for the renormalizability of the theory. In order to incorporate the non-zero particle masses in a gauge invariant way, one needs another essential ingredient of the standard model, i.e. the spontaneous electroweak symmetry breaking, which is realized by the Higgs-Brout-Englert-Guralnik-Hagen-Kibble mechanism [7] or the Higgs mechanism for short. Through the Higgs mechanism the gauge group $SU(3)_C \times SU(2)_L \times U(1)_Y$ breaks down to $SU(3)_C \times U(1)_Q$, where the color and charge symmetry are still preserved. In this way the weak gauge bosons acquire masses after the symmetry breaking, while the gluon and photon still stay massless as required. It turns out that the fermion masses can also be generated by the Higgs mechanism.

Before introducing the electroweak symmetry breaking, the standard model Lagrangian can be expressed in terms of the left- and right-handed fermionic matter fields and the gauge fields. The left and right fermionic fields are defined by $f_{L,R} = \frac{1}{2}(1 \mp \gamma_5)f$, where $P_L, R = \frac{1}{2}(1 \mp \gamma_5)$

are the projection operators. The left- and right-handed fermions reside in weak isodoublets and isosinglets, respectively,

$$\begin{aligned}
L_1 &= \begin{pmatrix} \nu_e \\ e^- \end{pmatrix}_L , \; e_{R_1} = e^-_R , \; Q_1 = \begin{pmatrix} u \\ d \end{pmatrix}_L , \; u_{R_1} = u_R , \; d_{R_1} = d_R \\
L_2 &= \begin{pmatrix} \nu_\mu \\ \mu^- \end{pmatrix}_L , \; e_{R_2} = \mu^-_R , \; Q_2 = \begin{pmatrix} c \\ s \end{pmatrix}_L , \; u_{R_2} = c_R \; , \; d_{R_2} = s_R \; ; \quad (I^3_f)_{L,R} = \pm\frac{1}{2}, 0 \; . \\
L_3 &= \begin{pmatrix} \nu_\tau \\ \tau^- \end{pmatrix}_L , \; e_{R_3} = \tau^-_R , \; Q_3 = \begin{pmatrix} t \\ b \end{pmatrix}_L , \; u_{R_3} = t_R \; , \; d_{R_3} = b_R
\end{aligned} \tag{2.1}$$

The fermionic hypercharge defined in terms of the third component of its weak isospin, I^3_f, and electric charge, Q_f, by $Y = 2(Q_f - I^3_f)$ leads to a vanishing sum of hypercharges in each generation, which is important for the cancellation of chiral anomalies and thus crucial for the renormalizability of the standard model. The gauge fields $G^a_\mu (a = 1...8)$, $W^i_\mu (i = 1...3)$ and B_μ correspond to the generators of the group $SU(3)_C$, $SU(2)_L$ and $U(1)_Y$. Their field strengths are given by

$$\begin{aligned}
G^a_{\mu\nu} &= \partial_\mu G^a_\nu - \partial_\nu G^a_\mu + g_3 f^{abc} G^b_\mu G^c_\nu \; , \\
W^i_{\mu\nu} &= \partial_\mu W^i_\nu - \partial_\nu W^i_\mu + g_2 \, \epsilon^{ijk} W^j_\mu W^k_\nu \; , \\
B_{\mu\nu} &= \partial_\mu B_\nu - \partial_\nu B_\mu \; ,
\end{aligned} \tag{2.2}$$

where f^{abc} and ϵ^{ijk} are the structure constants, and g_3, g_2 the coupling constants for the gauge groups $SU(3)_C$ and $SU(2)_L$, respectively. The interactions between matter and gauge fields are introduced by requiring the invariance of the Lagrangian under local gauge transformations. This gives rise to a minimal coupling through the covariant derivative

$$D_\mu = \partial_\mu - i g_3 T_a G^a_\mu - i g_2 I_i W^i_\mu - i g_1 \frac{Y}{2} B_\mu \; , \tag{2.3}$$

where T_a, I_i and Y are the generators of the respective gauge group and g_1 is the coupling constant for the gauge group $U(1)_Y$. The standard model Lagrangian can then be written in terms of the gauge and matter fields and the covariant derivative

$$\begin{aligned}
\mathcal{L}_{SM} &= -\frac{1}{4} G^a_{\mu\nu} G^{\mu\nu}_a - \frac{1}{4} W^a_{\mu\nu} W^{\mu\nu}_a - \frac{1}{4} B_{\mu\nu} B^{\mu\nu} + i \, \bar{L}_i D_\mu \gamma^\mu L_i + i \, \bar{e}_{R_i} D_\mu \gamma^\mu e_{R_i} \\
&+ i \, \bar{Q}_i D_\mu \gamma^\mu Q_i + i \, \bar{u}_{R_i} D_\mu \gamma^\mu u_{R_i} + i \, \bar{d}_{R_i} D_\mu \gamma^\mu d_{R_i} \; .
\end{aligned} \tag{2.4}$$

Here a sum over the indices is implicitly understood. There are no mass terms for the fermion and gauge fields in the above expression due to the requirement of gauge invariance. As mentioned before, these masses can be generated through the Higgs mechanism. The idea of the Higgs mechanism is to introduce new terms into the original Lagrangian in such a way that the Lagrangian is still invariant under the gauge symmetry but the vacuum is not. This is the so-called spontaneous breaking of symmetry. As a massless particle has two degrees of freedom, while a massive one has three, at least three degrees of freedom have to be introduced in order to generate masses for the weak gauge bosons $W^\pm$ and Z, which are mixtures of W and B bosons introduced above. The simplest possibility is to introduce a weak isospin doublet Φ of two complex scalar fields (so that Lorentz invariance is respected),

which couple to the vector bosons in a gauge invariant way. In order to achieve a spontaneous symmetry breaking that preserves the electric charge symmetry, only the electrically neutral field can acquire a non-vanishing vacuum expectation value. To allow for such a neutral component in the introduced doublet, the hypercharge of the doublet must be ± 1. One can choose either $+1$ or -1. We choose $+1$ here, so that

$$\Phi = \begin{pmatrix} \phi^+ \\ \phi^0 \end{pmatrix} . \tag{2.5}$$

The contribution of the scalar field part to the Lagrangian is given by

$$\mathcal{L}_S = (D^\mu \Phi)^\dagger (D_\mu \Phi) - \mu^2 \Phi^\dagger \Phi - \lambda (\Phi^\dagger \Phi)^2 \qquad \mu^2 < 0, \lambda > 0 \ . \tag{2.6}$$

The neutral component of the doublet develops a non-zero vacuum expectation value

$$\langle \Phi \rangle = \begin{pmatrix} 0 \\ v/\sqrt{2} \end{pmatrix} \qquad v = \sqrt{-\frac{\mu^2}{\lambda}} \ . \tag{2.7}$$

Expanding the doublet field Φ around the vacuum, one has

$$\Phi = \begin{pmatrix} \phi^+ \\ \phi^0 \end{pmatrix} = \begin{pmatrix} \phi^+ \\ \frac{1}{\sqrt{2}}(v + H + i\theta) \end{pmatrix} , \tag{2.8}$$

where the would-be Goldstone fields [8], ϕ^+, ϕ^- and θ are unphysical degrees of freedom, and can be eliminated by a transition into the unitary gauge via a gauge transformation. The three Goldstone bosons are absorbed by the gauge bosons $W^\pm$ and Z and form their longitudinal components so that they become massive. The leftover degree of freedom H is a physical field and gives rise to the physical Higgs boson. The Higgs boson is the only ingredient of the standard model that has not been observed so far [9,10]. The present lower limit on its mass from direct searches is 114.4 GeV at 95% CL [10], which is consistent with the electroweak precision data [11].

In the unitary gauge, one can easily extract the physical content by adding the contribution of the scalar field part, Eq. (2.6), to the standard model Lagrangian, Eq. (2.4), and expanding around the ground state. The physical gauge boson fields $W^\pm$, A and Z are mixtures of the W and B bosons,

$$W_\mu^\pm = \frac{1}{\sqrt{2}}(W_\mu^1 \mp i W_\mu^2) \ , \ Z_\mu = \frac{g_2 W_\mu^3 - g_1 B_\mu}{\sqrt{g_1^2 + g_2^2}} \ , \ A_\mu = \frac{g_2 W_\mu^3 + g_1 B_\mu}{\sqrt{g_1^2 + g_2^2}} \ , \tag{2.9}$$

where the mixing matrix for the neutral vector bosons defines the weak mixing angle θ_W with

$$\sin\theta_W = \frac{g_1}{\sqrt{g_1^2 + g_2^2}} \ , \quad \cos\theta_W = \frac{g_2}{\sqrt{g_1^2 + g_2^2}} \ . \tag{2.10}$$

The gauge boson masses arise from the terms bilinear in the physical gauge fields, yielding

$$M_W = \frac{1}{2} g_2 \, v \ , \ M_Z = \frac{1}{2}\sqrt{g_1^2 + g_2^2} \, v \ , \ M_A = 0 \ . \tag{2.11}$$

Note that the photon is still massless after the electroweak symmetry breaking as the charge symmetry is preserved. The electromagnetic coupling is related to the coupling constants g_1 and g_2 by

$$e = \sqrt{4\pi\alpha} = \frac{g_1 g_2}{\sqrt{g_1^2 + g_2^2}} = g_1 \cos\theta_W = g_2 \sin\theta_W \ . \tag{2.12}$$

The vacuum expectation value can be fixed by the Fermi constant determined from the muon decay

$$\frac{4G_\mu}{\sqrt{2}} = \frac{e^2}{2\sin^2\theta_W M_W^2} = \frac{2}{v^2} \implies v = \left(\frac{1}{\sqrt{2}G_\mu}\right)^{\frac{1}{2}} \approx 246\,\text{GeV}. \tag{2.13}$$

As previously mentioned, the explicit fermion mass terms in the Lagrangian are forbidden by gauge invariance, since such terms have the form of $m_f(\bar{f}_L f_R + \bar{f}_R f_L)$, which is obviously not gauge invariant since the left- and right-handed fermions belong to different representations of the gauge group (the former are weak isodoublets while the latter are weak isosinglets). This problem can be circumvented by the Higgs mechanism. One can generate fermion masses without disturbing gauge invariance through the Yukawa couplings between fermion and scalar fields. For this purpose, both the field Φ and its charge-conjugate $\Phi^c = i\tau_2\Phi^* = (\phi^{0*}, -\phi^-)$ are required, which generate masses for down-type and up-type fermions, respectively. The Yukawa interactions are described by the following terms

$$\mathcal{L}_Y = -\sum_{i,j}\left(\bar{L}_i Y^l_{ij} e_{R_j}\Phi + \bar{Q}_i Y^u_{ij} u_{R_j}\Phi^c + \bar{Q}_i Y^d_{ij} d_{R_j}\Phi + h.c.\right), \tag{2.14}$$

where $h.c.$ denotes the hermitian conjugate and Y^f_{ij} the Yukawa coupling matrices. Inserting Eq. (2.8) into these Yukawa interaction terms yields the following mass matrices for the leptons, up- and down-type quarks, respectively,

$$M^l_{ij} = \frac{1}{\sqrt{2}} Y^l_{ij}\, v \ , \qquad M^u_{ij} = \frac{1}{\sqrt{2}} Y^u_{ij}\, v \ , \qquad M^d_{ij} = \frac{1}{\sqrt{2}} Y^d_{ij}\, v \ . \tag{2.15}$$

These mass matrices may not be diagonal, which implies that the interaction eigenstates may be different from the mass eigenstates. In order to obtain the mass eigenstates, we apply a unitray transformation to the left- and right-handed fermions

$$f'_{i,L} = \sum_j U^f_{ij,L} f_{j,L} \ , \qquad f'_{i,R} = \sum_j U^f_{ij,R} f_{j,R} \ . \tag{2.16}$$

After these transformations the mass matrices become diagonal with the following entries

$$M_{f,i} = \frac{1}{\sqrt{2}} \sum_{j,k} U^f_{ij,L} Y^f_{jk} U^{f\dagger}_{ki,R}\, v \ . \tag{2.17}$$

Summing over the three parts in Eq. (2.4), (2.6) and (2.14) yields the classical Lagrangian for the standard model. An important feature of the standard model Higgs sector is that

the coupling of the Higgs boson with itself or with fermions or gauge bosons are proportional to their masses. The transformation matrices U_L^f and U_R^f drop out in the coupling of fermions and neutral gauge bosons due to their unitarity. This has the important consequence that the flavor-changing neutral current is absent at tree level. In the leptonic sector these transformation matrices also drop out. This is because the neutrinos are assumed to be massless in the standard model, its transformation is arbitrary and can be chosen to make the mass and interaction eigenstates of leptons coincide with each other. The transformation matrices survive only in the coupling of quarks and W gauge boson, leading to the Cabbibo-Kobayashi-Maskawa (CKM) mixing matrix [12, 13]

$$V = U_L^u U_L^{d\dagger} \ . \tag{2.18}$$

If the up- or down-type quarks have degenerate masses, this mixing matrix can also be eliminated.

So far we are only concerned with the classical Lagrangian of the standard model. There are other issues that have to be addressed when one tries to quantize this classical Lagrangian (detailed discussion can be found, e.g. in [14, 15]). Like the quantization of all non-abelian gauge theories, it is necessary to specify a gauge by adding gauge-fixing terms into the original Lagrangian of the standard model in order to avoid the integration over physically equivalent configurations that are related by a gauge transformation. For practical calculations, it is convenient to choose a renormalizable gauge in which the gauge boson propagators behave convergently at large momentum. The 't Hooft gauge [16] is a gauge of this kind. In this gauge the mixing between the gauge bosons and the Goldstone bosons introduced by the spontaneous symmetry breaking drops out, and the gauge-fixing terms are given by

$$\mathcal{L}_{GF} = -\frac{1}{2\xi_G}(C^G)^2 - \frac{1}{2\xi_A}(C^A)^2 - \frac{1}{2\xi_Z}(C^Z)^2 - \frac{1}{\xi_W}C^+C^- \tag{2.19}$$

with the linear gauge-fixing operators

$$\begin{aligned} C^G &= \partial^\mu G_\mu^a \ , \\ C^A &= \partial^\mu A_\mu \ , \\ C^Z &= \partial^\mu Z_\mu - M_Z \xi_Z \theta \ , \\ C^\pm &= \partial^\mu W_\mu^\pm \mp i M_W \xi_W \phi^\pm \ . \end{aligned} \tag{2.20}$$

In this thesis we use $\xi_\alpha = 1$, which corresponds to the 't Hooft-Feynman gauge. Note that by introducing the gauge-fixing terms into the original Lagrangian one includes the unphysical degrees of freedom of gauge fields, the effects of which are cancelled by the ghost term

$$\mathcal{L}_{FP} = \bar{u}^\alpha \frac{\delta C^\alpha}{\delta \theta^\beta} u^\beta \ , \tag{2.21}$$

where u^α, $\bar{u}^\alpha$ are the Faddeev-Popov ghosts [17], and $\delta\theta^\beta$ is the infinitesimal gauge transformation parametrized by θ^β. Adding these gauge-fixing and Faddeev-Popov ghost terms to the classical Lagrangian one achieves a complete renormalizable Lagrangian of the standard model, from which the computation of higher order corrections is possible.

2.2 Deficiencies of the standard model

In spite of the remarkable success of the standard model, there are a number of reasons that it can not be the ultimate theory. The standard model contains a number of free parameters, at least 19, which include the three gauge couplings, six quark and three lepton masses, three charged weak mixing angles and one CP-violating phase, the two parameters μ and λ parametrizing the Higgs sector, and an additional parameter describing the potential strong CP violation. Another compelling reason is that it does not incorporate gravity. Although gravity does not play a role at the energies accessible at current accelerators, it will come into play at the Planck scale $M_{pl} = (G_N/\hbar c)^{-1/2} \sim 1.2 \times 10^{19}$ GeV with G_N being the gravitational constant. The standard model is expected to break down at this scale. Even if gravity is ignored, the standard model is not asymptotically free, the electromagnetic coupling, for instance, will become strong at some high energy scale. This also indicates that the standard model is only a low energy effective theory of some more fundamental theory. The existence of dark matter from cosmological observations, as it is not built out of quarks and leptons, indicates clearly the incompleteness of the standard model. The baryon anti-baryon asymmetry is, too, not explicable within the standard model. The neutrino oscillation experiments imply massive neutrinos, which are beyond the scope of the standard model although they can be incorporated naturally by introducing Dirac mass terms, apart from the fact that the masses are unnaturally small. Of course, this procedure also introduces more free parameters into the standard model. In addition, there are some other theoretical and phenomenological issues that the standard model is not able to address, such as the problem of gauge coupling unification, the quantization of electric charges, the replication of fermion families and the hierarchical masses of them.

Besides all these, there is the hierarchy problem. Phenomenologically the mass of the standard model Higgs boson should be around the electroweak scale. However, its squared mass receives radiative corrections that are quadratically dependent on the ultraviolet cutoff Λ, which is supposed to be the energy scale at which the standard model breaks down and new physics enters. The natural value of the Higgs boson mass is thus of the order of the cutoff rather than the electroweak scale. To keep the Higgs boson mass at the electroweak scale, one needs a huge fine-tuning if the energy scale Λ is expected to be the grand unification (GUT) scale or the Planck scale. In contrast, the fermion mass, e.g. the electron mass in QED is not fine-tuned. The reason is that when the electron mass goes to zero, an additional symmetry arises, i.e. the chiral symmetry. When the electron mass moves away from zero, this chiral symmetry is broken, but the effects of this breaking comes only from the electron mass. Therefore the loop corrections are proportional to this mass and only logarithmically divergent. In this way massless fermions are protected from acquiring masses by the chiral symmetry. Likewise, the photon stays massless due to the gauge symmetry. For the scalar particle in the standard model, however, there is no such symmetry that can protect it from acquiring large masses from radiative corrections, thus leading to a destabilization of the mass hierarchy between the electroweak scale and GUT scale.

There have been proposals to solve at least some of these problems. Supersymmetry [18,19] is one of such proposals that has been extensively studied in literature. It is a symmetry that

relates fermions and bosons, and leads to a cancellation between the radiative corrections to the Higgs boson mass from fermionic and bosonic loops, thus stabilizes the huge mass hierarchy between the electroweak scale and the GUT scale. This can also be understood as follows. By pairing the scalar boson with a fermion through supersymmetry, the chiral symmetry that protects the fermion mass now serves as a protection mechanism for the boson mass as well. Supersymmetry can also explain how the hierarchy arises, can provide a natural dark matter candidate, and offers the possibility for the unification of gauge couplings. Another proposal is the so-called Technicolor theory [20], in which the inclusion of elementary scalar particles is avoided by proposing that the Higgs boson is a composite particle made of fermions. Theories with extra dimensions are also widely discussed in literature. They have the potential to provide solutions to the fermion family replication, to give explanations to the breaking of supersymmetry, and even to form a consistent quantum theory of gravity. It is clear that precise knowledge of both the standard model and its theoretical extensions is required, in order to verify and disentangle all these extended models. We will concentrate on the scenario with supersymmetry in this thesis. In the next chapter a brief description of the basic characteristics of supersymmetry will be given.

Chapter 3

Supersymmetry

3.1 Basics of supersymmetry

The attempts in the 1960's to combine in a non-trivial manner the internal symmetries with the space-time Poincaré symmetry turned out to fail. Indeed it was shown by Coleman and Mandula [21] that this is not possible within the context of Lie groups. Their proof was based on very general assumptions, such as the analyticity of the S-matrix, the existence of scattering at almost all energies etc. Later on it was realized that there was a possibility to evade this no-go theorem, namely by generalizing the notion of a Lie algebra in such a way that its defining relations involve both anticommutators as well as commutators. These are the graded Lie algebras. It was proven by Haag, Sohnius and Lopuszanski [22] that supersymmetry algebra is the only graded Lie algebra of symmetries of the S-matrix that is consistent with relativistic quantum field theory.

As mentioned at the end of the previous chapter, supersymmetry provides solutions to a number of theoretical and phenomenological problems, for instance, it can solve the hierarchy problem, and provide a nice cold dark matter candidate with the relic density of the right order of magnitude. Owing to the pairing between fermions and bosons, supersymmetric theories in general have better ultraviolet behavior compared to ordinary field theories. It turns out that all supersymmetric theories are free of quadratic divergences, and indeed any unrenormalized quantum field theory that has no quadratic divergences to all orders in perturbation theory must be supersymmetric [23, 24]. Supersymmetry even yields field theories that are completely finite to all orders in perturbation theory. For instance, the $N = 4$ super Yang-Mills theory in four space-time dimensions (where N denotes the number of supersymmetries) is finite to all orders [25–28]. Although supersymmetry can potentially provide solutions to many phenomenological problems, it was not invented for these purposes. Supersymmetry was first introduced in string theory in order to incorporate fermions in the model [29]. It was realized that supersymmetry could possibly be the solution of these phenomenological problems only after the construction of supersymmetric field theories in four space-time dimensions.

Since supersymmetry is a symmetry relating fermions and bosons, its generators must transform a fermionic state into a bosonic one, and vice versa. Thus the supersymmetry generators carry half-integer spin, and they are fermionic operators. The algebra of supersymmetry including the Poincaré algebra can be collected as follows [3, 30–36],

$$\begin{aligned}
\{Q^i_\alpha, \bar{Q}^j_{\dot{\beta}}\} &= 2\sigma^\mu_{\alpha\dot{\beta}} P_\mu \delta^{ij} \ , \\
\{Q^i_\alpha, Q^j_\beta\} &= \epsilon_{\alpha\beta} Z^{ij} \ , \quad \{\bar{Q}^i_{\dot{\alpha}}, \bar{Q}^j_{\dot{\beta}}\} = \epsilon_{\dot{\alpha}\dot{\beta}} (Z^{ij})^* \ , \\
[Q^i_\alpha, P_\mu] &= [\bar{Q}^i_{\dot{\alpha}}, P_\mu] = 0 \ , \\
[Q^i_\alpha, M_{\mu\nu}] &= (\sigma_{\mu\nu})^\beta_\alpha Q^i_\beta, \quad [\bar{Q}^i_{\dot{\alpha}}, M_{\mu\nu}] = (\bar{\sigma}_{\mu\nu})^{\dot{\beta}}_{\dot{\alpha}} \bar{Q}^i_{\dot{\beta}} \ , \\
[M_{\mu\nu}, M_{\rho\sigma}] &= i(g_{\nu\rho} M_{\mu\sigma} - g_{\mu\rho} M_{\nu\sigma} - g_{\nu\sigma} M_{\mu\rho} + g_{\mu\sigma} M_{\nu\rho}) \ , \\
[M_{\mu\nu}, P_\rho] &= i(g_{\rho\nu} P_\mu - g_{\rho\mu} P_\nu) \ , \\
[P_\mu, P_\nu] &= 0 \ ,
\end{aligned} \tag{3.1}$$

where P_μ and $M_{\mu\nu}$ are the generators of the Poincaré group, Q^i_α and its conjugate $\bar{Q}^i_{\dot{\alpha}}$ are the spinorial generators of supersymmetry with the Weyl spinor indices $\alpha, \dot{\alpha} = 1, 2$ and $i, j = 1...N$ denoting some integral space. σ^μ consist of the identity matrix and Pauli matrices. The operators Q^i and $\bar{Q}^i$ transform in the $(\frac{1}{2}, 0)$ and $(0, \frac{1}{2})$ representations of the Poincaré group respectively, hence the anticommutator of them must transform as $(\frac{1}{2}, \frac{1}{2})$, i.e. as a four-vector. From this consideration it is almost straightforward that the anticommutation relation in the first row of Eq. (3.1) takes that form. The operators $Z^{ij} = -Z^{ji}$ are the central charges, they commute with any operator and belong to an abelian invariant subalgebra of the internal symmetry group [30]. In the absence of the central charges, the supersymmetry algebra is invariant under a $U(N)$ transformation among the supersymmetry generators. For the simple $N = 1$ supersymmetry, the central charge automatically vanishes due to its anti-symmetry. The resulting $U(1)$ symmetry is the so-called R symmetry.

As one can see from Eq. (3.1) that the algebra of supersymmetry contains the Poincaré algebra as a subalgebra. From quantum field theory we know that particles correspond to irreducible representations of the Poincaré algebra, now the supersymmetry transformations will relate different particle representations. These particles form a supermultiplet and are related to each other by the spinorial operators Q^i and $\bar{Q}^i$, differing in spin by $\frac{1}{2}$. Within a supermultiplet, all particles have the same mass since the operator P^2 is still a Casimir operator, namely it commutes with all supersymmetry generators. Moreover, as one can easily show, a supermultiplet contains an equal number of bosonic and fermionic degrees of freedom.

In the following we will mainly concentrate on the $N = 1$ supersymmetry, since, for the reason that will be given at the end of this chapter, only this simple supersymmetry allows chiral fermions [3, 30–34, 37] and thus lays the foundation for the construction of phenomenologically viable models[1]. Moreover, the supersymmetry is assumed to be a global symmetry. The extended supersymmetry ($N > 1$) and local supersymmetry will be briefly described at the end of this chapter.

[1] Although, in principle, extended supersymmetry can be introduced into the gauge sector of phenomenological models (see e.g. ref. [38]), we will not discuss this possibility in this thesis.

For the $N = 1$ global supersymmetry, the simplest possible supermultiplets describing massless fields are the chiral and the vector supermultiplets. The former contains an irreducible representation formed by a single Weyl fermion with helicity $\frac{1}{2}$ and a real scalar, as well as its CPT-conjugate representation that consists of a Weyl fermion of helicity $-\frac{1}{2}$ and another real scalar. This is necessary for the construction of a Lorentz invariant theory. The chiral supermultiplet thus contains two fermionic and two bosonic degrees of freedom. The vector supermultiplet contains a massless spin-1 gauge boson and a Weyl fermion, where the fermion has to transform in the adjoint representation of the gauge group as the gauge boson does.

With these supermultiplets one can write down the supersymmetry transformations and construct invariants from the component fields belonging to the supermultiplets. However, this turns out to be rather complicated. The supersymmetry algebra can only be realized on-shell. In order to match the bosonic and fermionic degrees of freedom off-shell, one has to introduce auxiliary fields, whose transformation properties are then determined by the requirement that the algebra of supersymmetry can close off-shell. This can be greatly simplified by enlarging the space-time to include as well anticommuting variables, i.e. defining the superspace, and using the superfield formalism introduced by Salam and Strathdee [39,40], in which the superfields also include the auxiliary fields as components.

3.2 Superspace and superfields

In superspace, one has two additional anticommuting Grassmann coordinates θ_α and $\bar{\theta}_{\dot{\alpha}}$ (the properties of Grassmann variables will be briefly summarized in Appendix A), in addition to the ordinary coordinates x^μ. The elements of superspace are thus labeled by the set of coordinates $(x, \theta, \bar{\theta})$. In contrast to an ordinary field, which is a function of the space-time coordinates only, a superfield is a function of both the space-time and the anticommuting Grassmann coordinates. The component fields of the supermultiplet then arise as the coefficients in the expansion of the superfield in powers of the variables θ and $\bar{\theta}$. In particular, the auxiliary fields also arise as components of superfields.

The anticommutators of supersymmetry algebra can now be written in terms of commutators

$$[\xi Q, \bar{\xi}\bar{Q}] = 2\xi\sigma^\mu\bar{\xi}P_\mu \ , \tag{3.2}$$

where ξ and $\bar{\xi}$ are anticommuting parameters and $\xi Q = \xi^\alpha Q_\alpha$, $\bar{\xi}\bar{Q} = \bar{\xi}_{\dot{\alpha}}\bar{Q}^{\dot{\alpha}}$.

As the momentum operator generates infinitesimal translations in space-time, we can think of the supersymmetry generators as inducing infinitesimal translations in superspace with Grassmann parameters. Hence a finite supersymmetry group transformation can be constructed by the following exponentiation (there are different possibilities to write the group element, for which the supersymmetry generators Q, $\bar{Q}$ and the covariant derivatives given below will take different forms)

$$G(x, \theta, \bar{\theta}) = e^{i(-x^\mu P_\mu + \theta Q + \bar{\theta}\,\bar{Q})} \ . \tag{3.3}$$

A successive application of the group transformation leads to the following translation in superspace

$$(x^\mu, \theta, \bar{\theta}) \longrightarrow (x^\mu + a^\mu - i\xi\sigma^\mu\bar{\theta} + i\theta\sigma^\mu\bar{\xi}, \theta + \xi, \bar{\theta} + \bar{\xi}) \ . \tag{3.4}$$

Thus the supersymmetry generators Q and $\bar{Q}$ can be written as differential operators in superspace

$$iQ_\alpha = \frac{\partial}{\partial\theta^\alpha} - i\sigma^\mu_{\alpha\dot{\alpha}}\bar{\theta}^{\dot{\alpha}}\partial_\mu \ , \qquad\qquad i\bar{Q}_{\dot{\alpha}} = -\frac{\partial}{\partial\bar{\theta}^{\dot{\alpha}}} + i\theta^\alpha\sigma^\mu_{\alpha\dot{\alpha}}\partial_\mu \ . \tag{3.5}$$

A general superfield can be expanded in powers of θ and $\bar{\theta}$. Due to their anticommuting property, all powers of θ and $\bar{\theta}$ higher than two vanish in the expansion. Such superfields form representations of supersymmetry, but they contain many component fields and usually give reducible representations. In order to obtain irreducible ones, we have to impose certain constraint on the superfields that is invariant under the supersymmetry algebra. One possibility is to impose the reality condition, which can be used to construct the vector superfield, the component fields of which constitute the vector supermultiplet. Another possibility is to define a supersymmetric covariant derivative to eliminate extra component fields. This can be used to construct the chiral superfield, whose components form the chiral supermultiplet. Besides these, there are other possibilities to constrain a superfield and yield other types of supermultiplets, e.g. the linear superfield [41–43]. However, the interactions of linear superfields are no more general than those of chiral and vector superfields, therefore we will not discuss them further.

For the representation given by Eq. (3.3) the covariant derivatives are defined as

$$D_\alpha = \frac{\partial}{\partial\theta^\alpha} + i\sigma^\mu_{\alpha\dot{\alpha}}\bar{\theta}^{\dot{\alpha}}\partial_\mu \ , \qquad\qquad \bar{D}_{\dot{\alpha}} = -\frac{\partial}{\partial\bar{\theta}^{\dot{\alpha}}} - i\theta^\alpha\sigma^\mu_{\alpha\dot{\alpha}}\partial_\mu \ . \tag{3.6}$$

They themselves satisfy the anticommutation relations

$$\{D_\alpha, \bar{D}_{\dot{\alpha}}\} = 2i\sigma^\mu_{\alpha\dot{\alpha}}\partial_\mu \ , \qquad\qquad \{D_\alpha, D_\beta\} = \{D_{\dot{\alpha}}, D_{\dot{\beta}}\} = 0 \ , \tag{3.7}$$

and anticommute with the supersymmetry generators Q and $\bar{Q}$. A (left-) chiral superfield can be defined by the following condition, which is invariant under supersymmetry

$$\bar{D}_{\dot{\alpha}}\Phi = 0 \ . \tag{3.8}$$

The general form of a chiral superfield when expanding in powers of the Grassmann variables θ and $\bar{\theta}$ reads

$$\begin{aligned} \Phi(x^\mu, \theta, \bar{\theta}) &= \varphi(x) + \sqrt{2}\,\theta\psi(x) + \theta\theta F(x) + i\partial_\mu\varphi(x)\,\theta\,\sigma^\mu\bar{\theta} \\ &- \frac{i}{\sqrt{2}}\,\theta\theta\,\partial_\mu\psi(x)\sigma^\mu\bar{\theta} - \frac{1}{4}\partial_\mu\partial^\mu\varphi(x)\theta\theta\bar{\theta}\bar{\theta} \ , \end{aligned} \tag{3.9}$$

where φ and F are complex scalar fields and ψ is a Weyl spinor field. Note that the parameters θ and $\bar{\theta}$ have mass dimension $-\frac{1}{2}$, thus the coefficient F is the field with highest mass

dimension in this expansion. All coefficients associated with higher powers of θ and $\bar{\theta}$ are space-time derivatives. It turns out that the component field F of a chiral superfield always transform into a space-time derivative under supersymmetry transformations. This property is crucial for the construction of supersymmetric invariant actions. In addition, there is no kinetic term of the F field in Eq. (3.9), it thus represents a non-propagating degree of freedom. The conjugate field of Φ, Φ^+, satisfies the constraint $D_\alpha \Phi^+ = 0$ and is a right-chiral or anti-chiral superfield.

The product of left-chiral superfields is again a left-chiral superfield, since the operator $\bar{D}$ is a linear differential operator. However, the product of a left-chiral superfield and a right-chiral one is no longer a chiral superfield, but a general vector superfield, whose properties will be described below.

Vector superfields form another irreducible representation of supersymmetry. They are defined by imposing the reality condition

$$V = V^\dagger \ . \tag{3.10}$$

This condition is preserved by the supersymmetry transformation. A vector superfield in general contains four auxiliary scalar fields and an auxiliary fermion field. With the help of gauge invariance one can eliminate all but one of them, the remaining field is the so-called D field.

In terms of powers of θ and $\bar{\theta}$ one can expand a vector superfield as follows

$$\begin{aligned} V(x^\mu, \theta, \bar{\theta}) &= C(x) + i\theta\chi(x) - i\bar{\theta}\bar{\chi}(x) + \frac{i}{2}\theta\theta[M(x) + iN(x)] \\ &- \frac{i}{2}\bar{\theta}\bar{\theta}[M(x) - iN(x)] + \theta\sigma^\mu\bar{\theta}V_\mu(x) \\ &+ i\theta\theta\bar{\theta}[\bar{\lambda}(x) + \frac{i}{2}\bar{\sigma}^\mu\partial_\mu\chi(x)] - i\bar{\theta}\bar{\theta}\theta[\lambda(x) + \frac{i}{2}\sigma^\mu\partial_\mu\bar{\chi}(x)] \\ &+ \frac{1}{2}\theta\theta\bar{\theta}\bar{\theta}[D(x) - \frac{1}{2}\partial_\mu\partial^\mu C(x)] \ , \end{aligned} \tag{3.11}$$

where C, M, N, D are real scalar fields and V_μ is a real vector field, λ and χ are two Weyl spinor fields.

It is possible to construct a vector superfield from a chiral superfield Λ and an anti-chiral one $\Lambda^\dagger$ by taking $i(\Lambda - \Lambda^\dagger)$, which can be written in components as follows

$$\begin{aligned} i(\Lambda - \Lambda^\dagger) &= i(\varphi - \varphi^\dagger) + i\sqrt{2}(\theta\psi - \bar{\theta}\bar{\psi}) + i\theta\theta F - i\bar{\theta}\bar{\theta}F^\dagger \\ &- \theta\sigma^\mu\bar{\theta}\partial_\mu(\varphi + \varphi^\dagger) - \frac{1}{\sqrt{2}}\theta\theta\bar{\theta}\bar{\sigma}^\mu\partial_\mu\psi + \frac{1}{\sqrt{2}}\bar{\theta}\bar{\theta}\theta\sigma^\mu\partial_\mu\bar{\psi} \\ &- \frac{i}{4}\theta\theta\bar{\theta}\bar{\theta}\partial_\mu\partial^\mu(\varphi - \varphi^\dagger) \ . \end{aligned} \tag{3.12}$$

This suggests the following supersymmetric generalization of an abelian gauge transformation as it gives the correct transformation for the vector field V_μ

$$V \longrightarrow V + i(\Lambda - \Lambda^\dagger) \ . \tag{3.13}$$

This gauge transformation reflects the fact that the fields C, M, N and χ are unphysical degrees of freedom, since they can be eliminated from Eq. (3.11) by a proper adjustment of the component fields in Eq. (3.12), i.e. by a particular choice of gauge. The gauge in which these unphysical fields disappear is called Wess-Zumino gauge. Note that the Wess-Zumino gauge does not completely fix the gauge, actually it fixes all the gauge freedom except for the ordinary $U(1)$ gauge transformation of the vector field V_μ. The manifest supersymmetry is lost in this gauge. However, the expression of a vector superfield is greatly simplified to

$$V_{WZ}(x^\mu, \theta, \bar{\theta}) = \theta\sigma^\mu\bar{\theta}V_\mu(x) + i\theta\theta\bar{\theta}\bar{\lambda}(x) - i\bar{\theta}\bar{\theta}\theta\lambda(x) + \frac{1}{2}\theta\theta\bar{\theta}\bar{\theta}D(x) \ , \tag{3.14}$$

where the highest D component is the only leftover auxiliary field, and as the F term in the chiral superfield, it transforms into a total derivative under supersymmetry transformations. In addition, any power higher than two of V vanishes automatically.

For the non-abelian gauge group, the vector superfield transforms as follows

$$e^V \longrightarrow e^{-i\Lambda^\dagger} e^V e^{i\Lambda} \tag{3.15}$$

with $V = 2gV^a t^a$, where t^a represent the generators of the non-abelian gauge group.

In order to construct a supersymmetric gauge invariant theory, we need a field strength superfield and a gauge invariant combination of the vector superfield and the chiral matter superfield. For the abelian case, it turns out that the fields λ, $\bar{\lambda}$ and D, together with the field strength $V_{\mu\nu} = \partial_\mu V_\nu - \partial_\nu V_\mu$ form an irreducible representation of the supersymmetry algebra. In this representation the lowest-dimensional field λ has mass dimension $\frac{3}{2}$, this suggests that the field strength superfield that contains the field strength as component is a spinor superfield. One can thus define the following left- and right-handed spinor superfields by observing that λ and $\bar{\lambda}$ are also the lowest-dimensional component fields of them

$$W_\alpha = -\frac{1}{4}\bar{D}^2 D_\alpha V \ , \qquad\qquad \bar{W}_{\dot{\alpha}} = -\frac{1}{4}D^2 \bar{D}_{\dot{\alpha}} V \ . \tag{3.16}$$

They are gauge invariant chiral superfields and contain the gauge invariant field strength tensor as components, hence serve as the supersymmetric generalization of the field strength tensor for an abelian group. Moreover, they satisfy an additional covariant constraint

$$D^\alpha W_\alpha = \bar{D}_{\dot{\alpha}} \bar{W}^{\dot{\alpha}} \ . \tag{3.17}$$

The field strength superfields defined above can be generalized to the non-abelian case as

$$W_\alpha = -\frac{1}{4}\bar{D}^2 e^{-V} D_\alpha e^V \ , \qquad\qquad \bar{W}_{\dot{\alpha}} = -\frac{1}{4}D^2 e^{-V} \bar{D}_{\dot{\alpha}} e^V \ , \tag{3.18}$$

with $W_\alpha = W_\alpha^a t^a$. From the gauge transformation Eq. (3.13) and (3.15) it follows that in the non-abelian case, the gauge invariant coupling of the vector superfield V and the chiral matter superfield Φ is

$$\Phi^\dagger e^V \Phi \ , \tag{3.19}$$

provided the superfield Φ transforms as $\Phi \to e^{-i\Lambda}\Phi$.

The last piece that one needs for the construction of supersymmetric Lagrangians is the superpotential, which is an analytic function of chiral superfields only and determines the possible interactions other than the gauge interaction of the theory.

Now we have all the ingredients to write down a supersymmetric Lagrangian. For this purpose, the transformation properties of the F and D terms discussed above are crucial.

3.3 Construction of supersymmetric Lagrangians

A supersymmetric action can be constructed from the integral over superspace of the corresponding Lagrangian density. In order for the action to be invariant under supersymmetry transformations, the space-time Lagrangian density can at most change as a total space-time derivative under supersymmetry transformations. We have already seen in the previous section that the highest components of the superfields, i.e. the F term in a chiral superfield and the D term in a vector superfield, transform under supersymmetry transformations into total derivatives. Hence they are suitable for the construction of supersymmetric Lagrangians. The highest components can be projected out by integrating over the anticommuting parameters θ and $\bar{\theta}$. First, we have the D term contribution, which involves an integration over the full superspace

$$\mathcal{L}_D = \int d^4\theta \sum_i \Phi_i^\dagger e^V \Phi_i \ . \tag{3.20}$$

Second, we have the F term contributions, which can be extracted by an integration over half of the superspace. One of these contributions arises from the gauge kinetic term

$$\mathcal{L}_F = \int d^2\theta \frac{1}{16g^2} W_\alpha^a W^{a\alpha} + h.c. \ , \tag{3.21}$$

another contribution is the superpotential part

$$\mathcal{L}_W = \int d^2\theta W(\Phi_i) + h.c. \ . \tag{3.22}$$

Note that the superpotential $W(\Phi)$ is an analytic function of the chiral superfields Φ_is. For a renormalizable theory, apart from a possible tadpole term that is linear in the superfields Φ_i, it has the following form

$$W = \frac{1}{2} m_{ij} \Phi_i \Phi_j + \frac{1}{3} g_{ijk} \Phi_i \Phi_j \Phi_k \ . \tag{3.23}$$

Terms involving more than three superfields would have mass dimension higher than four after the integration over the superspace and hence are forbidden by renormalizability.

The full Lagrangian is the sum of the three parts in Eqs. (3.20-3.22). As previously discussed, the auxiliary F and D fields appear without derivatives, their equations of motion are thus algebraic and can be easily derived from the constructed Lagrangian. It turns out that the these auxiliary fields and their equations of motion fix completely the scalar

potential. This is a striking feature of supersymmetric theories. In contrast, the scalar potential in the standard model is arbitrary and can not be determined within the standard model itself. When constructing phenomenologically viable supersymmetric models, this feature has important implications, as we will see in the forthcoming chapter.

If we are not restricted to renormalizable theories, the most general globally supersymmetric theory of chiral and vector superfields has the Lagrangian [3]

$$\mathcal{L} = \int d^4\theta K(\Phi^\dagger e^V, \Phi) + \left[\int d^2\theta W(\Phi) + \int d^2\theta f(\Phi)(W_\alpha^a)^2 + h.c.\right] , \tag{3.24}$$

where Φ and V denote the chiral and vector superfields, $W(\Phi)$ is the superpotential, which, as well as the gauge kinetic function $f(\Phi)$, is an analytic function of the chiral superfields. If one requires renormalizability, it turns out that the function $f(\Phi)$ must be constant and $K(\Phi^\dagger e^V, \Phi)$ has to be of the form of $\Phi^\dagger e^V \Phi$, and the superpotential can only be a polynomial involving powers up to three of the chiral fields. This indeed shows that the terms given in Eq. (3.20), (3.21) and (3.22) define the most general renormalizable theory.

3.4 Non-renormalization theorem

One of the important features of supersymmetric theories is that they have better ultraviolet behavior than ordinary field theories. In addition, in ordinary field theories any term that is permitted by the symmetries of the theory tends to appear in the effective action, while this is not the case for supersymmetric theories. Indeed, there exists a theorem for the supersymmetric theories, i.e. the non-renormalization theorem [44,45], which states that the superpotential is not renormalized in perturbation theory. Thus any fine-tuning of the potential at tree-level will not receive any higher order loop contributions. This makes supersymmetry a potential solution to the hierarchy problem.

The original proof of this theorem based on detailed investigations of perturbation theory and supergraph techniques led to the consequence that any radiative correction to the effective action will be of the form of an integral over the full superspace. The F term, hence the superpotential, is not renormalized. Only the D term receives radiative corrections, which yield the usual wave function renormalization constants for the superfields. All other parameters like mass and coupling constants are renormalized entirely due to the wave function renormalization.

Seiberg proposed another fairly simple proof based on considerations of symmetry, analyticity and the idea that the coupling constants can be viewed as chiral superfields with only lowest components non-zero [46]. This is possible due to the fact that the supersymmetry generators are differential operators on superspace, thus a superfield whose only non-zero component is a constant lowest component will not spoil supersymmetry. Now since superpotential is an analytic function of chiral superfields, it must be an analytic function of these coupling constants as well. For the sake of illustration, consider a theory of one single chiral superfield Φ with the tree-level superpotential

$$W = m\Phi^2 + \lambda\Phi^3 . \tag{3.25}$$

This superpotential is invariant under a $U(1) \times U(1)_R$ global symmetry. The charge assignment of the field Φ is $(1, 1)$ under such symmetry, while the charges of the couplings m and λ are $(-2, 0)$ and $(-3, -1)$, respectively. Under the global $U(1)_R$ symmetry, the anticommuting parameter θ also has charge 1. The most general renormalized superpotential that is invariant under this global $U(1) \times U(1)_R$ symmetry has the following form

$$W_R = m\Phi^2 f\left(\frac{\lambda\Phi}{m}\right) \ , \tag{3.26}$$

where f is an analytic function and can be expanded as

$$f = \sum_n a_n m^{1-n} \lambda^n \Phi^{n+2} \ . \tag{3.27}$$

The limit of $\lambda \to 0$ corresponds to a free theory and should not yield any singularity, hence no negative power of λ can appear in the expansion of the function f. One can also take simultaneously the massless limit $m/\lambda \to 0$, requiring the absence of singularity in this limit forbids terms with $n \geq 2$. Therefore the renormalized superpotential must be

$$W_R = m\Phi^2 + \lambda\Phi^3 = W \ , \tag{3.28}$$

i.e. the superpotential is not renormalized. This result can be generalized to theories with arbitrary numbers of chiral and vector superfields.

Another important aspect of the non-renormalization theorem is the non-renormalization of the factor e^V [3]. It then follows that the gauge coupling renormalization is related to the wave function renormalization constant of the vector superfield. This plays an important role in the investigation of $N = 4$ super Yang-Mills theory, whose multiplicative renormalization constants are not only related among each other, but are all equal to unity as a consequence of symmetries. Hence this theory is completely finite.

3.5 Mechanisms of supersymmetry breaking

Obviously, if supersymmetry has anything to do with nature, it must be a broken symmetry, either spontaneously or explicitly, since supersymmetry requires that each standard model particle be degenerate in mass with its superpartner, a possibility that has been ruled out by experiments. Supersymmetry can be explicitly broken by adding to the Lagrangian extra terms that are not invariant under supersymmetry transformations. These non-invariant terms introduce arbitrariness into the theory, since they have to be put in by hand, leading to a number of free parameters lacking of theory explanation. This situation retains in the construction of phenomenologically viable models. There, the extra terms are restricted by the requirement of mass hierarchy stabilization, so that they can only break supersymmetry softly, i.e. without reintroducing quadratic divergences. Trying to achieve a satisfactory explanation for these somewhat arbitrary soft terms motivates an alternative possibility of supersymmetry breaking, the spontaneous supersymmetry breaking, in which the Lagrangian remains invariant under supersymmetry transformations while the vacuum does not. The

spontaneous breaking of supersymmetry is also required if supersymmetry can be promoted to a local symmetry. It turns out that high energy theories with spontaneous supersymmetry breaking can yield low energy effective theories with explicit soft supersymmetry breaking terms, and hence provide explanations for the presence of such terms.

The anticommutation relations of supersymmetry generators imply that the Hamiltonian of $N = 1$ supersymmetric theory has the following form

$$H = P^0 = \frac{1}{4}(Q_1\bar{Q}_{\dot{1}} + \bar{Q}_{\dot{1}}Q_1 + Q_2\bar{Q}_{\dot{2}} + \bar{Q}_{\dot{2}}Q_2) \ . \tag{3.29}$$

The spectrum of H is positive semi-definite and the supersymmetric vacuum state has zero energy. Supersymmetry is unbroken as long as the vacuum state has vanishing energy. Its spontaneous breaking can take place only if the potential is positive. As discussed previously, the scalar potential is fixed by the auxiliary F and D fields and their equations of motion, and it turns out to be quadratic in these fields. Hence to achieve supersymmetry breaking, we must require that either $\langle F\rangle \neq 0$ or $\langle D\rangle \neq 0$ or both. A straightforward approach to obtain the soft terms in phenomenological models is to break supersymmetry spontaneously by generating non-zero vacuum expectation values of the F and/or D fields at a low energy scale relevant for phenomenology (e.g. the TeV scale). The O'Raifeartaigh mechanism [47] does this job through non-zero F terms, while the Fayet-Iliopoulus mechanism [48] does through non-zero D terms. Both can be achieved by introducing linear terms into the Lagrangian. However, it turns out that this sort of tree-level spontaneous supersymmetry breaking leads to phenomenologically unacceptable particle spectrum. For the tree-level masses of particles with spin j, the following supertrace relation holds

$$\sum_j (-1)^{2j}(2j+1)m_j^2 = 0 \ , \tag{3.30}$$

which yields constraints too strict for the boson masses, and contradicts the experimental observations. Moreover, these breaking mechanisms may result in unacceptable symmetry breaking in phenomenological models, such as breaking of color or electromagnetism. Consequently it is rather difficult, if not impossible, to achieve explicit soft supersymmetry breaking terms from directly generating F/D term vacuum expectation values at a low energy scale in a renormalizable Lagrangian.

Owing to the difficulties of spontaneous supersymmetry breaking at low energy (or visible sector supersymmetry breaking), one is strongly motivated to consider the possibility of supersymmetry breaking at a high energy scale. One most common such scenario is the hidden sector scenario, in which supersymmetry is spontaneously broken in a hidden sector. The supersymmetry breaking is communicated to the visible sector via suppressed interactions that are shared by both sectors. The visible sector, in a phenomenological model such as the minimal supersymmetric standard model contains the standard model particles and their superpartners. There are no direct renormalizable couplings between the visible and hidden sectors, the suppressed interactions can be induced by loop effects or non-renormalizable operators. Consequently the soft supersymmetry breaking terms result in the low energy effective theories. In this approach the supertrace relation Eq. (3.30) needs not hold for the

visible sector fields, so that it is possible, in principle, to have a phenomenologically acceptable particle spectrum. One of the leading candidates for the mediation of the hidden sector supersymmetry breaking is the gravitational interaction, an interaction shared by all particles. This possibility can be naturally embedded in supergravity theory [49, 50], which is a non-renormalizable supersymmetric effective theory of gravity resulting from gauging global supersymmetry. In supergravity theory it is possible to compute the soft supersymmetry breaking terms directly from the supergravity Lagrangian. The soft terms determined in this way are values at the high energy scale, their values at the electroweak scale can then be obtained through the renormalization group evolution. In the gravity-mediated supersymmetry breaking scenario [3, 34, 51, 52], the spin 3/2 superpartner of graviton, the gravitino, acquires its mass by absorbing the Goldstino degree of freedom, which is the fermionic counterpart of Goldstone boson in the presence of spontaneous supersymmetry breaking. The gravitino mass then sets the scale of the soft terms in the visible sector. If one takes the simplest possibility to assume that the supergravity Kähler potential (a generalization of the $\Phi^\dagger\Phi$ term in the Lagrangian for one single chiral superfield Φ) takes a minimal canonical form

$$K(\Phi_i, \lambda_i) = \sum_i \lambda_i^\dagger \lambda_i + \sum_i \Phi_i^\dagger \Phi_i \ , \tag{3.31}$$

where Φ_i represent the superfields of the visible sector and λ_i the superfields of the hidden sector that are connected with supersymmetry breaking; and assumes furthermore a universal gauge kinetic function $f(\Phi)$ (defined previously in Eq. (3.24)) for all gauge groups, one achieves a universality of the soft terms at the high energy scale. This defines the minimal supergravity model [34, 52].

Another competing candidate for the mediation of supersymmetry breaking is the gauge interaction. In the gauge-mediated supersymmetry breaking scenario there is another sector consisting of the messenger fields, which couple to the fields of both the hidden sector and the visible sector. The supersymmetry breaking is communicated between these two sectors via radiative corrections to the visible sector field propagators through loop diagrams involving the messenger fields. Of course, in this scenario there is still gravitational communication between the visible and hidden sectors. It is, however, subdominant compared to the gauge interaction. In this scenario, the gravitino mass is much smaller than the scale of soft terms in the visible sector, as long as the characteristic mass of the messenger fields is much lower than the Planck scale.

From a phenomenological perspective, we do not need to worry about how supersymmetry is broken at the high energy scale, since the effects of supersymmetry breaking are parameterized in phenomenological models by explicit soft supersymmetry breaking terms. Girardello and Grisaru [53] have classified all such terms that are renormalizable as follows[2]

$$\begin{array}{ll}
(a) \text{ scalar mass terms}, & m^{ij}\varphi_i\varphi_j^* \ , \\
(b) \text{ gaugino mass terms}, & \tfrac{1}{2}m_\lambda \lambda^a\lambda^a \ , \\
(c) \text{ trilinear scalar interactions}, & A^{ijk}\varphi_i\varphi_j\varphi_k + h.c. \ , \\
(d) \text{ bilinear terms}, & B^{ij}\varphi_i\varphi_j + h.c. \ , \\
(e) \text{ linear terms}, & C^i\varphi_i \ .
\end{array} \tag{3.32}$$

[2] terms like $\lambda^{ijk}\varphi_i^*\varphi_j\varphi_k + h.c.$ may be allowed, but they lead to practical difficulties in realistic models with supersymmetry breaking and are usually omitted [52, 54].

All these terms have couplings with positive mass dimension. The gauginos transform non-trivially under continuous R symmetries, hence their mass terms do not respect such symmetries. In realistic models this kind of symmetry is usually needed to suppress the baryon- or lepton-violating terms in the effective Lagrangian. In order to allow the gaugino mass terms, one defines a discrete symmetry rather than a continuous one, i.e. the R parity, which is respected by the gaugino mass terms and sufficient to suppress those terms that violate baryon or lepton number conservation. This will be described in the next chapter.

3.6 Extended and local supersymmetry

In this section we will say a few words about theories with extended ($N > 1$) supersymmetry and local supersymmetry. Evidently one can introduce more than one set of supersymmetry generators to enlarge the supersymmetry algebra, each of the generators Q^i will change the particle spin by $\frac{1}{2}$. If one wants to construct a renormalizable supersymmetric gauge theory, in which the maximum value allowed for particle spin is 1, then the number of supersymmetries will be restricted to $N \leq 4$, since by applying the supersymmetry generators to a state with helicity 1 one can at most end with a helicity -1 state. Analogously if one allows a spin 2 particle in the theory, e.g. the graviton, then the number of supersymmetries is restricted to $N \leq 8$.

The drawback of theories with extended supersymmetry for the construction of phenomenologically viable models is clear. Suppose one has two sets of supersymmetry generators that anticommute with each other, starting from a fermionic state with maximum helicity $\frac{1}{2}$, one can obtain two scalar states by applying each generator once and one state with helicity $-\frac{1}{2}$ by applying both generators. Hence the left- and right-handed fermionic states are contained in the same representation and they should have the same transformation property under gauge groups [33]. This is a general feature of theories with extended supersymmetry and is bad news for phenomenology. Therefore, as we mentioned at the beginning of this chapter, only $N = 1$ supersymmetry needs to be taken seriously for low energy phenomenology. This is the starting point of the construction of the minimal supersymmetric extension of the standard model in the next chapter.

If supersymmetry is not merely an accident, it should be realized as a local symmetry. Local supersymmetry naturally includes the general coordinate invariance as a subsymmetry, hence is a theory of gravity, i.e. supergravity. At a low energy scale where the effects of gravity is negligible, local supersymmetry can appear as a global symmetry. One can expect that supergravity theory, as a more fundamental theory, might be able to solve some problems of the low energy phenomenological theory. In previous sections we have already mentioned some of these possibilities. Although adding more supersymmetries can improve on the convergence behavior of the theory, it turns out that supergravity, even with the maximum number of supersymmetries allowed ($N = 8$), is yet not finite or renormalizable. It seems that a consistent quantum theory of gravity can only be formulated within the framework of string theory, which is based on the idea that the fundamental objects are open/closed strings rather than point particles [55–57]. The spectrum of closed strings includes a spin 2 massless

state, which can be identified as the graviton. Hence gravity is naturally incorporated in string theory. Another appealing feature of string theory is that it does not suffer from the ultraviolet divergences that plague ordinary quantum field theories of point particles due to the completely different topological structure.

Chapter 4

The Minimal Supersymmetric Standard Model

4.1 Definition of the model

As its name suggests, the minimal supersymmetric standard model (MSSM) [3, 4, 34, 58] is the most economic way to extend the standard model (SM) to include supersymmetry. It has the same gauge group as the SM, i.e. the $SU(3)_C \times SU(2)_L \times U(1)_Y$ group. The SM fields are cast into superfields. For each SM particle, there exists only one superpartner as the consequence of minimal supersymmetry ($N = 1$). The gauge bosons and their spin $\frac{1}{2}$ superpartners (spin $\frac{3}{2}$ is not allowed for a renormalizable theory), called gauginos (8 gluinos, 3 winos and 1 bino corresponding to each gauge group) are in the vector supermultiplet. The three generation spin $\frac{1}{2}$ quarks and leptons and their spin 0 superpartners, the scalar quarks and leptons, or squarks and sleptons for short, reside in the chiral supermultiplets, so that the left-handed components of fermions are allowed to transform differently from the right-handed components under gauge groups. As in the SM, there are no right-handed neutrinos in the MSSM. The Higgs sector of the MSSM contains two Higgs chiral supermultiplets with opposite hypercharges. In the SM there is one single Higgs doublet, which acquires a non-vanishing vacuum expectation value so that the electroweak symmetry is spontaneously broken. The fermion masses are then generated by Yukawa couplings with the Higgs doublet itself or its conjugate. This is, however, not possible in the MSSM since the Yukawa interactions arise from the superpotential, which has to be an analytic function of superfields only, not of their conjugate fields. Hence one is forced to introduce two Higgs doublets in order to generate masses for both up- and down-type fermions. In addition, to ensure that the model is anomaly-free an even number of Higgs doublets with opposite hypercharges are required, two Higgs doublets in the MSSM are the simplest possibility.

The supermultiplets of the MSSM and their particle content are listed in Table 4.1 according to their transformation properties under the gauge groups. To determine their dynamic properties and interactions one needs to specify the Lagrangian of the model. As discussed in the previous chapter, supersymmetry has to be a broken symmetry at low energies. This

Superfields		Bosonic fields	Fermionic partners	$SU(3)_C$	$SU(2)_L$	$U(1)_Y$
Gauge multiplets						
$\hat{G}_a$	gluons, gluinos	G_a	$\tilde{G}_a$	8	1	0
$\hat{W}_a$	W bosons, winos	W_a	$\tilde{W}_a$	1	3	0
$\hat{B}$	B boson, bino	B	$\tilde{B}$	1	1	0
Matter multiplets						
$\hat{Q}_i$	squarks, quarks	$(\tilde{u}_L, \tilde{d}_L)_i$	$(u_L, d_L)_i$	3	2	$\frac{1}{3}$
$\hat{U}_i$		$\tilde{u}^*_{Ri}$	$\bar{u}_{Ri}$	$\bar{3}$	1	-$\frac{4}{3}$
$\hat{D}_i$		$\tilde{d}^*_{Ri}$	$\bar{d}_{Ri}$	$\bar{3}$	1	$\frac{2}{3}$
$\hat{L}_i$	sleptons, leptons	$(\tilde{\nu}, \tilde{e}_L)_i$	$(\nu, e_L)_i$	1	2	-1
$\hat{E}_i$		$\tilde{e}^*_{Ri}$	$\bar{e}_{Ri}$	1	1	2
$\hat{H}_1$	Higgses, higgsinos	(H_1^0, H_1^-)	$(\tilde{H}_1^0, \tilde{H}_1^-)$	1	2	-1
$\hat{H}_2$		(H_2^+, H_2^0)	$(\tilde{H}_2^+, \tilde{H}_2^0)$	1	2	1

Table 4.1: Particle content of the MSSM.

implies that, in addition to the supersymmetry-conserving part in the MSSM Lagrangian, there must exist a supersymmetry breaking part in the Lagrangian. In order that supersymmetry remains to be a solution for the hierarchy problem, only superrenormalizable soft terms are allowed. From the effective theory point of view, these terms are the most relevant supersymmetry breaking operators at low energies. The most general such terms have been classified in the previous chapter.

The supersymmetric Lagrangian consists of three parts, the gauge interacting part, the gauge kinetic term and the superpotential, which can be written as follows

$$\begin{aligned}
\mathcal{L}_{SUSY} = & \int d^4\theta \left\{ \hat{L}_i^\dagger e^{V_L+V_Y} \hat{L}_i + \hat{E}_i^\dagger e^{V_Y} \hat{E}_i + \hat{Q}_i^\dagger e^{V_C+V_L+V_Y} \hat{Q}_i \right. \\
& \left. + \hat{U}_i^\dagger e^{V_C+V_Y} \hat{U}_i + \hat{D}_i^\dagger e^{V_C+V_Y} \hat{D}_i + \hat{H}_i^\dagger e^{V_L+V_Y} \hat{H}_i \right\} \\
& + \int d^2\theta \left\{ \frac{1}{16 g_2^2} W_\alpha^a W^{a\alpha} + \frac{1}{16 g_1^2} W_\alpha W^\alpha + \frac{1}{16 g_3^2} W_\alpha^{a_s} W^{a_s \alpha} + h.c. \right\} \\
& + \int d^2\theta \left\{ \epsilon_{\alpha\beta} \Big[- (Y_u)_{ij} \hat{H}_2^\alpha \hat{Q}_i^\beta \hat{U}_j + (Y_d)_{ij} \hat{H}_1^\alpha \hat{Q}_i^\beta \hat{D}_j + (Y_e)_{ij} \hat{H}_1^\alpha \hat{L}_i^\beta \hat{E}_j \right. \\
& \left. - \mu \hat{H}_1^\alpha \hat{H}_2^\beta \Big] + h.c. \right\} , \qquad (4.1)
\end{aligned}$$

where V_C, V_L, V_Y and g_3, g_2, g_1 are the vector superfields and gauge couplings that correspond to the gauge groups $SU(3)_C$, $SU(2)_L$ and $U(1)_Y$, respectively. $\alpha, \beta = 1, 2$ are the $SU(2)_L$ doublet indices, and $\epsilon_{\alpha\beta}$ is a totally anti-symmetric tensor with $\epsilon_{12} = -\epsilon_{21} = 1$. i, j are family indices, $(Y_{u,d,e})_{ij}$ represent the Yukawa couplings. A summation over the indices is implied.

The terms in the first curly bracket dictate the gauge interactions between matter and gauge fields, those in the second are the kinetic terms for the gauge fields constructed from the field strength superfields, the superpotential in the third bracket defines all other supersymmetric interactions of the theory. The first three terms in the superpotential are the generalizations of the SM Yukawa couplings, while the last term is the supersymmetric Higgs mass term. The only dimensionful parameter in the supersymmetric Lagrangian is the parameter μ. Given as a superpotential parameter, it is expected to be of the order of a high energy scale, e.g. the GUT scale or the Planck scale. However, from the phenomenological perspective it should be roughly of the order of the electroweak scale so that the hierarchy problem is not restored. One can think of the μ parameter as, rather than a fundamental parameter, only a parametrization of some more fundamental physics associated with supersymmetry breaking at a high energy scale. It does not appear at tree-level and only arises as the vacuum expectation value of some new field. In this way understanding the μ parameter is intimately connected to understanding the breaking of supersymmetry, the parameter itself can be treated on the same footing as the soft terms and is roughly of the same order as the soft terms.

The soft supersymmetry breaking part of the MSSM Lagrangian is given by

$$\begin{aligned}\mathcal{L}_{soft} = &-\frac{1}{2}\Big[M_1\tilde{B}\tilde{B} + M_2\tilde{W}^a\tilde{W}^a + M_3\tilde{G}^a\tilde{G}^a\Big] \\ &+ \epsilon_{\alpha\beta}\Big[(A_u)_{ij}H_2^\alpha\tilde{Q}_i^\beta\tilde{U}_j - (A_d)_{ij}H_1^\alpha\tilde{Q}_i^\beta\tilde{D}_j - (A_e)_{ij}H_1^\alpha\tilde{L}_i^\beta\tilde{E}_j + B\mu H_1^\alpha H_2^\beta + h.c.\Big] \\ &- \Big[\tilde{Q}_i^\alpha {m_Q^2}_{ij}\tilde{Q}_j^{\alpha*} + \tilde{L}_i^\alpha {m_L^2}_{ij}\tilde{L}_j^{\alpha*} + \tilde{U}_i^* {m_U^2}_{ij}\tilde{U}_j + \tilde{D}_i^* {m_D^2}_{ij}\tilde{D}_j + \tilde{E}_i^* {m_E^2}_{ij}\tilde{E}_j\Big] \\ &- \Big[m_{H_2}^2 H_2^\dagger H_2 + m_{H_1}^2 H_1^\dagger H_1\Big] \ , \end{aligned} \tag{4.2}$$

where M_1, M_2 and M_3 represent the bino, wino and gluino masses respectively, $(A_{u,d,e})_{ij}$ specify the trilinear couplings between sfermions and Higgs bosons, and B determines the bilinear coupling of Higgs bosons. The last two lines are mass terms for sfermions and Higgs bosons.

Here we stress that there is an additional assumption when writing down the supersymmetry-preserving part of the MSSM Lagrangian. In the SM, baryon/lepton number (B/L) conservation are accidental symmetries of the model implied by gauge invariance, in the sense that if one requires gauge invariance of all possible interactions of the SM, the renormalizable terms with mass dimension four or less automatically preserve B/L. This is not the case in the MSSM. The MSSM superpotential can have renormalizable terms which are invariant under supersymmetry, Lorentz and gauge transformations but do not preserve B/L. These terms are

$$W_{NR} = \lambda_{ijk}\hat{L}_i\hat{L}_j\hat{E}_k + \lambda'_{ijk}\hat{L}_i\hat{Q}_j\hat{D}_k + \lambda''_{ijk}\hat{U}_i\hat{D}_j\hat{D}_k + \lambda'''_i\hat{L}_i\hat{H}_2 \ . \tag{4.3}$$

They violate L or B by 1 unit, and can lead to undesirable phenomenological consequences such as the proton decay, which is so far not observed experimentally. Hence such B/L violating terms should be avoided. Instead of simply postulating the conservation of B/L in the MSSM, one introduces a discrete symmetry, the matter parity [59], or equivalently, the

R parity [60], so that these terms are not allowed in the MSSM superpotential. The matter parity is defined as

$$P_M = (-1)^{3(B-L)} \ . \tag{4.4}$$

The terms in Eq. (4.3) would be disallowed if one requires all terms of the superpotential to have $P_M = 1$. This discrete symmetry of the low energy effective theory should be expected to arise from some new physics at a high energy scale, e.g. as the residual symmetry left over after the breaking of some continuous symmetry of high energy theories.

The R parity is defined by

$$P_R = (-1)^{3(B-L)+2S} \ , \tag{4.5}$$

where S is the spin of the particle. This is equivalent to the matter parity as long as angular momentum is conserved. The standard model particles and Higgs bosons have even R parity $P_R = +1$, whereas their superpartners have odd R parity $P_R = -1$. If R parity is exactly conserved, no mixing between ordinary particles and their superpartners can occur. This has important phenomenological implications, such as a superparticle must decay into an odd number of superparticles, and they must be produced in pairs at colliders. In addition, the lightest supersymmetric particle (LSP) must be absolutely stable since it cannot decay into the SM particles. The LSP at the end of decay chains gives the characteristic signature for supersymmetry at colliders. Moreover, the LSP can be neutral under the gauge groups, thus inevitably very weakly interacting. Therefore it is a nice cold dark matter candidate.

Adding to the Lagrangian the gauge-fixing and the Faddeev-Popov ghost part completes the construction of the MSSM Lagrangian. As one can clearly see, most of the free parameters in the MSSM are introduced by the soft supersymmetry breaking part of the Lagrangian. The mass spectrum of the model crucially depends on these soft parameters. In the next section we sketch the counting of independent parameters of the MSSM following Haber [61].

4.2 The MSSM parameters

The MSSM contains a lot of new parameters, in addition to the 19 parameters that are already present in the SM. As mentioned in the previous section, most of these new parameters are contained in the soft supersymmetry breaking Lagrangian. The mass matrices of squarks and sleptons are 3×3 Hermitian matrices. These lead to $6 \times 5 = 30$ real parameters and $3 \times 5 = 15$ imaginary parameters, where the imaginary parameters arise from the off-diagonal entries. The trilinear coupling matrices in general are 3×3 complex matrices, which give $9 \times 3 = 27$ real parameters and $9 \times 3 = 27$ imaginary ones. The μ parameter is treated on the same footing as the soft parameters, which, together with the bilinear coupling parameter B, can be complex, thus contribute two real and two imaginary degrees of freedom. In addition, the complex gaugino mass parameters M_1, M_2 and M_3 contribute three real and three imaginary degrees of freedom. The real soft Higgs mass parameters m_{H_1} and m_{H_2} contribute two real degrees of freedom, which are the same as the Higgs sector of the SM and thus need not be counted into the number of new degrees of freedom. All these add up to 109

parameters, but not all of them are physical. Certain symmetries arise if the superpotential couplings and the soft terms are switched off. These symmetries allow a redefinition of the global phase of the fields without changing the physics. In the SM, there exist the following global symmetries if the Yukawa couplings are switched off [52, 61]

$$U(3)_Q \times U(3)_U \times U(3)_D \times U(3)_L \times U(3)_E \ , \tag{4.6}$$

which correspond to three generations of the five multiplets: $(u_L, d_L)_i$, $\bar{u}_{Ri}$, $\bar{d}_{Ri}$, $(\nu, e_L)_i$, $\bar{e}_{Ri}$. Each of them has $3(3-1)/2 = 3$ real and $3(3+1)/2 = 6$ imaginary parameters. When the Yukawa couplings are reintroduced, they are broken down to four global $U(1)$ symmetries, namely the conservation of baryon number and the conservation of lepton numbers for each family. Hence these symmetries can be used to eliminate $3 \times 5 = 15$ real and $6 \times 5 - 4 = 26$ imaginary parameters in the SM. In the MSSM, the situation is slightly different. There is only one global lepton number conservation rather than three when the Yukawa couplings are switched on. Hence with these symmetries one can eliminate two more degrees of freedom, reducing the 109 newly introduced parameters to 107. Moreover, there are two additional global $U(1)$ symmetries in the absence of the μ term and the soft terms, the $U(1)_R \times U(1)_{PQ}$ symmetry [62], which can be used to further remove two degrees of freedom. Therefore one has 105 new parameters in the MSSM.

From the point of view of phenomenological analyses, it is a formidable task to scan over such a large parameter space with so many unknown parameters. In order to give predictions one usually makes additional assumptions on the soft supersymmetry breaking parameters. For example, a common assumption is that the soft parameters take a simple form at a higher energy scale, e.g. the GUT scale, so that the scalar mass parameters, the gaugino mass parameters and the trilinear couplings unify. Renormalization group equations can then be used to run these parameters down to the electroweak scale.

4.3 Particle spectrum of the MSSM

4.3.1 Higgs bosons

As previously mentioned, the Higgs sector of the MSSM consists of two Higgs doublets with opposite hypercharges. The tree-level scalar potential of the Higgs fields is given by the sum of the contributions from the F-term, the D-term and the soft supersymmetry breaking term [63]

$$\begin{aligned} V_H = &(|\mu|^2 + m_{H_1}^2)|H_1|^2 + (|\mu|^2 + m_{H_2}^2)|H_2|^2 + \frac{1}{8}(g_1^2 + g_2^2)(|H_1|^2 - |H_2|^2)^2 \\ &+ \frac{g_2^2}{2}|H_1^\dagger H_2|^2 - B\mu(\epsilon_{\alpha\beta} H_1^\alpha H_2^\beta + h.c.) \ . \end{aligned} \tag{4.7}$$

Specifically, the $|\mu|^2$ term arises from the F-term of the superpotential, the quartic terms are the D-term contributions and all the other terms come from the soft supersymmetry breaking part of the Lagrangian. Note that the quartic Higgs couplings are completely fixed in terms of the gauge couplings as a consequence of supersymmetry.

Spontaneous breaking of the electroweak symmetry takes place if the neutral components of the Higgs doublets acquire non-zero vacuum expectation values. The $SU(2)_L$ symmetry can always be used to set the vacuum expectation values of the charged components of the Higgs doublets to zero. Hence the electric charge symmetry is preserved. The only possible complex term $B\mu$ can also be made real by a redefinition of the global phase of the Higgs fields. Consequently the vacuum expectation values of both Higgs doublets can be chosen to be real and thus the CP symmetry is preserved by the tree-level Higgs potential. The Higgs mass eigenstates, therefore, have definite CP quantum numbers. After the electroweak symmetry breaking, three of the eight degrees of freedom of the two Higgs doublets are eaten by the weak gauge bosons and become their longitudinal components, resulting in five physical Higgs bosons. Two of them, h^0 and H^0, are CP-even, one is CP-odd, denoted as A^0, and the other two, $H^\pm$, are charged.

The requirements of electroweak symmetry breaking and that the potential should be bounded from below impose the following conditions on the parameters of the Higgs potential

$$\begin{aligned} (|\mu|^2 + m_{H_1}^2)(|\mu|^2 + m_{H_2}^2) &< (B\mu)^2 \ , \\ 2|\mu|^2 + m_{H_1}^2 + m_{H_2}^2 &\leq 2|B\mu| \ , \\ m_{H_1}^2 &\neq m_{H_2}^2 \ . \end{aligned} \tag{4.8}$$

The last relation indicates that the soft supersymmetry breaking Higgs masses must have non-vanishing value, revealing the fact that supersymmetry must be broken in order to realize the electroweak symmetry breaking.

The two Higgs doublets can be decomposed as

$$\begin{aligned} H_1 &= \begin{pmatrix} v_1 + \frac{1}{\sqrt{2}}(\phi_1 + i\chi_1) \\ H_1^- \end{pmatrix} = \begin{pmatrix} v\cos\beta + \frac{1}{\sqrt{2}}(\phi_1 + i\chi_1) \\ H_1^- \end{pmatrix} \ , \\ H_2 &= \begin{pmatrix} H_2^+ \\ v_2 + \frac{1}{\sqrt{2}}(\phi_2 + i\chi_2) \end{pmatrix} = \begin{pmatrix} H_2^+ \\ v\sin\beta + \frac{1}{\sqrt{2}}(\phi_2 + i\chi_2) \end{pmatrix} \ , \end{aligned} \tag{4.9}$$

where $v = \sqrt{v_1^2 + v_2^2} = 174\,\mathrm{GeV}$ and $\tan\beta = v_2/v_1$ with $0 < \beta < \pi/2$. The minimization conditions for the potential can be written as

$$\begin{aligned} B\mu &= \frac{(m_{H_1}^2 - m_{H_2}^2)\tan 2\beta}{2} + \frac{M_Z^2 \sin 2\beta}{2} \ , \\ |\mu|^2 &= \frac{m_{H_2}^2 \sin^2\beta - m_{H_1}^2 \cos^2\beta}{\cos 2\beta} - \frac{M_Z^2}{2} \ . \end{aligned} \tag{4.10}$$

Thereby the parameters B and μ can be determined up to an unknown phase. Substituting the decomposition Eq. (4.9) into the Higgs potential, Eq. (4.7), the terms bilinear in the Higgs fields define their masses. In the interaction basis, their mass matrices are not diagonal. These mass matrices can be diagonalized by unitary matrices. Applying these diagonalization matrices to the interaction eigenstates yields the mass eigenstates. For the CP-even, CP-odd

and charged Higgs bosons, the respective mass eigenstates are given by applying the following rotations

$$\begin{pmatrix} H^0 \\ h^0 \end{pmatrix} = \begin{pmatrix} \cos\alpha & \sin\alpha \\ -\sin\alpha & \cos\alpha \end{pmatrix} \begin{pmatrix} \phi_1 \\ \phi_2 \end{pmatrix} ,$$
$$\begin{pmatrix} G^0 \\ A^0 \end{pmatrix} = \begin{pmatrix} \cos\beta & \sin\beta \\ -\sin\beta & \cos\beta \end{pmatrix} \begin{pmatrix} \chi_1 \\ \chi_2 \end{pmatrix} ,$$
$$\begin{pmatrix} G^\pm \\ H^\pm \end{pmatrix} = \begin{pmatrix} \cos\beta & \sin\beta \\ -\sin\beta & \cos\beta \end{pmatrix} \begin{pmatrix} H_1^\pm \\ H_2^\pm \end{pmatrix} . \tag{4.11}$$

The tree-level masses of the CP-even Higgs bosons are then given by

$$M^2_{h^0,H^0} = \frac{1}{2}\Big[M^2_{A^0} + M^2_Z \mp \sqrt{(M^2_{A^0} + M^2_Z)^2 - 4M^2_{A^0} M^2_Z \cos^2 2\beta}\Big] . \tag{4.12}$$

The mass of the CP-odd Higgs boson is determined as

$$M^2_{A^0} = B\mu(\tan\beta + \cot\beta) = \frac{2B\mu}{\sin 2\beta} . \tag{4.13}$$

It is related to the charged Higgs boson mass via

$$M^2_{H^\pm} = M^2_{A^0} + M^2_W . \tag{4.14}$$

One can freely choose either M_{A^0} or $M_{H^\pm}$ as an input parameter for phenomenological analyses. Usually M_{A^0} is used for analyses within real MSSM, while $M_{H^\pm}$ is often chosen for analyses within complex MSSM since in the complex MSSM the CP-odd Higgs boson A^0 is no longer mass eigenstate beyond tree-level due to the CP-violating mixing effect [64]. In this thesis we will essentially concentrate on real MSSM. The mixing angle α between the two CP-even Higgs bosons H^0 and h^0 is determined as

$$\alpha = \frac{1}{2}\arctan\Big[\tan 2\beta \frac{M^2_{A^0} + M^2_Z}{M^2_{A^0} - M^2_Z}\Big] , \qquad -\frac{\pi}{2} < \alpha < 0 . \tag{4.15}$$

From Eq. (4.12) one can see that the mass M_{h^0} has an upper bound $M_{h^0} \leq |M_Z \cos 2\beta| \leq M_Z$, as a consequence of the fact that the Higgs self couplings are determined by the gauge couplings in the MSSM. In contrast, the Higgs self coupling in the SM is a free parameter, hence the Higgs mass is, too, a free parameter.

The couplings of Higgs bosons to vector bosons can be derived from the kinetic term of Higgs fields. CP invariance forbids certain couplings at tree-level, such as the $A^0W^+W^-$ and Zh^0h^0 vertices. The structure of the MSSM Higgs sector also implies constraints for those couplings that are present at tree-level. For example, the couplings of the two CP-even Higgs bosons and the W/Z gauge bosons

$$g_{h^0VV} = \frac{\sqrt{2}M^2_V}{v}\sin(\beta - \alpha) , \qquad g_{H^0VV} = \frac{\sqrt{2}M^2_V}{v}\cos(\beta - \alpha) \tag{4.16}$$

fulfill $g^2_{h^0VV} + g^2_{H^0VV} = (\sqrt{2}M_V^2/v)^2 = g^2_{HVV}$, where V denotes W or Z, and g_{HVV} is the coupling of the SM Higgs boson and the W/Z gauge bosons. Consequently in the limit that $\cos(\beta-\alpha) \to 0$, the light CP-even Higgs boson h^0 will behave like a SM Higgs boson, while in the limit that $\sin(\beta-\alpha) \to 0$, the heavy CP-even Higgs boson H^0 will resemble the SM Higgs boson. Note that the factor $\cos(\beta-\alpha)$ can be written as

$$\cos^2(\beta-\alpha) = \frac{M^2_{h^0}(M_Z^2 - M^2_{h^0})}{M^2_{A^0}(M^2_{H^0} - M^2_{h^0})} \ . \tag{4.17}$$

In the limit that M_{A^0} is much larger than M_Z, one obtains

$$\cos^2(\beta-\alpha) \approx \frac{M_Z^4 \sin^2 4\beta}{4M^4_{A^0}} \ , \tag{4.18}$$

hence the coupling g_{H^0VV} is negligibly small and g_{h^0VV} approaches the SM coupling. This is the so-called decoupling limit.

The Yukawa couplings of Higgs bosons and fermions are defined in the superpotential. As H_1 couples exclusively to down-type fermions and H_2 exclusively to up-type ones, the following relations between the Yukawa couplings and the fermion masses are expected

$$\lambda_u = \frac{m_u}{v_2} = \frac{m_u}{v\sin\beta} \ , \qquad \lambda_d = \frac{m_d}{v_1} = \frac{m_d}{v\cos\beta} \ . \tag{4.19}$$

In contrast to the Yukawa couplings in the SM, the MSSM Yukawa couplings involve an additional factor of $1/\sin\beta$ or $1/\cos\beta$. Consequently the down-type couplings can be significantly enhanced at large $\tan\beta$.

As previously shown, the mass of the light CP-even MSSM Higgs boson has an upper bound of M_Z at tree-level. If this is not significantly altered by radiative corrections, the MSSM would have been ruled out by the Higgs searches at LEP [65]. Fortunately, the higher order corrections indeed induce a considerable shift in this mass bound. The loop contributions have been computed with different methods, e.g. the effective potential approach [66–72] or the diagrammatic method [64, 73–82], which yield the complete results at one-loop level and partial corrections that are presumably dominant at two-loop level. At one-loop level, the dominant contribution arises from an incomplete cancellation between the top quark and top squark loops, which turns out to be proportional to the fourth power of the top quark mass. The fact that the top quark is heavy is crucial, since otherwise the radiative corrections might not be able to yield a significant shift to the upper bound of the light CP-even Higgs boson mass.

The relations between the Yukawa couplings and fermion masses will be modified by radiative corrections as well. In the tree-level Lagrangian the down-type fermions couple to the Higgs field H_1 only, whereas the up-type fermions couple only to H_2. Radiative corrections can not only yield modifications to the tree-level couplings, but also induce couplings of down-type fermions to the conjugate field of H_2 or up-type fermions to the conjugate field of H_1. These induced couplings are closely related to the soft breaking parameters. The effective Lagrangian that includes the induced couplings of Higgs bosons and fermions can

be written as [83]

$$-\mathcal{L}_Y = \epsilon_{\alpha\beta}\Big[(\lambda_u + \delta\lambda_u)\bar{u}_R Q_L^\alpha H_2^\beta + (\lambda_d + \delta\lambda_d)\bar{d}_R H_1^\alpha Q_L^\beta\Big] + \Delta\lambda_d \bar{d}_R Q_L^\alpha H_2^{\alpha *} + \Delta\lambda_u \bar{u}_R Q_L^\alpha H_1^{\alpha *} + h.c.\ , \tag{4.20}$$

which results in the following modification of the tree-level relations between the Yukawa couplings and fermion masses [84]

$$\begin{aligned} \lambda_u &= \frac{m_u}{v_2(1 + \frac{\delta\lambda_u}{\lambda_u} + \frac{\Delta\lambda_u \cot\beta}{\lambda_u})} = \frac{m_u}{v \sin\beta(1 + \Delta_u)}\ , \\ \lambda_d &= \frac{m_d}{v_1(1 + \frac{\delta\lambda_d}{\lambda_d} + \frac{\Delta\lambda_d \tan\beta}{\lambda_d})} = \frac{m_d}{v \cos\beta(1 + \Delta_d)}\ . \end{aligned} \tag{4.21}$$

Note that Δ_d contains corrections that are enhanced by $\tan\beta$ [84, 85]. From the effective Lagrangian, Eq. (4.20), and these modified relations one can then derive straightforwardly the effective Yukawa couplings in terms of the fermion masses $m_{u,d}$ and the $\Delta_{u,d}$ factors.

4.3.2 Sfermions

After the electroweak symmetry breaking, all particles of the same spin with the same $SU(3)_C \times U(1)_Q$ quantum numbers can mix. This will lead to 6×6 mixing matrices for up- and down-type squarks and charged sleptons, and 3×3 mixing matrix for sneutrinos. As phenomenological constraints on flavor changing neutral current processes require that the intergeneration mixing be small, we will not consider the mixing between squarks of different generations here. The mass matrix entries of squarks originate from the contribution of the F-term, D-term and soft supersymmetry breaking terms to the scalar potential. The F-term contributes both to the diagonal and off-diagonal entries, the D-term yields only diagonal contributions, while the soft terms contribute to the diagonal entries through the scalar mass terms and to the off-diagonal entries through the trilinear coupling terms when the Higgs fields acquire non-zero vacuum expectation values. Hence to parametrize the sfermion mass matrices, one needs μ, $\tan\beta$, the trilinear couplings and the corresponding left- and right-handed soft masses. In the gauge eigenstate basis $(\tilde{f}_L, \tilde{f}_R)$, the mass matrix can be written as

$$M_{\tilde{f}} = \begin{pmatrix} M_{\tilde{f}_L}^2 + m_f^2 + M_Z^2 \cos 2\beta (I_3^f - Q_f s_W^2) & m_f X_f \\ m_f X_f & M_{\tilde{f}_R}^2 + m_f^2 + M_Z^2 \cos 2\beta\, Q_f s_W^2 \end{pmatrix} \tag{4.22}$$

with m_f the SM fermion mass, and

$$X_f = A_f - \mu\{\cot\beta, \tan\beta\}\ , \tag{4.23}$$

where $\cot\beta, \tan\beta$ applies to the up- and down-type sfermions, respectively. The mass eigenstates can be obtained by applying a unitary transformation to the gauge eigenstates

$$\begin{pmatrix} \tilde{f}_1 \\ \tilde{f}_2 \end{pmatrix} = \begin{pmatrix} \cos\theta_{\tilde{f}} & \sin\theta_{\tilde{f}} \\ -\sin\theta_{\tilde{f}} & \cos\theta_{\tilde{f}} \end{pmatrix} \begin{pmatrix} \tilde{f}_L \\ \tilde{f}_R \end{pmatrix}\ . \tag{4.24}$$

The mixing angle is determined by requiring that the mass matrix be diagonal in the rotated basis. The mass eigenvalues are given by

$$m^2_{\tilde{f}_1,\tilde{f}_2} = m^2_f + \frac{1}{2}\Big[M^2_{\tilde{f}} + M^2_{\tilde{f}_R} + M^2_Z \cos 2\beta I^f_3 \mp \sqrt{[M^2_{\tilde{f}} - M^2_{\tilde{f}_R} + M^2_Z \cos 2\beta(I^f_3 - 2Q_f s^2_W)]^2 + 4m^2_f X^2_f}\Big] \ . \tag{4.25}$$

As one can see that the non-diagonal entries of the mass matrix in the gauge eigenstate basis is proportional to the fermion mass, thus the mixing in the stop sector is particularly important. Its contribution to the renormalization group equation decreases the stop masses when running down to the low energy scale and can yield a mass of the lighter stop smaller than any other squarks. Of course the stop mass can not run into negative values, since the color or electric charge symmetry should not be broken. This requirement would yield constraint on the corresponding trilinear coupling. In the sbottom sector, if $\tan\beta$ and μ are large, the mixing can be strongly enhanced and also become important.

In terms of the physical masses and the mixing angles the original mass matrix Eq. (4.22) can be written as

$$M_{\tilde{f}} = \begin{pmatrix} \cos\theta^2_{\tilde{f}} m^2_{\tilde{f}_1} + \sin\theta^2_{\tilde{f}} m^2_{\tilde{f}_2} & \sin\theta_{\tilde{f}}\cos\theta_{\tilde{f}}(m^2_{\tilde{f}_1} - m^2_{\tilde{f}_2}) \\ \sin\theta_{\tilde{f}}\cos\theta_{\tilde{f}}(m^2_{\tilde{f}_1} - m^2_{\tilde{f}_2}) & \sin\theta^2_{\tilde{f}} m^2_{\tilde{f}_1} + \cos\theta^2_{\tilde{f}} m^2_{\tilde{f}_2} \end{pmatrix} \tag{4.26}$$

and

$$A_f = \frac{\sin\theta_{\tilde{f}}\cos\theta_{\tilde{f}}(m^2_{\tilde{f}_1} - m^2_{\tilde{f}_2})}{m_f} + \mu\{\cot\beta, \tan\beta\} \ , \tag{4.27}$$

i.e. the trilinear coupling and the mixing angle of squarks can be related to each other. If one insists this relation beyond tree-level, the mixing angle of squarks usually needs be renormalized when renormalizing the squark sector [86, 87], since its renormalization is equivalent to the renormalization of the trilinear coupling.

4.3.3 Neutralinos and charginos

In this section we describe the mixing between neutral (charged) higgsinos and neutral (charged) gauginos. The neutral higgsinos $(\tilde{H}^0_1, \tilde{H}^0_2)$ and gauginos $(\tilde{B}, \tilde{W}^3)$ can mix to form four mass eigenstates, the neutralinos, while the charged higgsinos $(\tilde{H}^-_1, \tilde{H}^+_2)$ and gauginos $(\tilde{W}^-, \tilde{W}^+)$ can mix to yield charginos. The contribution to the neutralino and chargino mass matrices results from the soft gaugino mass terms, the higgsino mass terms and the couplings of Higgs fields to higgsino and gauginos when the Higgs fields acquire nonzero vacuum expectation values. In the neutral gaugino and higgsino basis $(\tilde{B}, \tilde{W}^3, \tilde{H}^0_1, \tilde{H}^0_2)$ the

mass matrix is given by

$$M_N = \begin{pmatrix} M_1 & 0 & -M_Z s_W \cos\beta & M_Z s_W \sin\beta \\ 0 & M_2 & M_Z c_W \cos\beta & M_Z c_W \sin\beta \\ -M_Z s_W \cos\beta & M_Z c_W \cos\beta & 0 & -\mu \\ M_Z s_W \sin\beta & M_Z c_W \sin\beta & -\mu & 0 \end{pmatrix} . \tag{4.28}$$

The symmetry of this mass matrix allows its diagonalization with only one unitary matrix N. Applying N to the gauge eigenstates yields the neutralino mass eigenstates

$$\begin{pmatrix} \tilde{\chi}_1^0 \\ \tilde{\chi}_2^0 \\ \tilde{\chi}_3^0 \\ \tilde{\chi}_4^0 \end{pmatrix} = N \begin{pmatrix} \tilde{B} \\ \tilde{W}^3 \\ \tilde{H}_1^0 \\ \tilde{H}_2^0 \end{pmatrix} . \tag{4.29}$$

The diagonalized neutralino mass matrix is given by

$$M_N^D = N^* M_N N^\dagger . \tag{4.30}$$

By appropriately choosing the diagonalization matrix N, M_N^D can be settled to have non-negative entries.

The mass term for the charginos in the Lagrangian can be written in the basis $\psi^+ = (\tilde{W}^+, \tilde{H}_2^+)$, $\psi^- = (\tilde{W}^-, \tilde{H}_1^-)$ as

$$-\frac{1}{2}(\psi^+, \psi^-) \begin{pmatrix} 0 & M_C^T \\ M_C & 0 \end{pmatrix} \begin{pmatrix} \psi^+ \\ \psi^- \end{pmatrix} + h.c. \tag{4.31}$$

with $\tilde{W}^\pm = \frac{1}{\sqrt{2}}(\tilde{W}^1 \mp i\tilde{W}^2)$ and the matrix

$$M_C = \begin{pmatrix} M_2 & \sqrt{2}\sin\beta M_W \\ \sqrt{2}\cos\beta M_W & \mu \end{pmatrix} . \tag{4.32}$$

The mass eigenstates are then obtained by two unitary rotation matrices since there are two independent mixings

$$\chi_i^+ = V_{ij}\psi_j^+, \qquad \chi_i^- = U_{ij}\psi_j^-, \quad i = 1, 2 , \tag{4.33}$$

leading to the following four-component Dirac spinors

$$\tilde{\chi}_i^+ = \begin{pmatrix} \chi_i^+ \\ \bar{\chi}_i^- \end{pmatrix}, \quad i = 1, 2 . \tag{4.34}$$

The diagonalized mass matrix is obtained by

$$M_C^D = U^* M_C V^\dagger \ . \tag{4.35}$$

In the case that both M_2 and μ are real, the rotation matrices can be written as

$$U = \mathcal{O}_-, \quad V = \begin{cases} \mathcal{O}_+ & \text{if} \quad \det M_C > 0 \\ \sigma_3 \mathcal{O}_+ & \text{if} \quad \det M_C < 0 \end{cases} , \quad \mathcal{O}_\pm = \begin{pmatrix} \cos\phi_\pm & \sin\phi_\pm \\ -\sin\phi_\pm & \cos\phi_\pm \end{pmatrix} , \tag{4.36}$$

where σ_3 is the Pauli matrix that is inserted to make the chargino masses positive. The angles $\phi_\pm$ satisfy

$$\tan 2\phi_+ = \frac{2\sqrt{2} M_W (M_2 \cos\beta + \mu \sin\beta)}{M_2^2 - \mu^2 - 2M_W^2 \cos 2\beta} , \quad \tan 2\phi_- = \frac{2\sqrt{2} M_W (M_2 \sin\beta + \mu \cos\beta)}{M_2^2 - \mu^2 + 2M_W^2 \cos 2\beta} . \tag{4.37}$$

This yields the following chargino masses

$$\begin{aligned} M^2_{\tilde{\chi}^+_{1,2}} = \frac{1}{2}\Big\{ & M_2^2 + \mu^2 + 2M_W^2 \\ & \mp \Big[(M_2^2 + \mu^2 + 2M_W^2)^2 - 4(\mu M_2 - M_W^2 \sin 2\beta)^2 \Big]^{\frac{1}{2}} \Big\} . \end{aligned} \tag{4.38}$$

4.3.4 Gluinos

As the superpartner of gluons, gluino is a color octet fermion and can not mix with any other particle in the MSSM. By $SU(3)_C$ invariance all gluinos have the same Majorana mass M_3, which is related to the bino and wino masses M_1 and M_2 in supersymmetric GUT theories

$$M_3 = \frac{\alpha_S}{\alpha} \sin^2\theta_W M_2 = \frac{3}{5} \frac{\alpha_S}{\alpha} \cos^2\theta_W M_1 \ , \tag{4.39}$$

where α_S and α are the strong and electromagnetic coupling constants, respectively.

4.4 Renormalization of the MSSM

In this section we will describe the renormalization of the MSSM, essentially focusing on the Higgs sector, which is most relevant for the computation that will be presented in the forthcoming chapters. Before the detailed investigation, the basic strategy of regularization and renormalization will be briefly illustrated.

4.4.1 Strategies of regularization and renormalization

The Lagrangian specifying a quantum field theory usually involves free parameters that have to be determined by experiments. At tree-level these free parameters can be directly related to

the experimentally measurable quantities. At perturbative higher orders these relations will, in general, no longer hold. Moreover, this is plagued by ultraviolet divergences that appear in the higher order loop diagrams. The appearance of these divergences is an indication that the theory under consideration is just a low energy effective theory which will break down at a higher energy scale where new physics enters. Nevertheless, for certain theories, it is possible to achieve a consistent treatment of the divergences by means of the regularization and renormalization procedure and thereby to make predictions that can be tested by experiments. The previously described SM and MSSM are theories of this kind. The idea of regularization is to render the unmanipulable divergent integrals finite by introducing a suitable convergence device, such as a cut-off to the energy scale, or equivalently, to the integrated loop momenta. In this way the original parameters in the Lagrangian (bare parameters) have no longer physical meaning since their relations to physical quantities become cut-off dependent. By means of renormalization the cut-off dependence can be absorbed into the bare parameters so that the relations between measurable physical quantities do not depend on the cut-off. After the renormalization procedure, one can express the observable quantities in terms of the free parameters determined by experiments, which absorb our ignorance of physics at high energy scales so that we are able to make predictions at a low energy scale.

Clearly the regularization procedure is purely mathematical and has no physical impacts. Accordingly the choice of regularization prescription is not unique, we list some of the commonly used regularization schemes below.

Regularization schemes

1. **Pauli-Villars regularization** [88]
In the Pauli-Villars regularizaton scheme one introduces fictitious fields whose mass acts as a cut-off on the momentum integrals. This regularization is the most intuitive choice. It preserves the Poincaré symmetry but might spoil gauge invariance when applying to non-abelian gauge theories, hence is not well-suited for the regularization of the SM.

2. **Dimensional regularization** [89, 90]
This regularization scheme originates from the observation that the ultraviolet divergences of momentum integrals can be removed if one goes to space-time dimension lower than four. The space-time dimension D is then treated as a continuous variable and acts as a regulator for the momentum integrals. The integrals are performed in D dimensions ($D < 4$), and then analytically continuated to four dimensions. The original divergences will show up as poles in $D - 4$. In this regularization scheme care has to be taken when generalizing the usual γ_5 matrix in four dimensions to arbitrary dimensions. Also an arbitrary mass parameter μ needs to be introduced to keep the dimension of the coupling constants correct. As the space-time dimension is used as the regulator, this scheme preserves properties of the theory that are independent of the space-time dimension, e.g. gauge invariance but not supersymmetry. Consequently this scheme is not suitable for the regularization of supersymmetric gauge theories. To obtain a suitable regularization scheme for supersymmetric gauge theories, one develops a variant of the dimensional regularization scheme, i.e. the dimensional reduction scheme, in which the continuation from four to D dimensions is carried out by compactification, or

dimensional reduction.

3. **Dimensional reduction** [91, 92]
The reason that the dimensional regularization scheme does not preserve supersymmetry is the following: in $D = 4$ dimensions the condition $2^{D/2} = D$ is fulfilled, thus the fermionic and bosonic degrees of freedom match in four dimensions. When moving away from four dimensions, this match is broken, hence supersymmetry is broken as well. Practically, when applying dimensional regularization to supersymmetric gauge theories, it is possible to restore supersymmetry by adding suitable finite corrections to the counter terms, whose existence is guaranteed by renormalizability of the theory [93–97]. This, however, will lead to complication since these finite terms do not originate from necessary renormalization. An elegant alternative that preserves supersymmetry is the regularization by dimensional reduction, in which only momenta are treated as D-dimensional, whereas fields and the Dirac algebra remain as 4-dimensional. Ambiguities related to the treatment of the γ_5 matrix also occur in this regularization scheme [98]. However, there has been proof that dimensional reduction can be formulated in a mathematically consistent manner [99].

Renormalization

There are different approaches of renormalization. One possibility is to compute physical quantities in terms of bare parameters and then express them in terms of finite renormalized parameters. Another alternative that is widely used in literature is the counter term approach. In the counter term approach, the original bare Lagrangian is separated into two pieces, one piece by replacing the bare parameters with finite renormalized parameters, and the other counter term piece that absorbs the unobservable infinite shifts between the bare and renormalized parameters. Apart from the renormalization constants that define the counter terms, these two pieces take the same form. In order to obtain finite S-matrix element as well as finite propagators and vertex functions, one has to perform not only the renormalization of the Lagrangian parameters, but also the field renormalization. The bare and renormalized parameters and fields can be related by multiplicative factors

$$g_0 = Z_g g = \left(1 + \sum_{n=1}^{\infty} \delta Z_g^{(n)}\right) g \ , \tag{4.40}$$

$$\Phi_0 = \sqrt{Z}_\Phi \Phi = \left(1 + \sum_{n=1}^{\infty} \delta Z_\Phi^{(n)}\right)^{\frac{1}{2}} \Phi \ , \tag{4.41}$$

where the subscript 0 denotes the bare quantities, and n the perturbative orders, $\delta Z_i^{(n)}$ are the respective renormalization constants. As mentioned above, the bare Lagrangian can be written as the sum of the basic Lagrangian depending on the renormalized quantities and the counter term Lagrangian

$$\mathcal{L}_0(g_0, \Phi_0) = \mathcal{L}(g, \Phi) + \mathcal{L}_{CT}(g, \Phi, \delta Z_g, \delta Z_\Phi) \ . \tag{4.42}$$

The renormalization constants or counter terms have to be determined by renormalization conditions. These conditions are arbitrary, since the definition of divergent parts to be

absorbed by the counter terms are arbitrary. One such definition can differ by finite parts from others. The prescription specifying the finite parts defines a renormalization scheme, any two such renormalization schemes are connected by a finite renormalization. As a consequence, calculations at fixed order perturbation theory are renormalization scheme dependent, i.e. they can differ from scheme to scheme by higher order contributions. Of course if one is able to perform exact calculations that include contributions from all perturbative orders the dependence on the renormalization schemes must drop out. In the following we list some of the widely used renormalization schemes.

1. **On-shell scheme**
In the on-shell scheme the renormalization conditions that determine the counter terms are formulated in such a way that the finite renormalized parameters are equal to physical parameters at all orders in perturbation theory. The renormalized masses of physical particles are required to be the physical masses, which arise as the real parts of the poles of the corresponding propagators. Obviously the on-shell renormalization for quarks are meaningless, since they are confined in hadrons and are not free particles. Thus the quark mass parameters have to be replaced by some other experimental inputs. The on-shell renormalization of fields are fixed by requiring that the renormalized fields are properly normalized, i.e. the residues of the renormalized propagators are equal to one. The on-shell renormalization scheme has been formulated for the SM [100, 101] and generalized to the MSSM [102].

2. **Minimal subtraction**
The minimal subtraction (MS) scheme [103] is specific to dimensional regularization. In this scheme the counter terms are defined so that only the pole terms $1/\varepsilon$ ($2\varepsilon = 4 - D$) that arise from dimensional regularization are eliminated. For calculations at fixed perturbative order, the arbitrary mass scale μ in the dimensional regularization introduces a scale dependence, namely the renormalization scale dependence. Of course if one performs an exact calculation, this dependence has to drop out. However, in practical perturbative calculations, the parameter used for perturbative expansion is the coupling constant, the renormalization scale dependence is not fully cancelled order by order in this expansion, consequently the results of perturbative calculations depend on the renormalization scale. The MS scheme and its variant, the so-called modified minimal subtraction scheme or $\overline{MS}$ scheme [104], are commonly used in QCD as the fundamental particle states, the quarks and gluons are not free particles and an on-shell renormalization is meaningless. The $\overline{MS}$ scheme is defined by observing that in dimensional regularization the pole terms are usually accompanied by constant terms. In this scheme not only the pole terms but also the constant terms are subtracted, namely the following term is subtracted

$$\Delta = \frac{1}{\varepsilon} - \gamma_E + \ln 4\pi \ , \tag{4.43}$$

where γ_E is the Euler constant. The renormalization scale in the MS and $\overline{MS}$ scheme are related by

$$\ln \mu^2_{MS} - \gamma_E + \ln 4\pi \to \ln \mu^2_{\overline{MS}} \ . \tag{4.44}$$

Note that in contrast to the MS scheme, there is no renormalization scale dependence in

the on-shell renormalization scheme as the masses of physical particles set natural scales at which the parameters can be defined.

3. $\overline{DR}$ **scheme**
The $\overline{DR}$ scheme is the analog of the $\overline{MS}$ scheme for regularization by dimensional reduction. The $\overline{DR}$ renormalization scale $\mu_{\overline{DR}}$ is defined analogously. As in the MS or $\overline{MS}$ scheme, for practical calculations, one usually sets this scale as the characteristic mass scale of processes under consideration.

Now we turn to the renormalization of the MSSM. In the following we will concentrate on the Higgs sector and describe its renormalization in detail.

4.4.2 Renormalization of the MSSM Higgs sector

As previously shown, in the MSSM two Higgs doublets with opposite hypercharges are required for consistency. These two doublets can be decomposed as in Eq. (4.9). Substituting this decomposition into the scalar potential (4.7) gives rise to linear (tadpole) and bilinear terms of the decomposed fields. These terms can be rewritten in terms of mass eigenstates as follows

$$\begin{aligned} V_{TB} = &-T_{h^0}h^0 - T_{H^0}H^0 + \frac{1}{2}\begin{pmatrix} h^0 & H^0 \end{pmatrix}\begin{pmatrix} M^2_{h^0} & M^2_{h^0H^0} \\ M^2_{h^0H^0} & M^2_{H^0} \end{pmatrix}\begin{pmatrix} h^0 \\ H^0 \end{pmatrix} \\ &+ \frac{1}{2}\begin{pmatrix} A^0 & G^0 \end{pmatrix}\begin{pmatrix} M^2_{A^0} & M^2_{A^0G^0} \\ M^2_{A^0G^0} & M^2_{G^0} \end{pmatrix}\begin{pmatrix} A^0 \\ G^0 \end{pmatrix} \\ &+ \begin{pmatrix} H^- & G^- \end{pmatrix}\begin{pmatrix} M^2_{H^\pm} & M^2_{H^-G^+} \\ M^2_{G^-H^+} & M^2_{G^\pm} \end{pmatrix}\begin{pmatrix} H^+ \\ G^+ \end{pmatrix} . \end{aligned} \tag{4.45}$$

Note that the tadpole terms for charged components do not appear in the above equation. The tadpole coefficients and mass matrix entries are related to the original parameters in the scalar potential. The CP-even, CP-odd and charged Higgs fields in Eq. (4.45) are given at the moment by the rotations defined by the mixing angles α, β_1 and β_2 rather than those in Eq. (4.11). The determination of these mixing angles will be given later. Due to the freedom of choosing $m^2_{H_1}$ and $m^2_{H_2}$, the scalar potential contains seven independent parameters, namely $m_1^2 = |\mu|^2 + m^2_{H_1}$, $m_2^2 = |\mu|^2 + m^2_{H_2}$, $m_3^2 = B\mu$, g_1, g_2, v_1 and v_2. They can be replaced by an equivalent set of free parameters consisting of T_{h^0}, T_{H^0}, e, M_W, M_Z, M_{A^0} and $\tan\beta$. Note that for complex MSSM, there exists one more free parameter, that is the CP-violating phase between the two Higgs doublets (at lowest order this phase can be eliminated, hence the tree-level Higgs potential is CP-conserving). In this case, one can introduce T_{A^0} into the equivalent set of parameters and replace M_{A^0} with $M_{H^\pm}$. In terms of the new parameters, the non-diagonal entries of the mass matrices describing mixing between Higgs bosons are

given by [64]

$$\begin{aligned}
M^2_{h^0H^0} &= -\frac{1}{2}M_Z^2 \sin 2(\alpha+\beta) + \frac{1}{2}M^2_{A^0}\sin 2(\alpha-\beta)/\cos^2(\beta-\beta_1) \\
&+ \frac{e}{2M_Z s_W c_W} T_{H^0}\sin(\alpha-\beta)\sin^2(\alpha-\beta_1)/\cos^2(\beta-\beta_1) \\
&- \frac{e}{2M_Z s_W c_W} T_{h^0}\cos(\alpha-\beta)\cos^2(\alpha-\beta_1)/\cos^2(\beta-\beta_1)\ , \\
M^2_{A^0G^0} &= -M^2_{A^0}\tan(\beta-\beta_1) - \frac{e}{2M_Z s_W c_W} T_{H^0}\sin(\alpha-\beta_1)/\cos(\beta-\beta_1) \\
&- \frac{e}{2M_Z s_W c_W} T_{h^0}\cos(\alpha-\beta_1)/\cos(\beta-\beta_1)\ , \\
M^2_{H^-G^+} &= -M^2_{H^\pm}\tan(\beta-\beta_2) - \frac{e}{2M_Z s_W c_W} T_{H^0}\sin(\alpha-\beta_2)/cos(\beta-\beta_2) \\
&- \frac{e}{2M_Z s_W c_W} T_{h^0}\cos(\alpha-\beta_2)/\cos(\beta-\beta_2)\ ,
\end{aligned} \tag{4.46}$$

where s_W and c_W denote the sine and cosine of the weak mixing angle, respectively. The condition that tadpoles and $M^2_{A^0G^0}$ and $M^2_{H^-G^+}$ vanish yields $\beta_1 = \beta_2 = \beta$, while $M^2_{h^0H^0} = 0$ fixes the mixing angle α as in Eq. (4.15). The expressions for diagonal entries lead to Eqs. (4.12), (4.14) and $M_{G^\pm} = M_{G^0} = 0$.

The computation of higher order corrections requires the renormalization of the Higgs sector. One can choose to renormalize the following parameters (the gauge-fixing term is kept invariant under renormalization)

$$\begin{aligned}
&T_{h^0} \to T_{h^0} + \delta T_{h^0}\ , \qquad T_{H^0} \to T_{H^0} + \delta T_{H^0}\ , \qquad \tan\beta \to \tan\beta + \delta\tan\beta\ , \\
&M_Z^2 \to M_Z^2 + \delta M_Z^2\ , \qquad M_W^2 \to M_W^2 + \delta M_W^2\ , \qquad M_{ij}^2 \to M_{ij}^2 + \delta M_{ij}^2\ ,
\end{aligned} \tag{4.47}$$

where M^2_{ij} represent the mass matrix entries in Eq. (4.45). Note that the mixing angles α and $\beta_{1,2}$ need not be renormalized, hence $\beta_{1,2} = \beta$ can be applied only after renormalization. The mass counter terms for M^2_{ij} (except the counter term for $M^2_{A^0}$) follow straightforwardly from their tree-level expressions. For example,

$$\begin{aligned}
\delta M^2_{h^0H^0} &= -\frac{1}{2}\delta M_Z^2 \sin 2(\alpha+\beta) + \frac{1}{2}\delta M^2_{A^0}\sin 2(\alpha-\beta) \\
&+ \frac{e}{2M_Z s_W c_W}[\delta T_{H^0}\sin^3(\alpha-\beta) - \delta T_{h^0}\cos^3(\alpha-\beta)] \\
&- \delta\tan\beta\cos^2\beta[M_Z^2\cos 2(\alpha+\beta) + M^2_{A^0}\cos 2(\alpha-\beta)]
\end{aligned} \tag{4.48}$$

is derived directly from the first equation in (4.46). Likewise, one finds

$$\begin{aligned}
\delta M^2_{h^0} &= \delta M_Z^2\sin^2(\alpha+\beta) + \delta M^2_{A^0}\cos^2(\alpha-\beta) \\
&+ \frac{e}{2M_Z s_W c_W}[\delta T_{H^0}\cos(\alpha-\beta)\sin^2(\alpha-\beta) + \delta T_{h^0}(1+\cos^2(\alpha-\beta))] \\
&+ \delta\tan\beta\cos^2\beta[M_Z^2\sin 2(\alpha+\beta) + M^2_{A^0}\sin 2(\alpha-\beta)]\ , \\
\delta M^2_{H^0} &= \delta M_Z^2\cos^2(\alpha+\beta) + \delta M^2_{A^0}\sin^2(\alpha-\beta) \\
&- \frac{e}{2M_Z s_W c_W}[\delta T_{H^0}\cos(\alpha-\beta)(1+\sin^2(\alpha-\beta)) + \delta T_{h^0}\sin(\alpha-\beta)\cos^2(\alpha-\beta)] \\
&- \delta\tan\beta\cos^2\beta[M_Z^2\sin 2(\alpha+\beta) + M^2_{A^0}\sin 2(\alpha-\beta)]\ ,
\end{aligned} \tag{4.49}$$

and

$$\begin{aligned}
\delta M^2_{A^0G^0} &= -\frac{e}{2M_Z s_W c_W}[\delta T_{H^0}\sin(\alpha-\beta)+\delta T_{h^0}\cos(\alpha-\beta)] - \delta\tan\beta\cos^2\beta M^2_{A^0}\ , \\
\delta M^2_{G^0} &= -\frac{e}{2M_Z s_W c_W}[\delta T_{H^0}\cos(\alpha-\beta)-\delta T_{h^0}\sin(\alpha-\beta)]\ , \\
\delta M^2_{H^-G^+} &= -\frac{e}{2M_Z s_W c_W}[\delta T_{H^0}\sin(\alpha-\beta)+\delta T_{h^0}\cos(\alpha-\beta)] - \delta\tan\beta\cos^2\beta M^2_{H^\pm}\ , \\
\delta M^2_{G^\pm} &= -\frac{e}{2M_Z s_W c_W}[\delta T_{H^0}\cos(\alpha-\beta)-\delta T_{h^0}\sin(\alpha-\beta)]\ . \qquad (4.50)
\end{aligned}$$

The counter term for $M^2_{H^\pm}$ is given by

$$\delta M^2_{H^\pm} = \delta M^2_{A^0} + \delta M^2_W\ . \qquad (4.51)$$

If one uses $M_{H^\pm}$ instead of M_{A^0} as an input parameter, then the counter term $\delta M^2_{A^0}$ will be a derived quantity. Note that the renormalization of the electric charge does not appear in the mass counter terms at the one-loop level [64]. The counter terms on the right-hand side of Eqs. (4.48-4.51) have to be determined by appropriately chosen renormalization conditions. The mass counter terms δM^2_Z, δM^2_W and $\delta M^2_{A^0}$ can be fixed by on-shell renormalization conditions

$$\mathrm{Re}\hat{\Sigma}^T_Z(M^2_Z)=0\ , \qquad \mathrm{Re}\hat{\Sigma}^T_W(M^2_W)=0\ , \qquad \mathrm{Re}\hat{\Sigma}_{A^0}(M^2_{A^0})=0\ , \qquad (4.52)$$

where $\hat{\Sigma}^T_{Z,W}$ denote the renormalized transverse gauge boson self energies. The third renormalization condition should be replaced by

$$\mathrm{Re}\hat{\Sigma}_{H^+H^-}(M^2_{H^\pm})=0 \qquad (4.53)$$

if $M^2_{H^\pm}$ is used instead as an input. The tadpole counter terms are fixed by requiring that the renormalized tadpoles vanish, which leads to

$$\delta T_{h^0} = -T_{h^0}\ , \qquad \delta T_{H^0} = -T_{H^0}\ . \qquad (4.54)$$

In order to have finite Green functions, the fields have to be renormalized as well. For the renormalization of the Higgs fields, we can choose to renormalize either the unrotated Higgs fields defined in Eq. (4.9) or the rotated ones given by Eq. (4.11). This is in analogy to the renormalization of gauge boson fields in the SM, where one can renormalize either W^3 and B bosons or alternatively their mixtures, the γ and Z bosons. In the SM the weak mixing angle is defined by $\sin^2\theta_W = 1 - M^2_W/M^2_Z$ in the on-shell scheme [101]. This defining relation is valid to all orders in perturbation theory. The weak mixing angle thus receives renormalization due to the renormalization of M_W and M_Z. In the Higgs sector of the MSSM, the relations between the mixing angles and input parameters hold only at tree-level. Hence the mixing angles can be kept unrenormalized.

The renormalization of the Higgs fields can be carried out by the following transformations

$$\begin{pmatrix} h^0 \\ H^0 \end{pmatrix} \to \begin{pmatrix} 1+\frac{1}{2}\delta Z_{h^0h^0} & \frac{1}{2}\delta Z_{h^0H^0} \\ \frac{1}{2}\delta Z_{H^0h^0} & 1+\frac{1}{2}\delta Z_{H^0H^0} \end{pmatrix} \begin{pmatrix} h^0 \\ H^0 \end{pmatrix}\ , \qquad (4.55)$$

$$\begin{pmatrix} A^0 \\ G^0 \end{pmatrix} \to \begin{pmatrix} 1+\frac{1}{2}\delta Z_{A^0A^0} & \frac{1}{2}\delta Z_{A^0G^0} \\ \frac{1}{2}\delta Z_{G^0A^0} & 1+\frac{1}{2}\delta Z_{G^0G^0} \end{pmatrix} \begin{pmatrix} A^0 \\ G^0 \end{pmatrix} ,$$
$$\begin{pmatrix} H^+ \\ G^+ \end{pmatrix} \to \begin{pmatrix} 1+\frac{1}{2}\delta Z_{H^+H^-} & \frac{1}{2}\delta Z_{H^-G^+} \\ \frac{1}{2}\delta Z_{G^-H^+} & 1+\frac{1}{2}\delta Z_{G^+G^-} \end{pmatrix} \begin{pmatrix} H^+ \\ G^+ \end{pmatrix} , \tag{4.56}$$

where the renormalization constants can be fixed by, e.g. on-shell conditions. For the CP-even Higgs bosons, the mass counter terms $\delta M^2_{h^0}$, $\delta M^2_{H^0}$ and $\delta M^2_{h^0H^0}$ have been determined by Eqs. (4.48) and (4.49). We can use the following on-shell conditions to fix the field renormalization constants for the CP-even Higgs bosons [102]

$$\begin{aligned} \mathrm{Re}\hat{\Sigma}'_{h^0}(M^2_{h^0}) &= 0, & \mathrm{Re}\hat{\Sigma}'_{H^0}(M^2_{H^0}) &= 0 . \\ \mathrm{Re}\hat{\Sigma}_{h^0H^0}(M^2_{h^0}) &= 0, & \mathrm{Re}\hat{\Sigma}_{h^0H^0}(M^2_{H^0}) &= 0 . \end{aligned} \tag{4.57}$$

The field renormalization constants for the CP-odd and charged Higgs bosons can be determined analogously.

Alternatively one can choose to renormalize the Higgs fields by defining a renormalization constant for each Higgs doublet

$$H_1 \to (1+\frac{1}{2}\delta Z_{H_1})H_1, \qquad H_2 \to (1+\frac{1}{2}\delta Z_{H_2})H_2 . \tag{4.58}$$

Their vacuum expectation values then renormalize as follows

$$\begin{aligned} v_1 &\to (1+\frac{1}{2}\delta Z_{H_1})(v_1-\delta v_1) = v_1(1+\frac{1}{2}\delta Z_{H_1}-\frac{\delta v_1}{v_1}) , \\ v_2 &\to (1+\frac{1}{2}\delta Z_{H_2})(v_2-\delta v_2) = v_2(1+\frac{1}{2}\delta Z_{H_2}-\frac{\delta v_2}{v_2}) . \end{aligned} \tag{4.59}$$

Note that the freedom of field renormalization allows to impose the condition $\frac{\delta v_1}{v_1} = \frac{\delta v_2}{v_2}$.

Keeping in mind that the mixing angles are not renormalized, the renormalization constants in the mass eigenstate basis can be expressed in terms of δZ_{H_1} and δZ_{H_2}. For instance, for the CP-even Higgs bosons, one has

$$\begin{pmatrix} 1+\frac{1}{2}\delta Z_{h^0h^0} & \frac{1}{2}\delta Z_{h^0H^0} \\ \frac{1}{2}\delta Z_{H^0h^0} & 1+\frac{1}{2}\delta Z_{H^0H^0} \end{pmatrix} =$$
$$\begin{pmatrix} -\sin\alpha & \cos\alpha \\ \cos\alpha & \sin\alpha \end{pmatrix} \begin{pmatrix} 1+\frac{1}{2}\delta Z_{H_1} & 0 \\ 0 & 1+\frac{1}{2}\delta Z_{H_2} \end{pmatrix} \begin{pmatrix} -\sin\alpha & \cos\alpha \\ \cos\alpha & \sin\alpha \end{pmatrix} , \tag{4.60}$$

giving rise to

$$\begin{aligned} \delta Z_{h^0h^0} &= \sin^2\alpha\delta Z_{H_1} + \cos^2\alpha\delta Z_{H_2} , \\ \delta Z_{h^0H^0} &= \delta Z_{H^0h^0} = \sin\alpha\cos\alpha(\delta Z_{H_2}-\delta Z_{H_1}) , \\ \delta Z_{H^0H^0} &= \cos^2\alpha\delta Z_{H_1} + \sin^2\alpha\delta Z_{H_2} . \end{aligned} \tag{4.61}$$

This implies that the renormalization transformation matrix can be set symmetrically. Likewise, one obtains the expressions of field renormalization constants for CP-odd and charged Higgs bosons by replacing α with β in the above equations.

For convenience, usually the $\overline{DR}$ scheme is used for the field renormalization as in this scheme possible occurrence of unphysical threshold effects can be avoided [64]. From Eq. (4.61), it is straightforward to fix the field renormalization constants for the two Higgs doublets in the $\overline{DR}$ scheme as follows

$$\begin{aligned}\delta Z_{H_1}^{\overline{DR}} &= -[\,\mathrm{Re}\Sigma'_{H^0}(M^2_{H^0})|_{\alpha=0}\,]^{\mathrm{div}}\ ,\\ \delta Z_{H_2}^{\overline{DR}} &= -[\,\mathrm{Re}\Sigma'_{h^0}(M^2_{h^0})|_{\alpha=0}\,]^{\mathrm{div}}\ .\end{aligned} \tag{4.62}$$

Now we turn to the renormalization of $\tan\beta$. The $\tan\beta$ renormalization follows from the renormalization of the vacuum expectation values of the two Higgs doublets. From Eq. (4.59), one obtains

$$\frac{\delta\tan\beta}{\tan\beta} = \frac{1}{2}(\delta Z_{H_2} - \delta Z_{H_1})\ . \tag{4.63}$$

In the $\overline{DR}$ scheme $\delta\tan\beta$ is fixed by Eq. (4.62). Another choice that is commonly used for the renormalization of $\tan\beta$ is to impose the following renormalization condition [74, 76]

$$\mathrm{Re}\hat{\Sigma}_{A^0Z}(M^2_{A^0}) = 0\ , \tag{4.64}$$

where the renormalized self energy is given by

$$\hat{\Sigma}_{A^0Z}(k^2) = \Sigma_{A^0Z}(k^2) - M_Z\frac{\sin 2\beta}{\tan\beta}\delta\tan\beta\ . \tag{4.65}$$

Consequently the counter term $\delta\tan\beta$ is fixed as

$$\frac{\delta\tan\beta}{\tan\beta} = \frac{1}{M_Z\sin 2\beta}\,\mathrm{Re}\Sigma_{A^0Z}(M^2_{A^0})\ . \tag{4.66}$$

Both schemes for the renormalization of $\tan\beta$ lead to gauge dependence, since they do not imply direct relations between $\tan\beta$ and physical observables. However, it has been shown that at one-loop level the $\overline{DR}$ scheme of $\tan\beta$ renormalization yields gauge independent results within the class of R_ξ gauges (the gauge dependence arises at two-loop level even within R_ξ gauges), while the other scheme does not [105]. Hence the $\overline{DR}$ scheme is a convenient choice for the evaluation of one-loop corrections. Moreover, this scheme has stable numerical behavior [105–107]. We will employ the field renormalization Eq. (4.58) and impose the $\overline{DR}$ renormalization conditions Eqs. (4.62) and (4.63) for the Higgs fields and $\tan\beta$ renormalization.

The renormalized self energies can be written in terms of the unrenormalized ones, the field renormalization constants and the mass counter terms. For the CP-even Higgs bosons, we have

$$\begin{aligned}\hat{\Sigma}_{h^0}(k^2) &= \Sigma_{h^0}(k^2) + \delta Z_{h^0h^0}(k^2 - M^2_{h^0}) - \delta M^2_{h^0}\ ,\\ \hat{\Sigma}_{H^0}(k^2) &= \Sigma_{H^0}(k^2) + \delta Z_{H^0H^0}(k^2 - M^2_{H^0}) - \delta M^2_{H^0}\ ,\\ \hat{\Sigma}_{h^0H^0}(k^2) &= \Sigma_{h^0H^0}(k^2) + \delta Z_{h^0H^0}(k^2 - \frac{1}{2}(M^2_{h^0} + M^2_{H^0})) - \delta M^2_{h^0H^0}\ .\end{aligned} \tag{4.67}$$

The renormalized self energies for the CP-odd and charged Higgs bosons can be written down analogously.

As mentioned previously, the light CP-even Higgs boson mass receives large radiative corrections. The higher-order corrected CP-even Higgs boson masses can be computed by finding the poles of the propagator matrix of (H^0, h^0) and then taking their real parts. The inverse of the Higgs propagator matrix can be written as

$$\Delta^{-1} = -i \begin{pmatrix} k^2 - M_{H^0}^2 + \hat{\Sigma}_{H^0}(k^2) & \hat{\Sigma}_{h^0H^0}(k^2) \\ \hat{\Sigma}_{h^0H^0}(k^2) & k^2 - M_{h^0}^2 + \hat{\Sigma}_{h^0}(k^2) \end{pmatrix} . \tag{4.68}$$

The propagator matrix is then given by

$$\Delta = i \begin{pmatrix} \Delta_{H^0}(k^2) & \Delta_{h^0H^0}(k^2) \\ \Delta_{h^0H^0}(k^2) & \Delta_{h^0}(k^2) \end{pmatrix} \tag{4.69}$$

with

$$\begin{aligned} \Delta_{H^0}(k^2) &= \frac{1}{k^2 - M_{H^0}^2 + \hat{\Sigma}_{H^0}(k^2) - \frac{\hat{\Sigma}^2_{h^0H^0}(k^2)}{k^2 - M^2_{h^0} + \hat{\Sigma}_{h^0}(k^2)}} , \\ \Delta_{h^0H^0}(k^2) &= -\frac{\hat{\Sigma}_{h^0H^0}(k^2)}{[k^2 - M_{h^0}^2 + \hat{\Sigma}_{h^0}(k^2)][k^2 - M_{H^0}^2 + \hat{\Sigma}_{H^0}(k^2)] - \hat{\Sigma}^2_{h^0H^0}(k^2)} , \\ \Delta_{h^0}(k^2) &= \frac{1}{k^2 - M_{h^0}^2 + \hat{\Sigma}_{h^0}(k^2) - \frac{\hat{\Sigma}^2_{h^0H^0}(k^2)}{k^2 - M^2_{H^0} + \hat{\Sigma}_{H^0}(k^2)}} . \end{aligned} \tag{4.70}$$

The poles of the matrix Δ can be determined by solving the following equation

$$[k^2 - M_{H^0}^2 + \hat{\Sigma}_{H^0}(k^2)][k^2 - M_{h^0}^2 + \hat{\Sigma}_{h^0}(k^2)] - [\hat{\Sigma}_{h^0H^0}(k^2)]^2 = 0 . \tag{4.71}$$

Due to the complicated momentum dependence, this equation is rather difficult to solve. Hence it is of particular interest to consider approximation methods. One such method is to approximate the renormalized self energies by their values evaluated at zero momentum, namely completely neglect their momentum dependence [108, 109]. This approximation is useful for comparisons with calculations from effective potential approaches [64]. Replacing $\hat{\Sigma}(k^2)$ with $\hat{\Sigma}(0)$, one can easily find the pole positions from Eq. (4.71) as

$$\begin{aligned} k^2_{H^0,h^0} = \frac{1}{2}&(M_{H^0}^2 - \hat{\Sigma}_{H^0}(0) + M_{h^0}^2 - \hat{\Sigma}_{h^0}(0) \\ &\pm \sqrt{(M_{H^0}^2 - \hat{\Sigma}_{H^0}(0) - M_{h^0}^2 + \hat{\Sigma}_{h^0}(0))^2 + 4\hat{\Sigma}^2_{h^0H^0}(0)} . \end{aligned} \tag{4.72}$$

Equivalently, the physical Higgs bosons masses within this approximation can be computed directly by diagonalizing the corrected Higgs boson mass matrix in (H^0, h^0) basis. The diagonalization matrix is given by

$$D(\Delta\alpha) = \begin{pmatrix} \cos\Delta\alpha & -\sin\Delta\alpha \\ \sin\Delta\alpha & \cos\Delta\alpha \end{pmatrix} , \tag{4.73}$$

where the angle $\Delta\alpha$ satisfies

$$\tan\Delta\alpha = \frac{\mathrm{Re}\hat{\Sigma}_{h^0H^0}(0)}{\mathrm{Re}\,k^2_{h^0} - M^2_{H^0} + \mathrm{Re}\hat{\Sigma}_{H^0}(0)} \ . \tag{4.74}$$

Note that the corrected Higgs mass matrix is transformed from (ϕ_1, ϕ_2) to (H^0, h^0) basis by the rotation matrix

$$D(\alpha) = \begin{pmatrix} \cos\alpha & -\sin\alpha \\ \sin\alpha & \cos\alpha \end{pmatrix} \ , \tag{4.75}$$

one can define an effective mixing angle $\alpha_{eff} = \alpha + \Delta\alpha$ so that $D(\alpha_{eff})$ diagonalizes the corrected Higgs mass matrix in the unrotated basis. Thus this zero momentum approximation is also known as the α_{eff} approximation.

Chapter 5

Electroweak Corrections to $h^0 \to WW^*/ZZ^* \to 4$ fermions

Deciphering the mechanism that breaks the electroweak symmetry and generates the masses of fundamental particles is one of the central tasks of current and future colliders. As discussed in previous chapters, in the SM the electroweak symmetry breaking is realized through the Higgs mechanism where the neutral component of an SU(2) complex scalar doublet acquires a non-zero vacuum expectation value. While in the MSSM, two Higgs doublets are required, resulting in five physical Higgs bosons. Two of them are CP-even, one CP-odd, and the other two are charged. The mass of the lightest CP-even Higgs boson is bounded from above by $M_{h^0} \lesssim 135\,\text{GeV}$, including radiative corrections up to two-loop order [78,81,82]. In this mass range, the Higgs boson decays dominantly to $b\bar{b}$ pair. However, this is not a promising channel for the discovery of the Higgs boson at hadron colliders due to the large QCD background [6]. Detailed investigations of other decay modes of the Higgs boson are thus necessary. Such investigations also have further implications. At the LHC at least one MSSM Higgs boson can be discovered over all of the MSSM parameter space. In the region where $\tan\beta$ and M_{A^0} take on moderate values and the region with large M_{A^0} values, only the lightest Higgs boson would be observable [110]. In this case, precision measurements of the Higgs decay properties would indicate if the Higgs boson originates from the SM or from the MSSM and for the latter case allow to derive indirect bounds on other MSSM parameters, e.g. on the mass of the CP-odd Higgs boson [111]. Over a large fraction of the MSSM parameter space more than one Higgs boson would be accessible. Then precision measurements of the lightest Higgs boson at the linear collider can provide valuable information for distinguishing between different soft SUSY-breaking scenarios [111].

For the decay of the SM Higgs boson to four fermions via a gauge boson pair, the complete $\mathcal{O}(\alpha)$ electroweak corrections for leptonic final states have been presented [112], for semi-leptonic and hadronic final states also complete $\mathcal{O}(\alpha_s)$ QCD corrections are available [113]; where the results are improved by corrections beyond $\mathcal{O}(\alpha)$ originating from heavy-Higgs effects and final state radiation.

In this chapter we consider similar processes in the CP-conserving MSSM with real pa-

rameters and compute the $\mathcal{O}(\alpha)$ electroweak corrections to the decay $h^0 \to WW^*/ZZ^* \to 4$ fermions. As discussed in the previous chapter, beyond the lowest order the propagator matrix of the CP-even Higgs bosons receives large radiative corrections, yielding shifts to their tree-level masses. These Higgs propagator corrections are numerically very important, we define an effective amplitude to account for such corrections. In addition, in the presence of the mixing between the two CP-even Higgs bosons, the coupling of the heavy CP-even Higgs boson to gauge bosons should be taken into account as well. Although this coupling is usually suppressed at tree-level, the radiative corrections to this coupling can be numerically relevant due to the presence of the heavy fermions/sfermions in the loop and thus should be taken into account. The numerical results are analyzed in the benchmark scenarios suggested in [114]. We also evaluate the results in the decoupling limit and compared with the corresponding SM results.

5.1 Amplitudes for on-shell Higgs bosons

For processes with external Higgs bosons, the radiative corrections to the Higgs propagators lead to finite wave function normalization factors for these external Higgs bosons. In order to ensure the correct normalization of S-matrix element, these wave function normalization factors have to be taken into account. In the most general case, the decay amplitude of a Higgs boson can be written as

$$\mathcal{M} = \sqrt{Z_i}(\mathcal{M}_i + Z_{ij}\mathcal{M}_j) \ , \tag{5.1}$$

where Z_i and Z_{ij} represent the wave function normalization factors, i, j denote the species of Higgs bosons and $i \neq j$. From the discussion in the previous chapter, the factors Z_i and Z_{ij} are given by

$$\begin{aligned} Z_i &= \frac{1}{1 + \mathrm{Re}\hat{\Sigma}_i'(k^2) - \mathrm{Re}\left(\frac{\hat{\Sigma}_{ij}^2(k^2)}{k^2 - M_j^2 + \hat{\Sigma}_j(k^2)}\right)'}\Big|_{k^2 = M_i'^2} \ , \\ Z_{ij} &= -\frac{\hat{\Sigma}_{ij}(M_i'^2)}{M_i'^2 - M_j^2 + \hat{\Sigma}_j(M_i'^2)} \ , \end{aligned} \tag{5.2}$$

with M_i' being the physical mass of the corresponding Higgs boson. These finite wave function normalization factors, as well as the physical masses of the Higgs bosons can be computed by the program package FeynHiggs [5], in which also the dominant two-loop corrections to the Higgs boson self energies are taken into account. For the processes considered in this chapter, the wave function normalization factors arising from the mixing between the two CP-even Higgs bosons are required.

5.2 Incorporation of gauge boson width

Due to the upper bound of the lightest Higgs boson mass, one of the intermediate gauge bosons in our decay processes can become resonant. We need to implement the width for

the resonant gauge boson in order to avoid the occurrence of singularities when it approaches on-shell. In this section the strategies to implement gauge boson width are briefly illustrated. A short summary of the properties of unstable particles is given in Appendix C, more detailed discussions can be found, e.g. in [115, 116].

5.2.1 Schemes for gauge boson width implementation

For the processes considered in this chapter, the unstable particle involved is the W or Z gauge boson. There are different schemes to implement the width of gauge bosons.

The simplest approach is the so-called fixed-width scheme, in which one replaces the gauge boson propagator $1/(p^2 - M_V^2)$ by $1/(p^2 - M_V^2 + iM_V\Gamma_V)$, namely one adds a constant width term to the propagator. In this scheme the $U(1)$ gauge invariance is respected, while the $SU(2)_L$ gauge invariance is violated [117]. Moreover, the replacement introduces a finite width also to space-like momenta $p^2 < 0$, which is unphysical since the imaginary part of the inverse propagator of gauge boson arises from fermionic loop contribution to its self energy and should vanish for space-like momenta [118, 119]. Such an unphysical width for space-like momenta can be avoided by multiplying the constant width term with a step function $\theta(p^2)$, or more accurately, by using $1/(p^2 - M_V^2 + ip^2\Gamma_V/M_V\theta(p^2))$ [118], i.e. taking into account the energy dependence of the self energy as well. The latter corresponds to the running-width scheme. This running-width scheme, however, violates the $U(1)$ as well as the $SU(2)_L$ gauge invariance.

Another possibility is based on the observation that the violation of gauge invariance is caused by self energy diagrams, thus one can include the minimal set of Feynman diagrams that is necessary to compensate the gauge violation. For gauge bosons, the lowest order widths arise from the imaginary part of fermionic one-loop contribution to their self energies, therefore one should include all other possible fermionic one-loop corrections to restore gauge invariance. This leads to the fermion-loop scheme [117–120]. The selected fermionic contributions form a gauge-independent subset and obey all Ward-identities exactly, even with resummed propagators. Note that in the leading order computation, near the resonance the inverse propagator of gauge boson behaves like $iM_V\Gamma_V$, which is already a one-loop effect. Therefore for the calculation at the next-to-leading order, it is necessary to take into account the next-to-leading order corrections to the width, which are two-loop effects. As fermion loops only yield the lowest order width, this scheme is not applicable to the computation of radiative corrections.

Alternatively one can choose the so-called pole scheme [121–127], in which the scattering amplitude is expanded according to its pole structure. This expansion corresponds to a systematic separation of orders in Γ_V. For processes involving a single resonance, the lowest order amplitude can be expanded as

$$\mathcal{M}_{0,pole} = \frac{W_0(p^2)}{p^2 - M_V^2} \sum_{n=0}^{\infty} \left(\frac{-\Sigma(p^2)}{p^2 - M_V^2} \right)^n + N_0(p^2) \ , \tag{5.3}$$

where $W_0(p^2)$ represents the contribution of production and decay of the unstable particle. Its

dependence on other kinematic variables is omitted here. $N_0(p^2)$ summarizes the contribution of non-resonant diagrams that are regular when the unstable particle approaches on-shell. In the first term a resummation of the geometric series is needed to avoid the occurrence of singularity. The contribution of the first term can be divided into resonant and non-resonant parts by isolating its pole structure after resumming the geometrical series, which yields

$$\frac{W_0(p^2)}{p^2 - M_V^2 + \Sigma(p^2)} = \frac{W_0(M^2)}{p^2 - M^2} \frac{1}{1 + \Sigma'(M^2)} + rem. \,, \tag{5.4}$$

where $M^2 = M_V^2 - iM_V\Gamma_V$ is the pole position and defined by $M^2 - M_V^2 + \Sigma(M^2) = 0$, $rem.$ denotes the remaining non-resonant contribution, which will be combined with the contribution of non-resonant diagrams $N_0(p^2)$. As the pole position can be extracted from experimental data, it is a gauge invariant physical quantity. Therefore the residue at the pole and the non-resonant remnant are separately gauge invariant as well since gauge cancellation can not occur between terms with different pole structure. The finite width can then be incorporated into the pole term without disturbing gauge invariance. The residue at the pole can be evaluated by performing an expansion around the real mass squared M_V^2. The pole scheme can also be used to consistently evaluate the radiative corrections of resonant processes in the region that is far beyond the production threshold of the unstable particle. At one-loop level, one can decompose the scattering amplitude as

$$\mathcal{M}_{1,pole} = \frac{W_1(p^2)}{p^2 - M_V^2} \sum_{n=0}^{\infty} \left(\frac{-\Sigma(p^2)}{p^2 - M_V^2} \right)^n + C_1(p^2) + N_1(p^2) \,, \tag{5.5}$$

where the first term is an analogue of the first term in Eq. (5.3). It arises from the so-called factorizable diagrams, in which the production and subsequent decay process of the unstable particle can be factorized. $W_1(p^2)$ describes the correction to the production or decay of the unstable particle. The second term summarizes the contribution of the non-factorizable diagrams, in which the production and decay processes are linked by a massless particle, such as a photon or gluon. These non-factorizable diagrams are not present at the lowest order. The third term comes from the non-resonant diagrams. The expansion of the first term is analogous to that in the lowest order and can be carried out as before, while the treatment of the second term that results from the non-factorizable diagrams is more complicated since it involves the divergent logarithm $\log(p^2 - M_V^2)$ (or on-shell singularity), as well as the pole term $1/(p^2 - M_V^2)$. The logarithm $\log(p^2 - M_V^2)$ arises when the momentum of the photon that links the production and decay process goes to zero and thus is an infrared singularity. A characteristic feature of the non-factorizable diagrams is that in the case of a single resonance, they develop a linear singularity when the resonant particle goes on-shell and the exchanged photon becomes soft. In the final result the divergent logarithm $\log(p^2 - M_V^2)$ should be replaced by $\log(p^2 - M^2)$. This replacement does not spoil gauge invariance, as a consequence of the fact that these logarithms arise only from scalar loop integrals, which are linearly independent and associated with gauge invariant coefficients [123]. After separating the full scattering amplitude into resonant and non-resonant parts and incorporating the width in the resonant contributions only, a gauge invariant implementation of width is achieved. The drawback of this scheme is that it is not reliable in the threshold region. Below the threshold no resummation should be performed and one encounters the original divergence

when approaching the threshold from below. When the threshold is approached from above, terms of the order of Γ_V/(distance from threshold) may appear and make the expansion around the threshold unreliable [123].

The gauge boson width may also be elegantly incorporated by the complex mass scheme [128]. In this scheme the gauge boson masses are taken as complex quantities defined by the poles of the propagators. Gauge invariance is preserved in this scheme if one introduces the complex gauge boson masses everywhere in the Feynman rules, in particular, also in the definition of the weak mixing angle. This scheme has been successfully applied to the evaluation of radiative corrections within the SM. However, the implementation of this scheme would require independent mass parameters, which is clearly not the case in the MSSM, since, for example, the CP-even Higgs boson masses depend on the gauge boson masses. Thus applying the complex mass scheme to the MSSM can be problematic.

Finally one can incorporate the width according to the factorization scheme [129–131]. In this scheme, for a single resonance, the lowest order amplitude receives a rescaling

$$\mathcal{M}_{0,fact} = \frac{p^2 - M_V^2}{p^2 - M_V^2 + iM_V\Gamma_V}\mathcal{M}_0 = \frac{p^2 - M_V^2}{p^2 - M_V^2 + iM_V\Gamma_V}\left(\frac{R_0(p^2)}{p^2 - M_V^2} + N_0(p^2)\right) , \quad (5.6)$$

where $\mathcal{M}_0$ is the lowest order amplitude before Dyson resummation, and $N_0(p^2)$ denotes the contribution of non-resonant diagrams. Gauge invariance is preserved by this rescaling, but the non-resonant terms are not correctly treated in this scheme since they are simply put to zero on the resonance. The resulting error is, however, of the order of $\mathcal{O}(\Gamma_V/M_V)$. Away from the resonance the rescaling also introduces an error of the order of $\mathcal{O}(\Gamma_V/M_V)$. Thus this prescription leads to a correct result to the leading order both on the resonance and away from it, as long as the non-resonant contributions are not enhanced. At one-loop level, one has to avoid the double-counting from the inclusion of width in the lowest order amplitude. This can be done by subtracting the width term from the self energy correction of the unstable particle, which gives

$$\mathcal{M}_{1,fact} = \frac{p^2 - M_V^2}{p^2 - M_V^2 + iM_V\Gamma_V}\left(\mathcal{M}_1 + \frac{iM_V\Gamma_V}{p^2 - M_V^2}\mathcal{M}_0\right) , \quad (5.7)$$

where $\mathcal{M}_1$ denotes the one-loop amplitude before Dyson resummation. The rescaled amplitude is gauge invariant since the two terms on the right-hand side are separately gauge invariant. As in the lowest order, the non-resonant contributions are treated incorrectly on the resonance, but the corresponding error is again of higher order.

5.3 Lowest order results

We consider the process

$$h^0(k_1) \to WW^*/ZZ^* \to f_1(k_2) + f_2(k_3) + f_3(k_4) + f_4(k_5) , \quad (5.8)$$

where the momenta of the particles are given in the parentheses, while the helicity indices are omitted. The masses of the external light fermions are neglected whenever possible, i.e.

we keep them only as regulators for collinear singularities that arise from collinear photon emission off final state fermions. As already mentioned, only one of the intermediate gauge bosons can become resonant due to the upper bound on the lightest Higgs boson mass. We implement the width of the gauge boson according to the factorization scheme, which yields a simple rescaling at the lowest order

$$\mathcal{M}_{born} = \frac{k_V^2 - M_V^2}{k_V^2 - M_V^2 + iM_V\Gamma_V}\mathcal{M}_{born}(\Gamma_V = 0) \ , \tag{5.9}$$

where k_V is the four-momentum of the resonant gauge boson. $\mathcal{M}_{born}(\Gamma_V = 0)$ denotes the decay amplitude before Dyson resummation. To account for the numerically important Higgs propagator corrections, we use the following effective Born amplitude

$$\begin{aligned}\mathcal{M}_{born}(\Gamma_V = 0) &= \sqrt{Z_{h^0}}(\mathcal{M}^0_{h^0}(\Gamma_V = 0) + Z_{h^0H^0}\mathcal{M}^0_{H^0}(\Gamma_V = 0)) \\ &= \sqrt{Z_{h^0}}\mathcal{M}^0_{h^0}(\Gamma_V = 0)(1 + \cot(\beta - \alpha)Z_{h^0H^0}) \ ,\end{aligned} \tag{5.10}$$

where $\mathcal{M}^0_{h^0}(\Gamma_V = 0)$ and $\mathcal{M}^0_{H^0}(\Gamma_V = 0)$ denote the respective tree-level decay amplitude of h^0 and H^0 before Dyson resummation, and the Z factors are defined in Eq.(5.2). In the second row we have written the decay amplitude $\mathcal{M}^0_{H^0}$ in terms of $\mathcal{M}^0_{h^0}$. The lowest order Feynman diagram including Higgs propagator corrections is shown in Fig. 5.1.

We start from the leptonic decay processes

$$h^0(k_1) \to WW^* \to e^-(k_2) + \bar{\nu}_e(k_3) + \mu^+(k_4) + \nu_\mu(k_5) \tag{5.11}$$

and

$$h^0(k_1) \to ZZ^* \to e^-(k_2) + e^+(k_3) + \mu^+(k_4) + \mu^-(k_5) \ . \tag{5.12}$$

For the first process, the tree-level amplitude reads

$$\begin{aligned}\mathcal{M}^0_{h^0}(\Gamma_W = 0) = &\frac{2\pi\alpha\, eM_W \sin(\beta - \alpha)}{s_W^3}\frac{1}{k_+^2 - M_W^2} \\ &\times \frac{1}{k_-^2 - M_W^2}[\bar{u}_{e^-}(k_2)\gamma_\rho\omega_- v_{\bar{\nu}_e}(k_3)][\bar{u}_{\nu_\mu}(k_5)\gamma^\rho\omega_- v_{\mu^+}(k_4)] \ ,\end{aligned} \tag{5.13}$$

and for the second

$$\begin{aligned}\mathcal{M}^0_{h^0}(\Gamma_Z = 0) = &\frac{\pi\alpha\, eM_W \sin(\beta - \alpha)}{c_W^4 s_W^3}\frac{1}{k_+^2 - M_Z^2}\frac{1}{k_-^2 - M_Z^2} \\ &\times [(-1 + 2s_W^2)\bar{u}_{e^-}(k_2)\gamma_\rho\omega_- v_{e^+}(k_3) + 2s_W^2\bar{u}_{e^-}(k_2)\gamma_\rho\omega_+ v_{e^+}(k_3)] \\ &\times [(-1 + 2s_W^2)\bar{u}_{\mu^-}(k_5)\gamma^\rho\omega_- v_{\mu^+}(k_4) + 2s_W^2\bar{u}_{\mu^-}(k_5)\gamma^\rho\omega_+ v_{\mu^+}(k_4)] \ ,\end{aligned} \tag{5.14}$$

where we have introduced the variables $k_\pm$ with $k_+ = k_2 + k_3, k_- = k_4 + k_5$ and $\omega_\pm = \frac{1}{2}(1 \pm \gamma_5)$. These decay amplitudes differ from their SM counterparts only by a factor of $\sin(\beta - \alpha)$.

The lowest order partial decay width is then given by

$$\Gamma_{born} = \frac{1}{2M'_{h^0}}\int \sum_{pol} |\mathcal{M}_{born}|^2 d\Phi \ , \tag{5.15}$$

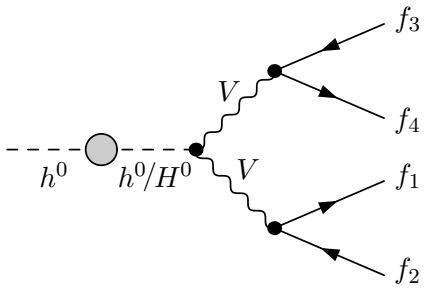

Figure 5.1: Lowest order diagram with Higgs propagator corrections indicated by the bubble.

with M'_{h^0} denoting the physical mass of the lightest Higgs boson, the squared matrix element is summed over the final state polarizations and the phase space factor is given by

$$d\Phi = \left(\prod_{i=2}^{5} \frac{d^3\mathbf{k}_i}{(2\pi)^3\ 2k_i^0} \right) (2\pi)^4 \delta^{(4)}(k_1 - \sum_{i=2}^{5} k_i) \ . \tag{5.16}$$

5.4 Virtual corrections

The evaluation of virtual corrections involves several additional issues. As in the lowest order amplitude, we use an effective one-loop amplitude to account for the wave function normalization factors for the external Higgs boson. In the presence of the mixing between Higgs bosons, the corrections to the coupling of H^0 to gauge bosons from loops involving fermions and sfermions, especially from those involving the third generation fermions and sfermions may yield sizeable contributions, since they involve potentially large Yukawa couplings, Y_t, Y_b, Y_τ, and the couplings to down-type fermions/sfermions can be enhanced at large $\tan\beta$ values. In addition, the photonic one-loop diagrams may contain not only soft and collinear singularities, but also on-shell singularities. The soft singularities originate from the diagrams with a virtual photon exchanged between two external charged particles, while collinear singularities arise if a massless external particle splits into two massless internal particles. On-shell singularities are closely related to the presence of resonant gauge boson propagator in the loop and have to be cured by including the finite width of gauge boson. For this purpose, the loop integrals that contribute to these on-shell singularities are computed analytically. As before, the final state fermion masses are neglected whenever possible in the evaluation of loop integrals. If the contribution of real photon emission processes is taken into account, the infrared singularities will drop out.

According to the factorization scheme, at one-loop level the gauge boson width can be incorporated as follows

$$\mathcal{M}_{loop} = \frac{k_V^2 - M_V^2}{k_V^2 - M_V^2 + iM_V\Gamma_V} \mathcal{M}_{loop}(\Gamma_V = 0) + \frac{i\,\mathrm{Im}\Sigma_V^T(M_V^2)}{k_V^2 - M_V^2} \mathcal{M}_{born}$$

$$= \frac{k_V^2 - M_V^2}{k_V^2 - M_V^2 + iM_V\Gamma_V}\mathcal{M}_{loop,no\ r.s.}(\Gamma_V = 0)$$
$$- \left(\frac{\Sigma_V^T(k_V^2) - \Sigma_V^T(M_V^2)}{k_V^2 - M_V^2} + \delta Z_V\right)\mathcal{M}_{born}\ , \tag{5.17}$$

where Σ_V^T denotes the transverse part of vector boson self energy and δZ_V the corresponding field renormalization constant. The $\mathcal{M}_{loop,no\ r.s.}$ term in the second row represents the one-loop corrections excluding the self energy corrections to the resonant gauge boson. The term involving the imaginary part of the vector boson self energy in the first line is required to avoid the double-counting from the inclusion of finite width in the lowest order amplitude, it is absorbed into the self energy corrections, yielding the last term in the above equation.

The effective amplitude $\mathcal{M}_{loop}(\Gamma_V = 0)$ can be written as

$$\mathcal{M}_{loop}(\Gamma_V = 0) = \sqrt{Z_{h^0}}\left(\mathcal{M}^1_{h^0}(\Gamma_V = 0) + Z_{h^0H^0}\mathcal{M}^1_{H^0\,3rd}(\Gamma_V = 0)\right)\ , \tag{5.18}$$

where the superscript 1 indicates the one-loop amplitude, and we include as well the corrections to the coupling of H^0 to gauge bosons from the third generation fermions and sfermions $\mathcal{M}^1_{H^0\,3rd}$, since they can potentially yield sizeable contributions. Note that only $\mathcal{M}^1_{h^0}$ term involves gauge boson self energy corrections, thus we can replace $\mathcal{M}_{born}$ in Eq. (5.17) by

$$\mathcal{M}'_{born} = \mathcal{M}_{born}|_{\mathcal{M}^0_{H^0}=0} \tag{5.19}$$

without introducing any double-counting. The squared matrix element can be written as

$$|\mathcal{M}|^2 \simeq |\mathcal{M}_{born}|^2 + 2\mathrm{Re}(\mathcal{M}^*_{born}\mathcal{M}_{loop}) + |\sqrt{Z_{h^0}}Z_{h^0H^0}\mathcal{M}^1_{H^0\,3rd}|^2\ , \tag{5.20}$$

where we also keep the square of $\mathcal{M}^1_{H^0\,3rd}$ term. Note that we can not simply include the square of the complete one-loop amplitude, since the one-loop photonic diagrams involve infrared singularities. In this work the Feynman diagrams are generated by the program package FeynArts [132]. FormCalc [133] and LoopTools [133, 134] are then used to algebraically simplify the amplitudes and evaluate the one-loop integrals that do not involve on-shell singularities.

In the following we describe in detail the computation of virtual corrections to the decay processes given in Eqs. (5.11) and (5.12).

5.4.1 Virtual corrections to $h^0 \to WW^* \to 4l$

The virtual corrections arise from the photonic, SM-like, genuine SUSY and counter term diagrams. The photonic diagrams are the same as in the SM, examples of these diagrams are shown in Fig. 5.2. Such photonic diagrams might contain infrared as well as on-shell singularities. Note that the diagrams with a photon exchanged between the two intermediate W bosons do not contribute to the on-shell singularities, due to the fact that only one of these W bosons can be at resonance. The on-shell singularities have to be rendered finite by incorporating the gauge boson width. In the factorization scheme, power counting tells us that

only scalar integrals resulting from the virtual photonic diagrams can contribute to the on-shell singularities. We will evaluate these scalar integrals analytically. The SM-like diagrams consist of diagrams involving other SM particles and the MSSM Higgs bosons in the loop. Examples of these diagrams are depicted in Fig. 5.3. In the decoupling limit $M_{A^0} \gg M_Z$, the lightest MSSM Higgs boson behaves like a SM Higgs boson and all other heavy Higgs boson decouple, thus the contribution of these diagrams will approach the corresponding SM contribution. This fact can be used as a useful check on our computation. The loop diagrams involving all other SUSY particles constitute the genuine SUSY diagrams, some representative of them are shown in Fig. 5.4. The counter term diagrams are depicted in Fig. 5.5.

The structure of the counter term contribution in the first four diagrams of Fig. 5.5 is as in the SM (see ref. [101]), while the last diagram yields (see e.g. [135])

$$\begin{aligned}
\mathcal{M}^{CT}_{h^0} &= \mathcal{M}^0_{h^0}\Big[\delta Z_e + \delta Z_W + \frac{1}{2}\frac{\delta M_W^2}{M_W^2} + \frac{\delta s_W}{s_W} + \frac{\cos(\beta-\alpha)}{\sin(\beta-\alpha)}\Big(\cos^2\beta\delta\tan\beta \\
&\quad + \frac{1}{2}\delta Z_{H^0h^0}\Big) + \frac{1}{2}\delta Z_{h^0h^0}\Big] \ , \\
\mathcal{M}^{CT}_{H^0} &= \mathcal{M}^0_{H^0}\Big[\delta Z_e + \delta Z_W + \frac{1}{2}\frac{\delta M_W^2}{M_W^2} + \frac{\delta s_W}{s_W} + \frac{\sin(\beta-\alpha)}{\cos(\beta-\alpha)}\Big(-\cos^2\beta\delta\tan\beta \\
&\quad + \frac{1}{2}\delta Z_{h^0H^0}\Big) + \frac{1}{2}\delta Z_{H^0H^0}\Big]
\end{aligned} \tag{5.21}$$

with

$$\mathcal{M}^0_{h^0,H^0} = \frac{k_V^2 - M_V^2}{k_V^2 - M_V^2 + iM_V\Gamma_V}\mathcal{M}^0_{h^0,H^0}(\Gamma_V = 0) \ . \tag{5.22}$$

The Higgs field renormalization constants $\delta Z_{h^0h^0}$, $\delta Z_{h^0H^0}$, $\delta Z_{H^0h^0}$, $\delta Z_{H^0H^0}$ and the counter term $\delta\tan\beta$ have been given by Eqs. (4.61), (4.62) and (4.63) in the previous chapter, the remaining counter terms are determined in the on-shell scheme as [101]

$$\begin{aligned}
\delta Z_e &= \frac{1}{2}\Sigma'\gamma(0) - \frac{s_W}{c_W}\frac{\Sigma^T_{\gamma Z}(0)}{M_Z^2} \ , \\
\delta Z_W &= -\mathrm{Re}\,\Sigma'^T_W(M_W^2) \ , \\
\delta M_W^2 &= \mathrm{Re}\,\Sigma^T_W(M_W^2) \ , \\
\delta M_Z^2 &= \mathrm{Re}\,\Sigma^T_Z(M_Z^2) \ , \\
\frac{\delta s_W}{s_W} &= \frac{1}{2}\frac{c_W^2}{s_W^2}\Big(\frac{\delta M_Z^2}{M_Z^2} - \frac{\delta M_W^2}{M_W^2}\Big) \ ,
\end{aligned} \tag{5.23}$$

where the prime indicates the derivative and the superscript T the transverse part of the corresponding self energy.

In the photonic diagrams the on-shell singularities can arise if the exchanged photon becomes soft. Now we turn to the extraction of these singularities from the virtual photonic contributions.

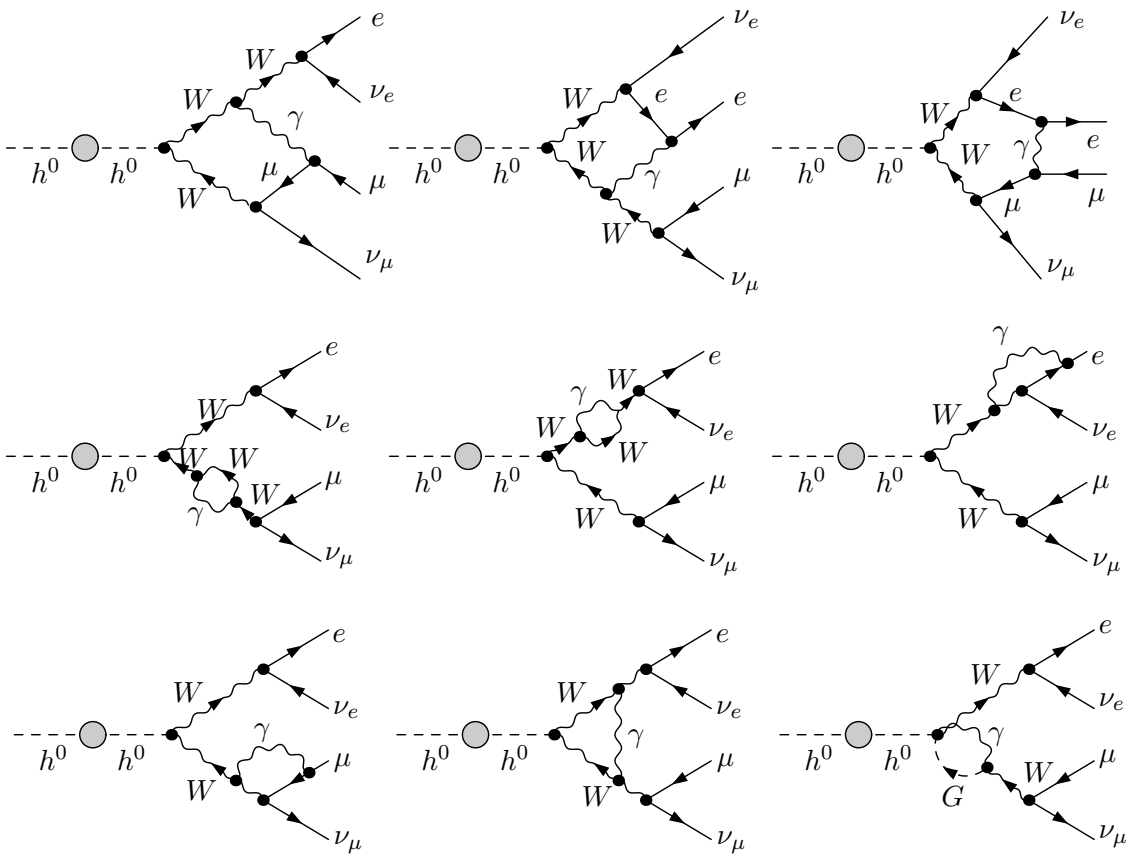

Figure 5.2: Examples of photonic diagrams for the process $h^0 \to WW^* \to 4l$.

On-shell singular virtual contributions

As previously mentioned, in the factorization scheme only scalar integrals resulting from the photonic diagrams can contribute to the on-shell singularities. In this section we calculate the relevant scalar integrals and extract from them the on-shell singular virtual contributions. The final state fermion masses are neglected unless they have to be kept as regulators for the collinear singularities. The scalar loop integrals are computed for zero gauge boson width. A finite width is inserted afterwards wherever a singularity arises when the resonant gauge boson approaches on-shell.

For the notation of the one-loop integrals, we follow the convention of [136]. The virtual 3-, 4- and 5-point functions are defined as follows

$$C_0(p_1, p_2, m_0, m_1, m_2) = \frac{1}{i\pi^2} \int d^4q \, \frac{1}{N_0 N_1 N_2} \, ,$$
$$D_{0,\mu}(p_1, p_2, p_3, m_0, m_1, m_2, m_3) = \frac{1}{i\pi^2} \int d^4q \, \frac{1, q_\mu}{N_0 N_1 N_2 N_3} \, , \tag{5.24}$$

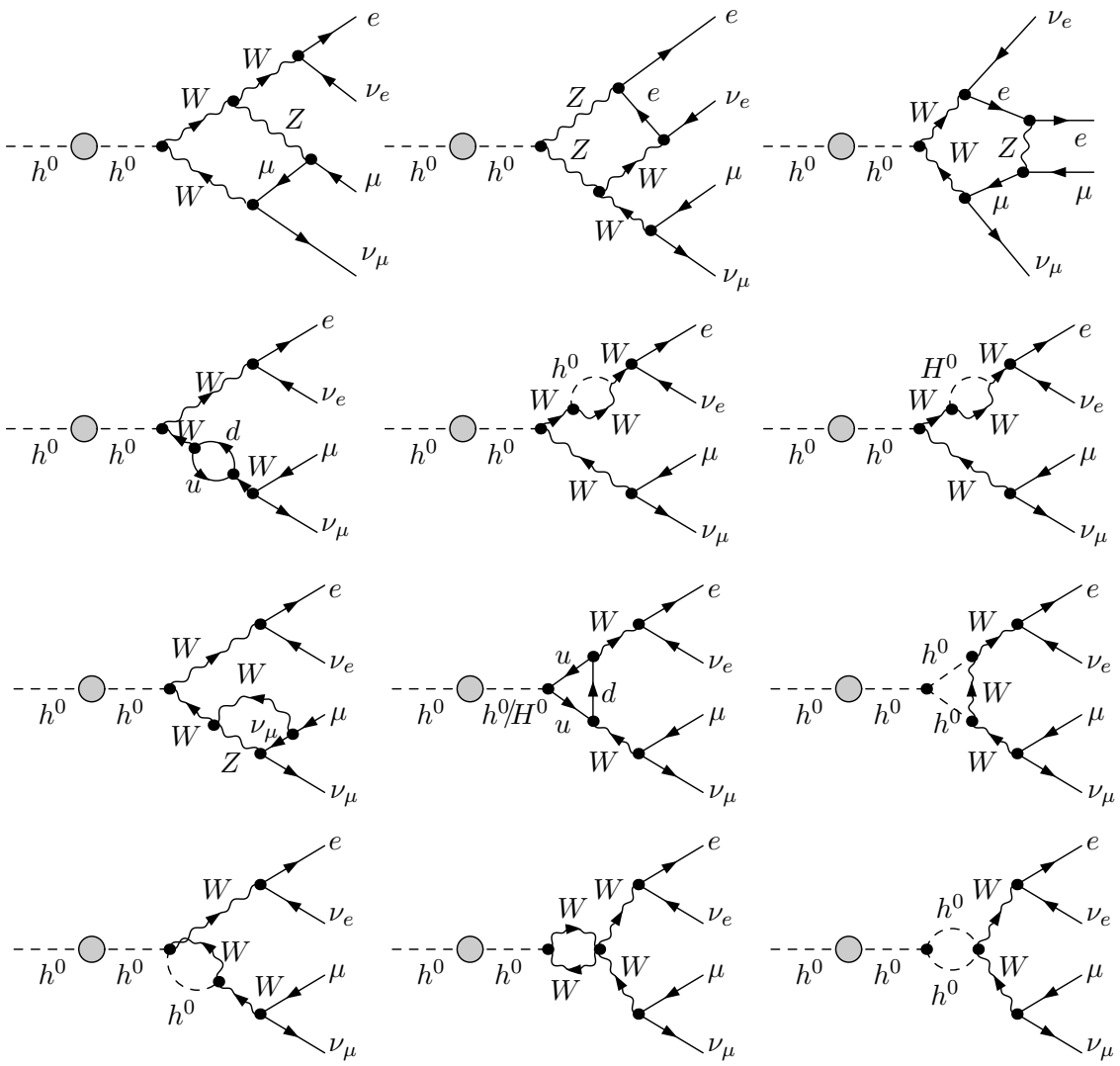

Figure 5.3: Examples of SM-like diagrams for the process $h^0 \to WW^* \to 4l$.

and

$$E_{0,\mu}(p_1, p_2, p_3, p_4, m_0, m_1, m_2, m_3, m_4) = \frac{1}{i\pi^2} \int d^4q \, \frac{1, q_\mu}{N_0 N_1 N_2 N_3 N_4} \ , \tag{5.25}$$

where the denominators are given by

$$N_0 = q^2 - m_0^2 + i\epsilon, \qquad N_i = (q + p_i)^2 - m_i^2 + i\epsilon, \qquad i = 1...4 \tag{5.26}$$

with the infinitesimal imaginary part $i\epsilon$ ($\epsilon > 0$).

The vector integrals can be decomposed in terms of the momenta appearing in the denominators and coefficient functions, for example

$$E_\mu = \sum_{i=1}^{4} p_{i_\mu} E_i \ . \tag{5.27}$$

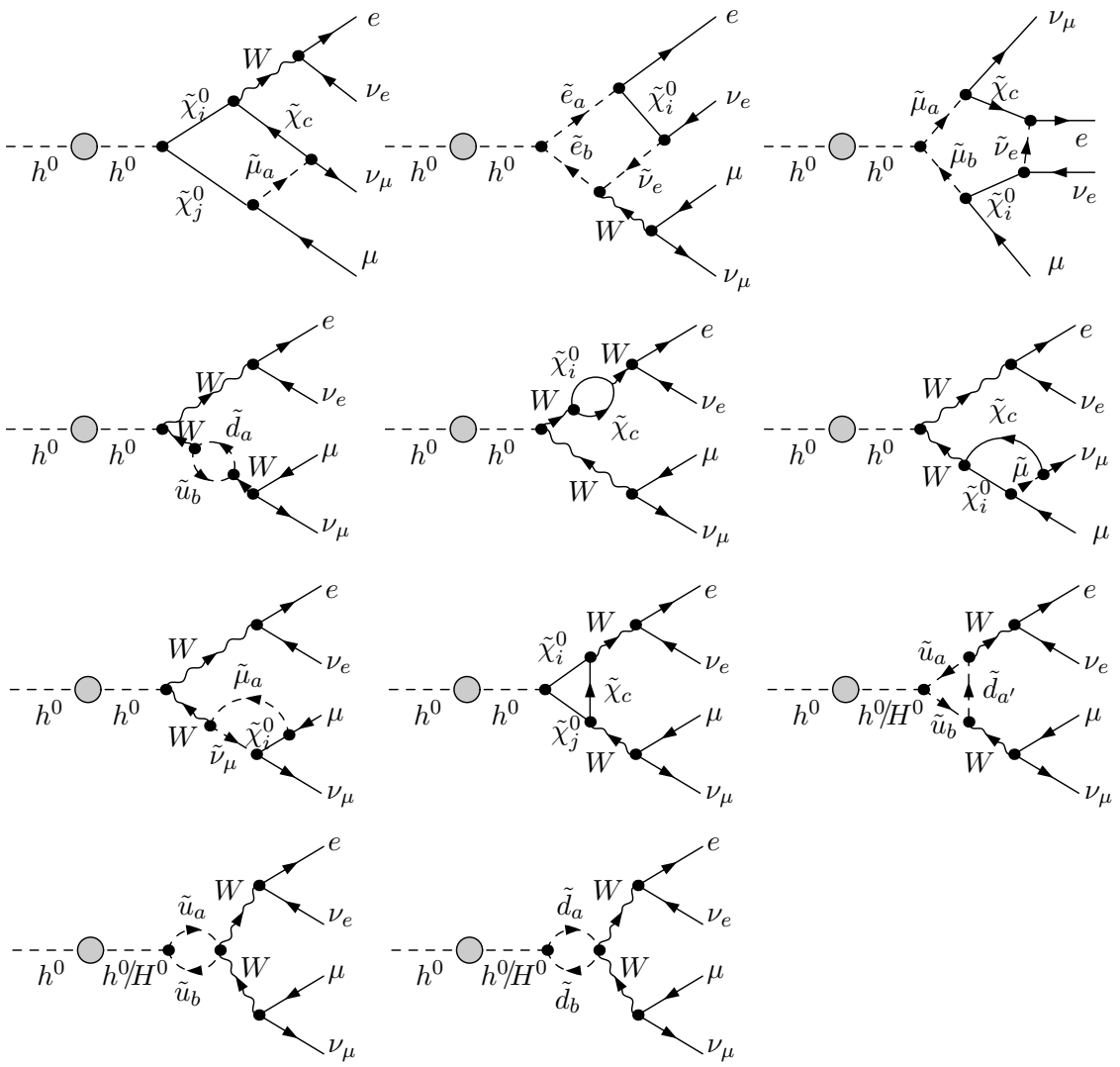

Figure 5.4: Examples of genuine SUSY diagrams for the process $h^0 \to WW^* \to 4l$.

Our evaluation of on-shell singular scalar integrals is based on the observation that only one of the intermediate gauge bosons can be resonant due to the upper bound of the mass of h^0. Therefore it is possible to make a decomposition of these scalar integrals by separating from them the non-resonant gauge boson propagator. This decomposition leaves the on-shell singular parts of the integrals intact but simplifies the extraction of such singularities from these integrals. We now illustrate this procedure by computing the on-shell singular scalar 5-point integral.

Assuming the gauge boson with four-momentum k_- is at resonance (the case that the other gauge boson is resonant can be obtained by simple substitution with the help of the explicit results for the integrals in Appendix B), the scalar 5-point integral arising from the photonic pentagon diagram in Fig. 5.2 can be decomposed by separating the non-resonant gauge boson propagator as follows (for convenience, we still use M_V to label the gauge boson mass in the

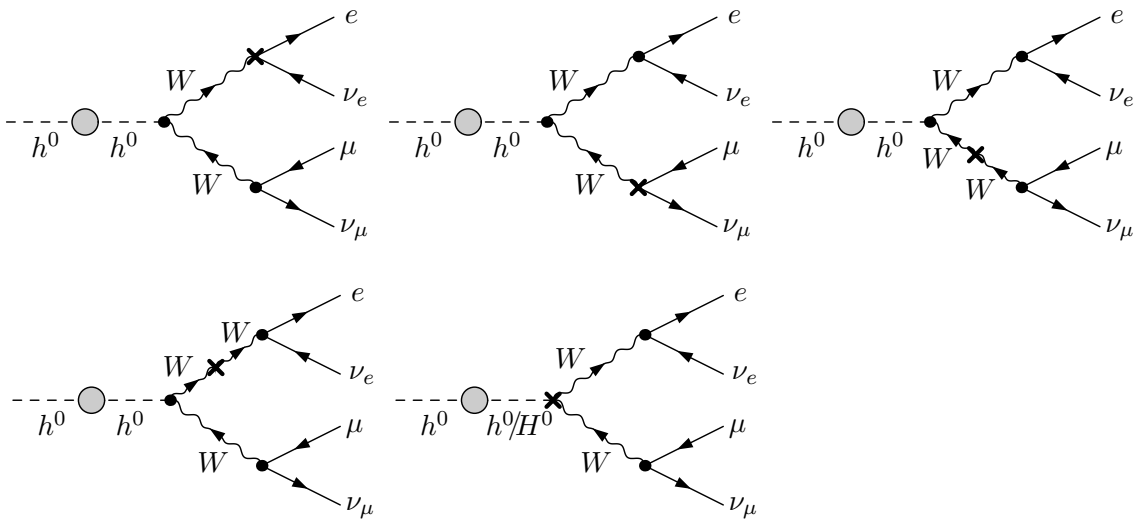

Figure 5.5: Counter term diagrams for the process $h^0 \to WW^* \to 4l$.

integrals. It should be replaced by M_W in the final result)

$$
\begin{aligned}
&E_0(-k_2,-k_+,k_-,k_4,\lambda,m_e,M_V,M_V,m_\mu)\\
&=\frac{1}{i\pi^2}\int d^4q \frac{1}{(q^2-\lambda^2)((q-k_2)^2-m_e^2)((q+k_4)^2-m_\mu^2)((q-k_+)^2-M_V^2)((q+k_-)^2-M_V^2)}\\
&=\frac{1}{i\pi^2}\,\frac{1}{k_+^2-M_V^2}\int d^4q \frac{1}{(q^2-\lambda^2)((q-k_2)^2-m_e^2)((q+k_4)^2-m_\mu^2)((q+k_-)^2-M_V^2)}\\
&+\frac{1}{i\pi^2}\,\frac{1}{k_+^2-M_V^2}\int d^4q \frac{-q^2+2q\cdot k_+}{q^2((q-k_2)^2-m_e^2)((q+k_4)^2-m_\mu^2)((q-k_+)^2-M_V^2)((q+k_-)^2-M_V^2)}\\
&=\frac{1}{k_+^2-M_V^2}\Big\{D_0(-k_2,k_-,k_4,\lambda,m_e,M_V,m_\mu)-D_0(k_2+k_4,-k_3,k_2+k_-,m_e,m_\mu,M_V,M_V)\\
&-S_{23}E_1(-k_2,-k_+,k_-,k_4,0,m_e,M_V,M_V,m_\mu)\\
&+(S_{24}+S_{34})E_2(-k_2,-k_+,k_-,k_4,0,m_e,M_V,M_V,m_\mu)\\
&-2S_{23}E_3(-k_2,-k_+,k_-,k_4,0,m_e,M_V,M_V,m_\mu)\\
&+(S_{24}+S_{25}+S_{34}+S_{35})E_4(-k_2,-k_+,k_-,k_4,0,m_e,M_V,M_V,m_\mu)\Big\}\,,
\end{aligned}
\tag{5.28}
$$

where $S_{ij}=(k_i+k_j)^2$. In this decomposition we have introduced a fictitious photon mass λ to regularize the soft singularity. This is allowed since Ward identities are still preserved in the presence of the photon mass. While the second scalar 4-point function in the curly bracket is finite, the first one contains both the singular logarithm $\ln(k_-^2-M_V^2+i\epsilon)$ and the resonant factor $1/(k_-^2-M_V^2)$, as well as the soft singularities, as we will see from Eq. (5.29) below. The coefficient functions E_i do not contain soft singularity. They may contain the singular logarithm $\ln(k_-^2-M_V^2+i\epsilon)$, but not the resonant factor $1/(k_-^2-M_V^2)$. Therefore it follows from Eqs. (5.17), (5.28) and (5.29) that when the gauge boson approaches on-shell, only the first scalar 4-point integral in Eq. (5.28) gives rise to a singular logarithm $\ln(k_-^2-M_V^2+i\epsilon)$.

Consequently, to incorporate the width of gauge boson we only need to calculate this 4-point integral instead of the original 5-point integral. The analytical result of this scalar 4-point integral is worked out with the help of ref. [137, 138] and listed as follows

$$\begin{aligned} D_0(-k_2,k_-,k_4,\lambda,m_e,M_V,m_\mu) = \frac{1}{S_{24}(k_-^2-M_V^2)}\Big\{ &-\mathrm{Li}_2\left(-\frac{S_{25}+k_-^2-M_V^2}{S_{24}}\right) \\ &+2\ln\left(-\frac{S_{24}}{m_e m_\mu - i\epsilon}\right)\ln\left(\frac{M_V^2-k_-^2}{\lambda M_V}-i\epsilon\right) \\ &-\ln^2\left(\frac{m_\mu}{M_V}\right)-\ln^2\left(\frac{M_V^2-k_-^2-S_{24}-S_{25}}{m_e M_V}-i\epsilon\right) \\ &-\frac{\pi^2}{3}\Big\}\,, \end{aligned} \tag{5.29}$$

where $\mathrm{Li}_2(x)$ is the usual dilogarithm

$$\mathrm{Li}_2(x) = -\int_0^x \frac{dt}{t}\ln(1-t)\,. \tag{5.30}$$

The singular logarithm $\ln(k_-^2 - M_V^2 + i\epsilon)$ has to be replaced by $\ln(k_-^2 - M_V^2 + iM_V\Gamma_V)$ in the final result, as will be done later on for other scalar integrals involving this singular logarithm. This replacement, as argued in previous sections, does not disturb gauge invariance.

The photonic box diagrams in Fig. 5.2 involve scalar 4-point integrals that might contribute to the on-shell singularities. These integrals can be decomposed analogously by separating the non-resonant gauge boson propagator, yielding

$$\begin{aligned} &D_0(-k_4,k_+,-k_-,0,m_\mu,M_V,M_V) \\ &= \frac{1}{k_+^2-M_V^2}\Big\{C_0(-k_4,-k_-,0,m_\mu,M_V) - C_0(-k_5,k_4+k_+,m_\mu,M_V,M_V) \\ &+ (S_{24}+S_{34})D_1(-k_4,k_+,-k_-,0,m_\mu,M_V,M_V) \\ &+ (S_{24}+S_{34}+S_{25}+S_{35})D_2(-k_4,k_+,-k_-,0,m_\mu,M_V,M_V) \\ &- 2S_{23}D_3(-k_4,k_+,-k_-,0,m_\mu,M_V,M_V)\Big\}\,, \\ &D_0(-k_2,k_-,-k_+,0,m_e,M_V,M_V) \\ &= \frac{1}{k_+^2-M_V^2}\Big\{C_0(-k_2,k_-,0,m_e,M_V) - C_0(-k_3,k_2+k_-,m_e,M_V,M_V) \\ &- S_{23}D_1(-k_2,k_-,-k_+,0,m_e,M_V,M_V) - 2S_{23}D_2(-k_2,k_-,-k_+,0,m_e,M_V,M_V) \\ &+ (S_{24}+S_{34}+S_{25}+S_{35})D_3(-k_2,k_-,-k_+,0,m_e,M_V,M_V)\Big\}\,. \end{aligned} \tag{5.31}$$

These integrals do not involve soft singularities. Note that in our case, only one of these two 4-point integrals can yield on-shell singular contributions. Here we do not give the analytical expressions for the on-shell singular scalar 3-point functions in Eq. (5.31), they are collected in Appendix B. For the evaluation of other loop integrals, the general strategies have been described, e.g. in [101, 136, 139–141].

With these decompositions, the on-shell singular virtual contributions can be extracted straightforwardly. Note that in the contribution of photonic box and pentagon diagrams only scalar integrals contain soft singularities. Therefore the analytical results of these scalar integrals can also be used to extract the soft singularities from virtual contributions and allow us to analytically check their cancellation when combining with real corrections. The soft and on-shell singular terms arising from the photonic box and pentagon diagrams can be written in terms of the lowest order amplitude and a correction factor that contains these singularities

$$\begin{aligned}\mathcal{M}_{h^0\,b,p}^{sing} &= \mathcal{M}_{h^0}^0 \delta_{b,p}^{sing} = \mathcal{M}_{h^0}^0 \Big\{ -\frac{\alpha}{2\pi}\Big(\frac{(S_{24}+S_{34})(k_-^2 - M_V^2)}{k_+^2 - M_V^2} C_0(-k_4, -k_-, 0, m_\mu, M_V) \\ &\quad + (S_{24}+S_{25}) C_0(-k_2, k_-, 0, m_e, M_V) \\ &\quad + S_{24}(k_-^2 - M_V^2) D_0(-k_2, k_-, k_4, \lambda, m_e, M_V, m_\mu)\Big)\Big\} \,. \end{aligned} \tag{5.32}$$

The photonic vertex and self energy diagrams also contribute to the soft and on-shell singularities. These contributions originate from the field renormalization constants of the external charged fermions, the photonic corrections to the Wff' vertex and the W boson self energy. The field renormalization constants of W boson give rise to soft singular contributions as well. However, they only appear in intermediate stages and cancel out in the full matrix element. Owing to the presence of one additional resonant propagator, the photonic self energy insertion gives rise to a correction factor to the lowest order amplitude of the form $B_0(k_-^2, 0, M_V)/(k_-^2 - M_V^2)$. After the W boson mass renormalization the correction factor is modified to be proportional to

$$\frac{B_0(k_-^2, 0, M_V) - B_0(M_V^2, 0, M_V)}{k_-^2 - M_V^2} = -\frac{1}{k_-^2} \ln\left(1 - \frac{k_-^2}{M_V^2} - i\epsilon\right) \,, \tag{5.33}$$

which is clearly on-shell singular and has to be regularized by the width of W boson. The photonic vertex correction gives rise to a correction factor involving the on-shell singular scalar 3-point integral. Putting all these together, one finds the following correction factor that contains the soft and on-shell singularities from the photonic vertex and self energy diagrams

$$\begin{aligned}\mathcal{M}_{h^0\,v,s}^{sing} &= \mathcal{M}_{h^0}^0 \delta_{v,s}^{sing} = \mathcal{M}_{h^0}^0 \Big\{ \frac{\alpha}{2\pi}\Big(k_+^2 C_0(-k_2, -k_+, 0, m_e, M_V) \\ &\quad + k_-^2 C_0(-k_4, -k_-, 0, m_\mu, M_V)\Big) + \frac{1}{2}(\delta Z_e^L + \delta Z_\mu^L)_{\rm IR} \\ &\quad - \frac{\alpha}{4\pi} \frac{5k_-^2 - M_V^2}{k_-^2} \ln\left(1 - \frac{k_-^2}{M_V^2} - i\epsilon\right)\Big\} \,, \end{aligned} \tag{5.34}$$

where the subscript IR denotes the infrared singular part of the field renormalization costants, whose expression can be found, e.g. in [101]. As before, the width of W boson should be included in the on-shell singular logarithms. The correction factors defined in Eq. (5.32) and (5.34) include all the soft singularities from virtual one-loop diagrams. The collinear singularities, however, are not fully contained in these correction factors, since the tensor integrals that are not accounted for in these factors, contain collinear singularities as well.

In the case that the other gauge boson becomes resonant, the correction factor resulting from the box and pentagon diagrams becomes

$$\begin{aligned}\mathcal{M}_{h^0\,b,p}^{\;sing} = \mathcal{M}_{h^0}^0 \delta_{b,p}^{sing} = \mathcal{M}_{h^0}^0 \Big\{ -\frac{\alpha}{2\pi}\Big(&\frac{(S_{24}+S_{25})(k_+^2 - M_V^2)}{k_-^2 - M_V^2} C_0(-k_2, -k_+, 0, m_e, M_V) \\ &+ (S_{24}+S_{34}) C_0(-k_4, k_+, 0, m_\mu, M_V) \\ &+ S_{24}(k_+^2 - M_V^2) D_0(-k_2, -k_+, k_4, \lambda, m_e, M_V, m_\mu)\Big)\Big\} \; . \end{aligned} \tag{5.35}$$

The correction factor from the self energy and vertex diagrams can be obtained from Eq. (5.34) by replacing k_-^2 with k_+^2 in the last term.

Now we are able to extract the on-shell singular virtual contributions from Eqs. (5.32), (5.34) and the results of the scalar integrals in Appendix B. This gives rise to the following correction factor after incorporating the width of the resonant gauge boson

$$\begin{aligned}\mathcal{M}_{h^0 on-shell,sing} = \mathcal{M}_{h^0}^0 \frac{\alpha}{2\pi} \Big\{ &\ln\Big(\frac{k_-^2}{M_V^2}\Big) + \ln\Big(\frac{S_{24}+S_{25}}{S_{24}}\Big)^2 - \frac{5k_-^2 - M_V^2}{2k_-^2}\Big\} \\ &\times \ln\Big(1 - \frac{k_-^2}{M_V^2} - i\frac{\Gamma_V}{M_V}\Big) \; . \end{aligned} \tag{5.36}$$

In the case that the other gauge boson becomes resonant, the correction factor describing on-shell singular virtual contributions can be obtained by making the following replacement in the above equation

$$S_{25} \to S_{34}, \qquad k_-^2 \to k_+^2 \; . \tag{5.37}$$

Soft and collinear singular virtual contributions

For the investigated process the photonic diagrams do not build a gauge invariant subset by themselves and their contributions are UV divergent. However, one can extract the infrared singularities and on-shell logarithms from them and combine with the real photon bremsstrahlung to build the QED-like corrections. The soft and collinear singular contributions from the virtual corrections can be extracted by making use of the well-known Kinoshita-Lee-Nauenberg (KLN) theorem [142], according to which the soft and collinear singularities are canceled out between the real and virtual corrections for sufficiently inclusive quantities. In the decay of h^0 to leptons, there is no initial state radiation of photons. The singular parts of the virtual corrections are exactly given by the singularities in the final state photon bremsstrahlung, but with opposite sign, which can be computed, e.g. with the dipole subtraction approach [143–146]. Following [146], the soft and collinear singular parts of the virtual contributions can be defined as

$$d\Gamma_{virt,sing} = d\Gamma_{born} \frac{\alpha}{2\pi} \sum_{i=2}^{5} \sum_{j=i+1}^{5} Q_i\, Q_j \Big(L(S_{ij}, m_i^2) + L(S_{ij}, m_j^2) - \frac{2\pi^2}{3} + 3 \Big) \; , \tag{5.38}$$

where $d\Gamma_{born}$ is the lowest order decay width, Q_i denote the charge of final state fermions, and the function $L(S_{ij}, m_i^2)$ is given by

$$L(S_{ij}, m_i^2) = \ln\left(\frac{m_i^2}{S_{ij}}\right)\ln\left(\frac{\lambda^2}{S_{ij}}\right) + \ln\left(\frac{\lambda^2}{S_{ij}}\right) - \frac{1}{2}\ln^2\left(\frac{m_i^2}{S_{ij}}\right) + \frac{1}{2}\ln\left(\frac{m_i^2}{S_{ij}}\right) , \tag{5.39}$$

Note that when computing these contributions, the soft and collinear singular parts that arise from the virtual photonic corrections to the mixed tree-level amplitude, i.e. to the second term in Eq. (5.10) should be excluded, since they are not included in Eq. (5.20). The definition of the soft and collinear singular virtual contribution is, of course, not unique, since finite terms can be redistributed between the singular and finite contributions. An alternative definition has been used in [147]. It differs from the definition used here only by finite terms.

The IR singular and on-shell singular virtual contributions combined with the contribution of real bremsstrahlung yield the QED-like correction. As previously mentioned, the soft singularities from photonic virtual diagrams are included in the correction factors $\delta_{b,p}^{sin}$ and $\delta_{v,s}^{sin}$ defined in Eqs. (5.32) and (5.34), subtracting from them the virtual singular factor in Eq. (5.38) (note that one has to take twice of the real part of the correction factor in (5.32) and (5.34)), the remnant must be free of soft singularities. This provides an analytic check on the cancellation of soft singularities. The cancellation of collinear singularities is, however, checked numerically since the collinear singularities appear not only in scalar integrals but also in tensor ones. The contribution of the latter is not accounted for in these correction factors.

5.4.2 Virtual corrections to $h^0 \to ZZ^* \to 4l$

The computation of virtual corrections to the decay of h^0 to four leptons via a Z boson pair can be carried out analogously. Consider the process

$$h^0(k_1) \to ZZ^* \to e^-(k_2) + e^+(k_3) + \mu^+(k_4) + \mu^-(k_5) , \tag{5.40}$$

where we define $k_+ = k_2 + k_3$ and $k_- = k_4 + k_5$ as before. The virtual one-loop diagrams can be classified as for the process $h^0 \to WW^* \to 4l$, and the h^0ZZ/H^0ZZ counter term contributions can be easily obtained from Eq. (5.21) by simple replacements: $\delta Z_W \to \delta Z_Z$, $\frac{\delta s_W}{s_W} \to \frac{\delta s_W}{s_W}\left(1 - 2\frac{s_W^2}{c_W^2}\right)$, while the structure of the other counter terms is as in the SM [101]. In Fig. 5.6 we depict only the photonic diagrams that contribute to the on-shell singularities. In this decay process, the intermediate gauge bosons are neutral, thus only pentagon diagrams with a photon exchanged between two external charged fermions can contribute to the on-shell singularities. The scalar 5-point integrals can again be decomposed by separating the non-resonant gauge boson propagator. Here we give explicitly the correction factor resulting from the photonic pentagon diagrams that contains the soft and on-shell singularities (assuming the gauge boson with four-momentum k_- is at resonance)

$$\begin{aligned}\delta_p^{sing} = -\frac{\alpha}{2\pi}\Big\{\Big[&- \mathrm{Li}_2\Big(-\frac{S_{25} + k_-^2 - M_V^2}{S_{24}}\Big) \\ &+ 2\ln\Big(-\frac{S_{24}}{m_e m_\mu} - i\epsilon\Big)\ln\Big(\frac{M_V^2 - k_-^2}{\lambda M_V} - i\epsilon\Big)\end{aligned}$$

$$
\begin{aligned}
&- \ln^2\Big(\frac{m_\mu}{M_V}\Big) - \ln^2\Big(\frac{M_V^2 - k_-^2 - S_{24} - S_{25}}{m_e M_V} - i\epsilon\Big) - \frac{\pi^2}{3}\Big] \\
&+ (2 \leftrightarrow 3, 4 \leftrightarrow 5) - (2 \leftrightarrow 3) - (4 \leftrightarrow 5)\Big\} \,, \qquad (5.41)
\end{aligned}
$$

where the expressions in the parentheses are obtained from that in the squared bracket by interchange of indices. In the case that the other gauge boson is resonant, the correction factor reads

$$
\begin{aligned}
\delta_p^{sing} = -\frac{\alpha}{2\pi}\Big\{\Big[&- \mathrm{Li}_2\Big(-\frac{S_{34} + k_+^2 - M_V^2}{S_{24}}\Big) \\
&+ 2\ln\Big(-\frac{S_{24}}{m_e m_\mu} - i\epsilon\Big)\ln\Big(\frac{M_V^2 - k_+^2}{\lambda M_V} - i\epsilon\Big) \\
&- \ln^2\Big(\frac{m_e}{M_V}\Big) - \ln^2\Big(\frac{M_V^2 - k_+^2 - S_{24} - S_{34}}{m_\mu M_V} - i\epsilon\Big) - \frac{\pi^2}{3}\Big] \\
&+ (2 \leftrightarrow 3, 4 \leftrightarrow 5) - (2 \leftrightarrow 3) - (4 \leftrightarrow 5)\Big\} \,. \qquad (5.42)
\end{aligned}
$$

As before, M_V^2 should be replaced by $M_V^2 - iM_V\Gamma_V$ in the on-shell singular logarithm. The on-shell singular virtual contributions can be easily extracted from these correction factors. The photonic corrections to the $Zf\bar{f}$ vertex and the field renormalization constants of the external charged fermions contribute to the soft singularities, but not to the on-shell singularities. There is no contribution to these singularities from Z boson self energy corrections.

5.4.3 Application to semileptonic and hadronic final states

In the discussions above, we only consider the decay of h^0 to leptonic final states. The procedure used there can, in principle, be applied to semileptonic and hadronic final states as well. For semileptonic and hadronic final states, the number of photonic diagrams involving on-shell singularities may increase, but their evaluation can be carried out in complete analogy to what we did for leptonic final state. With simple substitution of momenta and mass parameters, the analytical results for the scalar integrals in Appendix B can still be used to extract the on-shell singularities from the virtual contributions. The soft and collinear singular virtual contributions are again given by Eq. (5.38). The only possible exception in which the procedure used for our computation can not be straightforwardly applied is that the final state involves heavy down-type fermions, e.g. b quarks. Note that in our computation we keep the final state fermion masses only as regulators for collinear singularities and neglect them elsewhere. If the final state involves b quarks, we can not neglect their masses, since their coupling to Higgs bosons can be enhanced at large $\tan\beta$ and give rise to numerically important effects.

5.5 Real corrections

As can be seen from the computation of virtual corrections, the exchange of a virtual photon between two external charged particles leads to IR divergences. In order to achieve

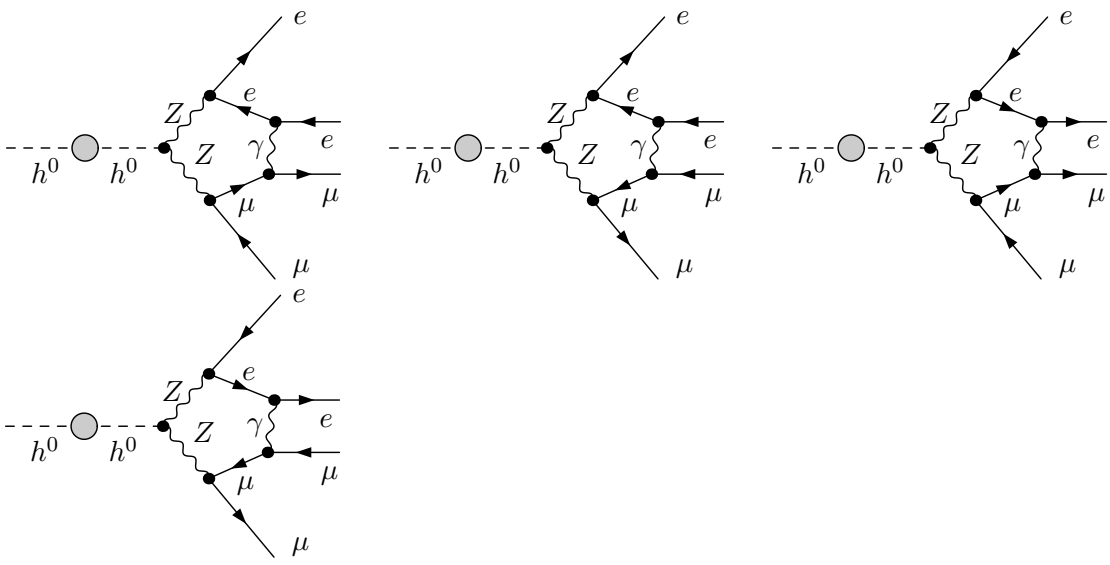

Figure 5.6: Photonic diagrams that contribute to the on-shell singularities.

an IR finite physical result, the combination with real photon emission process is required, as a consequence of the fact that the experimental resolution of soft photons is limited. The KLN theorem guarantees that the IR singularities from virtual and real corrections cancel with each other in physical observables.

We consider the following bremsstrahlung processes

$$h^0(k_1) \to e^-(k_2) + \bar{\nu}_e(k_3) + \mu^+(k_4) + \nu_\mu(k_5) + \gamma(k_6) \tag{5.43}$$

and

$$h^0(k_1) \to e^-(k_2) + e^+(k_3) + \mu^+(k_4) + \mu^-(k_5) + \gamma(k_6)\ . \tag{5.44}$$

In the evaluation of hard bremsstrahlung contribution a constant width is introduced in each gauge boson propagator. As previously mentioned, not all intermediate gauge bosons are resonant. For the propagator that is not resonant, the corresponding error is of higher order and negligible.

The contribution of the real photon bremsstrahlung to the partial decay width can be written as

$$\Gamma_\gamma = \frac{1}{2M'_{h^0}} \int \sum_{pol} |\mathcal{M}_\gamma|^2 \, d\Phi_\gamma \tag{5.45}$$

with the squared matrix element $|\mathcal{M}_\gamma|^2$ summed over the final state polarizations and the phase space factor

$$d\Phi_\gamma = \left(\prod_{i=2}^{6} \frac{d^3\mathbf{k}_i}{(2\pi)^3\ 2k_i^0} \right) (2\pi)^4 \delta^{(4)}(k_1 - \sum_{i=2}^{6} k_i)\ . \tag{5.46}$$

As in the evaluation of virtual corrections, the masses of light fermions are consistently neglected unless they have to be kept as regulators. Soft and collinear real photon emission give rise to singularities, which are regularized by the photon mass λ and the fermion mass m_f, respectively. These soft and collinear singularities are treated within two different approaches, which will be discussed below.

5.5.1 Treatment of soft and collinear photon emission

In this section we describe the methods used to treat the soft and collinear photon emission, i.e. the phase space slicing and the dipole subtraction approach. In the former approach one needs to impose cut-offs on the photon energy and the emission angle, while in the latter no cut-off is needed. Another advantage of the subtraction method is that the integration error within this method is much (typically one order of magnitude) smaller than that of the slicing method.

Phase space slicing

For the real photon bremsstrahlung the phase space integral diverges in certain regions. One can divide the phase space into singular and non-singular regions. In the non-singular region the integral is finite and can be evaluated numerically without regulators. In the singular region the integral has to be evaluated analytically with regulators. The singular region consists of the soft region, where the photon energy is smaller than a given cutoff ΔE; and the collinear region, in which the photon is emitted collinearly (but not soft) to a charged fermion, namely the angle between the emitted photon and the charged fermion is smaller than an angular cutoff $\Delta\theta$. The real correction can be decomposed as follows

$$d\Gamma^{h^0\to 4f\gamma} = d\Gamma_{soft} + d\Gamma_{coll} + d\Gamma^{h^0\to 4f\gamma}_{finite} \ . \tag{5.47}$$

In the soft and collinear regions, the squared matrix element $|\mathcal{M}^{h^0\to 4l\gamma}|^2$ factorizes into the lowest order squared matrix element $|\mathcal{M}^{h^0\to 4l}|^2$ and a universal soft or collinear factor. The five particle phase space also factorizes into four particle phase space and a photon part, so that the photon momentum can be integrated over analytically. In the soft region, the soft photon approximation can be applied, in which the photon 4-momentum is omitted everywhere except in the IR singular propagators. Then one obtains [101]

$$\begin{aligned} d\Gamma_{soft} &= d\Gamma_{born}\frac{\alpha}{4\pi^2}\sum_{i=2}^{5}\sum_{j=i+1}^{5} Q_i\,Q_j \int_{E_\gamma<\Delta E}\frac{d^3\mathbf{k}}{E_\gamma}\left(\frac{q_i^\mu}{kq_i}-\frac{q_j^\mu}{kq_j}\right)^2 \\ &= d\Gamma_{born}\frac{\alpha}{2\pi}\sum_{i=2}^{5}\sum_{j=i+1}^{5} Q_i\,Q_j[I_{ii}+I_{jj}-2I_{ij}] \ , \end{aligned} \tag{5.48}$$

where the basic integrals are given by [101, 139]

$$I_{ij} = \frac{1}{2\pi}\int_{E_\gamma<\Delta E}\frac{d^2\mathbf{k}}{E_\gamma}\frac{q_iq_j}{(kq_i)(kq_j)} \ . \tag{5.49}$$

As mentioned before, we keep the fermion masses only as regulators for the collinear singularities. Consequently, the soft photon correction factor can be written as [146]

$$d\Gamma_{soft} = d\Gamma_{born}\,\frac{\alpha}{\pi}\sum_{i=2}^{5}\sum_{j=i+1}^{5} Q_iQ_j\Bigg\{2\ln\left(\frac{2\Delta E}{\lambda}\right)\left[1-\ln\left(\frac{S_{ij}}{m_im_j}\right)\right]-\ln\left(\frac{4k_i^0k_j^0}{m_im_j}\right) + \ln^2\left(\frac{2k_i^0}{m_i}\right)+\ln^2\left(\frac{2k_j^0}{m_j}\right)+\frac{\pi^2}{3}+\mathrm{Li}_2\left(1-\frac{4k_i^0k_j^0}{S_{ij}}\right)\Bigg\}\,, \tag{5.50}$$

where S_{ij} are defined as before, k_i^0 and m_i denote the energy and mass of the final state fermions.

In the collinear region, the squared matrix element and the phase space also factorize as in the soft region, and the collinear factor that describes the collinear final state radiation is given by

$$d\Gamma_{coll} = d\Gamma_{born}\,\frac{\alpha}{2\pi}\sum_{i=2}^{5} Q_i^2\Bigg\{\left[\frac{3}{2}+2\ln\left(\frac{\Delta E}{k_i^0}\right)\right]\left[1-2\ln\left(\frac{\Delta\theta k_i^0}{m_i}\right)\right]+3-\frac{2\pi^2}{3}\Bigg\}\,, \tag{5.51}$$

where the cutoff parameters ΔE and $\Delta\theta$ should be chosen sufficiently small so that the soft photon and leading-pole approximations apply. On the other hand, they should not be too small so that the instabilities of numerical integration can be avoided. Also note that this result assumes that a photon emitted collinearly to a charged fermion is treated inclusively, namely it is combined to the emitting charged fermion. As a result, all dependence on the photon and fermion masses will drop out in the final result. If the collinearly emitted photon is not treated inclusively, for example, in the evaluation of distributions of final state muons, then in the collinear region one has

$$d\Gamma_{coll} = \sum_{i=2}^{5}\frac{\alpha}{2\pi}\,Q_i^2\,d\Gamma_{born}(\tilde{k}_i)\int_0^{1-\frac{\Delta E}{\tilde{k}_i^0}} dz_i\Bigg\{p_{ff}(z_i)\left[2\ln\left(\frac{\Delta\theta\tilde{k}_i^0}{m_i}z_i\right)-1\right] + (1-z_i)\Bigg\}\Theta(z_i) \tag{5.52}$$

with $z_i = k_i^0/\tilde{k}_i^0$ and the splitting function

$$P_{ff}(z_i) = \frac{1+z_i^2}{1-z_i}\,. \tag{5.53}$$

Here $\tilde{k}_i^0$ and k_i^0 denote the energy of the charged fermion before and after emitting the collinear photon, the function $\Theta(z_i)$ summarizes the phase space cuts. The integration over z_i in Eq. (5.52) is constrained by the phase space cuts $\Theta(z_i)$ and cannot be performed analytically. Consequently the fermion mass singularities are not fully canceled in the combination of virtual and real corrections and thus become visible. If the photon is treated inclusively, the integration over z_i will not be constrained by any phase space cut, and thus can be performed analytically, leading to Eq. (5.51).

Dipole subtraction

In this approach [143–145] one constructs an auxiliary function which contains the same singularities as the real bremsstrahlung integrand. Subtracting this auxiliary function from the bremsstrahlung integrand thus cancels all soft and collinear singularities and the difference can be integrated numerically, even in the singular region. In this numerical integration no regulators are needed for the soft and collinear singularities. The auxiliary function can then be integrated analytically (regulators are required) and readded to the original integral. Within the subtraction method there is no singular contribution involved in the numerical integration. Hence for computations within this method, the statistical uncertainty is smaller than that of the slicing method, in which the singular contributions are present in the numerical integration. The auxiliary function must possess the same asymptotic behavior as the original integrand in the soft and collinear limit, and has to be simple enough to be integrated over the singular regions analytically. In our case, soft and collinear singularities occur only in the final state. As the masses of the final state light fermions can be consistently neglected, the expression of the auxiliary function is fairly simple [144]

$$|\mathcal{M}_{sub}(\Phi_{4f\gamma})|^2 = -\sum_{\substack{i,j=2\\ i\neq j}}^{5} Q_i\, Q_j\, g_{ij}^{sub}(k_i,k_j,k)|\mathcal{M}_{born}(\tilde{\Phi}_{4f,ij})|^2 \;, \tag{5.54}$$

where k_i and k denote the respective momenta of final state fermions and photon, and the functions g_{ij}^{sub} contain the soft and collinear singularities

$$g_{ij}^{sub}(k_i,k_j,k) = \frac{1}{(k_ik)(1-y_{ij})}\Big[\frac{2}{1-z_{ij}(1-y_{ij})} - 1 - z_{ij}\Big] \tag{5.55}$$

with the variables

$$y_{ij} = \frac{k_ik}{k_ik_j + k_ik + k_jk} \;, \qquad z_{ij} = \frac{k_ik_j}{k_ik_j + k_jk} \;. \tag{5.56}$$

The mapping between the phase space of the radiative and non-radiative process, $\Phi_{4f\gamma}$ and $\tilde{\Phi}_{4f}$, is defined as

$$\tilde{k}_i^\mu = k_i^\mu + k^\mu - \frac{y_{ij}}{1-y_{ij}}k_j^\mu \;, \qquad \tilde{k}_j^\mu = \frac{1}{1-y_{ij}}k_j^\mu \tag{5.57}$$

with all other momenta unchanged. The contribution of the auxiliary function should be computed analytically. After integrating over the photon momentum the result reads

$$\int d\Phi_{4f\gamma}|\mathcal{M}_{sub}(\Phi_{4f\gamma})|^2 = -\frac{\alpha}{2\pi}\sum_{\substack{i,j=2\\ i\neq j}}^{5} Q_i\, Q_j \int d\tilde{\Phi}_{4f,ij}\, G_{ij}^{sub}(S_{ij})|\mathcal{M}_{born}(\tilde{\Phi}_{4f,ij})|^2 \tag{5.58}$$

with the function

$$G_{ij}^{sub}(S_{ij}) = L(S_{ij},m_i^2) - \frac{\pi^2}{3} + \frac{3}{2} \;, \tag{5.59}$$

where $L(S_{ij},m_i^2)$ has been defined in Eq. (5.39).

5.6 Higher order final state radiation

The emission of photons collinear to the charged fermions leads to corrections enhanced by large logarithms involving the fermion masses. These logarithms will cancel out if the collinearly emitted photon is treated inclusively, i.e. if it is combined with the emitting charged fermion. If this is not the case, for instance, in the evaluation of distributions of muons in the final state, this logarithm will survive and give rise to sizeable effects. Therefore one should take into account the corresponding higher order corrections. This can be done by the structure-function method [125, 148] based on the mass factorization theorem, according to which the decay width with leading logarithmic final state radiation can be written as

$$\int d\Gamma_{\rm LL} = \Pi_{i,Q_i\neq 0} \int_0^1 dz_i \Gamma_{ii}^{\rm LL}(z_i, Q^2) \int d\Gamma_{born} \Theta(z_i) \ , \tag{5.60}$$

where z_i is again the energy fraction of the charged fermion after and before the collinear photon emission, and Q is the relevant energy scale in the process, which can be taken as the physical mass of the lightest CP-even Higgs boson mass M'_{h^0} in our case. The leading logarithmic structure function including terms up to $\mathcal{O}(\alpha^3)$ is given by [125]

$$\begin{aligned}
\Gamma_{ii}^{\rm LL}(z_i, Q^2) = & \frac{\exp\left(-\frac{1}{2}\beta_i\gamma_E + \frac{3}{8}\beta_i\right)}{\Gamma(1+\frac{1}{2}\beta_i)} \frac{\beta_i}{2}(1-z_i)^{\frac{\beta_i}{2}-1} - \frac{\beta_i}{4}(1+z_i) \\
& - \frac{\beta_i^2}{32}\left\{\frac{1+3z_i^2}{1-z_i}\ln(z_i) + 4(1+z_i)\ln(1-z_i) + 5 + z_i\right\} \\
& - \frac{\beta_i^3}{384}\left\{(1+z_i)\left[6{\rm Li}_2(z_i) + 12\ln^2(1-z_i) - 3\pi^2\right]\right. \\
& + \frac{1}{1-z_i}\left[\frac{3}{2}(1+8z_i+3z_i^2)\ln(z_i) + 6(z_i+5)(1-z_i)\ln(1-z_i)\right. \\
& + 12(1+z_i^2)\ln(z_i)\ln(1-z_i) - \frac{1}{2}(1+7z_i^2)\ln^2(z_i) \\
& \left.\left. + \ \frac{1}{4}(39-24z_i-15z_i^2)\right]\right\} \ ,
\end{aligned} \tag{5.61}$$

where γ_E and $\Gamma(x)$ are the Euler constant and the Gamma function, the function β_i is given by

$$\beta_i = \frac{2\alpha}{\pi}\left[\ln\left(\frac{Q^2}{m_i^2}\right) - 1\right] \ . \tag{5.62}$$

For practical calculations, one can expand the structure function $\Gamma_{ii}^{\rm LL}$ in terms of β_i and keep terms up to $\mathcal{O}(\alpha^3)$. When adding the contribution in Eq. (5.60) to the one-loop result, the lowest order and one-loop contributions $d\Gamma_{\rm LL,1}$ should be subtracted, since they are already contained in our results

$$\int d\Gamma_{\rm LL,1} = \int d\Gamma_{born} + \sum_{i,Q_i\neq 0} \int_0^1 dz_i \Gamma_{ii}^{\rm LL,1}(z_i, Q^2) \int d\Gamma_{born} \Theta(z_i) \ , \tag{5.63}$$

where the one-loop contribution to the structure function $\Gamma_{ii}^{\mathrm{LL},1}$ reads

$$\Gamma_{ii}^{\mathrm{LL},1}(z_i, Q^2) = \frac{\beta_i}{4}\left(\frac{1+z_i^2}{1-z_i}\right)_+ \tag{5.64}$$

with the following +-prescription

$$\int_0^1 dx\, f(x)\, g(x)_+ = \int_0^1 dx\, (f(x) - f(1))g(x)\ , \tag{5.65}$$

or equivalently

$$g(x)_+ = \lim_{\epsilon\to 0}\left[\theta(1-x-\epsilon)g(x) - \delta(1-x-\epsilon)\int_0^{1-\epsilon} g(y)d(y)\right]\ . \tag{5.66}$$

This yields

$$\Gamma_{ii}^{\mathrm{LL},1}(z_i, Q^2) = \frac{\beta_i}{4}\lim_{\epsilon\to 0}\left[\delta(1-z_i)\left(\frac{3}{2} + 2\ln\epsilon\right) + \theta(1-z_i-\epsilon)\frac{1+z_i^2}{1-z_i}\right]\ , \tag{5.67}$$

where ϵ is a regulator for the otherwise divergent numerical integration, the dependence on which will drop out in the final result.

5.7 Numerical results

In this section we discuss the numerical results. Before that we briefly summarize the strategies for the computation of electroweak radiative corrections to our decay processes. In the evaluation of virtual corrections, the gauge boson width is incorporated via the factorization scheme, in which we separate the gauge boson self energy diagrams from other virtual diagrams and treat them differently in order to avoid the double counting from the inclusion of gauge boson width in the lowest order matrix element. If the intermediate gauge boson is charged, the contribution of photonic self energy diagrams diverges when the gauge boson approaches on-shell. To render it finite, we have to include the gauge boson width. This is done by computing analytically the scalar two-point integrals that contribute to these on-shell singularities and replace afterwards the real gauge boson mass in the singular terms by a complex one. Due to the upper bound of the lightest CP-even Higgs boson mass, only one of the intermediate gauge bosons can be resonant. Power counting tells that in the factorization scheme only scalar integrals potentially contribute to the on-shell singularities. The evaluation of scalar 4- and 5-point integrals are simplified by extracting the non-resonant gauge boson propagator from the integrals. In this way only analytical expressions for the resulting singular scalar 3- and 4-point integrals are required. For the evaluation of real corrections, we use two different approaches, i.e. the phase space slicing and the dipole subtraction approach. With the help of these methods we are able to extract the soft singularities from the real corrections and check analytically their cancellation with their counterparts in the virtual corrections. The extraction of collinear singularities from the real corrections is straightforward. However, in the virtual corrections they occur not only in scalar loop integrals, but

also in tensor ones, whose analytical evaluation is rather involved. Therefore we check the cancellation of collinear singularities numerically by varying the masses of light fermions in the final state, which act as regulators for collinear singularities. If the collinearly emitted photons are not combined to the emitting fermions, the large logarithms involving final state fermion masses can survive and become visible. In this case we also include the corrections resulting from the higher order final state radiation.

For the numerical evaluation, the following inputs for the SM parameters are used [9, 149]

$$\begin{aligned} G_\mu &= 1.16637 \times 10^{-5}\mathrm{GeV}^{-2} , & \alpha &= 1/137.03599968 , \\ M_W &= 80.403\,\mathrm{GeV} , & \Gamma_W &= 2.141\,\mathrm{GeV} , \\ M_Z &= 91.1876\,\mathrm{GeV} , & \Gamma_Z &= 2.4952\,\mathrm{GeV} , \\ M_t &= 172.7\,\mathrm{GeV} , & M_b &= 4.2\,\mathrm{GeV} . \end{aligned}$$

The lowest order matrix element is parametrized in such a way that it absorbs the running of the electromagnetic coupling and the leading universal corrections to the ρ parameter, i.e. we use the effective coupling derived from the Fermi constant

$$\alpha_{G_\mu} = \frac{\sqrt{2} G_\mu M_W^2 s_W^2}{\pi} \tag{5.68}$$

for the Born amplitude. In the relative $\mathcal{O}(\alpha)$ corrections, we use the coupling $\alpha = \alpha(0)$, which is an appropriate choice for the real photon emission. In order to avoid double-counting from using α_{G_μ} in the lowest order amplitude, the charge renormalization constant in Eq. (5.23) is modified to

$$\delta\tilde{Z}_e = \delta Z_e - \frac{1}{2}\Delta r , \tag{5.69}$$

where Δr summarizes the radiative corrections to the muon decay. In the evaluation of distributions, a real photon closer than 5 degrees to a charged fermion or with energy less than 1 GeV is combined with the charged fermion in the inclusive treatment.

As previously discussed, the Higgs field renormalization constants and the counter term $\delta \tan\beta$ are determined in the $\overline{DR}$ scheme. We choose the renormalization scale as $\mu^{\overline{DR}} = 1.5 M_W$, which is the scale of the physical mass of the lightest CP-even Higgs boson for moderate values of $\tan\beta$ and M_{A^0}.

From the discussions in the previous chapter, there are a large number of free parameters in the MSSM, most of which arise from the soft supersymmetry breaking Lagrangian. The complete scan over the MSSM parameter space is thus a formidable task. In our numerical analysis we investigate the results in several suggested benchmark scenarios [114, 150], which are defined so that the two parameters that govern the tree-level Higgs sector, M_{A^0} and $\tan\beta$, are varied while the other parameters that enter via radiative corrections are fixed. In these scenarios a common soft supersymmetry breaking parameter M_{SUSY}, as well as the same trilinear coupling for the third generation slepton and squark, is chosen for simplicity. The $U(1)$ gaugino mass parameter is given by the GUT relation

$$M_1 = \frac{5}{3}\frac{s_W^2}{c_W^2} M_2 . \tag{5.70}$$

The experimental mass exclusion limits from direct search of supersymmetric particles and the upper bound on the SUSY corrections to the electroweak ρ parameter [9] have been taken into account throughout the parameter scan. In the region that we are interested, the bound derived from the BR($B \to X_s\gamma$) prediction has ruled out the gluophobic scenario [151], therefore we will not discuss this scenario here. The investigated scenarios are listed below :

1. The $m_h^{\max}$ scenario
This scenario yields a maximal value of the lightest CP-even Higgs boson as a function of $\tan\beta$ for fixed top quark mass and common soft supersymmetry breaking scale $M_{\rm SUSY}$. The parameters are given by

$$\begin{aligned} &m_t = 172.7\,\text{GeV}\ , \qquad M_{\rm SUSY} = 1\,\text{TeV}\ , \qquad \mu = 200\,\text{GeV}\ , \qquad M_2 = 200\,\text{GeV}\ , \\ &X_t = 2M_{\rm SUSY}\ , \qquad A_b = A_t = A_\tau\ , \qquad m_{\tilde g} = 0.8 M_{\rm SUSY}\ . \end{aligned} \tag{5.71}$$

where X_t is the mixing parameter of the top squark sector and $m_{\tilde g}$ is the gluino mass.

2. The no-mixing scenario
This scenario differs from the $m_h^{\max}$ scenario by the vanishing mixing in the scalar top sector and a higher SUSY mass scale, which is chosen to avoid the exclusion bounds from the LEP Higgs searches [10, 152]. The parameters in this scenario read

$$\begin{aligned} &m_t = 172.7\,\text{GeV}\ , \qquad M_{\rm SUSY} = 2\,\text{TeV}\ , \qquad \mu = 200\,\text{GeV}\ , \qquad M_2 = 200\,\text{GeV}\ , \\ &X_t = 0\ , \qquad A_b = A_t = A_\tau\ , \qquad m_{\tilde g} = 0.8 M_{\rm SUSY}\ . \end{aligned} \tag{5.72}$$

3. The small-$\alpha_{\rm eff}$ scenario
In this scenario the higher order MSSM corrections can lead to a significant suppression of the $h^0 b\bar b$ coupling and give rise to an enhancement of BR($h^0 \to WW^*$). The parameters are

$$\begin{aligned} &m_t = 172.7\,\text{GeV}\ , \qquad M_{\rm SUSY} = 800\,\text{GeV}\ , \qquad \mu = 2.5 M_{\rm SUSY}\ , \qquad M_2 = 500\,\text{GeV}\ , \\ &X_t = -1100\,\text{GeV}\ , \qquad A_b = A_t = A_\tau\ , \qquad m_{\tilde g} = 500\,\text{GeV}\ . \end{aligned} \tag{5.73}$$

For the decay process $h^0 \to WW^* \to e^-\bar\nu_e\mu^+\nu_\mu$, the contribution of photonic one-loop diagrams are UV divergent. Extracting the infrared and on-shell singular contributions from these diagrams and combining with the contribution of real photon emission yields the QED-like correction to the partial decay width, which is both UV and IR finite. It is independent of the cutoff parameters ΔE, $\Delta\theta$ within the phase space slicing approach. This is illustrated in Fig. 5.7, where we show the relative size of the QED-like corrections

$$\delta = \frac{\Gamma_{corr} - \Gamma_{born}}{\Gamma_{born}} \tag{5.74}$$

for $\tan\beta = 25$, $M_{A^0} = 500\,\text{GeV}$ in the $m_h^{\max}$ scenario. Γ_{corr} denotes the partial decay width corrected by the QED-like contributions. The results of phase space slicing method is correct up to $\mathcal{O}(\Delta E/\sqrt{S})$ or $\mathcal{O}(\Delta\theta)$. For small cutoff parameters, terms of these orders are negligible and the result is independent of the cutoffs. For large cutoff parameters, such terms become relevant and their effects become visible.

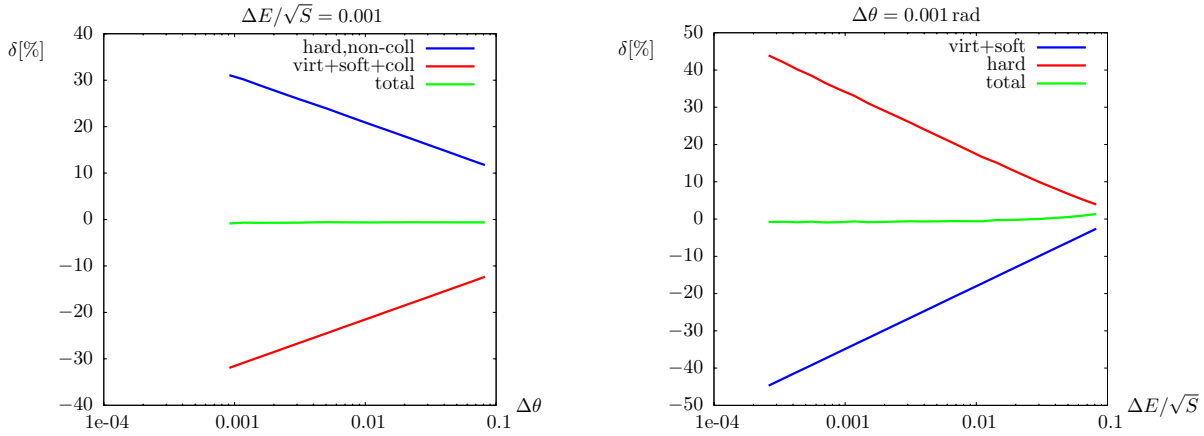

Figure 5.7: Cutoff dependence of the QED-like corrections to the decay $h^0 \to e^-\bar{\nu}_e\mu^+\nu_\mu$ for the $m_h^{\max}$ scenario with $\tan\beta = 25$, $M_A^0 = 500\,\text{GeV}$ in the phase space slicing approach. The left plot shows the dependence on the angular cutoff $\Delta\theta$ (with $\Delta E/\sqrt{S} = 0.001$), while the dependence on the energy cutoff of soft photon is shown in the right plot (with $\Delta\theta = 0.001\,\text{rad}$).

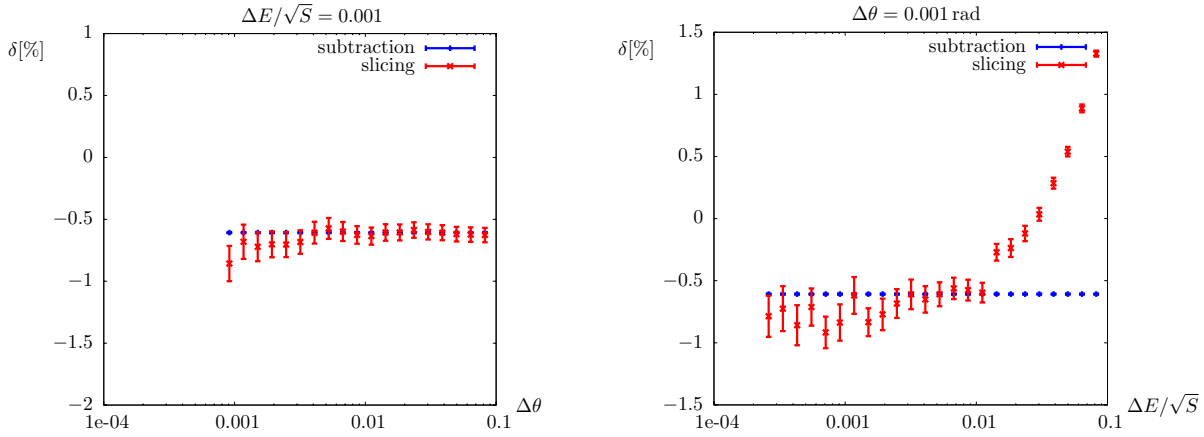

Figure 5.8: Comparison of the QED-like corrections to the decay $h^0 \to e^-\bar{\nu}_e\mu^+\nu_\mu$ for the $m_h^{\max}$ scenario with $\tan\beta = 25$, $M_A^0 = 500\,\text{GeV}$ in the phase space slicing and dipole subtraction approach.

For comparison purpose, the results computed within the slicing and the subtraction approach are shown in Fig. 5.8. From the plots one can find an agreement between the results of the two approaches, and that the subtraction approach yields smaller integration errors than the slicing method. In addition, the integration error within the slicing approach increases when the value of the cutoff parameter decreases, since the original IR singularity will appear if the cutoff parameter goes to zero.

In our decay processes, only SM particles are involved in the final state. It is interesting to compare the SM and the MSSM predictions for the partial decay widths. As discussed previously, in the limit that the mass parameter M_{A^0} is much larger than the electroweak scale, all the heavy Higgs bosons will decouple and the contribution from loop diagrams involving the SM particles and Higgs bosons will approach the SM prediction for a Higgs boson with the same mass. In order to compare the partial decay width of h^0 to four leptons in this limiting case with the SM result, we also perform the computation with the SM input parameters defined in [112], and choose the SUSY parameters $M_{\rm SUSY}$, μ and M_2 to be $M_{\rm SUSY} = \mu = M_2 = M_{A^0}$, so that the supersymmetric particles decouple when M_{A^0} becomes large. The remaining parameters are chosen as in the $m_h^{\rm max}$ scenario. In Fig. 5.9 we show the one-loop corrected partial decay width of h^0 to four leptons excluding the contribution of genuine SUSY diagrams as a function of M_{A^0}. In the limiting case that M_{A^0} gets large ($M_{A^0} > 1.5\,\text{TeV}$), the SM results for the partial decay width in [112] are reproduced. However, in [112] the distributions are evaluated for a Higgs boson with mass beyond the upper mass bound of h^0, thus a comparison of distributions is not possible.

If the generic mass scale of SUSY particles $M_{\rm SUSY}$ is not much larger than the electroweak scale, these genuine SUSY particles do not decouple even in the limiting case that $M_{A^0} \gg M_Z$. To investigate their numerical effects, we compare the one-loop corrected partial decay width of h^0 including/excluding these genuine SUSY loop contributions. In Fig. 5.10 the lowest order and corrected partial decay widths of h^0 to four leptons are depicted for $M_{\rm SUSY} = \mu = M_2 = M_{A^0}$, with the remaining parameters chosen as in the $m_h^{\rm max}$ scenario. The numerically most important one-loop corrections have been incorporated into the lowest order result by using the effective amplitude and the G_μ scheme. For the decay $h^0 \to e^-\bar{\nu}_e\mu^+\nu_\mu$, the relative loop corrections vary between -2.5% and -2% for $\tan\beta = 5$, while vary between -2% and -1.5% for $\tan\beta = 29$. For the process $h^0 \to e^-e^+\mu^+\mu^-$, the relative corrections change from -3% to -2% and from -4% to -3% for $\tan\beta = 5$ and 29, respectively. As can be seen from the plots, for both processes, at large M_{A^0} the blue curve that includes the genuine SUSY loop contributions and the red curve that does not are almost indistinguishable from each other, which indicates that the effects of the genuine SUSY loop contributions are negligible in the large M_{A^0} limit. In Fig. 5.11 we choose a relatively small value 300 GeV for $M_{\rm SUSY}$, all other parameters are chosen as in the $m_h^{\rm max}$ scenario, so that the genuine SUSY spectrum is not too heavy. The relative corrections vary from -2.5% to -1.5% and from -3% to -1% for $\tan\beta = 5$ and 29, respectively. However, the genuine SUSY loop contributions again yield negligible effects in the large M_{A^0} limit (while for small value of M_{A^0}, their contributions can reach several percent). This implies that in our case the decoupling behavior is essentially dominated by the mass parameter M_{A^0}. Thus it is rather difficult to distinguish the lightest MSSM Higgs boson from the SM Higgs boson in the limit that M_{A^0} gets large, even if one-loop corrections are taken into account.

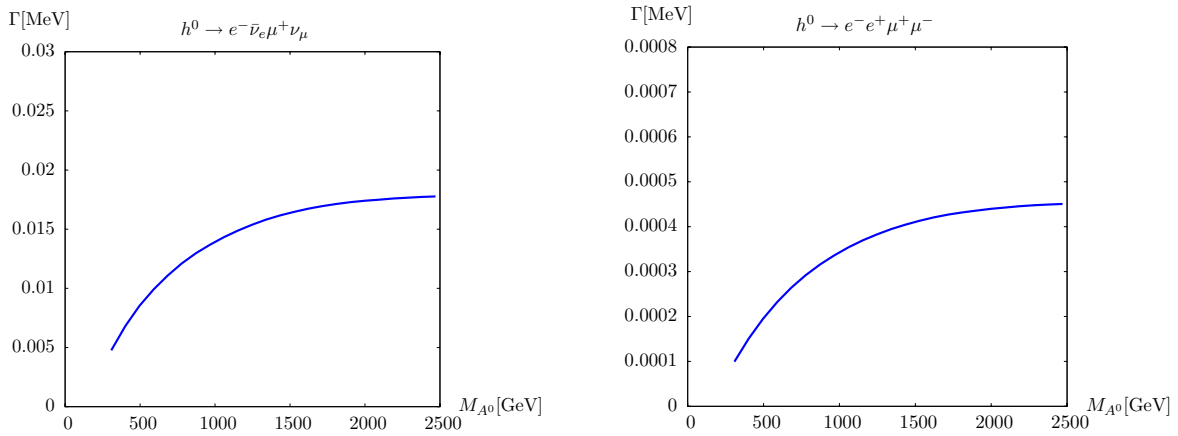

Figure 5.9: Corrected partial decay width of h^0 excluding the genuine SUSY one-loop contribution as a function of M_{A^0}, with $M_{\rm SUSY} = \mu = M_2 = M_{A^0}$ and $\tan\beta = 6$. All other parameters are chosen as in the $m_h^{\rm max}$ scenario.

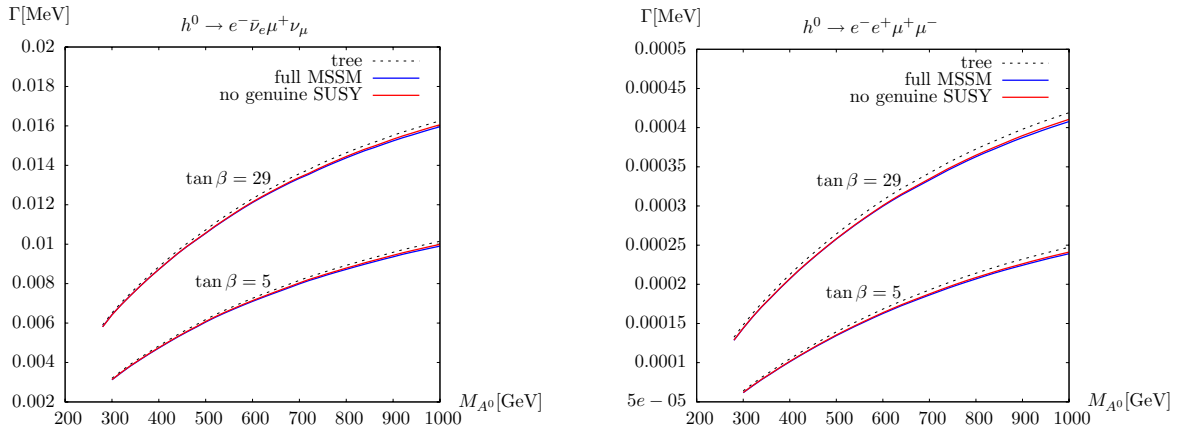

Figure 5.10: Partial decay width of h^0 as a function of M_{A^0}, with $M_{\rm SUSY} = \mu = M_2 = M_{A^0}$ and $\tan\beta = 5, 29$. All other parameters are chosen as in the $m_h^{\rm max}$ scenario. The dashed line denotes the tree-level result. The blue line shows the width with full MSSM corrections, including the genuine SUSY loop contributions, which are not included in the red line.

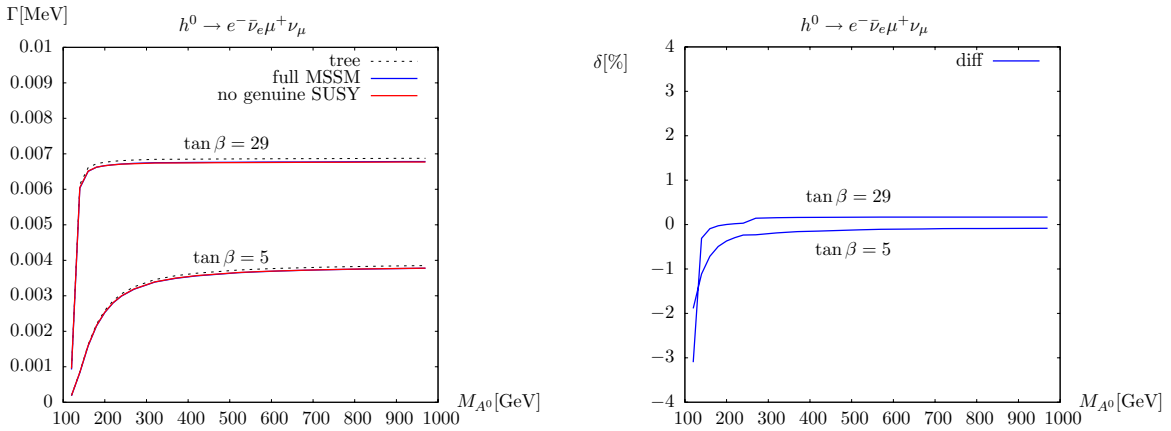

Figure 5.11: Partial decay width of h^0 as a function of M_{A^0}, with $M_{\rm SUSY} = 300\,\text{GeV}$ and $\tan\beta = 5, 29$. All other parameters are chosen as in the $m_h^{\rm max}$ scenario. The right plot shows the effects of the genuine SUSY contributions.

A generic scan over the most relevant parameters of the Higgs sector, M_{A^0} and $\tan\beta$, has also been performed. Fig. 5.12 shows the results for the one-loop corrected partial decay width of $h^0 \to e^-\bar{\nu}_e\mu^+\nu_\mu$ including the full MSSM corrections in three different scenarios, where the corrections to the H^0WW vertex from loops involving the third generation fermions and sfermions are not included. For $M_{A^0} > 500\,\text{GeV}$, the results hardly vary with M_{A^0} and therefore are not shown there. For small M_{A^0} values ($M_{A^0} < 140\,\text{GeV}$), the decay width is rather small due to a cancellation between the two parts of the effective Born amplitude Eq. (5.10). When M_{A^0} and $\tan\beta$ increase, the Higgs boson mass and thus the decay width increases rapidly in all three scenarios and reach a plateau after $\tan\beta > 15$ and $M_{A^0} > 220\,\text{GeV}$. In the small-$\alpha_{\rm eff}$ scenario there is a slight decrease with M_{A^0} for moderate and large $\tan\beta$ and $M_{A^0} > 220\,\text{GeV}$. This is basically due to the slight decrease of the light CP-even Higgs boson mass with M_{A^0} in this region. The relative corrections are typically of the order of $-1.5\% \sim 1\%$ and $-3\% \sim -2\%$ respectively in the $m_h^{\rm max}$ and no-mixing scenarios; in the small-$\alpha_{\rm eff}$ scenario they do not exceed -4% unless for small M_{A^0} values ($M_{A^0} < 140\,\text{GeV}$), where the cancellation between the two parts of the effective Born amplitude Eq. (5.10) can yield a very small lowest order result, and the size of the radiative correction is comparable to the lowest order result. This is not shown in Fig. 5.12 so that the generic size of the relative corrections can be clearly seen.

Owing to the mixing between the two CP-even Higgs bosons, the coupling of H^0 to gauge bosons needs to be taken into account as well. Although at tree-level this coupling is usually suppressed, the one-loop correction can be numerically relevant, since the fermionic and sfermionic loops involve potentially large Yukawa couplings and their contribution can thus get enhanced. In Fig. 5.13 we show the correction to the partial decay width of $h^0 \to e^-\bar{\nu}_e\mu^+\nu_\mu$ due to the third generation fermionic and sfermionic loop contribution to the H^0WW coupling. Such correction involves both the Yukawa couplings and the wave function normalization factors resulting from the mixing between the two CP-even Higgs bosons. While the latter can lead to a suppression/enhancement to the correction when

$M_{A^0}/\tan\beta$ increase, the former tend to enhance the correction when $\tan\beta$ increases. The combination of these effects may lead to local extremum in the $M_{A^0} - \tan\beta$ plane. For our scan, a maximum appears at $\tan\beta = 9$, $M_{A^0} = 140\,\text{GeV}$ in the $m_h^{\max}$ scenario and at $\tan\beta = 19$, $M_{A^0} = 120\,\text{GeV}$ in the no-mixing scenario. In the small-α_{eff} scenario, there is a maximum at $\tan\beta = 9$, $M_{A^0} = 140\,\text{GeV}$. The relative corrections are positive and stay below 1.5% in the $m_h^{\max}$ and no-mixing scenarios, and vary from -0.5% to 1% in the small-α_{eff} scenario. In all three scenarios the contribution of these fermionic and sfermionic loops decreases very rapidly when M_{A^0} becomes large.

In Fig. 5.14 and 5.15 we show the same plots for $h^0 \to e^-e^+\mu^+\mu^-$, which exhibits similar features as in Fig. 5.12 and 5.13. As shown in Fig. 5.14, the relative corrections are all negative in the three scenarios. In the $m_h^{\max}$ scenario the relative correction varies from -3% to -0.5%, while it stays between -5.5% and -3% in the other two scenarios. In the small-α_{eff} scenario where the cancellation in the effective Born amplitude can occur, the relative correction can reach 95%. One can find from Fig. 5.15 that there is a maximum at $\tan\beta = 11$, $M_{A^0} = 140\,\text{GeV}$ in the $m_h^{\max}$ scenario. The maximum occurs at $\tan\beta = 23$, $M_{A^0} = 120\,\text{GeV}$ in the no-mixing scenario and at $\tan\beta = 9$, $M_{A^0} = 140\,\text{GeV}$ in the small-α_{eff} scenario.

Fig. 5.16 shows the invariant mass distribution of the $\mu^+\nu_\mu$ pair resulting from the decay of the W boson in the process $h^0 \to e^-\bar{\nu}_e\mu^+\nu_\mu$ in the $m_h^{\max}$ scenario, where the parameters are chosen to be $\tan\beta = 30$, $M_{A^0} = 120\,\text{GeV}$ and $400\,\text{GeV}$. As the mass of h^0 stays below the production threshold of the gauge boson pair, only one intermediate gauge boson can be resonant. From the plots it can be seen that in addition to the peak around the W boson mass, there is another broad peak at small invariant mass. This is the point where the other W boson gets resonant. In the right plot the broad peak is closer to the W resonance peak, as the Higgs boson mass is larger. In Fig. 5.17 we show the relative corrections to the invariant mass distribution of the $\mu^+\nu_\mu$ pair in the $m_h^{\max}$ scenario. From the plots one can find an enhancement at low invariant mass due to the emission of photon off the final state fermions. In the case that the collinear photon is not combined with the emitting fermions, the logarithm involving the light fermion mass would survive and give rise to large corrections. This is shown by the blue curves in Fig. 5.17, while the red curves show the results with photon combinations, i.e. the collinear photon is combined with the emitting fermion. If the fermion masses are consistently neglected, the invariant mass distribution of the $e^-\bar{\nu}_e$ pair with photon combination coincides with the red curves in the plots. In Fig. 5.18 we show the relative contributions due to the higher order final state radiation discussed in section 5.6, and the corrections of the third generation fermions and sfermions to the H^0WW coupling, where in the right plot the latter is not shown since it is strongly suppressed by the wave function normalization factors and is completely negligible for large M_{A^0} values. For both M_{A^0} values, the higher order final state radiation can lead to corrections less than 2%. The corrections of the third generation fermions/sfermions to the H^0WW coupling give rise to a contribution less than 1% for $M_{A^0} = 120\,\text{GeV}$. In Fig. 5.19 the invariant mass distributions of the $\mu^+\nu_\mu$ pair without photon combination in the no-mixing and small-α_{eff} scenarios are shown with $\tan\beta = 30$ and $M_{A^0} = 400\,\text{GeV}$. The relative corrections can reach $\sim 25\%$ in both scenarios.

Fig. 5.20 to 5.23 show the corresponding invariant mass distributions for the process $h^0 \to$

$e^-e^+\mu^+\mu^-$ in the three benchmark scenarios. In the left plot of Fig. 5.20 the broad peak at low invariant mass is not clearly visible in the depicted region because of the larger mass of Z boson compared to the W boson mass. As shown in Fig. 5.22, for both M_{A^0} values, the higher order final state radiation gives rise to larger corrections than in the previous process, as the final state now involves two muons. While the contribution to the H^0ZZ vertex leads to a correction of 1% for $M_{A^0} = 120\,\text{GeV}$ in the m_h^{max} scenario, it is completely negligible for $M_{A^0} = 400\,\text{GeV}$. In Fig. 5.23 the invariant mass distributions in the no-mixing and small-α_{eff} scenarios are depicted with $\tan\beta = 30$ and $M_{A^0} = 400\,\text{GeV}$ (no photon combination). In both scenarios, the relative corrections vary from -30% to 10%.

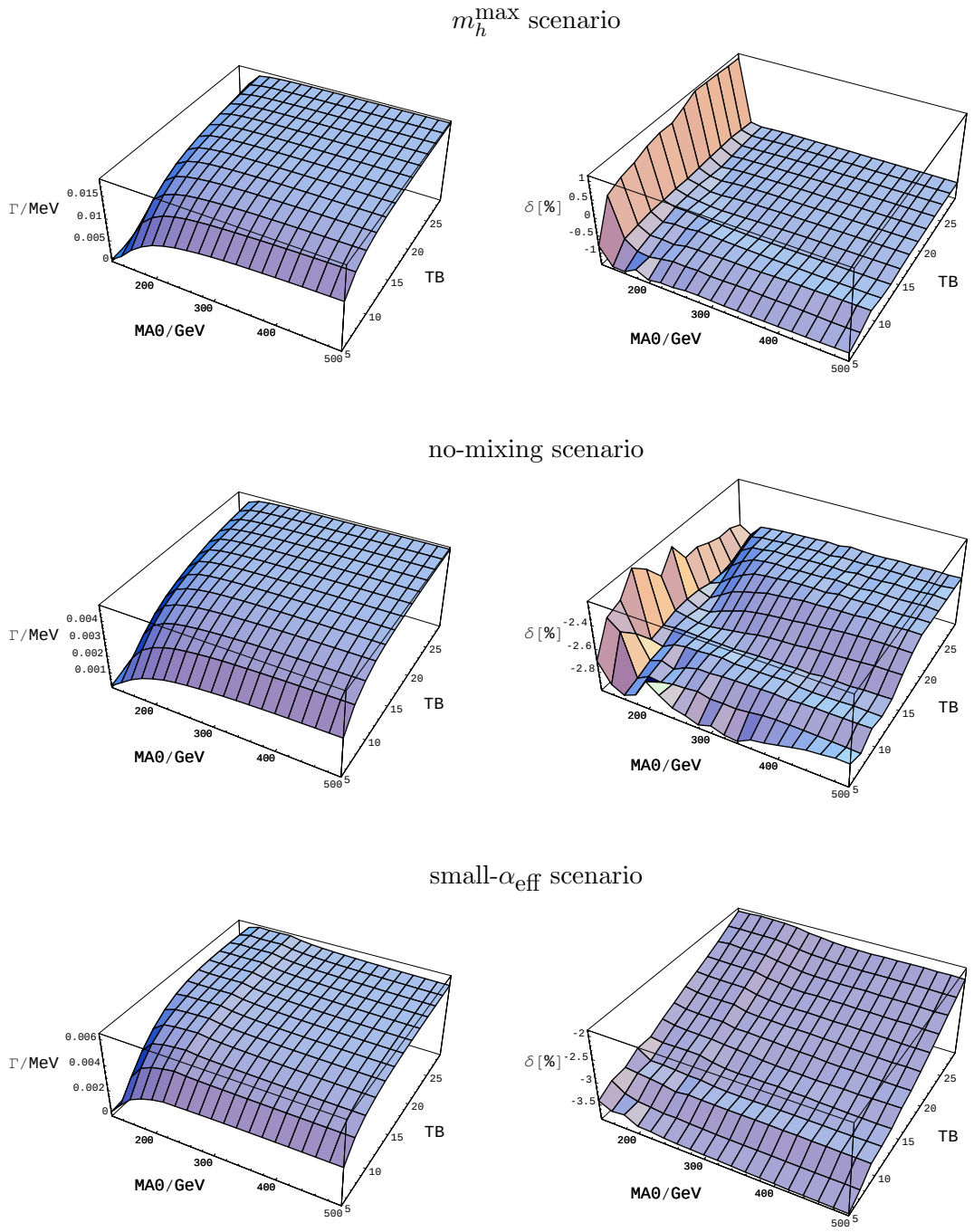

Figure 5.12: Results for the partial decay width of $h^0 \to WW^* \to e^-\bar{\nu}_e\mu^+\nu_\mu$ in three different benchmark scenarios (the contribution due to the third generation fermion and sfermion loop corrections to the H^0WW coupling is not included. TB denotes $\tan\beta$). The left column shows the corrected partial decay width, while the right column shows the relative corrections.

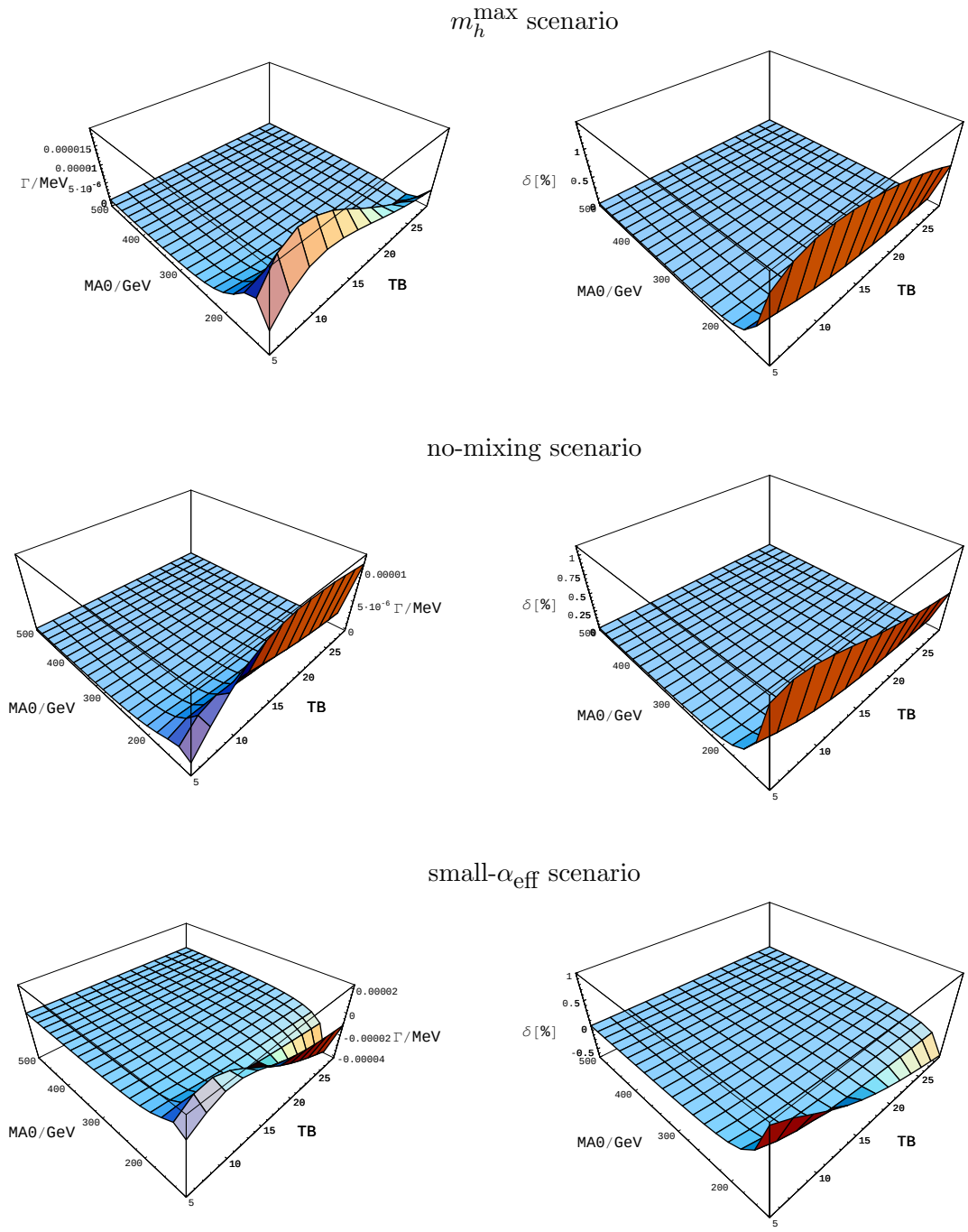

Figure 5.13: Contribution to the partial decay width of $h^0 \to WW^* \to e^-\bar{\nu}_e\mu^+\nu_\mu$ due to the correction to the H^0WW coupling from the third generation fermions and sfermions in three different benchmark scenarios (TB denotes $\tan\beta$). The left column shows the corrections to the partial decay width, while the right column shows their relative size.

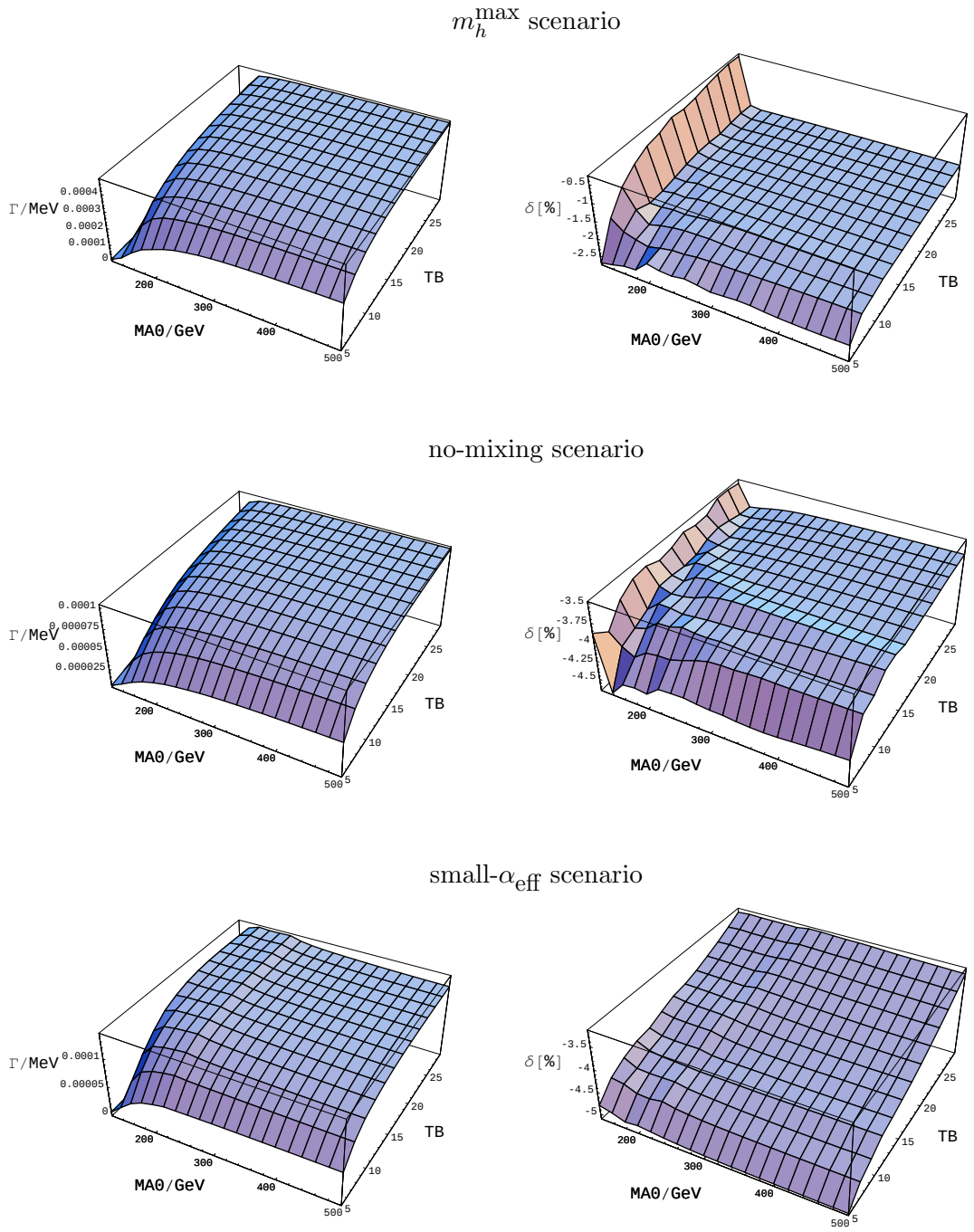

Figure 5.14: Results for the partial decay width of $h^0 \to ZZ^* \to e^-e^+\mu^+\mu^-$ in three different benchmark scenarios (the contribution due to the third generation fermion and sfermion loop corrections to the H^0ZZ coupling is not included. TB denotes $\tan\beta$). The left column shows the corrected partial decay width, while the right column shows the relative corrections.

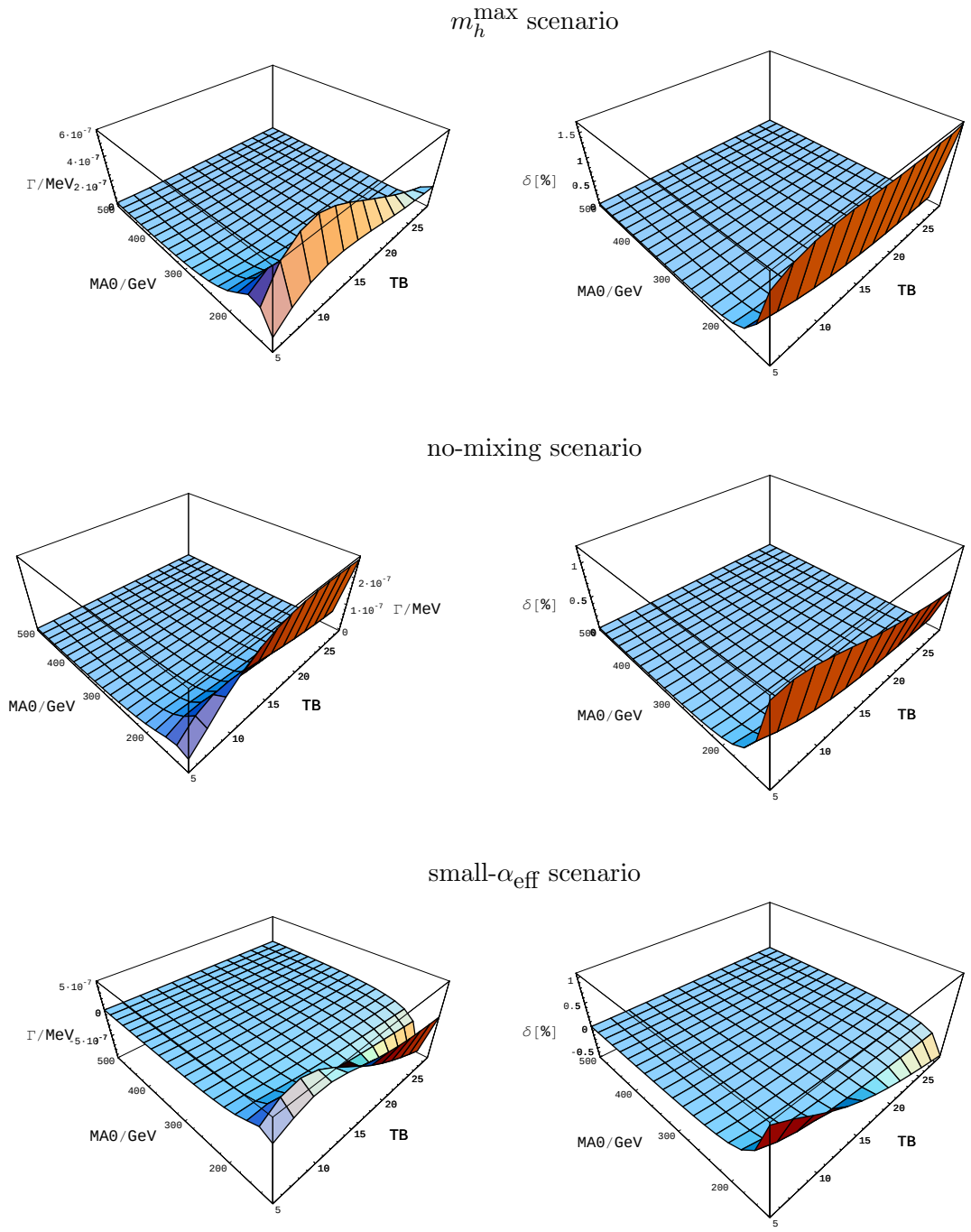

Figure 5.15: Contribution to the partial decay width of $h^0 \to ZZ^* \to e^-e^+\mu^+\mu^-$ due to the correction to the H^0ZZ coupling from the third generation fermions and sfermions in three different benchmark scenarios (TB denotes $\tan\beta$). The left column shows the corrections to the partial decay width, while the right column shows their relative size.

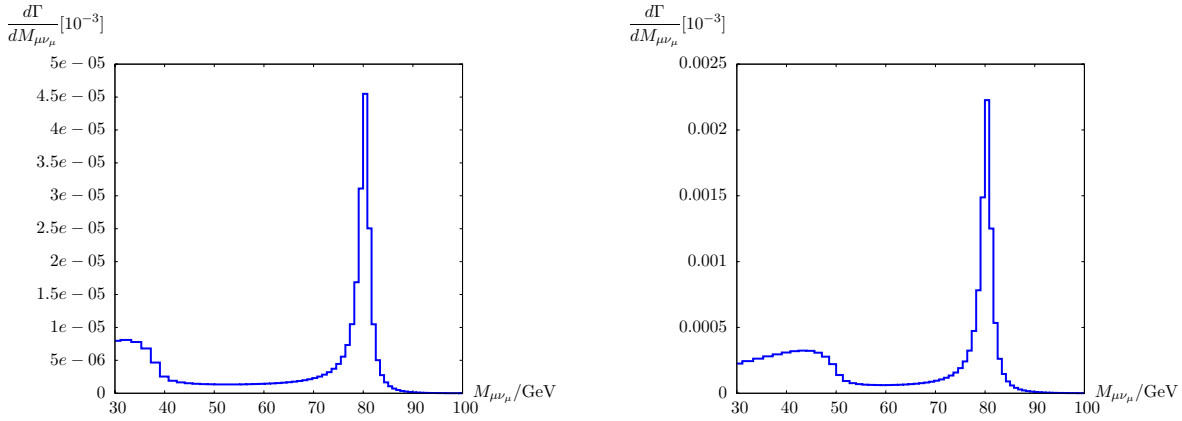

Figure 5.16: Invariant mass distribution of $\mu^+\nu_\mu$ in the decay $h^0 \to e^-\bar{\nu}_e\mu^+\nu_\mu$ (corrected, no photon combination, the contribution from the H^0WW vertex correction is not included) in the $m_h^{\max}$ scenario, with $\tan\beta = 30$, $M_{A^0} = 120\,\text{GeV}$ (left) and $\tan\beta = 30$, $M_{A^0} = 400\,\text{GeV}$ (right).

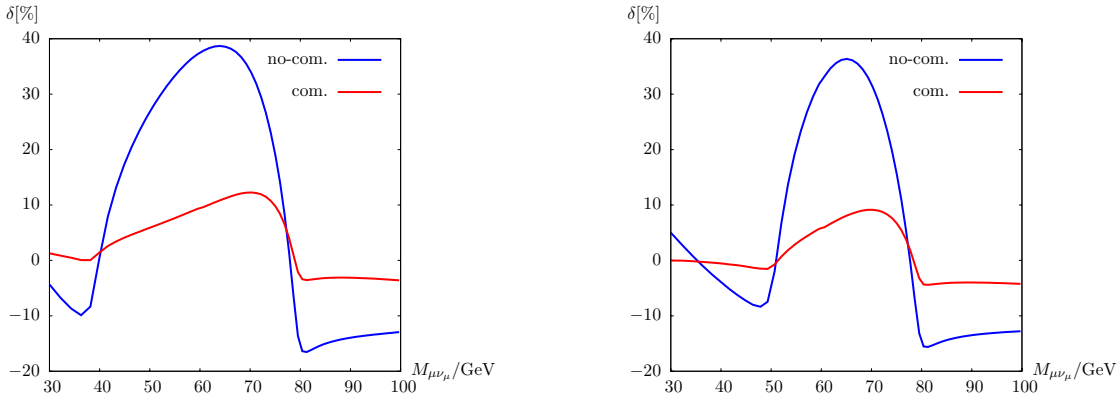

Figure 5.17: Relative correction to the invariant mass distribution of $\mu^+\nu_\mu$ in the decay $h^0 \to e^-\bar{\nu}_e\mu^+\nu_\mu$ (the contribution from the H^0WW vertex correction is not included) in the $m_h^{\max}$ scenario, with $\tan\beta = 30$, $M_{A^0} = 120\,\text{GeV}$ (left) and $\tan\beta = 30$, $M_{A^0} = 400\,\text{GeV}$ (right). "com." and "no-com." indicate the results with and without photon combination, respectively.

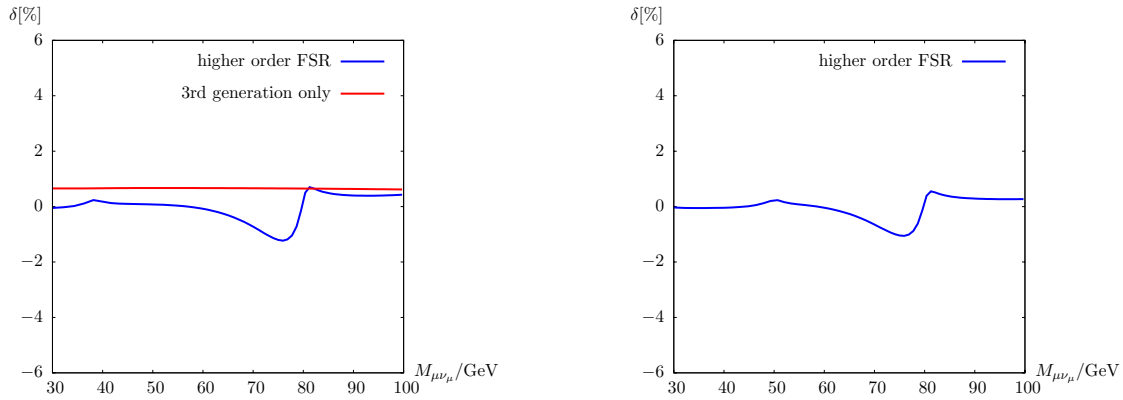

Figure 5.18: Relative contribution to the invariant mass distribution of $\mu^+\nu_\mu$ in the decay $h^0 \to e^-\bar{\nu}_e\mu^+\nu_\mu$ from the higher order final state radiation (higher order FSR) and from the H^0WW vertex correction (3rd generation only) in the $m_h^{\max}$ scenario, with $\tan\beta = 30$, $M_{A^0} = 120\,\text{GeV}$ (left) and $\tan\beta = 30$, $M_{A^0} = 400\,\text{GeV}$ (right).

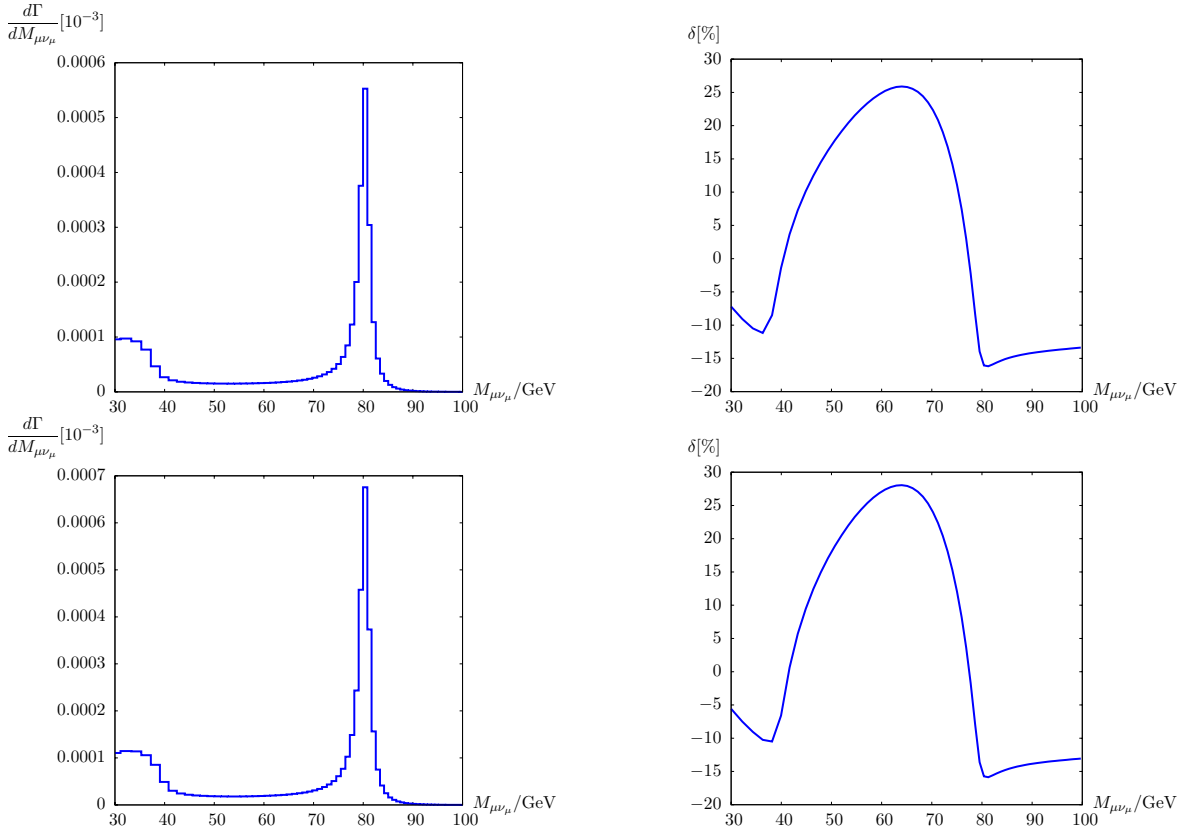

Figure 5.19: Invariant mass distribution and relative correction to the invariant mass distribution of $\mu^+\nu_\mu$ in the decay $h^0 \to e^-\bar{\nu}_e\mu^+\nu_\mu$ (no photon combination) in the no-mixing scenario (upper) and the small-α_{eff} scenario (lower), with $\tan\beta = 30$, $M_{A^0} = 400\,\text{GeV}$.

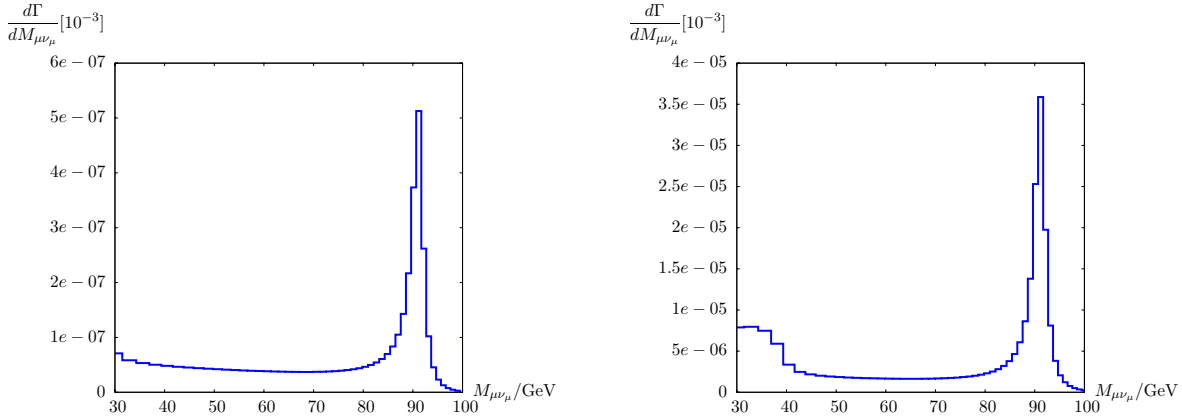

Figure 5.20: Invariant mass distribution of $\mu^+\mu^-$ in the decay $h^0 \to e^-e^+\mu^+\mu^-$ (corrected, no photon combination, the contribution from the H^0ZZ vertex correction is not included) in the $m_h^{\max}$ scenario, with $\tan\beta = 30$, $M_{A^0} = 120\,\text{GeV}$ (left) and $\tan\beta = 30$, $M_{A^0} = 400\,\text{GeV}$ (right).

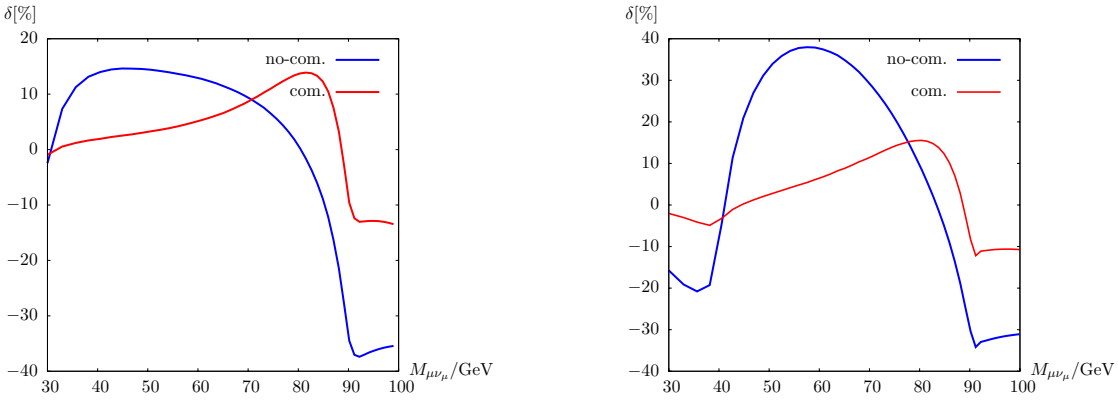

Figure 5.21: Relative correction to the invariant mass distribution of $\mu^+\mu^-$ in the decay $h^0 \to e^-e^+\mu^+\mu^-$ (the contribution from the H^0ZZ vertex correction is not included) in the $m_h^{\max}$ scenario, with $\tan\beta = 30$, $M_{A^0} = 120\,\text{GeV}$ (left) and $\tan\beta = 30$, $M_{A^0} = 400\,\text{GeV}$ (right). "com." and "no-com." indicate the results with and without photon combination, respectively.

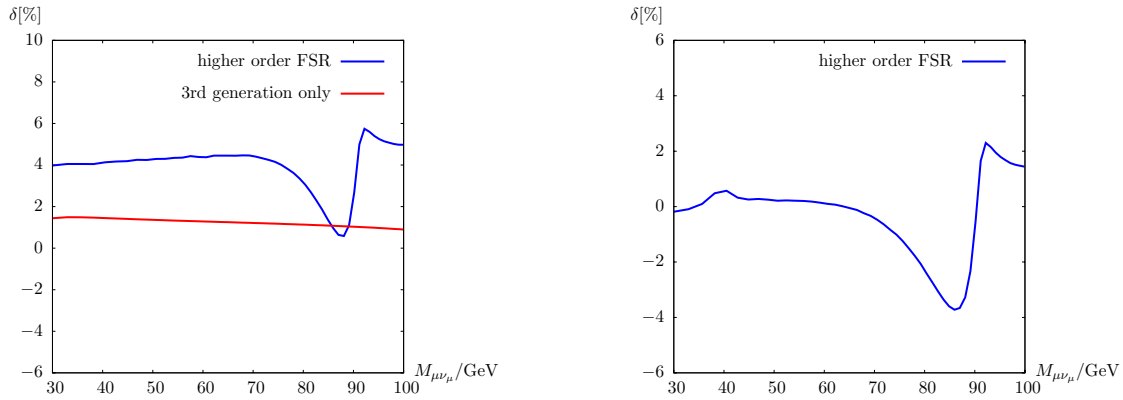

Figure 5.22: Relative contribution to the invariant mass distribution of $\mu^+\mu^-$ in the decay $h^0 \to e^-e^+\mu^+\mu^-$ from the higher order final state radiation (higher order FSR) and from the H^0ZZ vertex correction (3rd generation only) in the $m_h^{\max}$ scenario, with $\tan\beta = 30$, $M_{A^0} = 120\,\text{GeV}$ (left) and $\tan\beta = 30$, $M_{A^0} = 400\,\text{GeV}$ (right).

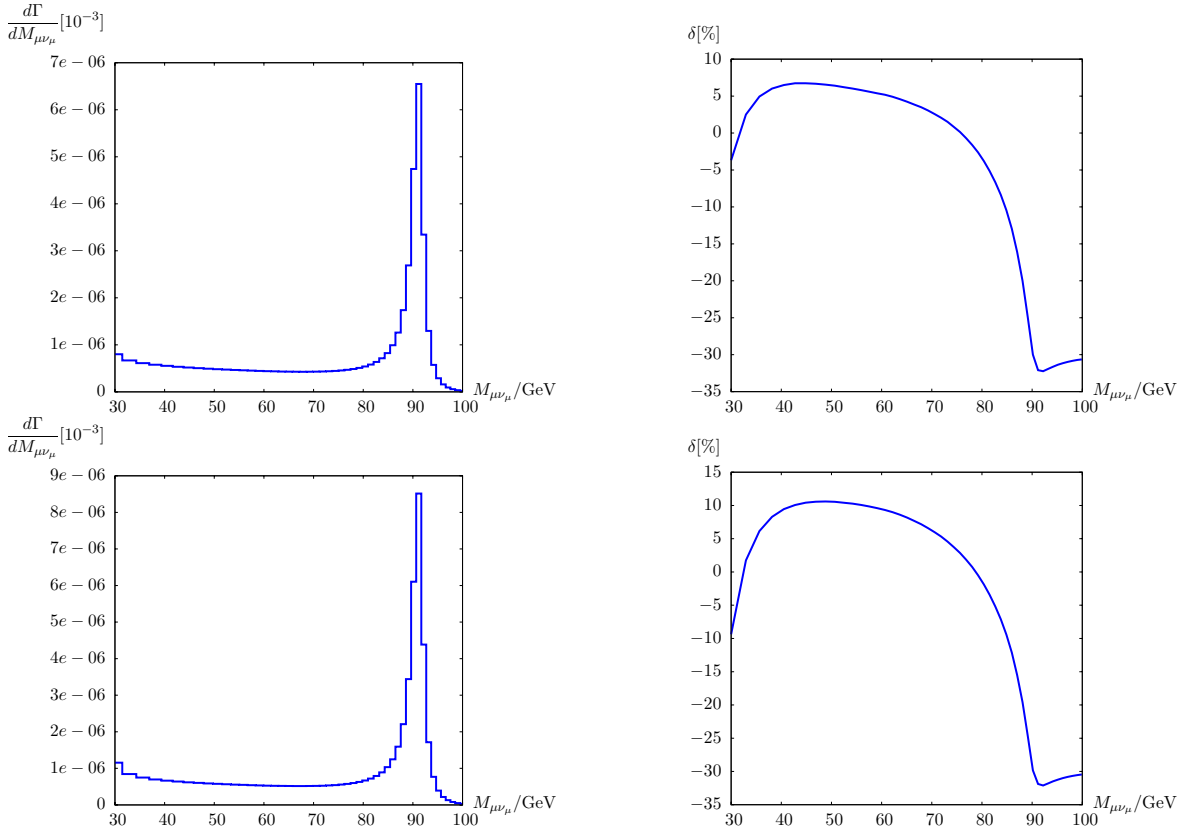

Figure 5.23: Invariant mass distribution and relative correction to the invariant mass distribution of $\mu^+\mu^-$ in the decay $h^0 \to e^-e^+\mu^+\mu^-$ (no photon combination) in the no-mixing scenario (upper) and the small-α_{eff} scenario (lower), with $\tan\beta = 30$, $M_{A^0} = 400\,\text{GeV}$.

Chapter 6

EW Corrections to Decay of H^0 to off/on-shell WW/ZZ Pair

The Higgs mechanism, as a widely discussed candidate for the electroweak symmetry breaking, in its minimal implementation in the SM, results in one physical Higgs boson. In the MSSM, two complex Higgs doublets are required for consistency. Moreover, two doublets are needed to bring the gauge couplings unified at some high energy scale [41]. Consequently five physical Higgs bosons result after the electroweak symmetry breaking. As discussed in previous chapters, among these physical Higgs bosons the lightest one resembles the SM Higgs boson in certain limits, hence it is possible that the discovery of only one light Higgs boson is compatible with both the SM and the MSSM predictions and thus one can not straightforwardly distinguish between them. However, the observation of additional heavy Higgs bosons would be a clear signature for physics beyond the SM. Precision measurements of the decay properties of such heavy Higgs bosons can then help to distinguish the MSSM from other models describing physics beyond the SM.

In the MSSM, the tree-level coupling of the heavy CP-even Higgs boson, H^0, to vector boson pair is suppressed by a factor $\cos(\beta - \alpha)$, compared to the coupling of the SM Higgs boson to vector boson pair, where α is the angle that diagonalizes the CP-even Higgs sector and $\tan\beta = v_2/v_1$ represents the ratio of the vacuum expectation values of the two Higgs doublets in the MSSM. Radiative corrections induce important modifications to this coupling. One potential source of large corrections is the contribution of loops involving fermions and sfermions, especially those involving the third generation fermions and sfermions, since they contain potentially large Yukawa couplings. The mixing between Higgs bosons can give rise to significant contributions as well. We will concentrate on CP-conserving MSSM with real parameters, hence the heavy CP-even Higgs boson can only mix with the light CP-even one. In certain parameter regions of the MSSM, the tree-level coupling is strongly suppressed. Investigating the impact of radiative corrections in these regions is particularly interesting.

The electroweak $\mathcal{O}(\alpha)$ radiative corrections to the decay of the SM Higgs boson to vector boson pair have been available for a long time, see e.g. [153–155]. In these computations all three external legs can be off-shell, hence the results there can be used for more complicated

process that involves the coupling of the SM Higgs boson and vector boson pair. Here we evaluate the $\mathcal{O}(\alpha)$ electroweak corrections to the decay of H^0 to vector boson pair in the same way, and give the analytical expression for the one-loop contributions from diagrams involving the third generation fermions and sfermions, so that our results can be straightforwardly implemented into other processes that contain the process under consideration as a subprocess.

In section 6.1 we discuss the one-loop corrections to the coupling H^0WW/H^0ZZ and work out the analytical results for the contribution of fermionic and sfermionic loops, where all three particles can be off-shell. Then we apply the results to on-shell particles and compute the electroweak corrections to the decay of H^0 to gauge boson pair in section 6.2. The numerical results are discussed in section 6.3.

6.1 Corrections to the H^0WW/H^0ZZ vertices

6.1.1 Correction to the H^0WW vertex

We start from the following process where all three particles are taken to be off-shell

$$H^0(k_1) \to W^-(k_2,\mu) + W^+(k_3,\nu) \ . \tag{6.1}$$

$k_i\,(i=1\ldots3)$ denote the momenta of the particles with $k_1 = k_2 + k_3$ and μ, ν are Lorentz indices for the two vector bosons. At tree-level, the H^0WW coupling is given by

$$V^{\mu\nu}_{H^0,0} = \frac{eM_W}{s_W}\cos(\beta-\alpha)g^{\mu\nu} \equiv V_{H^0}\cos(\beta-\alpha)g^{\mu\nu} \ , \tag{6.2}$$

which differs from the coupling of the SM Higgs boson to W bosons only by a factor of $\cos(\beta-\alpha)$. When the mass of the CP-odd Higgs boson M_{A^0} gets large, the angle $\beta-\alpha \to \pi/2$ and the factor $\cos(\beta-\alpha)$ approaches 0 as $\mathcal{O}(M_Z^2\sin^2 4\beta/(2M_{A^0}^2))$, thus the tree-level coupling Eq. (6.2) is strongly suppressed, this is known as the decoupling limit.

At one-loop level (ignore the mixing between Higgs bosons for the moment), the corrected vertex H^0WW possesses the following structure

$$\begin{aligned} V^{\mu\nu}_{H^0} &= V^{\mu\nu}_{H^0,0} + V^{\mu\nu}_{H^0,1} \\ &= V^{\mu\nu}_{H^0,0} + V_{H^0}(Ak_2^\mu k_2^\nu + Bk_3^\mu k_3^\nu + Ck_2^\mu k_3^\nu + Dk_3^\mu k_2^\nu + Eg^{\mu\nu} - iF\epsilon^{\mu\nu\rho\sigma}k_{2\rho}k_{3\sigma}) \ , \end{aligned} \tag{6.3}$$

where $\epsilon^{\mu\nu\rho\sigma}$ is totally antisymmetric with $\epsilon^{0123}=1$. As in ref. [155], we concentrate on the cases that the gauge bosons can either become on-shell or couple to conserved currents, thus only the D, E and F terms can contribute as a consequence of transversality requirement or current conservation. In particular, if the gauge bosons are on-shell, the contribution of the F term would vanish due to the antisymmetry of the ϵ tensor. In the following we focus on the one-loop vertex corrections arising from fermions and sfermions, in particular from the third generation fermions and sfermions, which involve potentially large Yukawa couplings and are expected to yield sizeable contribution. For instance, they give rise to contributions

enhanced by m_t^2. We give the analytical expressions for the one-loop vertex corrections due to the third generation fermions and sfermions, the results can be extended straightforwardly to include all fermions and sfermions. Fig. 6.1 shows the relevant Feynman diagrams.

Now we write down the analytical expressions for the contributions to the D, E and F terms from loops involving the third generation squarks, sleptons, and leptons and quarks, respectively. Note that the F term receives contribution only from the lepton and quark loops. The contribution of stop and sbottom loops to the coefficient D is given by

$$\begin{aligned} D_{\tilde{q}} = \frac{\alpha}{2\pi \sin 2\beta M_W^2 c_W s_W^2} \Big\{ \sum_{i,j,k} \big(& -\cos\beta (U_{\tilde{b}})_{k1} (U_{\tilde{b}}^*)_{k1} (U_{\tilde{t}})_{i1} (U_{\tilde{t}}^*)_{j1} ((U_{\tilde{t}})_{j1} \mathcal{A}_i + (U_{\tilde{t}})_{j2} \mathcal{B}_i) \\ & \times (C_1 + C_{11} + C_{12})[k_1^2, k_3^2, k_2^2, m_{\tilde{t}_i}^2, m_{\tilde{t}_j}^2, m_{\tilde{b}_k}^2] + \sin\beta (U_{\tilde{b}})_{j1} (U_{\tilde{b}}^*)_{i1} (U_{\tilde{t}})_{k1} (U_{\tilde{t}}^*)_{k1} \\ & \times ((U_{\tilde{b}})_{i1} \mathcal{C}_j + (U_{\tilde{b}})_{i2} \mathcal{D}_j)(C_1 + C_{11} + C_{12})[k_1^2, k_3^2, k_2^2, m_{\tilde{b}_i}^2, m_{\tilde{b}_j}^2, m_{\tilde{t}_k}^2]) \Big\} \ , \end{aligned} \tag{6.4}$$

where $U_{\tilde{t}}$ and $U_{\tilde{b}}$ denote the mixing matrices of the stop and sbottom sector that diagonalize the corresponding squark mass matrices discussed in previous chapters, while A_t, A_b represent the corresponding trilinear couplings, $i, j, k = 1, 2$. C_1, C_{11} and C_{12} represent the vector and tensor coefficient functions of the 3-point integrals. For brevity we put together all integrals with the same arguments, and adopt the convention defined in [133, 134] in writing the arguments of the integrals. The abbreviations read

$$\begin{aligned} \mathcal{A}_i &= (\cos(\alpha+\beta)\sin\beta M_W M_Z(-3+4s_W^2) - 6c_W \sin\alpha m_t^2)(U_{\tilde{t}}^*)_{i1} \\ &\quad + 3c_W m_t(\cos\alpha\mu - \sin\alpha A_t^*)(U_{\tilde{t}}^*)_{i2} \ , \\ \mathcal{B}_i &= 3c_W m_t(-\sin\alpha A_t + \cos\alpha\mu^*)(U_{\tilde{t}}^*)_{i1} \\ &\quad - 2(2\cos(\alpha+\beta)\sin\beta M_W M_Z s_W^2 + 3\sin\alpha c_W m_t^2)(U_{\tilde{t}}^*)_{i2} \ , \\ \mathcal{C}_i &= (\cos(\alpha+\beta)\cos\beta M_W M_Z(-3+2s_W^2) + 6c_W \cos\alpha m_b^2)(U_{\tilde{b}}^*)_{i1} \\ &\quad + 3c_W m_b(-\sin\alpha\mu + \cos\alpha A_b^*)(U_{\tilde{b}}^*)_{i2} \ , \\ \mathcal{D}_i &= 3c_W m_b(\cos\alpha A_b - \sin\alpha\mu^*)(U_{\tilde{b}}^*)_{i1} \\ &\quad - 2(\cos(\alpha+\beta)\cos\beta M_W M_Z s_W^2 - 3\cos\alpha c_W m_b^2)(U_{\tilde{b}}^*)_{i2} \ , \end{aligned} \tag{6.5}$$

where μ is the Higgsino mass parameter and the asterisk indicates the complex conjugate, although it is irrelevant here since we assume real MSSM parameters. The contributions of stop and sbottom loops to the coefficients E and F read

$$\begin{aligned} E_{\tilde{q}} = \frac{\alpha}{8\pi \sin 2\beta M_W^2 c_W s_W^2} \Big\{ & \sum_{i,j} \big(\sin\beta (U_{\tilde{b}})_{i1} (U_{\tilde{b}}^*)_{j1} (-(U_{\tilde{b}})_{j1} \mathcal{C}_i - (U_{\tilde{b}})_{j2} \mathcal{D}_i) \\ & \times B_0[k_1^2, m_{\tilde{b}_i}^2, m_{\tilde{b}_j}^2] + \cos\beta (U_{\tilde{t}})_{i1} (U_{\tilde{t}}^*)_{j1} ((U_{\tilde{t}})_{j1} \mathcal{A}_i + (U_{\tilde{t}})_{j2} \mathcal{B}_i) B_0[k_1^2, m_{\tilde{t}_i}^2, m_{\tilde{t}_j}^2]\big) \\ & + \sum_{i,j,k} 4\big(\cos\beta (U_{\tilde{b}})_{k1} (U_{\tilde{b}}^*)_{k1} (U_{\tilde{t}})_{i1} (U_{\tilde{t}}^*)_{j1} (-(U_{\tilde{t}})_{j1} \mathcal{A}_i - (U_{\tilde{t}})_{j2} \mathcal{B}_i) \\ & \times C_{00}[k_1^2, k_3^2, k_2^2, m_{\tilde{t}_i}^2, m_{\tilde{t}_j}^2, m_{\tilde{b}_k}^2] + \sin\beta (U_{\tilde{b}})_{j1} (U_{\tilde{b}}^*)_{i1} (U_{\tilde{t}})_{k1} (U_{\tilde{t}}^*)_{k1} \\ & \times ((U_{\tilde{b}})_{i1} \mathcal{C}_j + (U_{\tilde{b}})_{i2} \mathcal{D}_j) C_{00}[k_1^2, k_3^2, k_2^2, m_{\tilde{b}_i}^2, m_{\tilde{b}_j}^2, m_{\tilde{t}_k}^2]) \Big\} \ , \\ F_{\tilde{q}} = 0 \ , & \end{aligned} \tag{6.6}$$

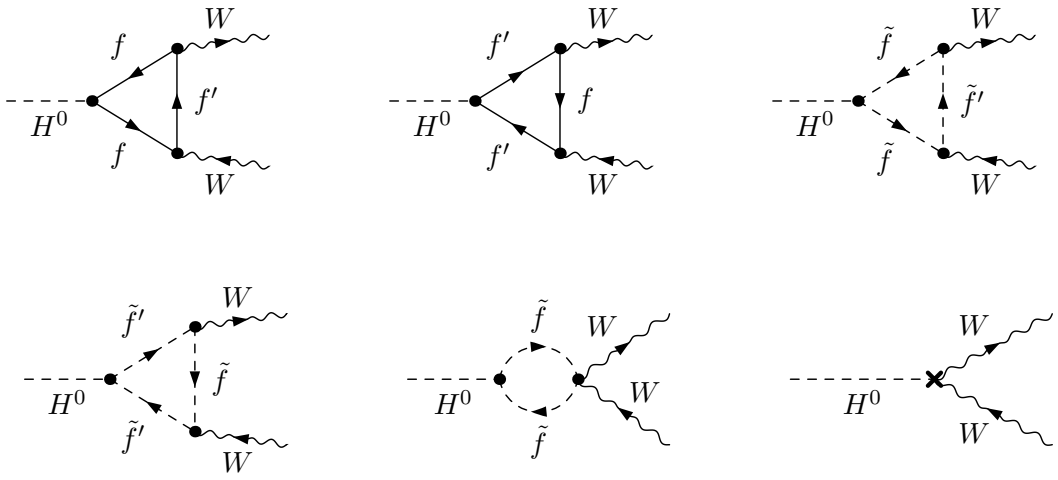

Figure 6.1: One-loop vertex diagrams and counter term diagram for H^0WW.

where B_0 denotes the scalar 2-point function, $\mathcal{A}_i$, $\mathcal{B}_i$, $\mathcal{C}_i$ and $\mathcal{D}_i$ are defined in Eq. (6.5).

The slepton loop contribution can be written as

$$\begin{aligned} D_{\tilde{l}} = \frac{\alpha}{4\pi M_W c_W s_W^2}\Big\{ & \sum_i \cos(\alpha+\beta) M_Z (C_1 + C_{11} + C_{12})[k_1^2, k_3^2, k_2^2, m_{\tilde{\nu}_\tau}^2, m_{\tilde{\nu}_\tau}^2, m_{\tilde{\tau}_i}^2] \\ & \times (U_{\tilde{\tau}})_{i1}(U_{\tilde{\tau}}^*)_{i1} + \sum_{i,j} \frac{1}{\cos\beta M_W}(U_{\tilde{\tau}}^*)_{i1}(U_{\tilde{\tau}})_{j1}((U_{\tilde{\tau}})_{i1}\mathcal{E}_j + (U_{\tilde{\tau}})_{i2}\mathcal{F}_j) \\ & \times C_{12}[k_2^2, k_1^2, k_3^2, m_{\tilde{\nu}_\tau}^2, m_{\tilde{\tau}_i}^2, m_{\tilde{\tau}_j}^2]\Big\} \ , \end{aligned} \tag{6.7}$$

and

$$\begin{aligned} E_{\tilde{l}} = \frac{\alpha}{16\pi \cos\beta M_W^2 c_W s_W^2}\Big\{ & -\cos(\alpha+\beta)\cos\beta M_W M_Z B_0[k_1^2, m_{\tilde{\nu}_\tau}^2, m_{\tilde{\nu}_\tau}^2] \\ & + \sum_i 4\cos(\alpha+\beta)\cos\beta M_W M_Z (U_{\tilde{\tau}})_{i1}(U_{\tilde{\tau}}^*)_{i1} C_{00}[k_1^2, k_3^2, k_2^2, m_{\tilde{\nu}_\tau}^2, m_{\tilde{\nu}_\tau}^2, m_{\tilde{\tau}_i}^2] \\ & + \sum_{i,j} -4\, C_{00}[k_2^2, k_1^2, k_3^2, m_{\tilde{\nu}_\tau}^2, m_{\tilde{\tau}_i}^2, m_{\tilde{\tau}_j}^2](U_{\tilde{\tau}})_{j1}(U_{\tilde{\tau}}^*)_{i1}((U_{\tilde{\tau}})_{i1}\mathcal{E}_j + (U_{\tilde{\tau}})_{i2}\mathcal{F}_j) \\ & + B_0[k_1^2, m_{\tilde{\tau}_i}^2, m_{\tilde{\tau}_j}^2](U_{\tilde{\tau}})_{i1}(U_{\tilde{\tau}}^*)_{j1}((U_{\tilde{\tau}})_{j1}\mathcal{E}_i + (U_{\tilde{\tau}})_{j2}\mathcal{F}_i)\Big\} \ , \\ F_{\tilde{l}} = 0 \end{aligned} \tag{6.8}$$

with the abbreviations

$$\begin{aligned} \mathcal{E}_i &= (\cos(\alpha+\beta)\cos\beta M_W M_Z(1-2s_W^2) - 2\cos\alpha c_W M_\tau^2)(U_{\tilde{\tau}}^*)_{i1} \\ &\quad + c_W(\mu\sin\alpha - \cos\alpha A_\tau^*) M_\tau (U_{\tilde{\tau}}^*)_{i2} \ , \\ \mathcal{F}_i &= c_W(-\cos\alpha A_\tau + \sin\alpha\mu^*) m_\tau (U_{\tilde{\tau}}^*)_{i1} \\ &\quad + 2(\cos(\alpha+\beta)\cos\beta M_W M_Z s_W^2 - \cos\alpha c_W M_\tau^2)(U_{\tilde{\tau}}^*)_{i2} \ . \end{aligned} \tag{6.9}$$

Note the factor $1/\cos\beta$ in these contributions, it leads to enhancement of the contribution of down-type fermions and sfermions at large $\tan\beta$.

The lepton and quark loop contributions to the coefficients are given by

$$\begin{aligned}
D_{lq} = \frac{\alpha}{4\pi \sin 2\beta M_W^2 s_W^2}\Big\{ & -3\sin\alpha\cos\beta m_t^2\big(C_0 + C_2 + 4(C_1 + C_{11} \\
& + C_{12})\big)[k_1^2, k_3^2, k_2^2, m_t^2, m_t^2, m_b^2] + \cos\alpha\sin\beta\big(m_\tau^2(C_1 + 4C_{12} \\
& + C_2)[k_2^2, k_1^2, k_3^2, 0, m_\tau^2, m_\tau^2] + 3m_b^2(C_1 + 4C_{12} + C_2)[k_2^2, k_1^2, k_3^2, m_t^2, m_b^2, m_b^2]\big)\Big\} \,, \qquad (6.10)
\end{aligned}$$

and

$$\begin{aligned}
E_{lq} = \frac{\alpha}{8\pi \sin 2\beta M_W^2 s_W^2}\Big\{ & 3\sin\alpha\cos\beta m_t^2\big(4B_0[k_3^2, m_b^2, m_t^2] + \big((k_1^2 + k_2^2 - k_3^2 + 4m_t^2)C_0 \\
& - 8C_{00} + 2(2k_1^2 + k_2^2 - k_3^2)C_1 + (k_1^2 + 5k_2^2 - k_3^2)C_2\big)[k_1^2, k_3^2, k_2^2, m_t^2, m_t^2, m_b^2]\big) \\
& + \cos\alpha\sin\beta\big(12m_b^2 B_0[k_1^2, m_b^2, m_b^2] + 4m_\tau^2 B_0[k_1^2, m_\tau^2, m_\tau^2] - m_\tau^2\big(8C_{00} \\
& + (k_1^2 - 3k_2^2 - k_3^2)C_1 + (k_1^2 - k_2^2 - 3k_3^2)C_2\big)[k_2^2, k_1^2, k_3^2, 0, m_\tau^2, m_\tau^2] \\
& - 3m_b^2\big(-4m_t^2 C_0 + 8C_{00} + (k_1^2 - 3k_2^2 - k_3^2)C_1 \\
& + (k_1^2 - k_2^2 - 3k_3^2)C_2\big)[k_2^2, k_1^2, k_3^2, m_t^2, m_b^2, m_b^2]\big)\Big\} \,, \\
F_{lq} = -\frac{\alpha}{4\pi \sin 2\beta M_W^2 s_W^2}\Big\{ & 3\sin\alpha\cos\beta m_t^2(C_0 + 2C_1 + C_2)[k_1^2, k_3^2, k_2^2, m_t^2, m_t^2, m_b^2] \\
& + \cos\alpha\sin\beta\big(m_\tau^2(C_1 - C_2)[k_2^2, k_1^2, k_3^2, 0, m_\tau^2, m_\tau^2] \\
& + 3m_b^2(C_1 - C_2)[k_2^2, k_1^2, k_3^2, m_t^2, m_b^2, m_b^2]\big)\Big\} \,. \qquad (6.11)
\end{aligned}$$

The vertex counter term contribution can be written as (see e.g. [135])

$$\begin{aligned}
V^{\mu\nu}_{H^0,CT} = V^{\mu\nu}_{H^0,0}\Big[& \delta Z_e + \delta Z_W + \frac{1}{2}\frac{\delta M_W^2}{M_W^2} + \frac{\delta s_W}{s_W} + \frac{\sin(\beta-\alpha)}{\cos(\beta-\alpha)}(-\cos^2\beta\delta\tan\beta + \frac{1}{2}\delta Z_{h^0H^0}) \\
& + \frac{1}{2}\delta Z_{H^0H^0}\Big] \,, \qquad (6.12)
\end{aligned}$$

where δZ_e is the charge renormalization constant, δZ_W is the field renormalization constant for the W boson, and δM_W^2 the mass counter term of the W boson. δs_W is the renormalization constant for the weak mixing angle. $\delta Z_{h^0H^0}$ and $\delta Z_{H^0H^0}$ are the Higgs field renormalization constants in the mass eigenstate basis, which, together with $\delta Z_{h^0h^0}$ and $\delta Z_{H^0h^0}$, are given in the $\overline{DR}$ scheme as (see the discussion of chapter 4)

$$\begin{aligned}
\delta Z_{h^0h^0} &= -[\mathrm{Re}\,\Sigma'_{h^0h^0}(M_{h^0}^2)]^{\mathrm{div}} \,, \\
\delta Z_{H^0H^0} &= -[\mathrm{Re}\,\Sigma'_{H^0H^0}(M_{H^0}^2)]^{\mathrm{div}} \,, \\
\delta Z_{h^0H^0} &= \delta Z_{H^0h^0} = \frac{\sin\alpha\cos\alpha}{\cos 2\alpha}(\delta Z_{h^0h^0} - \delta Z_{H^0H^0}) \qquad (6.13)
\end{aligned}$$

with M_{h^0}, M_{H^0} denoting the tree-level masses of the two CP-even Higgs bosons. The counter term for $\tan\beta$ is introduced, as in chapter 4, via $\tan\beta \to \tan\beta + \delta\tan\beta$, and is given by

$$\frac{\delta\tan\beta}{\tan\beta} = \left(\frac{\delta\tan\beta}{\tan\beta}\right)^{\overline{DR}} = \frac{1}{2\cos 2\alpha}\left[\delta Z_{h^0h^0} - \delta Z_{H^0H^0}\right]^{\mathrm{div}} \,. \qquad (6.14)$$

As the renormalization scale, we choose $\mu^{\overline{DR}} = M_{A^0}$. The remaining counter terms in Eq. (6.12) and (6.24) below are fixed by on-shell renormalization conditions as in the previous chapter.

Due to the fact that the two CP-even Higgs bosons can mix beyond the tree-level, we need to evaluate the loop corrections to the vertex h^0WW as well. This can be done by simple substitutions. The h^0WW tree-level coupling is obtained by replacing $\cos(\beta-\alpha)$ in Eq. (6.2) with $\sin(\beta-\alpha)$. The corresponding one-loop contributions can be obtained by making the following replacements in Eqs. (6.4-6.11)

$$\sin\alpha \to \cos\alpha \ , \qquad \cos\alpha \to -\sin\alpha \ , \qquad \cos(\alpha+\beta) \to -\sin(\alpha+\beta) \ , \tag{6.15}$$

while the corresponding counter term contribution reads

$$V^{\mu\nu}_{h^0,CT} = V_{H^0}\sin(\beta-\alpha)g^{\mu\nu}\Big[\delta Z_e + \delta Z_W + \frac{1}{2}\frac{\delta M_W^2}{M_W^2} + \frac{\delta s_W}{s_W} + \frac{\cos(\beta-\alpha)}{\sin(\beta-\alpha)}(\cos^2\beta\delta\tan\beta + \frac{1}{2}\delta Z_{H^0h^0}) + \frac{1}{2}\delta Z_{h^0h^0}\Big] \ . \tag{6.16}$$

6.1.2 Correction to the H^0ZZ vertex

Now we turn to the process

$$H^0(k_1) \to Z(k_2,\mu) + Z(k_3,\nu) \ . \tag{6.17}$$

As before, all the three particles can be off-shell.

The tree-level H^0ZZ coupling reads

$$V'^{\mu\nu}_{H^0,0} = \frac{eM_W}{c_W^2 s_W}\cos(\beta-\alpha)g^{\mu\nu} \equiv V'_{H^0}\cos(\beta-\alpha)g^{\mu\nu} \ , \tag{6.18}$$

which, as the tree-level H^0WW coupling, differs from the coupling of the SM Higgs boson and Z bosons by a factor of $\cos(\beta-\alpha)$ and gets strongly suppressed in the decoupling limit $M_{A^0} \gg M_Z$.

The corrected vertex has the same structure as Eq. (6.3), with V_{H^0} replaced by V'_{H^0}. The correction from loops involving the third generation fermions and sfermions to the H^0ZZ vertex can be computed analogously and the corresponding correction to the h^0ZZ vertex follows from the same replacement defined in Eq. (6.15). Due to charge conjugation invariance, the coefficient F vanishes in this case. The contribution of the stop and sbottom loops to the coefficients can be written as

$$\begin{aligned} D_{\tilde{q}} = \frac{\alpha}{36\pi\sin 2\beta M_W^2 c_W s_W^2}\Big\{ & \sum_{i,j,k}\sin\beta(C_1+C_{11}+C_{12})[k_1^2,k_3^2,k_2^2,m^2_{\tilde{b}_i},m^2_{\tilde{b}_j},m^2_{\tilde{b}_k}] \\ & \times \big(\mathcal{G}_{ik}\mathcal{G}^*_{jk}(\mathcal{C}^*_j(U^*_{\tilde{b}})_{i1} + \mathcal{D}^*_j(U^*_{\tilde{b}})_{i2}) + \mathcal{G}_{jk}\mathcal{G}^*_{ik}(\mathcal{C}^*_i(U^*_{\tilde{b}})_{j1} + \mathcal{D}^*_i(U^*_{\tilde{b}})_{j2})\big) \\ & - \cos\beta(C_1+C_{11}+C_{12})[k_1^2,k_3^2,k_2^2,m^2_{\tilde{t}_i},m^2_{\tilde{t}_j},m^2_{\tilde{t}_k}]\big(\mathcal{H}_{ik}\mathcal{H}^*_{jk}(\mathcal{A}^*_j(U^*_{\tilde{t}})_{i1} + \mathcal{B}^*_j(U^*_{\tilde{t}})_{i2}) \\ & + \mathcal{H}_{jk}\mathcal{H}^*_{ik}(\mathcal{A}^*_i(U^*_{\tilde{t}})_{j1} + \mathcal{B}^*_i(U^*_{\tilde{t}})_{j2})\big)\Big\} \ , \end{aligned}$$

$$
\begin{aligned}
E_{\tilde{q}} = \frac{\alpha}{72\pi \sin 2\beta M_W^2 c_W s_W^2} \Big\{ & \sum_{i,j} - \sin\beta B_0[k_1^2, m_{\tilde{b}_i}^2, m_{\tilde{b}_j}^2](\mathcal{C}_j^*(U_{\tilde{b}}^*)_{i1} + \mathcal{D}_j^*(U_{\tilde{b}}^*)_{i2}) \\
& \times \big((3-2s_W^2)^2 (U_{\tilde{b}})_{i1}(U_{\tilde{b}}^*)_{j1} + 4s_W^4 (U_{\tilde{b}})_{i2}(U_{\tilde{b}}^*)_{j2}\big) + \cos\beta B_0[k_1^2, m_{\tilde{b}_i}^2, m_{\tilde{b}_j}^2] \\
& \times (\mathcal{A}_j^*(U_{\tilde{t}}^*)_{i1} + \mathcal{B}_j^*(U_{\tilde{t}}^*)_{i2})\big((3-4s_W^2)^2 (U_{\tilde{t}})_{i1}(U_{\tilde{t}}^*)_{j1} + 16 s_W^4 (U_{\tilde{t}})_{i2}(U_{\tilde{t}}^*)_{j2}\big) \\
& + \sum_{i,j,k} 2\sin\beta C_{00}[k_1^2, k_3^2, k_2^2, m_{\tilde{b}_i}^2, m_{\tilde{b}_j}^2, m_{\tilde{b}_k}^2]\big(\mathcal{G}_{ik}\mathcal{G}_{jk}^*(\mathcal{C}_j^*(U_{\tilde{b}}^*)_{i1} + \mathcal{D}_j^*(U_{\tilde{b}}^*)_{i2}) \\
& + \mathcal{G}_{jk}\mathcal{G}_{ik}^*(\mathcal{C}_i^*(U_{\tilde{b}}^*)_{j1} + \mathcal{D}_i^*(U_{\tilde{b}}^*)_{j2})\big) - 2\cos\beta C_{00}[k_1^2, k_3^2, k_2^2, m_{\tilde{t}_i}^2, m_{\tilde{t}_j}^2, m_{\tilde{t}_k}^2] \\
& \times \big(\mathcal{H}_{ik}\mathcal{H}_{jk}^*(\mathcal{A}_j^*(U_{\tilde{t}}^*)_{i1} + \mathcal{B}_j^*(U_{\tilde{t}}^*)_{i2}) + \mathcal{H}_{jk}\mathcal{H}_{ik}^*(\mathcal{A}_i^*(U_{\tilde{t}}^*)_{j1} + \mathcal{B}_i^*(U_{\tilde{t}}^*)_{j2})\big)\Big\} \,, \qquad (6.19)
\end{aligned}
$$

where the abbreviations $\{\mathcal{A}, \mathcal{B}, \mathcal{C}, \mathcal{D}\}_i$ have been given in Eq. (6.5) and

$$
\begin{aligned}
\mathcal{G}_{ij} &= (-3 + 2s_W^2)(U_{\tilde{b}})_{i1}(U_{\tilde{b}}^*)_{j1} + 2s_W^2 (U_{\tilde{b}})_{i2}(U_{\tilde{b}}^*)_{j2} \,, \\
\mathcal{H}_{ij} &= (-3 + 4s_W^2)(U_{\tilde{t}})_{i1}(U_{\tilde{t}}^*)_{j1} + 4s_W^2 (U_{\tilde{t}})_{i2}(U_{\tilde{t}}^*)_{j2} \,. \qquad (6.20)
\end{aligned}
$$

The contribution of slepton loops are given by

$$
\begin{aligned}
D_{\tilde{l}} = \frac{\alpha}{8\pi M_W c_W s_W^2} \Big\{ & 2\cos(\alpha+\beta) M_Z (C_{12} + C_2 + C_{22})[k_2^2, k_3^2, k_1^2, m_{\tilde{\nu}_\tau}^2, m_{\tilde{\nu}_\tau}^2, m_{\tilde{\nu}_\tau}^2] \\
& - \frac{1}{\cos\beta M_W}(C_1 + C_{11} + C_{12})[k_1^2, k_3^2, k_2^2, m_{\tilde{\tau}_i}^2, m_{\tilde{\tau}_j}^2, m_{\tilde{\tau}_k}^2]\big(\mathcal{M}_{ik}\mathcal{M}_{jk}^*(\mathcal{E}_j^*(U_{\tilde{\tau}}^*)_{i1} + \mathcal{F}_j^*(U_{\tilde{\tau}}^*)_{i2}) \\
& + \mathcal{M}_{jk}\mathcal{M}_{ik}^*(\mathcal{E}_i^*(U_{\tilde{\tau}}^*)_{j1} + \mathcal{F}_i^*(U_{\tilde{\tau}}^*)_{j2})\big)\Big\} \,, \\
E_{\tilde{l}} = \frac{\alpha}{16\pi \cos\beta M_W^2 c_W s_W^2} \Big\{ & -\cos(\alpha+\beta)\cos\beta M_W M_Z (B_0[k_1^2, m_{\tilde{\nu}_\tau}^2, m_{\tilde{\nu}_\tau}^2] \\
& - 4C_{00}[k_2^2, k_3^2, k_1^2, m_{\tilde{\nu}_\tau}^2, m_{\tilde{\nu}_\tau}^2, m_{\tilde{\nu}_\tau}^2]) + \sum_{i,j} B_0[k_1^2, m_{\tilde{\tau}_i}^2, m_{\tilde{\tau}_j}^2](\mathcal{E}_j^*(U_{\tilde{\tau}}^*)_{i1} + \mathcal{F}_j^*(U_{\tilde{\tau}}^*)_{i2}) \\
& \times \big((1-2s_W^2)^2 (U_{\tilde{\tau}})_{i1}(U_{\tilde{\tau}}^*)_{j1} + 4s_W^4 (U_{\tilde{\tau}})_{i2}(U_{\tilde{\tau}}^*)_{j2}\big) - \sum_{i,j,k} 2C_{00}[k_1^2, k_3^2, k_2^2, m_{\tilde{\tau}_i}^2, m_{\tilde{\tau}_j}^2, m_{\tilde{\tau}_k}^2] \\
& \times \big(\mathcal{M}_{ik}\mathcal{M}_{jk}^*(\mathcal{E}_j^*(U_{\tilde{\tau}}^*)_{i1} + \mathcal{F}_j^*(U_{\tilde{\tau}}^*)_{i2}) + \mathcal{M}_{jk}\mathcal{M}_{ik}^*(\mathcal{E}_i^*(U_{\tilde{\tau}}^*)_{j1} + \mathcal{F}_i^*(U_{\tilde{\tau}}^*)_{j2})\big)\Big\} \qquad (6.21)
\end{aligned}
$$

with

$$
\mathcal{M}_{ij} = (-1 + 2s_W^2)(U_{\tilde{\tau}})_{i1}(U_{\tilde{\tau}}^*)_{j1} + 2s_W^2 (U_{\tilde{\tau}})_{i2}(U_{\tilde{\tau}}^*)_{j2} \,, \qquad (6.22)
$$

while the lepton and quark loop contributions read

$$
\begin{aligned}
D_{lq} = -\frac{\alpha}{12\pi \sin 2\beta M_W^2 s_W^2} \Big\{ & 3\cos\alpha \sin\beta m_\tau^2 \big((1 - 4s_W^2 + 8s_W^4) C_0 + C_1 \\
& + 4(1 - 4s_W^2 + 8s_W^4)(C_{12} + C_2 + C_{22})\big)[k_2^2, k_3^2, k_1^2, m_\tau^2, m_\tau^2, m_\tau^2] + \sin\alpha\cos\beta m_t^2 \\
& \times \big((9 + 8s_W^2(-3 + 4s_W^2))C_0 + 9C_1 + 4(9 + 8s_W^2(-3 + 4s_W^2))(C_{12} + C_2 \\
& + C_{22})\big)[k_2^2, k_3^2, k_1^2, m_t^2, m_t^2, m_t^2] + \cos\alpha\sin\beta m_b^2 \big((9 + 4s_W^2(-3 + 2s_W^2))C_0 \\
& + 9C_1 + 4(9 + 4s_W^2(-3 + 2s_W^2))(C_{12} + C_2 + C_{22})\big)[k_2^2, k_3^2, k_1^2, m_b^2, m_b^2, m_b^2]\Big\} \,,
\end{aligned}
$$

$$
\begin{aligned}
E_{lq} = \frac{\alpha}{24\pi \sin 2\beta M_W^2 s_W^2} \Big\{ & 3\cos\alpha \sin\beta m_\tau^2 \big(4(1-2s_W^2+4s_W^4)B_0[k_3^2, m_\tau^2, m_\tau^2] \\
& + \big((k_1^2+k_2^2-k_3^2+4m_\tau^2 - 4(k_1^2+k_2^2-k_3^2)s_W^2 + 8(k_1^2+k_2^2-k_3^2)s_W^4)C_0 - 8C_{00} \\
& + (k_1^2+5k_2^2-k_3^2)C_1 + 2(2k_1^2+k_2^2-k_3^2)C_2 - 8s_W^2(-1+2s_W^2)(4C_{00} - 2k_2^2 C_1 \\
& - (k_1^2+k_2^2-k_3^2)C_2)\big)[k_2^2, k_3^2, k_1^2, m_\tau^2, m_\tau^2, m_\tau^2]\big) + \sin\alpha\cos\beta m_t^2 \big(4(9+4s_W^2(-3+4s_W^2)) \\
& \times B_0[k_3^2, m_t^2, m_t^2] + \big((36m_t^2 + (k_1^2+k_2^2-k_3^2)(9+8s_W^2(-3+4s_W^2)))C_0 - 72C_{00} \\
& + 9(k_1^2+5k_2^2-k_3^2)C_1 + 18(2k_1^2+k_2^2-k_3^2)C_2 - 16s_W^2(-3+4s_W^2)(4C_{00} - 2k_2^2 C_1 \\
& - (k_1^2+k_2^2-k_3^2)C_2)\big)[k_2^2, k_3^2, k_1^2, m_t^2, m_t^2, m_t^2]\big) + \cos\alpha\sin\beta m_b^2 \big(4(9-6s_W^2+4s_W^4) \\
& \times B_0[k_3^2, m_b^2, m_b^2] + \big((36m_b^2 + (k_1^2+k_2^2-k_3^2)(9+4s_W^2(-3+2s_W^2)))C_0 - 72C_{00} \\
& + 9(k_1^2+5k_2^2-k_3^2)C_1 + 18(2k_1^2+k_2^2-k_3^2)C_2 - 8s_W^2(-3+2s_W^2)(4C_{00} - 2k_2^2 C_1 \\
& - (k_1^2+k_2^2-k_3^2)C_2)\big)[k_2^2, k_3^2, k_1^2, m_b^2, m_b^2, m_b^2]\big)\Big\} \, . \qquad (6.23)
\end{aligned}
$$

The corresponding counter term contribution is

$$
\begin{aligned}
V'^{\mu\nu}_{H^0,CT} = V'^{\mu\nu}_{H^0,0}\Big[& \delta Z_e + \delta Z_Z + \frac{1}{2}\frac{\delta M_W^2}{M_W^2} - \frac{\delta s_W}{s_W}\left(2\frac{s_W^2}{c_W^2} - 1\right) + \frac{\sin(\beta-\alpha)}{\cos(\beta-\alpha)}\left(-\cos^2\beta\delta\tan\beta\right. \\
& \left. + \frac{1}{2}\delta Z_{h^0H^0}\right) + \frac{1}{2}\delta Z_{H^0H^0}\Big] \, , \qquad (6.24)
\end{aligned}
$$

and analogously

$$
\begin{aligned}
V'^{\mu\nu}_{h^0,CT} = V'_{H^0}\sin(\beta-\alpha) g^{\mu\nu} \Big[& \delta Z_e + \delta Z_Z + \frac{1}{2}\frac{\delta M_W^2}{M_W^2} - \frac{\delta s_W}{s_W}\left(2\frac{s_W^2}{c_W^2} - 1\right) \\
& + \frac{\cos(\beta-\alpha)}{\sin(\beta-\alpha)}\left(\cos^2\beta\delta\tan\beta + \frac{1}{2}\delta Z_{H^0h^0}\right) + \frac{1}{2}\delta Z_{h^0h^0}\Big] \, . \qquad (6.25)
\end{aligned}
$$

The analytical results presented here for the one-loop corrections to the H^0WW/H^0ZZ coupling can be used as building blocks for more involved processes involving these couplings. If the G_μ scheme described in the previous chapter is chosen for the numerical computation, one can use in the counter term contribution the modified charge renormalization constant $\delta\tilde{Z}_e$

$$
\delta\tilde{Z}_e = \delta Z_e - \frac{1}{2}\Delta r \, , \qquad (6.26)
$$

in which the Δr contribution is incorporated that summarizes the radiative corrections to the muon decay.

6.2 Decay to on-shell gauge bosons

In this section we consider the case that the particles involved in the previously discussed processes are real and compute the corresponding radiative corrections. The decay amplitude can be obtained from the coupling vertex in the previous section by putting all off-shell

momenta on-shell and multiplying with the polarization vectors for the gauge bosons. As discussed in chapter 5, the finite wave function normalization factors for the external Higgs boson has to be taken into account in order to ensure the correct normalization of the S matrix. We define the effective Born amplitude as in chapter 5, which absorbs the Higgs propagator corrections

$$\begin{aligned}\mathcal{M}_{born} &= \sqrt{Z_{H^0}}(\mathcal{M}^0_{H^0} + Z_{H^0h^0}\mathcal{M}^0_{h^0}) \\ &= \sqrt{Z_{H^0}}\mathcal{M}^0_{H^0}(1 + \tan(\beta-\alpha)Z_{H^0h^0}) \ , \end{aligned} \tag{6.27}$$

where Z_{H^0} and $Z_{H^0h^0}$ are the finite wave function normalization factors that are determined by the renormalized self energies of Higgs bosons given in previous chapters by

$$\begin{aligned} Z_{H^0} &= \frac{1}{1 + \mathrm{Re}\hat{\Sigma}'_{H^0}(k^2) - \mathrm{Re}\left(\frac{\hat{\Sigma}^2_{h^0H^0}(k^2)}{k^2 - M^2_{h^0} + \hat{\Sigma}_{h^0}(k^2)}\right)'}\Big|_{k^2 = M'^{\,2}_{H^0}} \ , \\ Z_{H^0h^0} &= -\frac{\hat{\Sigma}_{h^0H^0}(M'^{\,2}_{H^0})}{M'^{\,2}_{H^0} - M^2_{h^0} + \hat{\Sigma}_{h^0}(M'^{\,2}_{H^0})} \end{aligned} \tag{6.28}$$

with M_{h^0} and M'_{H^0} the tree-level mass of h^0 and the physical mass of H^0, respectively. $\mathcal{M}^0_{H^0}$ in Eq. (6.27) denotes the tree-level decay amplitude of H^0. For the decay to W boson pair, it is given by

$$\mathcal{M}^0_{H^0} = V^{\mu\nu}_{H^0,0}\epsilon_\mu\epsilon_\nu \ , \tag{6.29}$$

where $V^{\mu\nu}_{H^0,0}$ is defined in Eq. (6.2) and ϵ_μ is the polarization vector of the external gauge boson. The amplitude for the decay of H^0 into Z bosons can be obtained by straightforward substitutions.

At one-loop level, the decay amplitude can be written as

$$\mathcal{M}_{loop} = \sqrt{Z_{H^0}}(\mathcal{M}^1_{H^0} + Z_{H^0h^0}\mathcal{M}^1_{h^0}) \ . \tag{6.30}$$

For W boson final state, $\mathcal{M}^1_{H^0} = V^{\mu\nu}_{H^0,1}\epsilon_\mu\epsilon_\nu$ with $V^{\mu\nu}_{H^0,1}$ defined in Eq. (6.3). $\mathcal{M}^1_{h^0}$ follows from $\mathcal{M}^1_{H^0}$ by the replacements in Eq. (6.15).

When computing the corrected decay width, the square of the one-loop amplitude $|\mathcal{M}_{loop}|^2$ needs to be included as well, due to the fact that the tree-level coupling can be suppressed so that the square of the one-loop amplitude becomes comparable to the tree-level result. For the decay process $H^0 \to WW$, we compute the one-loop contribution from loops involving all fermions and sfermions and from loops involving only the 3rd generation fermions and sfermions. The full one-loop corrections are not presented, since the full one-loop amplitude is not infrared finite, the numerically important contribution from the square of this amplitude can not be included without a full exploration of the photonic corrections beyond one-loop. However, for the decay $H^0 \to ZZ$, the full one-loop amplitude is infrared finite, hence we also compute the full one-loop corrections for this process.

6.3 Numerical discussions

For the numerical evaluation, we choose the same SM input parameters and SUSY scenarios as in the previous chapter and use the G_μ scheme, i.e. we parametrize the lowest order result with the Fermi constant. The experimental exclusion limits from direct search of supersymmetric particles and the upper bound on the SUSY corrections to the electroweak ρ parameter are taken into account throughout the scan over the SUSY parameter space.

To illustrate the numerical importance of the one-loop corrections, especially in the limit where the CP-odd Higgs boson mass M_{A^0} becomes large, we show in Fig. 6.2 and 6.3, as an example, the dependence of the lowest order and the one-loop corrected partial decay widths on M_{A^0} in the $m_h^{\max}$ scenario for different values of $\tan\beta$. From these figures one can find that for large M_{A^0} values ($M_{A^0} \gtrsim 250\,\text{GeV}$), the one-loop corrections are of significant importance both for small and large $\tan\beta$ values. The tree-level width for $\tan\beta = 30$ is much smaller than that for $\tan\beta = 5$. This is because for relatively large M_{A^0}, the tree-level coupling of H^0 to vector boson pair is suppressed by $\tan\beta$ as well, as one can see from the discussions below Eq. (6.2). In the fermionic and sfermionic sector, the leading contribution is from the third generation fermions and sfermions. For $\tan\beta = 30$, due to a cancellation between the two parts of the effective Born amplitude Eq. (6.27), the tree-level decay width is extremely small at $M_{A^0} \sim 420\,\text{GeV}$. For the decay $H^0 \to ZZ$ (see Fig. 6.3), the decay width falls off rapidly when M_{A^0} goes below $\sim 200\,\text{GeV}$, this is because for such M_{A^0} values, the Higgs boson mass is just above the production threshold of Z boson pair, thus the result is strongly suppressed by the allowed phase space. In Fig. 6.3 we also show the results including the complete one-loop corrections as well as that including only the fermionic and sfermionic corrections. The difference between them indicates that the contributions from other sectors are comparable to the fermionic and sfermionic ones. Although the tree-level decay width decreases quite rapidly with M_{A^0}, the one-loop corrected width for large M_{A^0} turns out to be of comparable size as that for small M_{A^0} values.

Fig. 6.4 and 6.5 show the lowest order and the one-loop corrected partial decay widths as a function of $\tan\beta$ in the $m_h^{\max}$ scenario for different values of M_{A^0}. For both small and large M_{A^0} values, the partial decay width decreases with $\tan\beta$. When M_{A^0} is small, the one-loop contribution yields relatively small corrections, while for large M_{A^0} the one-loop corrections are important and can exceed the lowest order result due to the strong suppression of the tree-level coupling. As in previous plots, the leading contribution from the fermionic and sfermionic sector is from the third generation fermions and sfermions. In Fig. 6.5 also the results including the complete one-loop corrections are depicted. It turns out that the contributions from other sectors are comparable to the fermionic and sfermionic ones for both small and large M_{A^0} values. Due to the identical particles in the final state, for large values of M_{A^0} the decay width of $H^0 \to ZZ$ is roughly half of the decay width of $H^0 \to WW$.

In Fig. 6.6 we show the one-loop corrected partial decay width as well as the relative size of the one-loop corrections for $H^0 \to WW$ in the $m_h^{\max}$ scenario, where the results with the contribution from all fermion and sfermion loops and the results with the contribution only from the third generation fermions and sfermions are depicted. For the size of the width and the relative corrections see the caption of the figure. As illustrated there, the width is

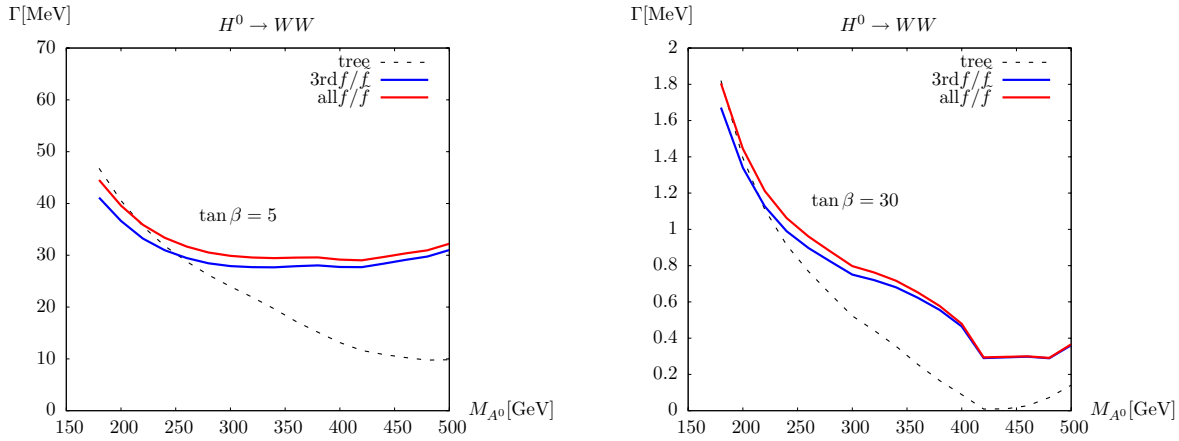

Figure 6.2: The tree-level and one-loop corrected partial decay widths for $H^0 \to WW$ as a function of M_{A^0} in the $m_h^{\max}$ scenario for $\tan\beta = 5, 30$. The results including the contribution from the third generation fermion and sfermion loops, and that including the contribution from all fermion and sfermion loops are depicted.

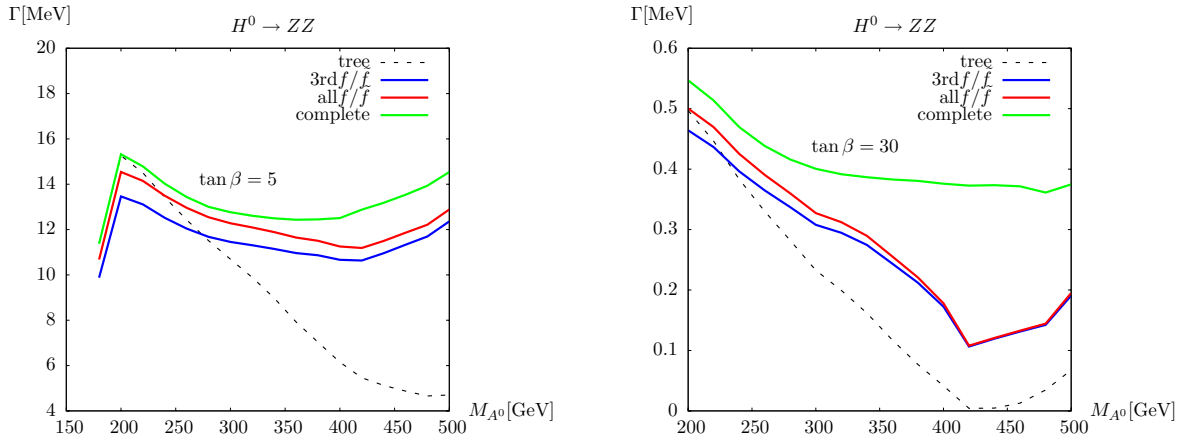

Figure 6.3: The tree-level and one-loop corrected partial decay widths for $H^0 \to ZZ$ as a function of M_{A^0} in the $m_h^{\max}$ scenario for $\tan\beta = 5, 30$. The results with the contribution from the third generation fermion and sfermion loops, with the contribution from all fermion and sfermion loops and with the complete one-loop corrections are depicted.

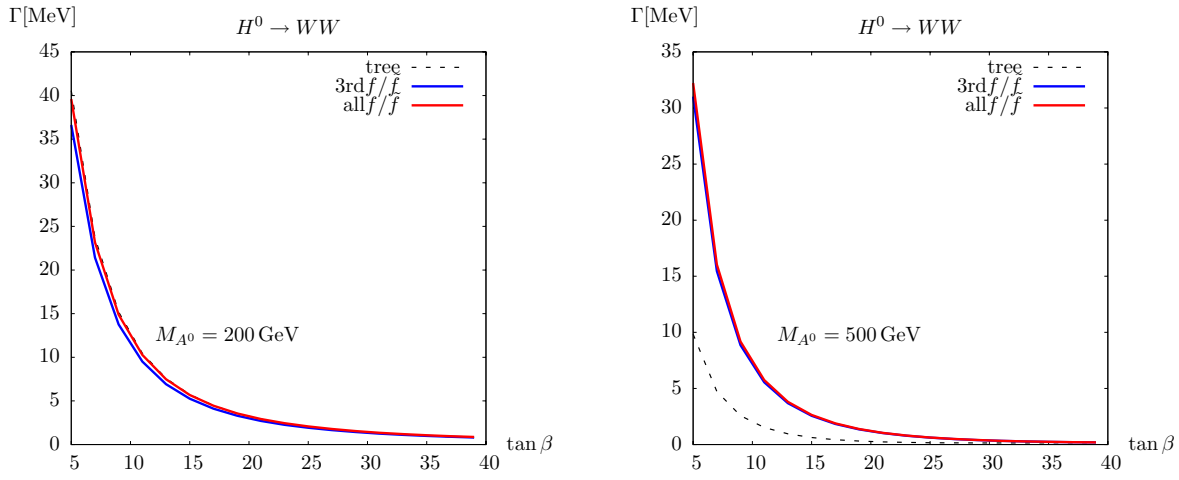

Figure 6.4: The tree-level and one-loop corrected partial decay widths for $H^0 \to WW$ as a function of $\tan\beta$ in the $m_h^{\max}$ scenario for $M_{A^0} = 200, 500\,\mathrm{GeV}$.

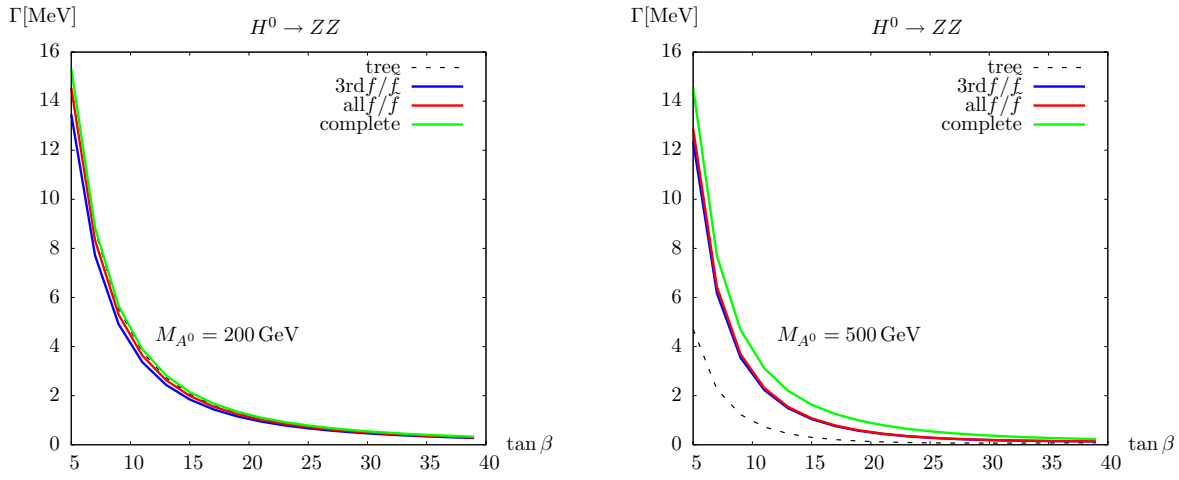

Figure 6.5: The tree-level and one-loop corrected partial decay widths for $H^0 \to ZZ$ as a function of $\tan\beta$ in the $m_h^{\max}$ scenario for $M_{A^0} = 200, 500\,\mathrm{GeV}$, where the results including the complete one-loop corrections are also shown.

rather small for large $\tan\beta$ and M_{A^0} values. It becomes larger when $\tan\beta$ decreases, and the relative size of the loop corrections increases rapidly with M_{A^0} and exceeds the tree-level result when $M_{A^0} > 300 \sim 350\,\text{GeV}$ depending on the values of $\tan\beta$. With the Higgs propagator corrections absorbed into the lowest order result, the other genuine one-loop corrections are negative for small M_{A^0} values, while they are positive for large M_{A^0}.

Fig. 6.7 shows the results in the no-mixing scenario. The region with small $\tan\beta$ and M_{A^0} values is excluded by the limits on the light CP-even Higgs boson mass. The corrected width increases when $\tan\beta$ decreases, the fermionic and sfermionic contributions are negative over a large fraction of the scanned parameter space. In Fig. 6.8 we show the results in the small-α_{eff} scenario. The corrected decay width increases when $\tan\beta$ decreases unless for very large $\tan\beta$ values, where the partial decay width is significantly increased by the Higgs propagator corrections. The relative correction is nearly always negative in the lower half M_{A^0}-$\tan\beta$ plane. At large $\tan\beta$ values, the relative size of the loop corrections increases with $\tan\beta$ and exceeds 100% quite rapidly.

Fig. 6.9, 6.10, and 6.11 illustrate the results for $H^0 \to ZZ$ in the three different scenarios, where we show as well the corrected width including the complete one-loop corrections. These results exhibit similar features to those shown in previous plots for $H^0 \to WW$, but the corresponding width is smaller due to the identical particles in the final state. As illustrated in Fig. 6.9, in the m_h^{max} scenario, at small M_{A^0} values the loop correction is positive if the complete one-loop contribution is taken into account, while it is negative if taking into account only the contribution from the (third generation) fermions and sfermions. This indicates that the contribution from other sectors is positive and larger than that from the fermionic and sfermionic sector for small M_{A^0}. For large M_{A^0} values, the contributions from the fermionic/sfermionic sector and other sectors are both positive. For the no-mixing scenario, in the regions where the loop contributions from the (third generation) fermions and sfermions are negative, they are also compensated by the loop corrections from the other sectors.

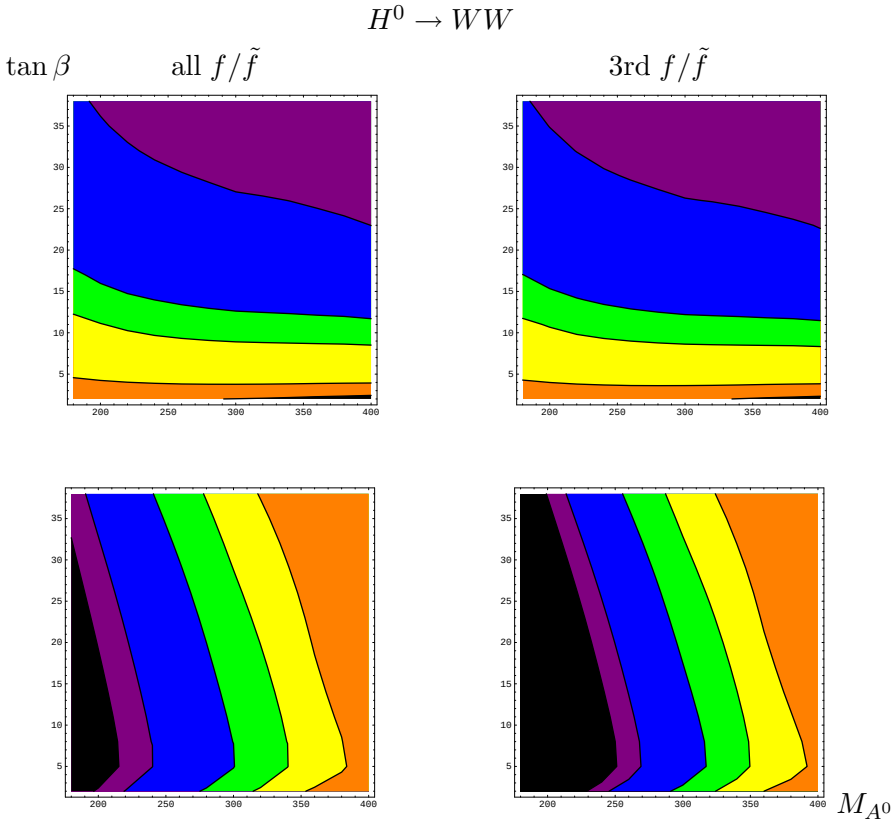

Figure 6.6: Results for the decay width of $H^0 \to WW$ in the $m_h^{\max}$ scenario. The upper row (from left to right) shows the corrected decay width including the contribution from all fermions and sfermions, and that including the contribution only from the third generation, respectively. The purple region corresponds to $\Gamma_{H^0} < 1$MeV, the blue region to 1MeV $< \Gamma_{H^0} < 5$MeV, the green region to 5MeV $< \Gamma_{H^0} < 10$MeV, the yellow region to 10MeV $< \Gamma_{H^0} < 50$MeV, the orange region to 50MeV $< \Gamma_{H^0} < 100$MeV and the black region to $\Gamma_{H^0} > 100$MeV. The lower row shows the corresponding relative correction δ. The purple region corresponds to $0 < \delta < 5\%$, the blue region to $5\% < \delta < 25\%$, the green region to $25\% < \delta < 50\%$, the yellow region to $50\% < \delta < 100\%$, and the orange region to $\delta > 100\%$, the black region corresponds to negative relative correction.

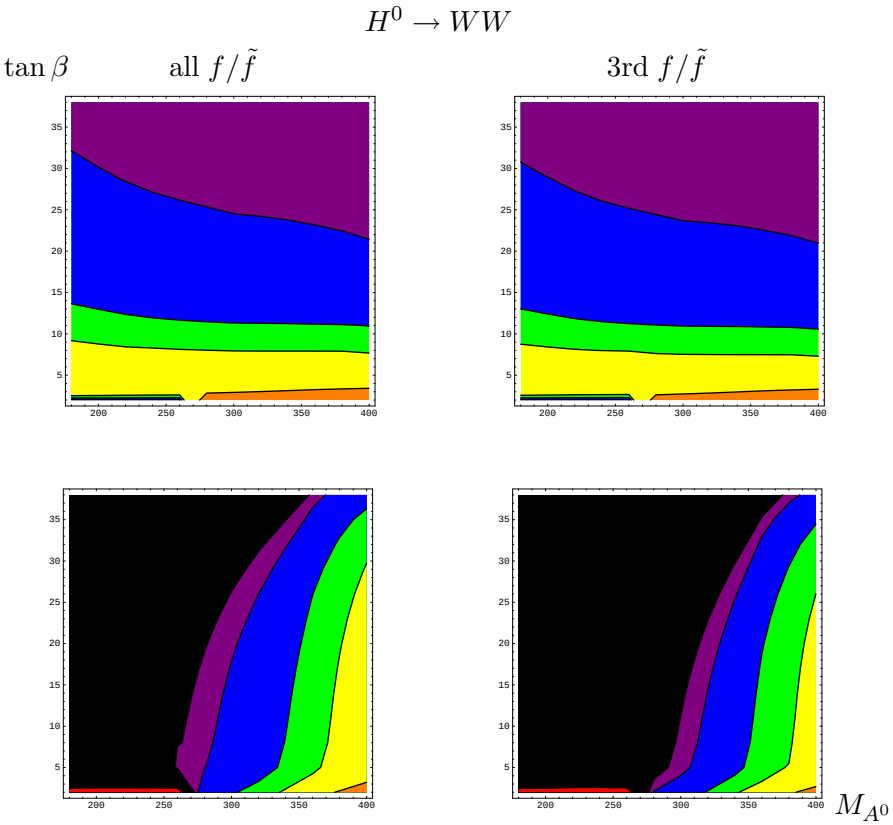

Figure 6.7: Results for the decay width of $H^0 \to WW$ in the no-mixing scenario. The upper row (from left to right) shows the corrected decay width including the contribution from all fermions and sfermions, and that including the contribution only from the third generation, respectively. The sliced region in the lower left corner of each plot is excluded. The lower row shows the corresponding relative correction δ. As in the upper row, the sliced region in the lower left corner of each plot is the excluded region. The color coding here is the same as in Fig. 6.6.

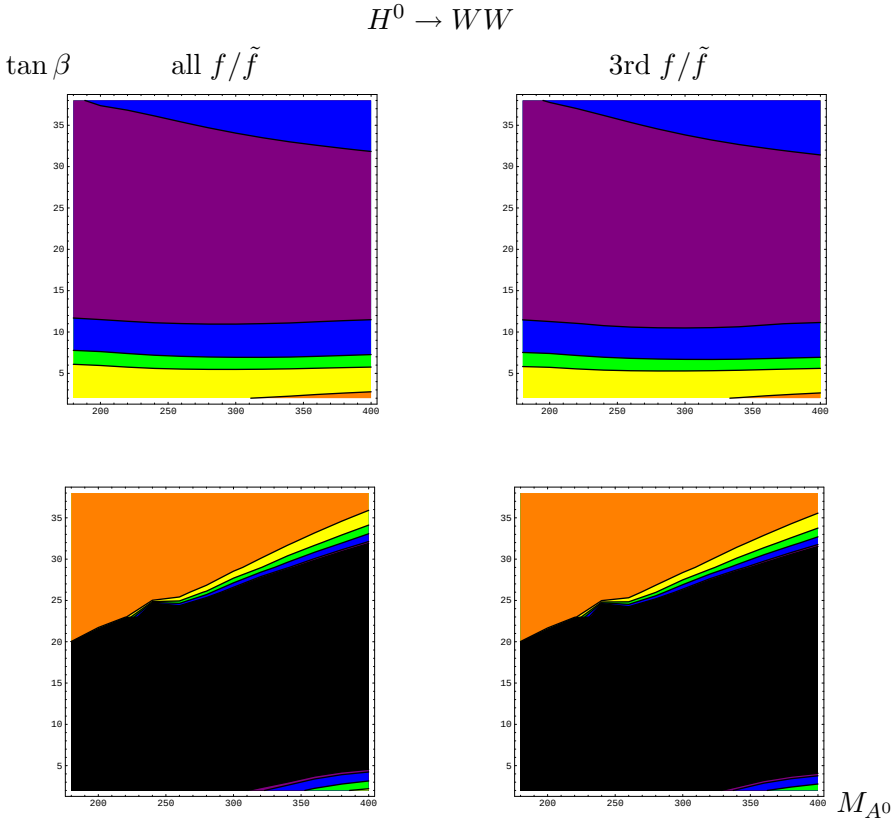

Figure 6.8: Results for the decay width of $H^0 \to WW$ in the small-$\alpha_{\rm eff}$ scenario. The upper row (from left to right) shows the corrected decay width including the contribution from all fermions and sfermions, and that including the contribution only from the third generation, respectively. The lower row shows the corresponding relative correction δ. The color coding is the same as in Fig. 6.6.

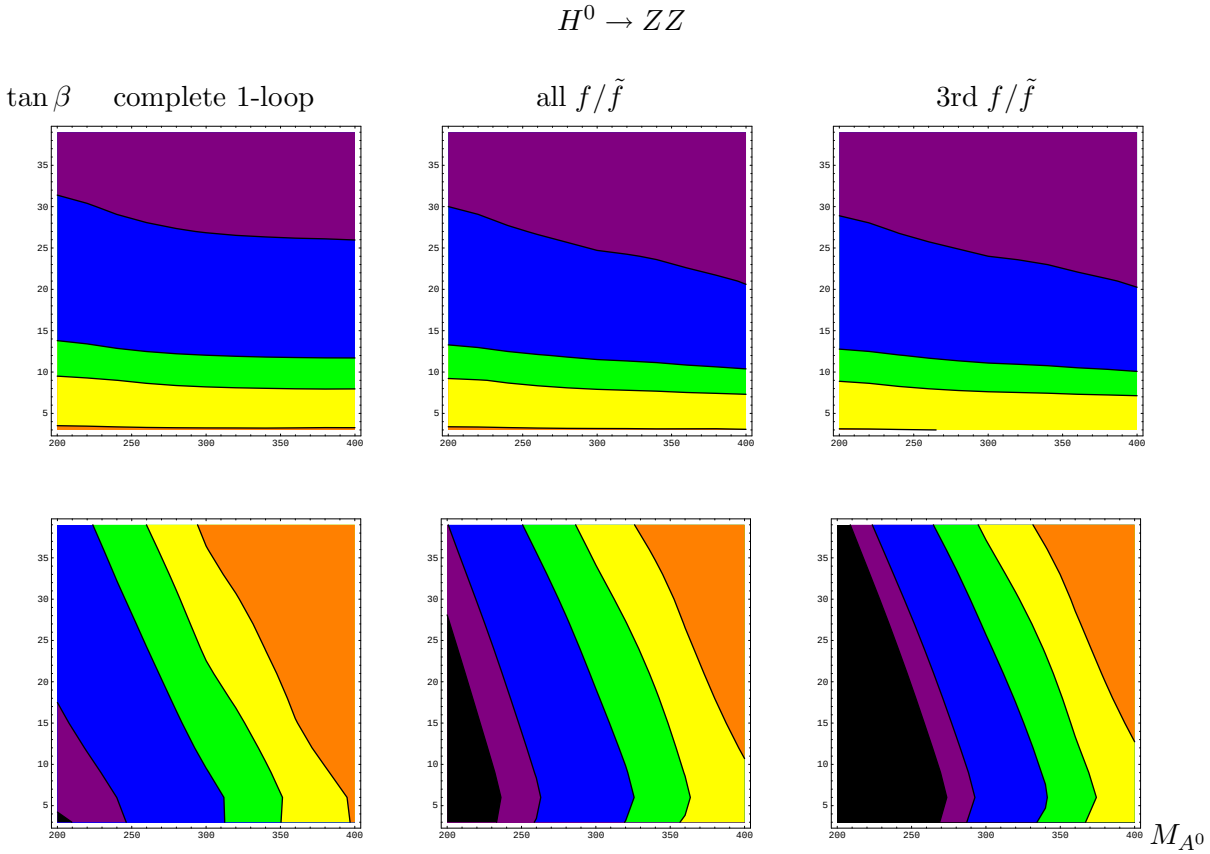

Figure 6.9: Results for the decay width of $H^0 \to ZZ$ in the $m_h^{\max}$ scenario. The upper row (from left to right) shows the corrected decay width including the complete one-loop contributions, that including all fermion and sfermion contributions and that including only the third generation fermion and sfermion contributions, respectively. The purple region corresponds to $\Gamma_{H^0} < 0.5\text{MeV}$, the blue region to $0.5\text{MeV} < \Gamma_{H^0} < 2.5\text{MeV}$, the green region to $2.5\text{MeV} < \Gamma_{H^0} < 5\text{MeV}$, the yellow region to $5\text{MeV} < \Gamma_{H^0} < 25\text{MeV}$, and the orange region to $25\text{MeV} < \Gamma_{H^0} < 50\text{MeV}$. The lower row shows the corresponding relative correction δ. The purple region corresponds to $0 < \delta < 5\%$, the blue region to $5\% < \delta < 25\%$, the green region to $25\% < \delta < 50\%$, the yellow region to $50\% < \delta < 100\%$, and the orange region to $\delta > 100\%$, the black region corresponds to negative relative correction.

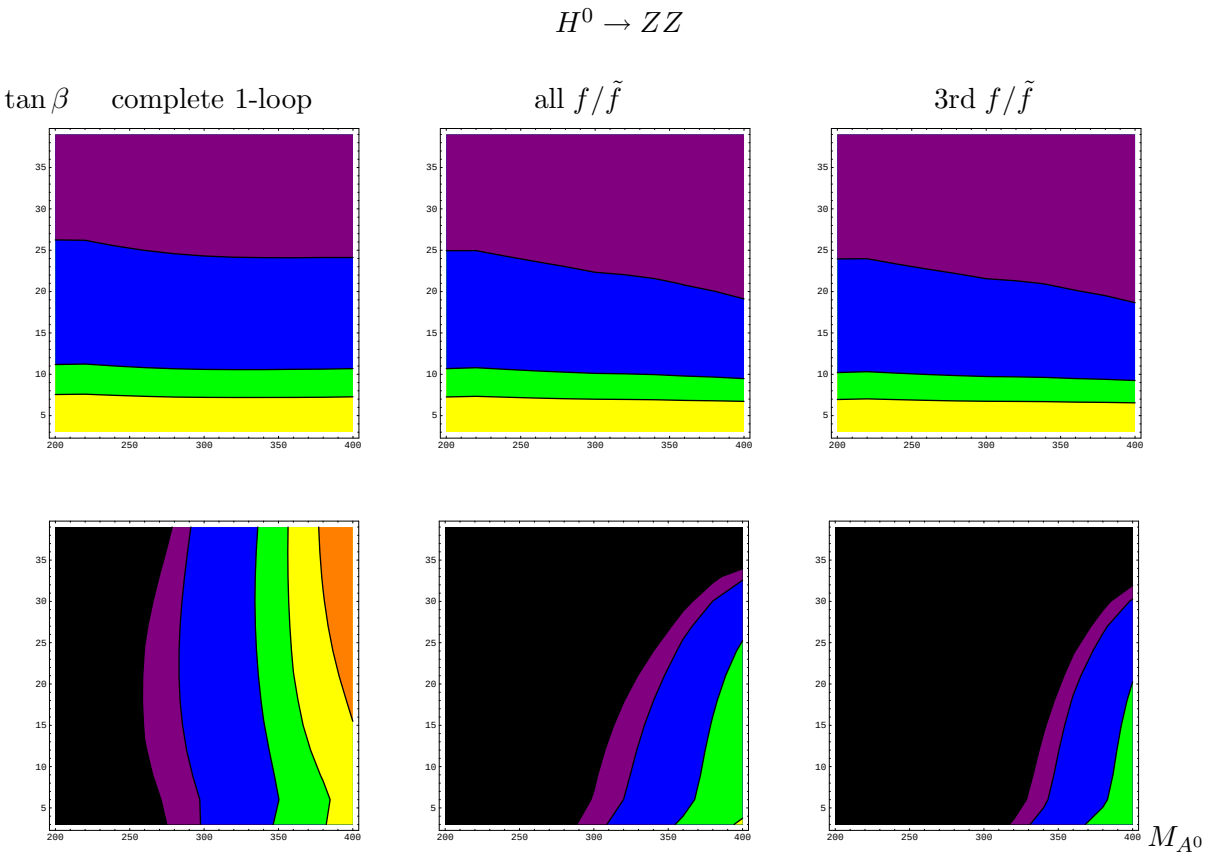

Figure 6.10: Results for the decay width of $H^0 \to ZZ$ in the no-mixing scenario. The upper row (from left to right) shows the corrected decay width including the complete one-loop contributions, that including all fermion and sfermion contributions and that including only the third generation fermion and sfermion contributions, respectively. The lower row shows the corresponding relative correction δ. The color coding is the same as in Fig. 6.9.

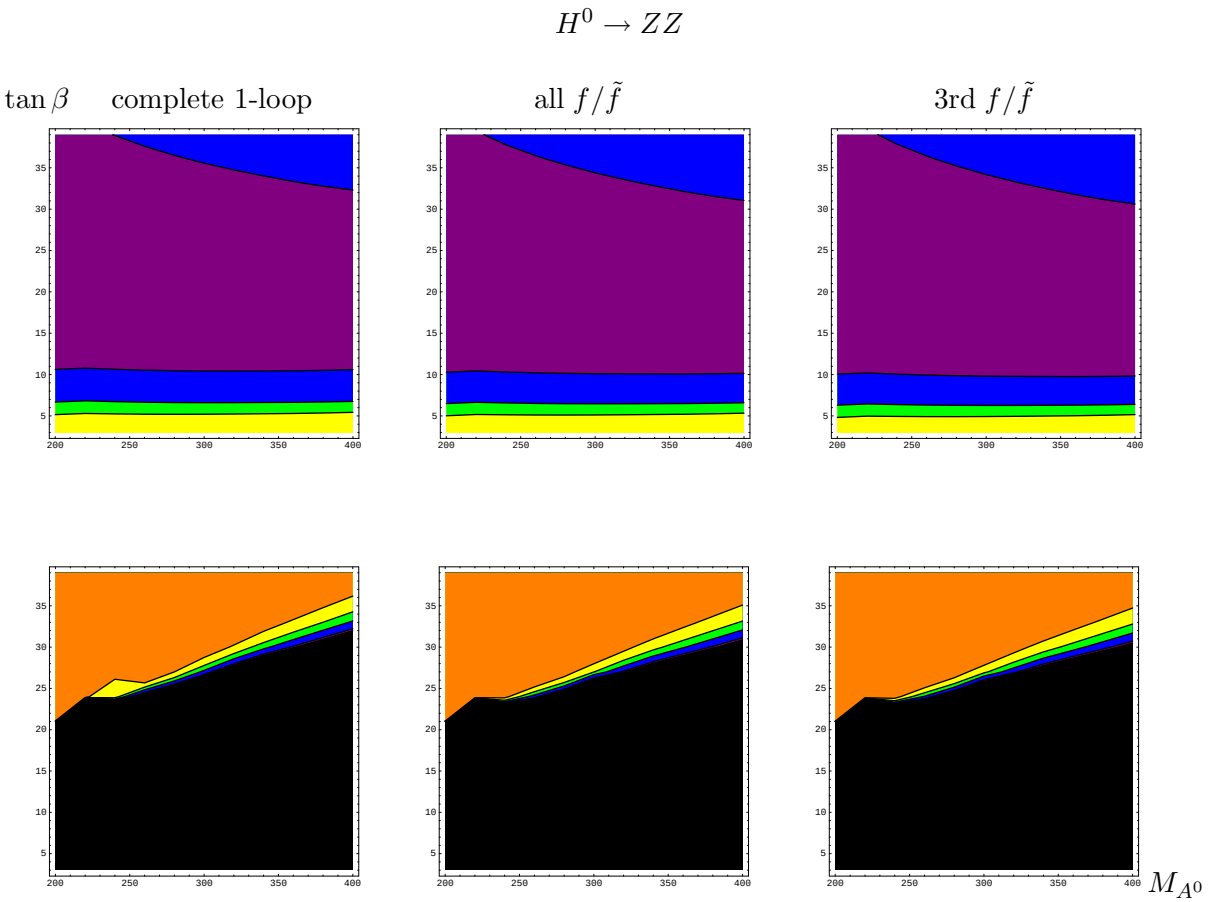

Figure 6.11: Results for the decay width of $H^0 \to ZZ$ in the small-$\alpha_{\rm eff}$ scenario. The upper row (from left to right) shows the corrected decay width including the complete one-loop contributions, that including all fermion and sfermion contributions and that including only the third generation fermion and sfermion contributions, respectively. The lower row shows the corresponding relative correction δ. The color coding is the same as in Fig. 6.9.

Chapter 7

Conclusions

In this thesis we investigated the decay processes of the light and heavy CP-even Higgs bosons in the MSSM and computed the relative $\mathcal{O}(\alpha)$ electroweak corrections, improved by the two-loop corrections provided in the program package FeynHiggs.

The tree-level coupling of the light CP-even Higgs boson in the MSSM, h^0, with the SM fermions or gauge bosons approaches that of the SM Higgs boson with these particles in the decoupling limit. Consequently the lowest order decay width for h^0 or a SM Higgs boson of the same mass to SM fermions will be indistinguishable from each other in this limit. It is therefore of particular interest to investigate the effects of radiative corrections to such decay processes. For the decay of h^0, the virtual corrections arise not only from loops involving the SM particles, but also from loops involving the non-SM particles, i.e. the additional Higgs bosons from the two Higgs doublets of the MSSM and the superpartners of the SM particles. In the decoupling limit, the corrections excluding the genuine SUSY contribution should approach the SM prediction, as in this limit all heavy Higgs bosons decouple. We computed such corrections to the partial decay width of h^0 to fermions via gauge boson pair in the decoupling limit and recovered the SM result. The decoupling of the genuine SUSY particles is governed by their characteristic mass scale. If this mass scale is not much larger than the electroweak scale, they may give rise to sizeable contributions, even in the decoupling limit. However, our results show that they only yield negligible effects in the decoupling limit, indicating that in our case the decoupling behavior is essentially dominated by the mass of the CP-odd Higgs boson mass, even if the one-loop corrections are included. As a consequence, it is rather difficult to distinguish between the light CP-even Higgs boson and the SM one, if the mass of the CP-odd Higgs boson is large.

Care has been taken with the treatment of unstable particles in our process. The width of unstable particles was incorporated according to the factorization scheme. This procedure, however, does not fully eliminate all the singularities that arise when the unstable particle goes on-shell. The scalar loop integrals arising from the photonic diagrams can still contain on-shell singular logarithms. We computed these scalar integrals analytically and included the width of resonant gauge boson afterwards in these singular logarithms. Owing to the upper bound on the light CP-even Higgs boson mass, only one of the intermediate gauge

bosons can become resonant. This allowed us to separate the propagator of the non-resonant gauge boson from the scalar integrals and greatly simplified the analytical evaluation of these integrals. As a byproduct, an analytical expression of the soft singular virtual contribution was obtained, which allowed an explicit check on its cancellation when combining with the real bremsstrahlung contribution. For the treatment of soft and collinear divergences in the real correction, we used two different approaches, namely the phase space slicing and the dipole subtraction approach.

The mixing between Higgs bosons beyond the lowest order can lead to numerically important Higgs propagator corrections. We have absorbed these corrections into the tree-level amplitude. In the presence of the Higgs boson mixing, the contribution due to corrections to the coupling of the heavy CP-even Higgs boson to gauge bosons might play a role. We have taken into account such contributions induced by fermionic and sfermionic loops, especially by loops involving the third generation fermions and sfermions, as they contain potentially large Yukawa couplings and are expected to yield sizeable contributions. It turns out that for the SUSY scenarios investigated in this thesis, these contributions yield visible effects only for small values of the CP-odd Higgs boson mass, and are completely negligible if the CP-odd Higgs boson mass gets large.

We have evaluated invariant mass distributions of the reconstructed gauge boson for different choice of SUSY parameters. If the collinearly emitted photon off the final state fermions is treated inclusively, i.e. if it is combined with the emitting fermion, the relative correction is usually of the order of several percent. If the collinear photon is not combined with the emitting fermion, the relative correction can become much larger. In this case we took into account as well the contribution of the higher order final state radiation. The size of such contribution is usually at percent level.

In the last chapter of this thesis, we also studied the decay of the heavy CP-even Higgs boson of the MSSM into gauge boson pair. The precise knowledge of the decay properties of the heavy Higgs boson can help to distinguish MSSM from other frameworks describing physics beyond the SM. Although the coupling of the heavy CP-even Higgs boson to gauge bosons is usually suppressed at tree-level, it receives numerically important corrections at the one-loop level. In order that our results can be used for more complicated process that involves this coupling, we allowed all three external particles to be off-shell but assumed that the gauge bosons couple to conserved currents. We computed analytically the one-loop corrections to this coupling from fermionic and sfermionic sector, especially from the third generation fermions and sfermions. Owing to the mixing between the Higgs bosons, we gave explicitly the analytical results for the correction to the coupling of the light CP-even Higgs boson to gauge bosons as well. These results were then applied to the decay of the heavy CP-even Higgs boson to on-shell external gauge bosons. After including the Higgs propagator corrections into the tree-level decay amplitude, the lowest order decay width can become extremely small for some value of CP-odd Higgs boson mass and $\tan\beta$. However, it turns out that after including the one-loop radiative corrections, the decay width at small values of M_{A^0} is comparable with that at large M_{A^0} values for a given $\tan\beta$. To illustrate the numerical importance of the loop contribution from different sectors, we showed a comparison of the correction from the third generation fermions and sfermions, the correction from all fermions

and sfermions and the complete one-loop correction. The correction of the third generation fermions and sfermions turned out to be the dominant contribution in the fermionic and sfermionic sector. The contribution from other sectors is comparable to the fermionic and sfermionic contributions and become particularly important for large CP-odd Higgs boson mass.

Appendix A

Spinors

In this Appendix we briefly describe the properties of spinors, more details can be found, e.g. in [156–160].

A.1 Clifford algebra

A Clifford algebra is defined as a set of matrices which satisfy the following anticommutation relations

$$\{\gamma_M, \gamma_N\} = \gamma_M\gamma_N + \gamma_N\gamma_M = 2\,\eta_{MN} \ , \tag{A.1}$$

where M, N can take $0, 1, \ldots, D-1$ for D space-time dimensions, and η_{MN} is the flat metric. Here we assume that only one of the D dimensions is time dimension, since this is the case of most interest. The corresponding metric is then given by $\eta_{MN} = diag(+1, -1, \ldots, -1)$.

Under multiplication the matrices γ_M generate a finite group $CL(D)$ consisting of the following elements

$$CL(D) = \{\pm 1, \pm\gamma_{M_1}, \pm\gamma_{M_1M_2\ldots}, \pm\gamma_{M_1\ldots M_D}\} \ , \tag{A.2}$$

where the indices $M_1, M_2 \ldots$ are all different and $\gamma_{M_1M_2\ldots} = \gamma_{M_1}\gamma_{M_2}\ldots$. The number of elements (or the order) of the group is $2 \times 2^D = 2^{D+1}$. In the case that the space-time dimensions D is even, this group has $2^D + 1$ conjugate classes [1]

$$[\pm 1], [\gamma_{M_1}], [\gamma_{M_1M_2}], \ldots, [\gamma_{M_1\ldots M_D}] \ . \tag{A.3}$$

As the number of irreducible representations of a finite dimensional group equals the number of its conjugate classes [161], the group $CL(D)$ has 2^D+1 irreducible representations. For any

[1] The conjugate class is formed by the elements of a group conjugate to one another, e.g. for an element a of group G, its conjugate elements are given by $g\,a\,g^{-1}$ for any $g \in G$, thus the conjugate class $[a]$ is given by $[a] = \{g\,a\,g^{-1}, \forall g \in G\}$.

two elements γ_A, γ_B, we have $\gamma_A\gamma_B = \pm\gamma_B\gamma_A$, thus $\gamma_A\gamma_B\gamma_A^{-1}\gamma_B^{-1} = \pm 1$, hence the commutator subgroup of $CL(D)$, denoted as $[CL(D), CL(D)]$, which is generated by $\gamma_A\gamma_B\gamma_A^{-1}\gamma_B^{-1}$, has two elements ± 1. In other words, it has order 2. The number of one-dimensional irreducible representations of $CL(D)$ is given by the order of $CL(D)$ divided by the order of $[CL(D), CL(D)]$, which yields $2^{D+1}/2 = 2^D$. Consequently there is only one irreducible representation of $CL(D)$ that is not one-dimensional, its dimension is determined by Burnside's theorem [161] as

$$(2^{D+1} - 1 \times 2^D)^{\frac{1}{2}} = 2^{D/2} \ . \tag{A.4}$$

This representation is also the only irreducible representation of the Clifford algebra that has dimension greater than one, and is known as the spinor representation. Given the irreducible representation of the Clifford algebra γ_M, its transpose γ_M^T forms a representation of the same algebra as well. Due to the fact that there is only one irreducible representation with dimension greater than one, these two representations must be equivalent, thus there exists a matrix C relating them as follows

$$\gamma_M^T = -C\gamma_M C^{-1} \ . \tag{A.5}$$

The matrix C is the so-called charge conjugation matrix.

In the case that the space-time dimensions D is odd, the matrix

$$\gamma_D = \gamma_0\gamma_1\cdots\gamma_{D-1} \tag{A.6}$$

commutes with all matrices $\gamma_M (M = 0, 1, \ldots, D-1)$ and their products. Thus in addition to γ_D, $-\gamma_D$ also forms a conjugate class by itself. The number of conjugate classes of $CL(D)$ in odd dimensions is one more than that in even dimensions. This implies that the group $CL(D)$ has $2^D + 2$ irreducible representations. As in the even dimensions case, 2^D of them are one-dimensional, which means that in odd space-time dimensions the group $CL(D)$ has two irreducible representations that have dimension greater than one. The dimensions of these two representations should divide 2^{D+1} [161], the order of the group $CL(D)$, hence they can be written as 2^i and 2^j respectively. Burnside's theorem then yields

$$2^{2i} + 2^{2j} = 2^D \ , \tag{A.7}$$

thus $i = j = \frac{D-1}{2}$. Actually, the fact that γ_D commutes with all γ_M matrices implies that it must be a multiple of the identity matrix, therefore the matrix γ_{D-1} can be expressed in terms of the other $D-2$ matrices with the help of the defining anticommutation relation of the Clifford algebra as

$$\gamma_{D-1} = a\,\gamma_0\gamma_1\cdots\gamma_{D-2} \ , \tag{A.8}$$

where a can take two different values depending on D [159, 160]. The two irreducible representations are indeed generated by the unique irreducible representation for $\gamma_M (M = 0, 1, \ldots, D-1)$ with the two choices of a for the matrix γ_{D-1}, respectively. So both of them should be of dimension $2^{\frac{D-1}{2}}$.

A Dirac spinor ψ can be represented by a vector of $2^{D/2}$ or $2^{\frac{D-1}{2}}$ components for even or odd space-time dimensions D, respectively. Its infinitesimal transformation is generated by γ_{MN}

$$\delta\psi = \frac{1}{4}\omega^{MN}\gamma_{MN}\,\psi \ . \tag{A.9}$$

The conjugate Dirac spinor is defined as

$$\bar{\psi} = \psi^\dagger\gamma^0 \ , \tag{A.10}$$

so that the combination $\bar{\psi}\psi$ is invariant under the transformation (A.9). Dirac spinors are reducible spinors. There are two possibilities to obtain from it irreducible spinors. For even space-time dimensions, one can construct the following matrix

$$\gamma_{D+1} = \eta\gamma_0\gamma_1\ldots\gamma_{D-1} \ , \tag{A.11}$$

which commutes with γ_{MN}, thus applying γ_{D+1} to a spinor just yields another spinor. This matrix can be used to construct projection operators. For this purpose, one requires $(\gamma_{D+1})^2 = 1$, which leads to

$$\eta^2 = (-1)^{\frac{D-2}{2}} \ . \tag{A.12}$$

The projection operators can be defined as

$$P_\pm = \frac{1}{2}(1 \pm \gamma_{D+1}) \ , \tag{A.13}$$

which clearly satisfy

$$P_\pm P_\mp = 0 \ , \qquad P_\pm^2 = P_\pm \ , \qquad P_\pm + P_\mp = 1 \ . \tag{A.14}$$

The Dirac spinor can be decomposed into two inequivalent Weyl spinors by applying the projection operators

$$\psi_\pm = P_\pm\psi \ . \tag{A.15}$$

Note that the construction of γ_{D+1} is possible only for even space-time dimensions, therefore Weyl spinors exist only in even space-time dimensions.

Another possibility to obtain irreducible spinors is to impose the reality condition or Majorana condition

$$\psi^c = C\bar{\psi}^T = \psi \ , \tag{A.16}$$

where ψ^c is the charge conjugate of ψ. This condition is equivalent to requiring the Majorana conjugate $\bar{\psi}^M$ of spinor ψ be equal to its Dirac conjugate $\bar{\psi}$

$$\bar{\psi}^M = \psi^T C = \bar{\psi} = \psi^\dagger\gamma^0 \ . \tag{A.17}$$

This condition selects the allowed space-time dimensions for the existence of Majorana spinors to be $D = 2, 4, 10, 12\ldots$ [159,160], i.e. in odd space-time dimensions, there are no Majorana spinors. In ordinary quantum field theories, we are mainly concerned with the case that the space-time dimensions $D = 4$, in which both Weyl and Majorana spinors are allowed.

A.2 Spinors in four dimensions

In four space-time dimensions, a Dirac spinor ψ is represented by a vector with four components. The projection operators can be written as

$$P_{\pm} = \frac{1}{2}(1 \pm \gamma_5) \tag{A.18}$$

with the matrix

$$\gamma_5 = \gamma^5 = -i\gamma_0\gamma_1\gamma_2\gamma_3 \ . \tag{A.19}$$

In the chiral or Weyl representation of the gamma matrices are given by

$$\gamma^\mu = \begin{pmatrix} 0 & \sigma^\mu \\ \bar{\sigma}^\mu & 0 \end{pmatrix}$$

with

$$\begin{aligned} \sigma^\mu &= (I, \sigma) \ , \\ \bar{\sigma}^\mu &= (I, -\sigma) = \sigma_\mu \ , \end{aligned} \tag{A.20}$$

where I represents the two-dimensional identity matrix and σ the Pauli matrices, the matrix γ_5 takes a diagonal form

$$\gamma_5 = \begin{pmatrix} -I & 0 \\ 0 & I \end{pmatrix} \ .$$

In this representation the projection operator $\frac{1}{2}(1-\gamma_5)$ projects out the upper two components of the Dirac spinor, which have left chirality, while $\frac{1}{2}(1+\gamma_5)$ projects out the lower two components which have right chirality. A Dirac spinor can thus be decomposed as

$$\psi = \psi_L + \psi_R \ , \tag{A.21}$$

where ψ_L and ψ_R are Weyl spinors with

$$\psi_L = \begin{pmatrix} \lambda_\alpha \\ 0 \end{pmatrix} \ , \qquad \psi_R = \begin{pmatrix} 0 \\ \bar{\chi}^{\dot{\alpha}} \end{pmatrix} \ ,$$

where different labels $\alpha, \dot{\alpha}$ are used to indicate that these two Weyl spinors transform differently under the Lorentz group and $\alpha, \dot{\alpha} = 1, 2$. The action of the Lorentz group on the Weyl spinors can be represented by a matrix M of $SL(2, C)$, which yields the following transformation properties

$$\begin{aligned} &\lambda_\alpha \to M_\alpha^{\ \beta} \lambda_\beta \ , && \lambda^\alpha \to (M^{-1})_\beta^{\ \alpha} \lambda^\beta \ , \\ &\bar{\chi}_{\dot{\alpha}} \to (M^*)_{\dot{\alpha}}^{\ \dot{\beta}} \bar{\chi}_{\dot{\beta}} \ , && \bar{\chi}^{\dot{\alpha}} \to [(M^*)^{-1}]_{\dot{\beta}}^{\ \dot{\alpha}} \bar{\chi}^{\dot{\beta}} \ , \end{aligned} \tag{A.22}$$

where $\bar{\chi}_{\dot{\alpha}} = (\chi_\alpha)^*$, $\bar{\chi}^{\dot{\alpha}} = (\chi^\alpha)^*$ and the spinor indices are raised and lowered as follows

$$\begin{aligned} \lambda^\alpha &= \epsilon^{\alpha\beta}\lambda_\alpha \ , & \lambda_\alpha &= \epsilon_{\alpha\beta}\lambda^\alpha \ , \\ \bar{\chi}^{\dot{\alpha}} &= \epsilon^{\dot{\alpha}\dot{\beta}}\bar{\chi}_{\dot{\beta}} \ , & \bar{\chi}_{\dot{\alpha}} &= \epsilon_{\dot{\alpha}\dot{\beta}}\bar{\chi}^{\dot{\beta}} \end{aligned} \tag{A.23}$$

with

$$\epsilon_{\alpha\beta} = \epsilon_{\dot{\alpha}\dot{\beta}} = \begin{pmatrix} 0 & 1 \\ -1 & 0 \end{pmatrix} \ , \qquad \epsilon^{\alpha\beta} = \epsilon^{\dot{\alpha}\dot{\beta}} = \begin{pmatrix} 0 & -1 \\ 1 & 0 \end{pmatrix} \ .$$

As a consequence, the following identities hold

$$\begin{aligned} \chi^\alpha\lambda_\alpha &= -\chi_\alpha\lambda^\alpha = \lambda^\alpha\chi_\alpha \ , \\ \bar{\chi}_{\dot{\alpha}}\bar{\lambda}^{\dot{\alpha}} &= -\bar{\chi}^{\dot{\alpha}}\bar{\lambda}_{\dot{\alpha}} = \bar{\lambda}_{\dot{\alpha}}\bar{\chi}^{\dot{\alpha}} \ , \\ \chi^\alpha(\sigma^\mu)_{\alpha\dot{\alpha}}\bar{\lambda}^{\dot{\alpha}} &= \chi_\alpha(\bar{\sigma}^\mu)^{\dot{\alpha}\alpha}\bar{\lambda}_{\dot{\alpha}} = -\bar{\lambda}_{\dot{\alpha}}(\bar{\sigma}^\mu)^{\dot{\alpha}\alpha}\chi_\alpha \ . \end{aligned} \tag{A.24}$$

Given a two-component Weyl spinor λ, one can always construct a four-component Majorana spinor

$$\psi_M = \begin{pmatrix} \lambda_\alpha \\ \bar{\lambda}^{\dot{\alpha}} \end{pmatrix} \ ,$$

which clearly has the same number of degrees of freedom as a Weyl spinor. In the Majorana representation of gamma matrices, which is a representation equivalent to the Weyl representation with purely imaginary gamma matrices, the Majorana spinors can be realized as real spinors.

In four dimensions, the following identities hold for the gamma matrices

$$\begin{aligned} \gamma^\mu\gamma_\mu &= 4 \ , \\ \gamma^\mu\gamma^\nu\gamma^\mu &= -2\gamma^\nu \ , \\ \gamma^\mu\gamma^\nu\gamma^\rho\gamma_\mu &= 4g^{\nu\rho} \ , \\ \gamma^\mu\gamma^\nu\gamma^\rho\gamma^\sigma\gamma_\mu &= -2\gamma^\sigma\gamma^\rho\gamma^\nu \ , \\ \gamma^\mu\gamma^\nu\gamma^\rho\gamma^\sigma\gamma^\lambda\gamma_\mu &= 2(\gamma^\lambda\gamma^\nu\gamma^\rho\gamma^\sigma + \gamma^\sigma\gamma^\rho\gamma^\nu\gamma^\lambda) \ , \end{aligned} \tag{A.25}$$

while the traces of the gamma matrices fulfill

$$\begin{aligned} \mathrm{Tr}(\gamma^\mu) &= \mathrm{Tr}(\gamma_5) = 0 \ , \\ \mathrm{Tr}(\gamma^\mu\gamma_5) &= \mathrm{Tr}(\gamma^\mu\gamma^\nu\gamma_5) = 0 \ , \\ \mathrm{Tr}(\gamma^{\mu_1}\gamma^{\mu_2}\cdots\gamma^{\mu_n}) &= 0 \quad \text{for } n \text{ odd} \ , \\ \mathrm{Tr}(\gamma^\mu\gamma^\nu) &= 4g^{\mu\nu} \ , \\ \mathrm{Tr}(\gamma^\mu\gamma^\nu\gamma^\rho\gamma^\sigma) &= 4(g^{\mu\nu}g^{\rho\sigma} - g^{\mu\rho}g^{\nu\sigma} + g^{\mu\sigma}g^{\nu\rho}) \ , \\ \mathrm{Tr}(\gamma^\mu\gamma^\nu\gamma^\rho\gamma^\sigma\gamma_5) &= -4i\epsilon^{\mu\nu\rho\sigma} \ . \end{aligned} \tag{A.26}$$

A.3 Grassmann variables

In the discussion of superspace in chapter 3, anticommuting Grassmann variables have been introduced. The basic feature of such variables is that they satisfy the anticommutation relations

$$\{\theta_\alpha, \theta_\beta\} = \{\theta_\alpha, \bar{\theta}_{\dot{\beta}}\} = \{\bar{\theta}_{\dot{\alpha}}, \bar{\theta}_{\dot{\beta}}\} = 0 \ , \tag{A.27}$$

which clearly indicates that

$$\theta_\alpha^2 = \bar{\theta}_{\dot{\alpha}}^2 = 0 \ . \tag{A.28}$$

The derivatives of Grassmann variables also anticommute

$$\{\frac{\partial}{\partial\theta_\alpha}, \frac{\partial}{\partial\theta_\beta}\} = \{\frac{\partial}{\partial\theta_\alpha}, \frac{\partial}{\partial\bar{\theta}_{\dot{\beta}}}\} = \{\frac{\partial}{\partial\bar{\theta}_{\dot{\alpha}}}, \frac{\partial}{\partial\bar{\theta}_{\dot{\beta}}}\} = 0 \ . \tag{A.29}$$

The integration over Grassmann variables is defined such that

$$\int d\theta_\alpha = \int d\bar{\theta}_{\dot{\alpha}} = 0 \ , \tag{A.30}$$

and

$$\int d\theta_\alpha \, \theta_\alpha = \int d\bar{\theta}_{\dot{\alpha}} \, \bar{\theta}_{\dot{\alpha}} = 1 \ , \tag{A.31}$$

where no summation over the indices is implied. The volume elements in superspace are defined as

$$d^4\theta = d^2\theta \, d^2\bar{\theta} \tag{A.32}$$

with

$$\begin{aligned} d^2\theta &= -\frac{1}{4} d\theta^\alpha \, d\theta_\alpha \ , \\ d^2\bar{\theta} &= -\frac{1}{4} d\bar{\theta}_{\dot{\alpha}} \, d\bar{\theta}^{\dot{\alpha}} \ . \end{aligned} \tag{A.33}$$

When integrating over the superspace, only the following integrals are non-zero

$$\int d^2\theta \, \theta^2 = 1 \ , \qquad \int d^2\bar{\theta} \, \bar{\theta}^2 = 1 \ . \tag{A.34}$$

Other useful identities concerning the Grassmann variables can be found, e.g. in ref. [30].

Appendix B

Loop Integrals

In this Appendix we discuss the one-loop integrals relevant for this thesis. As discussed in previous chapters, the one-loop photonic diagrams can lead to infrared singularities and/or on-shell singularities in the soft photon region. These singularities are contained in the scalar integrals resulting from such diagrams. The analytical results of these scalar integrals are listed at the end of this Appendix. For other loop integrals that do not involve the on-shell singularities, we used LoopTools [133, 134], which is a program package based on FF [162], to perform a numerical evaluation.

B.1 One-loop integrals

We closely follow the conventions and notation of refs. [136, 138]. The general one-loop tensor N-point integrals can be written as

$$T^N_{\mu_1\ldots\mu_p}(p_1,\ldots,p_{N-1},m_0,\ldots,m_{N-1}) = \frac{(2\pi\mu)^{4-D}}{i\pi^2}\int d^Dq \frac{q_{\mu_1}\cdots q_{\mu_p}}{N_0N_1\cdots N_{N-1}} \tag{B.1}$$

with the denominators given by

$$N_i = (q+p_i)^2 - m_i^2 + i\epsilon\ , \quad i=0,\ldots,N-1\ , \quad p_0 = 0\ , \tag{B.2}$$

where the loop momentum q is integrated over D space-time dimensions. The momenta in the parentheses of the above equation represent the momenta of the internal propagators, and $i\epsilon$ ($\epsilon > 0$) is an infinitesimal imaginary part that gives rise to imaginary part of the S-matrix element. The parameter μ has mass dimension and is introduced to keep the mass dimension of the integral fixed when varying the space-time dimension D.

The one-loop tensor integrals can be decomposed into tensors constructed from the momenta appearing in the denominators and the metric tensor with symmetric coefficient func-

tions according to Lorentz covariance. For instance,

$$T^N_{\mu_1} = \sum_{i=1}^{N-1} p_{i\mu_1} T^N_i \ ,$$
$$T^N_{\mu_1\mu_2} = \sum_{i,j=1}^{N-1} p_{i\mu_1} p_{j\mu_2} T^N_{ij} + g_{\mu_1\mu_2} T^N_{00} \ , \tag{B.3}$$

where the coefficient functions can be iteratively reduced to scalar integrals [140]. Note that for $N > 4$, the term involving the metric tensor $g_{\mu_1\mu_2}$ in the decomposition is redundant, since the metric can be expressed in terms of four linearly dependent momentum vectors that span the Minkowski space [136].

Within this thesis, up to five-point integrals are involved. We will denote the one- to five-point integrals by A, B, C, D, E following [139]. The corresponding scalar integrals are denoted by a subscript 0. The simplest scalar integral is the scalar one-point integral A_0, the explicit result of which is given by

$$A_0(m) = m^2(\Delta - \ln\frac{m^2}{\mu^2} + 1) + \mathcal{O}(D-4) \ , \tag{B.4}$$

with

$$\Delta = \frac{2}{4-D} - \gamma_E + \ln 4\pi \ , \tag{B.5}$$

where $\Gamma(x)$ is the Gamma function, and $\gamma_E = 0.5772\ldots$ is the Euler constant. The UV divergence is contained in Δ.

The result of the scalar two-point integral reads

$$B_0(p_1, m_0, m_1) = \Delta + 2 - \ln\frac{m_0 m_1}{\mu^2} + \frac{m_0^2 - m_1^2}{p_1^2}\ln\frac{m_1}{m_0}$$
$$- \frac{m_0 m_1}{p_1^2}\left(\frac{1}{r} - r\right)\ln r + \mathcal{O}(D-4) \ , \tag{B.6}$$

where the variable r satisfies

$$r + \frac{1}{r} = \frac{m_0^2 + m_1^2 - p_1^2 - i\epsilon}{m_0 m_1} \ . \tag{B.7}$$

Note that the scalar two-point integral itself is IR finite, only its derivative with respect to its momentum argument can be IR divergent. The expressions for the scalar three- and four-point integrals are rather lengthy and can be found in ref. [101].

The tensor integrals can be reduced to scalar integrals by inverting their covariant decompositions. For example, the decomposition equation of the vector two-point integral

$$B_\mu(p_1, m_0, m_1) = p_{1\mu} B_1 \tag{B.8}$$

can be inverted as

$$B_1 = \frac{1}{p_1^2} p_1^\mu B_\mu \ , \tag{B.9}$$

where the right-hand side can be expanded as a linear combination of one- and two-point scalar integrals, yielding

$$B_1(p_1, m_0, m_1) = \frac{1}{2p_1^2} \left(A_0(m_0) - A_0(m_1) - (p_1^2 + m_0^2 - m_1^2) B_0(p_1, m_0, m_1) \right) \ . \tag{B.10}$$

Analogously one obtains

$$\begin{aligned} B_{00} &= \frac{1}{2(D-1)} \left(A_0(m_1) + 2m_0^2 B_0(p_1, m_0, m_1) + (p_1^2 + m_0^2 - m_1^2) B_1(p_1, m_0, m_1) \right) \ , \\ B_{11} &= \frac{1}{2(D-1)p_1^2} \left((D-2) A_0(m_1) - 2m_0^2 B_0(p_1, m_0, m_1) \right. \\ &\quad \left. - D(p_1^2 + m_0^2 - m_1^2) B_1(p_1, m_0, m_1) \right) \ . \end{aligned} \tag{B.11}$$

The results for the coefficient functions of the three- and four-point tensor integrals can be found in ref. [136].

The drawback of this reduction procedure is that it involves the inverse of the Gram determinant, which is a determinant constructed from the scalar products of the momenta appearing in the tensor integral. At the boundary of phase space where the momenta become linearly dependent, the Gram determinant becomes vanishing and leads to numerical instability. For the N-point integrals with $N \leq 4$ usually the Gram determinant vanishes only at the boundary of phase space, while for $N > 4$, the Gram determinant can also vanish within the phase space. In ref. [136] a reduction method of five-point integrals has been developed in which the occurrence of the inverse Gram determinant can be avoided. This reduction method has been implemented in LoopTools [133].

In the following we list the UV-divergent parts of the commonly used tensor integrals

$$\begin{aligned} A_0(m_0) &= -\frac{2m_0^2}{D-4} \ , \\ B_0(p_1, m_0, m_1) &= -\frac{2}{D-4} \ , \\ B_1(p_1, m_0, m_1) &= \frac{1}{D-4} \ , \\ B_{00}(p_1, m_0, m_1) &= \frac{1}{6(D-4)} (p_1^2 - 3m_0^2 - 3m_1^2) \ , \\ B_{11}(p_1, m_0, m_1) &= -\frac{2}{3(D-4)} \ , \\ C_{00}(p_1, p_2, m_0, m_1, m_2) &= -\frac{1}{2(D-4)} \ , \\ C_{00i}(p_1, p_2, m_0, m_1, m_2) &= \frac{1}{6(D-4)} \ , \\ D_{0000}(p_1, p_2, p_3, m_0, m_1, m_2, m_3) &= -\frac{1}{12(D-4)} \ . \end{aligned} \tag{B.12}$$

The momentum dependence of the UV-divergent part of the coefficient function B_{00} indicates that its derivative is also UV-divergent, the derivation of its UV-divergent part is straightforward.

B.2 Analytical results for on-shell singular scalar integrals

In the following we give explicitly the analytical expressions of the scalar integrals that involve the on-shell singularities discussed in chapter 5. The variables k_i, S_{ij} and the mass parameters are also defined there. These integrals are computed for zero gauge boson width. The real squared mass M_V^2 should be replaced by the complex squared mass $M_V^2 - iM_V\Gamma_V$ in the result, if singularities arise when $k_\pm^2$ approaches M_V^2.

$$B_0(k_-^2, 0, M_V) = \Delta + 2 + \ln\left(\frac{\mu^2}{M_V^2}\right) + \left(\frac{M_V^2}{k_-^2} - 1\right)\ln\left(1 - \frac{k_-^2}{M_V^2} - i\epsilon\right) \ ,$$

$$\begin{aligned} C_0(-k_4, -k_-, 0, m_\mu, M_V) = \frac{1}{k_-^2}\Big\{ & \ln\frac{k_-^2}{m_\mu^2}\,\ln\Big(1 - \frac{k_-^2}{M_V^2} - i\epsilon\Big) + \mathrm{Li}_2\Big(1 - \frac{k_-^2}{M_V^2} - i\epsilon\Big) \\ & - \frac{\pi^2}{6}\Big\} \ , \end{aligned}$$

$$\begin{aligned} C_0(-k_2, k_-, 0, m_e, M_V) = \frac{1}{S_{24} + S_{25}}\Big\{ & \Big[\ln\Big(M_V^2 m_e^2\Big) - 2\ln\Big(-S_{24} - S_{25} - i\epsilon\Big)\Big] \\ & \times \ln\Big(M_V^2 - k_-^2 - i\epsilon\Big) - \ln\Big(M_V^2 - k_-^2 - S_{24} - S_{25} - i\epsilon\Big) \\ & \times \Big[\ln\Big(M_V^2 m_e^2\Big) - \ln\Big(M_V^2 - k_-^2 - S_{24} - S_{25} - i\epsilon\Big)\Big] \\ & + \ln^2\Big(-S_{24} - S_{25} - i\epsilon\Big) + 2\mathrm{Li}_2\Big(\frac{M_V^2 - k_-^2}{S_{24} + S_{25}}\Big) \\ & + \mathrm{Li}_2\Big(\frac{k_-^2 + S_{24} + S_{25}}{M_V^2}\Big) - \mathrm{Li}_2\Big(\frac{k_-^2}{M_V^2}\Big) + \frac{\pi^2}{3}\Big\} \ , \end{aligned}$$

$$\begin{aligned} D_0(-k_2, k_-, k_4, \lambda, m_e, M_V, m_\mu) = \frac{1}{S_{24}(k_-^2 - M_V^2)}\Big\{ & -\mathrm{Li}_2\Big(-\frac{S_{25} + k_-^2 - M_V^2}{S_{24}}\Big) \\ & + 2\ln\Big(-\frac{S_{24}}{m_e m_\mu} - i\epsilon\Big)\ln\Big(\frac{M_V^2 - k_-^2}{\lambda M_V} - i\epsilon\Big) \\ & - \ln^2\Big(\frac{m_\mu}{M_V}\Big) - \ln^2\Big(\frac{M_V^2 - k_-^2 - S_{24} - S_{25}}{m_e M_V} - i\epsilon\Big) \\ & - \frac{\pi^2}{3}\Big\} \ , \end{aligned}$$

$$
\begin{aligned}
D_0(-k_2,-k_+,k_4,\lambda,m_e,M_V,m_\mu) = \frac{1}{S_{24}(k_+^2-M_V^2)}\Big\{ &-\mathrm{Li}_2\Big(-\frac{S_{34}+k_+^2-M_V^2}{S_{24}}\Big)\\
&+2\ln\Big(-\frac{S_{24}}{m_e m_\mu}-i\epsilon\Big)\ln\Big(\frac{M_V^2-k_+^2}{\lambda M_V}-i\epsilon\Big)\\
&-\ln^2\Big(\frac{m_e}{M_V}\Big)-\ln^2\Big(\frac{M_V^2-k_+^2-S_{24}-S_{34}}{m_\mu M_V}-i\epsilon\Big)\\
&-\frac{\pi^2}{3}\Big\}\,. \qquad \text{(B.13)}
\end{aligned}
$$

Appendix C

Properties of Unstable Particles

Most particles in the SM and beyond are unstable, experimentally these unstable particles manifest themselves as resonances in scattering amplitudes. There exists no S-matrix element for external unstable particles, since they can not be defined as asymptotic states. In perturbation theory unstable particles can be viewed as intermediate states and are associated with poles in S-matrix with finite imaginary parts and lie below the real axis in the p^2 plane. The emergence of imaginary part can be understood as follows. Stable particles do not decay, it follows from the optical theorem that the imaginary part of the sum of all one-particle-irreducible (1PI) insertions to the propagator of the stable particle, hence the imaginary part of the pole vanishes. Unstable particles do decay, optical theorem then implies a non-zero imaginary part of the pole. A proper description of unstable particles in perturbation theory requires a resummation of 1PI insertions to its propagator (Dyson resummation). It has been shown that unitarity and causality are preserved in renormalizable theories involving unstable particles [163].

For processes that involve an unstable particle as intermediate state, singularities can occur in the lowest order calculations due to the presence of the propagator of the unstable particle. These singularities can be avoided by including higher-order self energy corrections of the unstable particle, the imaginary part of which, behaves as a regulator in the vicinity of the resonance and produces the Breit-Wigner shape of resonance. The inclusion of higher-order self energy corrections corresponds to the following resummation

$$\begin{aligned} D(p^2) &= \frac{i}{p^2 - m_0^2 + i\epsilon}(1 + \frac{-\Sigma(p^2)}{p^2 - m_0^2 + i\epsilon} + \cdots) \\ &= \frac{i}{p^2 - m_0^2 + \Sigma(p^2)} \,, \end{aligned} \tag{C.1}$$

where m_0 denotes the unrenormalized bare mass and $\Sigma(p^2)$ denotes the 1PI self energy.

From a practical point of view, the incorporation of the resummed propagator into the amplitude of a resonant process is not trivial. If this is done naively, for example, simply replacing the bare propagator in the tree-level amplitude by the dressed (resummed) one, usually the fulfillment of basic field theoretical requirements, e.g. gauge invariance of the

S-matrix element will be spoiled. This is not surprising, since this naive replacement only takes into account higher-order corrections to part of the tree-level amplitude and thereby mixes different perturbative orders, while gauge invariance is guaranteed order by order in perturbation theory. There have been different proposals to implement the width of unstable particles in a consistent manner, each of them has its own advantage and disadvantage and may be suitable for different circumstances. We have described some of such proposals in Chapter 5.

Another issue related to unstable particle is the definition of its mass and width. In the usual field theoretic treatment, the inverse propagator of a stable particle has a real pole position, which can be identified as the physical mass of the stable particle

$$D^{-1}(m_{ph}^2) = m_{ph}^2 - m_0^2 + \Sigma(m_{ph}^2) = 0 \ , \tag{C.2}$$

thus

$$m_{ph}^2 = m_0^2 - \Sigma(m_{ph}^2) \ . \tag{C.3}$$

When generalizing to unstable particles, the pole position becomes complex, one defines the pole of the real part of the inverse propagator as the on-shell mass

$$\mathrm{Re}\, D^{-1}(m_{os}^2) = m_{os}^2 - m_0^2 + \mathrm{Re}\, \Sigma(m_{os}^2) = 0 \ , \tag{C.4}$$

yielding

$$m_{os}^2 = m_0^2 - \mathrm{Re}\, \Sigma(m_{os}^2) \ . \tag{C.5}$$

From this definition the propagator can be expanded as

$$D(p^2) = \frac{\left(1 + \mathrm{Re}\, \Sigma'(m_{os}^2)\right)^{-1}}{p^2 - m_{os}^2 + i\frac{\mathrm{Im}\, \Sigma(p^2)}{1+\mathrm{Re}\, \Sigma'(m_{os}^2)}} \ . \tag{C.6}$$

It then follows that the on-shell width can be defined as

$$m_{os}\Gamma_{os} = \frac{\mathrm{Im}\, \Sigma(m_{os}^2)}{1 + \mathrm{Re}\, \Sigma'(m_{os}^2)} \ . \tag{C.7}$$

Sirlin [164] showed that the on-shell definition of the unstable particle mass is gauge-dependent beyond the one-loop order. This gauge dependence can be erased by going to a more fundamental "pole definition" that involves the position of the entire complex pole, which is an intrinsic property of the S-matrix. According to the pole definition, the mass and width of the unstable particle are defined by the following decomposition of the pole

$$m^2 = m_0^2 - \Sigma(m^2) = m_p^2 - i m_p \Gamma_p \ . \tag{C.8}$$

Note that the width Γ_p is a higher-order effect, expanding the self energy in Γ_p/m_p yields

$$\begin{aligned} m_p^2 &= m_0^2 - \mathrm{Re}\, \Sigma(m_p^2) - \mathrm{Im}\, \Sigma(m_p^2)\mathrm{Im}\, \Sigma'(m_p^2) + \mathcal{O}(\alpha^3) \ , \\ m_p\Gamma_p &= \mathrm{Im}\, \Sigma(m_p^2)[1 - \mathrm{Re}\, \Sigma'(m_p^2) + (\mathrm{Re}\, \Sigma'(m_p^2))^2 - \frac{1}{2}\mathrm{Im}\, \Sigma(m_p^2)\mathrm{Im}\, \Sigma''(m_p^2) + \mathcal{O}(\alpha^3)] \ . \end{aligned} \tag{C.9}$$

From Eq. (C.5) and (C.9) one can see that these two definitions coincide at one-loop level and differ only by two-loop contributions, thus the on-shell mass is, as the pole mass, gauge invariant at one-loop order. The higher order contributions lead to a difference of the definition of unstable particle masses in these two schemes. For example, for the W boson the mass difference is 27 MeV, and for the Z boson it is 34 MeV.

Bibliography

[1] S. L. Glashow, *Partial Symmetries of Weak Interactions*, *Nucl. Phys.* **22** (1961) 579–588.

S. Weinberg, *A Model of Leptons*, *Phys. Rev. Lett.* **19** (1967) 1264–1266.

A. Salam, *Weak and Electromagnetic Interactions*, . Originally printed in *Svartholm: Elementary Particle Theory, Proceedings Of The Nobel Symposium Held 1968 At Lerum, Sweden*, Stockholm 1968, 367-377.

[2] M. Gell-Mann, *A Schematic Model of Baryons and Mesons*, *Phys. Lett.* **8** (1964) 214–215.

H. Fritzsch, M. Gell-Mann, and H. Leutwyler, *Advantages of the Color Octet Gluon Picture*, *Phys. Lett.* **B47** (1973) 365–368.

G. 't Hooft unpublisher remarks at the Marseille Conference on Yang-Mills Fields, 1972.

D. J. Gross and F. Wilczek, *Ultraviolet Behavior of Non-abelian Gauge Theories*, *Phys. Rev. Lett.* **30** (1973) 1343–1346.

H. D. Politzer, *Reliable Perturbative Results for Strong Interactions?*, *Phys. Rev. Lett.* **30** (1973) 1346–1349.

[3] H. P. Nilles, *Supersymmetry, Supergravity and Particle Physics*, *Phys. Rept.* **110** (1984) 1–162.

[4] H. E. Haber and G. L. Kane, *The Search for Supersymmetry: Probing Physics Beyond the Standard Model*, *Phys. Rept.* **117** (1985) 75–263.

[5] S. Heinemeyer, W. Hollik, and G. Weiglein, *FeynHiggs: A Program for the Calculation of the Masses of the Neutral CP-even Higgs Bosons in the MSSM*, *Comput. Phys. Commun.* **124** (2000) 76–89, [hep-ph/9812320].

T. Hahn, W. Hollik, S. Heinemeyer, and G. Weiglein, *Precision Higgs Masses with FeynHiggs 2.2*, hep-ph/0507009.

T. Hahn *et al.*, *Higher-order Corrected Higgs Bosons in FeynHiggs 2.5*, *Pramana* **69** (2007) 861–870, [hep-ph/0611373].

[6] **CMS** Collaboration, G. L. Bayatian *et al.*, *CMS Technical Design Report, Volume II: Physics performance*, *J. Phys.* **G34** (2007) 995–1579.

[7] P. W. Higgs, *Broken Symmetries and the Masses of Gauge Bosons*, *Phys. Rev. Lett.* **13** (1964) 508–509.

P. W. Higgs, *Spontaneous Symmetry Breakdown Without Massless Bosons*, *Phys. Rev.* **145** (1966) 1156–1163.

F. Englert and R. Brout, *Broken Symmetry and the Mass of Gauge Vector Mesons*, *Phys. Rev. Lett.* **13** (1964) 321–322.

G. S. Guralnik, C. R. Hagen, and T. W. B. Kibble, *Global Conservation Laws and Massless Particles*, *Phys. Rev. Lett.* **13** (1964) 585–587.

T. W. B. Kibble, *Symmetry Breaking in Non-abelian Gauge Theories*, *Phys. Rev.* **155** (1967) 1554–1561.

[8] J. Goldstone, *Field Theories with Superconductor Solutions*, *Nuovo Cim.* **19** (1961) 154–164.

J. Goldstone, A. Salam, and S. Weinberg, *Broken Symmetries*, *Phys. Rev.* **127** (1962) 965–970.

[9] **Particle Data Group** Collaboration, W. M. Yao *et al.*, *Review of Particle Physics*, *J. Phys.* **G33** (2006) 1–1232.

[10] **LEP Working Group for Higgs Boson Searches** Collaboration, R. Barate *et al.*, *Search for the Standard Model Higgs Boson at LEP*, *Phys. Lett.* **B565** (2003) 61–75, [hep-ex/0306033].

[11] **LEP** Collaboration, J. Alcaraz *et al.*, *Precision Electroweak Measurements and Constraints on the Standard Model*, 0712.0929.

[12] N. Cabibbo, *Unitary Symmetry and Leptonic Decays*, *Phys. Rev. Lett.* **10** (1963) 531–532.

[13] M. Kobayashi and T. Maskawa, *CP Violation in the Renormalizable Theory of Weak Interaction*, *Prog. Theor. Phys.* **49** (1973) 652–657.

[14] M. E. Peskin and D. V. Schroeder, *An Introduction to Quantum Field Theory*. Reading, USA: Addison-Wesley (1995) 842 p.

S. Weinberg, *The Quantum Theory of Fields. Vol. 1: Foundations*. Cambridge, UK: Univ. Pr. (1995) 609 p.

S. Weinberg, *The Quantum Theory of Fields. Vol. 2: Modern Applications*. Cambridge, UK: Univ. Pr. (1996) 489 p.

M. Bohm, A. Denner, and H. Joos, *Gauge Theories of the Strong and Electroweak Interaction*. Stuttgart, Germany: Teubner (2001) 784 p.

M. Kaku, *Quantum Field Theory: A Modern Introduction*. New York, USA: Oxford Univ. Pr. (1993) 785 p.

S. Pokorski, *Gauge Field Theories*. Cambridge, Uk: Univ. Pr. (1987) 394 P. (Cambridge Monographs On Mathematical Physics).

[15] A. Djouadi, *The Anatomy of Electro-weak Symmetry Breaking. I: The Higgs Boson in the Standard Model*, *Phys. Rept.* **457** (2008) 1–216, [hep-ph/0503172].

[16] G. 't Hooft, *Renormalization of Massless Yang-Mills Fields*, *Nucl. Phys.* **B33** (1971) 173–199.

G. 't Hooft, *Renormalizable Lagrangians for Massive Yang-Mills Fields*, *Nucl. Phys.* **B35** (1971) 167–188.

[17] L. D. Faddeev and V. N. Popov, *Feynman Diagrams for the Yang-Mills Field*, *Phys. Lett.* **B25** (1967) 29–30.

[18] Y. A. Golfand and E. P. Likhtman, *Extension of the Algebra of Poincare Group Generators and Violation of p Invariance*, *JETP Lett.* **13** (1971) 323–326.

D. V. Volkov and V. P. Akulov, *Is the Neutrino a Goldstone Particle?*, *Phys. Lett.* **B46** (1973) 109–110.

[19] J. Wess and B. Zumino, *Supergauge Transformations in Four-Dimensions*, *Nucl. Phys.* **B70** (1974) 39–50.

[20] W. A. Bardeen, C. T. Hill, and M. Lindner, *Minimal Dynamical Symmetry Breaking of the Standard Model*, *Phys. Rev.* **D41** (1990) 1647.

E. Farhi and L. Susskind, *Technicolor*, *Phys. Rept.* **74** (1981) 277.

[21] S. R. Coleman and J. Mandula, *All Possible Symmetries of the S Matrix*, *Phys. Rev.* **159** (1967) 1251–1256.

[22] R. Haag, J. T. Lopuszanski, and M. Sohnius, *All Possible Generators of Supersymmetries of the S Matrix*, *Nucl. Phys.* **B88** (1975) 257.

[23] S. Weinberg, *Gauge Hierarchies*, *Phys. Lett.* **B82** (1979) 387.

M. J. G. Veltman, *The Infrared - Ultraviolet Connection*, *Acta Phys. Polon.* **B12** (1981) 437.

R. K. Kaul and P. Majumdar, *Cancellation of Quadratically Divergent Mass Corrections in Globally Supersymmetric Spontaneously Broken Gauge Theories*, *Nucl. Phys.* **B199** (1982) 36.

[24] T. Inami, H. Nishino, and S. Watamura, *Cancellation of Quadratic Divergences and Uniqueness of Softly Broken Supersymmetry*, *Phys. Lett.* **B117** (1982) 197.

N. G. Deshpande, R. J. Johnson, and E. Ma, *On the Uniqueness of Supersymmetry for the Cancellation of Quadratic Divergences*, *Phys. Lett.* **B130** (1983) 61.

[25] L. Brink, O. Lindgren, and B. E. W. Nilsson, *N=4 Yang-Mills Theory on the Light Cone*, *Nucl. Phys.* **B212** (1983) 401.

L. Brink, O. Lindgren, and B. E. W. Nilsson, *The Ultraviolet Finiteness of the N=4 Yang-Mills Theory*, *Phys. Lett.* **B123** (1983) 323.

[26] S. Mandelstam, *Light Cone Superspace and the Ultraviolet Finiteness of the N=4 Model*, *Nucl. Phys.* **B213** (1983) 149–168.

[27] M. F. Sohnius and P. C. West, *Conformal Invariance in N=4 Supersymmetric Yang-Mills Theory*, *Phys. Lett.* **B100** (1981) 245.

[28] P. S. Howe, K. S. Stelle, and P. C. West, *A Class of Finite Four-Dimensional Supersymmetric Field Theories*, *Phys. Lett.* **B124** (1983) 55.

[29] A. Neveu and J. H. Schwarz, *Factorizable Dual Model of Pions*, *Nucl. Phys.* **B31** (1971) 86–112.

P. Ramond, *Dual Theory for Free Fermions*, *Phys. Rev.* **D3** (1971) 2415–2418.

[30] J. Wess and J. Bagger, *Supersymmetry and Supergravity.* Princeton, USA: Univ. Pr. (1992) 259 p.

[31] P. C. West, *Introduction to Supersymmetry and Supergravity.* Singapore, Singapore: World Scientific (1990) 425 p.

[32] D. Bailin and A. Love, *Supersymmetric Gauge Field Theory and String Theory.* Bristol, UK: IOP (1994) 322 p. (Graduate student series in physics).

[33] M. F. Sohnius, *Introducing Supersymmetry*, *Phys. Rept.* **128** (1985) 39–204.

[34] S. P. Martin, *A Supersymmetry Primer*, `hep-ph/9709356`.

D. I. Kazakov, *Beyond the Standard Model (in search of supersymmetry)*, `hep-ph/0012288`.

[35] J. D. Lykken, *Introduction to Supersymmetry*, `hep-th/9612114`.

[36] A. Bilal, *Introduction to Supersymmetry*, `hep-th/0101055`.

[37] P. D. B. Collins, A. D. Martin, and E. J. Squires, *Particle Physics and Cosmology.* NEW YORK, USA: WILEY (1989) 496p.

[38] M. M. Nojiri *et al.*, *Physics Beyond the Standard Model: Supersymmetry*, `0802.3672`.

[39] A. Salam and J. A. Strathdee, *Supergauge Transformations*, *Nucl. Phys.* **B76** (1974) 477–482.

[40] S. Ferrara, J. Wess, and B. Zumino, *Supergauge Multiplets and Superfields*, *Phys. Lett.* **B51** (1974) 239.

[41] S. Weinberg, *The Quantum Theory of fields. Vol. 3: Supersymmetry.* Cambridge, UK: Univ. Pr. (2000) 419 p.

[42] P. Argyres, "An Introduction to Global Supersymmetry." http://www.physics.uc.edu/ argyres/661/index.html.

[43] R. N. Mohapatra, *Unification and Supersymmetry. The Frontiers of Quark - Lepton Physics.* Berlin, Germany: Springer (1986) 309 P. (Contemporary Physics).

[44] A. Salam and J. A. Strathdee, *On Superfields and Fermi-Bose Symmetry*, *Phys. Rev.* **D11** (1975) 1521–1535.

[45] M. T. Grisaru, W. Siegel, and M. Rocek, *Improved Methods for Supergraphs*, *Nucl. Phys.* **B159** (1979) 429.

[46] N. Seiberg, *Naturalness Versus Supersymmetric Nonrenormalization Theorems*, *Phys. Lett.* **B318** (1993) 469–475, [hep-ph/9309335].

N. Seiberg, *The Power of Holomorphy: Exact Results in 4-D Susy Field Theories*, hep-th/9408013.

[47] L. O'Raifeartaigh, *Spontaneous Symmetry Breaking for Chiral Scalar Superfields*, *Nucl. Phys.* **B96** (1975) 331.

[48] P. Fayet and J. Iliopoulos, *Spontaneously Broken Supergauge Symmetries and Goldstone Spinors*, *Phys. Lett.* **B51** (1974) 461–464.

[49] D. Z. Freedman, P. van Nieuwenhuizen, and S. Ferrara, *Progress Toward a Theory of Supergravity*, *Phys. Rev.* **D13** (1976) 3214–3218.

S. Deser and B. Zumino, *Consistent Supergravity*, *Phys. Lett.* **B62** (1976) 335.

[50] P. Van Nieuwenhuizen, *Supergravity*, *Phys. Rept.* **68** (1981) 189–398.

[51] M. A. Luty, *2004 TASI Lectures on Supersymmetry Breaking*, hep-th/0509029.

[52] D. J. H. Chung *et al.*, *The Soft Supersymmetry-breaking Lagrangian: Theory and Applications*, *Phys. Rept.* **407** (2005) 1–203, [hep-ph/0312378].

[53] L. Girardello and M. T. Grisaru, *Soft Breaking of Supersymmetry*, *Nucl. Phys.* **B194** (1982) 65.

[54] M. Drees, *An Introduction to Supersymmetry*, hep-ph/9611409.

[55] M. B. Green, J. H. Schwarz, and E. Witten, *Superstring Theory. Vol. 1: Introduction*. Cambridge, Uk: Univ. Pr. (1987) 469 P. (Cambridge Monographs On Mathematical Physics).

M. B. Green, J. H. Schwarz, and E. Witten, *Superstring Theory. Vol. 2: Loop Amplitudes, Anomalies and Phenomenology*. Cambridge, Uk: Univ. Pr. (1987) 596 P. (Cambridge Monographs On Mathematical Physics).

J. Polchinski, *String Theory. Vol. 1: An Introduction to the Bosonic String*. Cambridge, UK: Univ. Pr. (1998) 402 p.

J. Polchinski, *String Theory. Vol. 2: Superstring Theory and Beyond*. Cambridge, UK: Univ. Pr. (1998) 531 p.

[56] M. Dine, *Supersymmetry and String Theory: Beyond the Standard Model*. Cambridge, UK: Cambridge Univ. Pr. (2007) 515 p.

[57] K. Becker, M. Becker, and J. H. Schwarz, *String Theory and M-Theory: A Modern Introduction*. Cambridge, UK: Cambridge Univ. Pr. (2007) 739 p.

[58] H. E. Haber, *Introductory Low-energy Supersymmetry*, `hep-ph/9306207`.

[59] S. Dimopoulos and H. Georgi, *Softly Broken Supersymmetry and SU(5)*, *Nucl. Phys.* **B193** (1981) 150.

S. Weinberg, *Supersymmetry at Ordinary Energies. 1. Masses and Conservation Laws*, *Phys. Rev.* **D26** (1982) 287.

N. Sakai and T. Yanagida, *Proton Decay in a Class of Supersymmetric Grand Unified Models*, *Nucl. Phys.* **B197** (1982) 533.

S. Dimopoulos, S. Raby, and F. Wilczek, *Proton Decay in Supersymmetric Models*, *Phys. Lett.* **B112** (1982) 133.

[60] G. R. Farrar and P. Fayet, *Phenomenology of the Production, Decay, and Detection of New Hadronic States Associated with Supersymmetry*, *Phys. Lett.* **B76** (1978) 575–579.

[61] H. E. Haber, *The Status of the Minimal Supersymmetric Standard Model and Beyond*, *Nucl. Phys. Proc. Suppl.* **62** (1998) 469–484, [`hep-ph/9709450`].

[62] S. Dimopoulos and S. D. Thomas, *Dynamical Relaxation of the Supersymmetric CP Violating Phases*, *Nucl. Phys.* **B465** (1996) 23–33, [`hep-ph/9510220`].

[63] J. F. Gunion, H. E. Haber, G. L. Kane, and S. Dawson, *The Higgs Hunter's Guide*. SCIPP-89/13.

J. F. Gunion, H. E. Haber, G. L. Kane, and S. Dawson, *Errata for the Higgs Hunter's Guide*, `hep-ph/9302272`.

[64] M. Frank *et al.*, *The Higgs Boson Masses and Mixings of the Complex MSSM in the Feynman-Diagrammatic Approach*, *JHEP* **02** (2007) 047, [`hep-ph/0611326`].

[65] http://lephiggs.web.cern.ch/LEPHIGGS/papers/index.html.

[66] Y. Okada, M. Yamaguchi, and T. Yanagida, *Upper Bound of the Lightest Higgs Boson Mass in the Minimal Supersymmetric Standard Model*, *Prog. Theor. Phys.* **85** (1991) 1–6.

J. R. Ellis, G. Ridolfi, and F. Zwirner, *Radiative Corrections to the Masses of Supersymmetric Higgs Bosons*, *Phys. Lett.* **B257** (1991) 83–91.

[67] S. P. Li and M. Sher, *Upper Limit to the Lightest Higgs Mass in Supersymmetric Models*, *Phys. Lett.* **B140** (1984) 339.

R. Barbieri and M. Frigeni, *The Supersymmetric Higgs Searches at LEP after Radiative Corrections*, *Phys. Lett.* **B258** (1991) 395–398.

M. Drees and M. M. Nojiri, *One Loop Corrections to the Higgs Sector in Minimal Supergravity Models*, *Phys. Rev.* **D45** (1992) 2482–2492.

J. A. Casas, J. R. Espinosa, M. Quiros, and A. Riotto, *The Lightest Higgs Boson Mass in the Minimal Supersymmetric Standard Model*, *Nucl. Phys.* **B436** (1995) 3–29, [hep-ph/9407389].

[68] J. R. Ellis, G. Ridolfi, and F. Zwirner, *On Radiative Corrections to Supersymmetric Higgs Boson Masses and Their Implications for LEP Searches*, *Phys. Lett.* **B262** (1991) 477–484.

[69] R.-J. Zhang, *Two-Loop Effective Potential Calculation of the Lightest CP-even Higgs-Boson Mass in the MSSM*, *Phys. Lett.* **B447** (1999) 89–97, [hep-ph/9808299].

[70] J. R. Espinosa and R.-J. Zhang, *MSSM Lightest CP-even Higgs Boson Mass to O(alpha(s) alpha(t)): The Effective Potential Approach*, *JHEP* **03** (2000) 026, [hep-ph/9912236].

[71] J. R. Espinosa and R.-J. Zhang, *Complete Two-loop Dominant Corrections to the Mass of the Lightest CP-even Higgs Boson in the Minimal Supersymmetric Standard Model*, *Nucl. Phys.* **B586** (2000) 3–38, [hep-ph/0003246].

A. Brignole, G. Degrassi, P. Slavich, and F. Zwirner, *On The O(alpha(t)**2) Two-Loop Corrections to the Neutral Higgs Boson Masses in the MSSM*, *Nucl. Phys.* **B631** (2002) 195–218, [hep-ph/0112177].

[72] A. Brignole, G. Degrassi, P. Slavich, and F. Zwirner, *On the Two-Loop Sbottom Corrections to the Neutral Higgs Boson Masses in the MSSM*, *Nucl. Phys.* **B643** (2002) 79–92, [hep-ph/0206101].

[73] H. E. Haber and R. Hempfling, *Can the Mass of the Lightest Higgs Boson of the Minimal Supersymmetric Model Be Larger than m(Z)?*, *Phys. Rev. Lett.* **66** (1991) 1815–1818.

[74] P. H. Chankowski, S. Pokorski, and J. Rosiek, *Charged and Neutral Supersymmetric Higgs Boson Masses: Complete One Loop Analysis*, *Phys. Lett.* **B274** (1992) 191–198.

P. H. Chankowski, S. Pokorski, and J. Rosiek, *Complete On-Shell Renormalization Scheme for the Minimal Supersymmetric Higgs Sector*, *Nucl. Phys.* **B423** (1994) 437–496, [hep-ph/9303309].

[75] A. Yamada, *Radiative Corrections to the Higgs Masses in the Minimal Supersymmetric Standard Model*, *Phys. Lett.* **B263** (1991) 233–238.

A. Yamada, *The Higgs Sector of the Minimal Supersymmetric Standard Model Including Radiative Corrections*, *Z. Phys.* **C61** (1994) 247–263.

[76] A. Dabelstein, *The One Loop Renormalization of the MSSM Higgs Sector and its Application to the Neutral Scalar Higgs Masses*, *Z. Phys.* **C67** (1995) 495–512, [hep-ph/9409375].

A. Dabelstein, *Fermionic Decays of Neutral MSSM Higgs Bosons at the One Loop Level*, *Nucl. Phys.* **B456** (1995) 25–56, [hep-ph/9503443].

[77] R. Hempfling and A. H. Hoang, *Two Loop Radiative Corrections to the Upper Limit of the Lightest Higgs Boson Mass in the Minimal Supersymmetric Model*, *Phys. Lett.* **B331** (1994) 99–106, [hep-ph/9401219].

[78] S. Heinemeyer, W. Hollik, and G. Weiglein, *QCD Corrections to the Masses of the Neutral CP-even Higgs Bosons in the MSSM*, *Phys. Rev.* **D58** (1998) 091701, [hep-ph/9803277].

S. Heinemeyer, W. Hollik, and G. Weiglein, *Precise Prediction for the Mass of the Lightest Higgs Boson in the MSSM*, *Phys. Lett.* **B440** (1998) 296–304, [hep-ph/9807423].

S. Heinemeyer, W. Hollik, and G. Weiglein, *The Masses of the Neutral CP-even Higgs Bosons in the MSSM: Accurate Analysis at the Two-Loop Level*, *Eur. Phys. J.* **C9** (1999) 343–366, [hep-ph/9812472].

S. Heinemeyer, W. Hollik, and G. Weiglein, *The Mass of the Lightest MSSM Higgs Boson: A Compact Analytical Expression at the Two-Loop Level*, *Phys. Lett.* **B455** (1999) 179–191, [hep-ph/9903404].

S. Heinemeyer, W. Hollik, H. Rzehak, and G. Weiglein, *High-precision Predictions for the MSSM Higgs Sector at O(alpha(b) alpha(s))*, *Eur. Phys. J.* **C39** (2005) 465–481, [hep-ph/0411114].

[79] A. Dedes, G. Degrassi, and P. Slavich, *On the Two-Loop Yukawa Corrections to the MSSM Higgs Boson Masses at Large tan(beta)*, *Nucl. Phys.* **B672** (2003) 144–162, [hep-ph/0305127].

[80] S. Heinemeyer, W. Hollik, H. Rzehak, and G. Weiglein, *The Higgs Sector of the Complex MSSM at Two-Loop Order: QCD Contributions*, *Phys. Lett.* **B652** (2007) 300–309, [0705.0746].

[81] B. C. Allanach, A. Djouadi, J. L. Kneur, W. Porod, and P. Slavich, *Precise determination of the neutral Higgs boson masses in the MSSM*, *JHEP* **09** (2004) 044, [hep-ph/0406166].

[82] G. Degrassi, S. Heinemeyer, W. Hollik, P. Slavich, and G. Weiglein, *Towards high-precision predictions for the MSSM Higgs sector*, *Eur. Phys. J.* **C28** (2003) 133–143, [hep-ph/0212020].

[83] M. S. Carena and H. E. Haber, *Higgs Boson Theory and Phenomenology. ((V))*, *Prog. Part. Nucl. Phys.* **50** (2003) 63–152, [hep-ph/0208209].

[84] M. S. Carena, D. Garcia, U. Nierste, and C. E. M. Wagner, *Effective Lagrangian for the anti-t b H+ interaction in the MSSM and charged Higgs phenomenology*, *Nucl. Phys.* **B577** (2000) 88–120, [hep-ph/9912516].

[85] M. S. Carena, M. Olechowski, S. Pokorski, and C. E. M. Wagner, *Electroweak symmetry breaking and bottom - top Yukawa unification*, *Nucl. Phys.* **B426** (1994) 269–300, [hep-ph/9402253].

R. Hempfling, *Yukawa coupling unification with supersymmetric threshold corrections*, *Phys. Rev.* **D49** (1994) 6168–6172.

D. M. Pierce, J. A. Bagger, K. T. Matchev, and R.-j. Zhang, *Precision corrections in the minimal supersymmetric standard model*, *Nucl. Phys.* **B491** (1997) 3–67, [hep-ph/9606211].

[86] W. Hollik and H. Rzehak, *The sfermion mass spectrum of the MSSM at the one-loop level*, *Eur. Phys. J.* **C32** (2003) 127–133, [hep-ph/0305328].

[87] S. Heinemeyer, W. Hollik, and G. Weiglein, *Electroweak precision observables in the minimal supersymmetric standard model*, *Phys. Rept.* **425** (2006) 265–368, [hep-ph/0412214].

[88] W. Pauli and F. Villars, *On the Invariant Regularization in Relativistic Quantum Theory*, *Rev. Mod. Phys.* **21** (1949) 434–444.

[89] G. 't Hooft and M. J. G. Veltman, *Regularization and Renormalization of Gauge Fields*, *Nucl. Phys.* **B44** (1972) 189–213.

[90] J. C. Collins, *Renormalization. An Introduction to Renormalization, the Renormalization Group, and the Operator Product Expansion.* Cambridge, Uk: Univ. Pr. (1984) 380p.

[91] W. Siegel, *Supersymmetric Dimensional Regularization via Dimensional Reduction*, *Phys. Lett.* **B84** (1979) 193.

D. M. Capper, D. R. T. Jones, and P. van Nieuwenhuizen, *Regularization by Dimensional Reduction of Supersymmetric and Nonsupersymmetric Gauge Theories*, *Nucl. Phys.* **B167** (1980) 479.

[92] I. Jack and D. R. T. Jones, *Regularisation of Supersymmetric Theories*, hep-ph/9707278.

[93] W. Beenakker, R. Hopker, and P. M. Zerwas, *SUSY-QCD Decays of Squarks and Gluinos*, *Phys. Lett.* **B378** (1996) 159–166, [hep-ph/9602378].

[94] W. Hollik, E. Kraus, and D. Stockinger, *Renormalization and Symmetry Conditions in Supersymmetric QED*, *Eur. Phys. J.* **C11** (1999) 365–381, [hep-ph/9907393].

W. Hollik and D. Stockinger, *Regularization and Supersymmetry-restoring Counterterms in Supersymmetric QCD*, *Eur. Phys. J.* **C20** (2001) 105–119, [hep-ph/0103009].

I. Fischer, W. Hollik, M. Roth, and D. Stockinger, *Restoration of Supersymmetric Slavnov-Taylor and Ward Identities in Presence of Soft and Spontaneous Symmetry Breaking*, *Phys. Rev.* **D69** (2004) 015004, [hep-ph/0310191].

[95] P. L. White, *An Analysis of the Cohomology Structure of Super Yang-Mills Coupled to Matter*, *Class. Quant. Grav.* **9** (1992) 1663–1682.

[96] N. Maggiore, O. Piguet, and S. Wolf, *Algebraic Renormalization of N=1 Supersymmetric Gauge Theories*, *Nucl. Phys.* **B458** (1996) 403–429, [hep-th/9507045].

N. Maggiore, O. Piguet, and S. Wolf, *Algebraic Renormalization of $N = 1$ Supersymmetric Gauge Theories with Supersymmetry Breaking Masses*, *Nucl. Phys.* **B476** (1996) 329–350, [hep-th/9604002].

[97] W. Hollik, E. Kraus, and D. Stockinger, *Renormalization of Supersymmetric Yang-Mills Theories with Soft Supersymmetry Breaking*, *Eur. Phys. J.* **C23** (2002) 735–747, [hep-ph/0007134].

W. Hollik *et al.*, *Renormalization of the Minimal Supersymmetric Standard Model*, *Nucl. Phys.* **B639** (2002) 3–65, [hep-ph/0204350].

[98] W. Siegel, *Inconsistency of Supersymmetric Dimensional Regularization*, *Phys. Lett.* **B94** (1980) 37.

L. V. Avdeev, *Noninvariance of Regularization by Dimensional Reduction: An Explicit Example of Supersymmetry Breaking*, *Phys. Lett.* **B117** (1982) 317.

L. V. Avdeev and A. A. Vladimirov, *Dimensional Regularization and Supersymmetry*, *Nucl. Phys.* **B219** (1983) 262.

[99] D. Stockinger, *Regularization by Dimensional Reduction: Consistency, Quantum Action Principle, and Supersymmetry*, *JHEP* **03** (2005) 076, [hep-ph/0503129].

[100] M. Bohm, H. Spiesberger, and W. Hollik, *On the One Loop Renormalization of the Electroweak Standard Model and Its Application to Leptonic Processes*, *Fortsch. Phys.* **34** (1986) 687–751.

W. F. L. Hollik, *Radiative Corrections in the Standard Model and Their Role for Precision Tests of the Electroweak Theory*, *Fortschr. Phys.* **38** (1990) 165–260.

[101] A. Denner, *Techniques for Calculation of Electroweak Radiative Corrections at the One Loop Level and Results for W Physics at LEP-200*, *Fortschr. Phys.* **41** (1993) 307–420, [0709.1075].

[102] T. Fritzsche, *Berechnung von Observablen zur Supersymmetrischen Teilchenerzeugung an Hochenenergie-Collidern unter Einschluß Höherer Ordnungen*. PhD thesis, Universität Karlsruhe, 2005.

[103] G. 't Hooft, *Dimensional Regularization and the Renormalization Group*, *Nucl. Phys.* **B61** (1973) 455–468.

[104] W. A. Bardeen, A. J. Buras, D. W. Duke, and T. Muta, *Deep Inelastic Scattering Beyond the Leading Order in Asymptotically Free Gauge Theories*, *Phys. Rev.* **D18** (1978) 3998.

[105] A. Freitas and D. Stockinger, *Gauge Dependence and Renormalization of tan(beta) in the MSSM*, *Phys. Rev.* **D66** (2002) 095014, [hep-ph/0205281].

[106] A. Brignole, *Radiative Corrections to the Supersymmetric Neutral Higgs Boson Masses*, *Phys. Lett.* **B281** (1992) 284–294.

[107] M. Frank, S. Heinemeyer, W. Hollik, and G. Weiglein, *FeynHiggs1.2: Hybrid MS-bar / On-Shell Renormalization for the CP-even Higgs Boson Sector in the MSSM*, `hep-ph/0202166`.

[108] S. Heinemeyer, W. Hollik, and G. Weiglein, *Decay Widths of the Neutral CP-even MSSM Higgs Bosons in the Feynman-Diagrammatic Approach*, *Eur. Phys. J.* **C16** (2000) 139–153, [`hep-ph/0003022`].

[109] S. Heinemeyer, *MSSM Higgs Physics at Higher Orders*, *Int. J. Mod. Phys.* **A21** (2006) 2659–2772, [`hep-ph/0407244`].

[110] *ATLAS Detector and Physics Performance. Technical Design Report. Vol. 2*, . CERN-LHCC-99-15.

[111] A. Dedes, S. Heinemeyer, S. Su, and G. Weiglein, *The Lightest Higgs Boson of mSUGRA, mGMSB and mAMSB at Present and Future Colliders: Observability and Precision Analyses*, *Nucl. Phys.* **B674** (2003) 271–305, [`hep-ph/0302174`].

[112] A. Bredenstein, A. Denner, S. Dittmaier, and M. M. Weber, *Precise Predictions for the Higgs-boson Decay $H \to W\,W\,/\,Z\,Z \to 4$ leptons*, *Phys. Rev.* **D74** (2006) 013004, [`hep-ph/0604011`].

[113] A. Bredenstein, A. Denner, S. Dittmaier, and M. M. Weber, *Radiative Corrections to the Semileptonic and Hadronic Higgs-boson Decays $H \to W\,W\,/\,Z\,Z \to 4$ fermions*, *JHEP* **02** (2007) 080, [`hep-ph/0611234`].

[114] M. S. Carena, S. Heinemeyer, C. E. M. Wagner, and G. Weiglein, *Suggestions for Benchmark Scenarios for MSSM Higgs Boson Searches at Hadron Colliders*, *Eur. Phys. J.* **C26** (2003) 601–607, [`hep-ph/0202167`].

[115] R. G. Stuart, *Unstable Particles*, `hep-ph/9504308`.

[116] A. Denner, "Lectures on Unstable Particles in Gauge Theories." Second Graduate School in Physics at Colliders, Torino, July 2003.

[117] W. Beenakker *et al.*, *The Fermion-loop Scheme for Finite-width Effects in e+ e- Annihilation into Four Fermions*, *Nucl. Phys.* **B500** (1997) 255–298, [`hep-ph/9612260`].

[118] E. N. Argyres *et al.*, *Stable Calculations for Unstable Particles: Restoring Gauge Invariance*, *Phys. Lett.* **B358** (1995) 339–346, [`hep-ph/9507216`].

[119] U. Baur and D. Zeppenfeld, *Finite Width Effects and Gauge Invariance in Radiative W Productions and Decay*, *Phys. Rev. Lett.* **75** (1995) 1002–1005, [`hep-ph/9503344`].

[120] W. Beenakker and A. Denner, *Radiative Corrections to Off-shell Gauge-boson Pair Production*, *Acta Phys. Polon.* **B29** (1998) 2821–2838, [`hep-ph/9806475`].

[121] R. G. Stuart, *Gauge Invariance, Analyticity and Physical Observables at the Z0 Resonance*, *Phys. Lett.* **B262** (1991) 113–119.

R. G. Stuart, *Gauge Invariant Perturbation Theory Near a Gauge Resonance*, . Invited Talk at the Workshop on High Energy Phenomenology, Mexico City, Mexico, Jul 1-10, 1991.

R. G. Stuart, *The Structure of the Z0 Resonance and the Physical Properties of the Z0 Boson*, *Phys. Rev. Lett.* **70** (1993) 3193–3196.

R. G. Stuart, *Production Cross-Sections for Unstable Particles*, *Nucl. Phys.* **B498** (1997) 28–38, [hep-ph/9504215].

[122] A. Aeppli, F. Cuypers, and G. J. van Oldenborgh, *O(Gamma) Corrections to W Pair Production in e+ e- and Gamma Gamma Collisions*, *Phys. Lett.* **B314** (1993) 413–420, [hep-ph/9303236].

[123] A. Aeppli, G. J. van Oldenborgh, and D. Wyler, *Unstable Particles in One Loop Calculations*, *Nucl. Phys.* **B428** (1994) 126–146, [hep-ph/9312212].

[124] H. G. J. Veltman, *Mass and Width of Unstable Gauge Bosons*, *Z. Phys.* **C62** (1994) 35–52.

[125] W. Beenakker *et al.*, *WW Cross-sections and Distributions*, hep-ph/9602351.

W. Beenakker, F. A. Berends, and A. P. Chapovsky, *Radiative Corrections to Pair Production of Unstable Particles: Results for e+ e- → 4 fermions*, *Nucl. Phys.* **B548** (1999) 3–59, [hep-ph/9811481].

[126] S. Dittmaier and M. Kramer, *Electroweak Radiative Corrections to W-boson Production at Hadron Colliders*, *Phys. Rev.* **D65** (2002) 073007, [hep-ph/0109062].

[127] D. Wackeroth and W. Hollik, *Electroweak Radiative Corrections to Resonant Charged Gauge Boson Production*, *Phys. Rev.* **D55** (1997) 6788–6818, [hep-ph/9606398].

[128] A. Denner, S. Dittmaier, M. Roth, and D. Wackeroth, *Predictions for All Processes e+ e- → 4 fermions + gamma*, *Nucl. Phys.* **B560** (1999) 33–65, [hep-ph/9904472].

A. Denner, S. Dittmaier, M. Roth, and L. H. Wieders, *Electroweak Corrections to Charged-Current e+ e- → 4 fermion Processes: Technical Details and Further Results*, *Nucl. Phys.* **B724** (2005) 247–294, [hep-ph/0505042].

[129] U. Baur, J. A. M. Vermaseren, and D. Zeppenfeld, *Electroweak Vector Boson Production in High-energy e p Collisions*, *Nucl. Phys.* **B375** (1992) 3–44.

[130] Y. Kurihara, D. Perret-Gallix, and Y. Shimizu, *e+ e- → e- anti-electron-neutrino u anti-d from LEP to Linear Collider Energies*, *Phys. Lett.* **B349** (1995) 367–374, [hep-ph/9412215].

[131] A. Denner, S. Dittmaier, M. Roth, and M. M. Weber, *Electroweak radiative corrections to e+ e- → nu anti-nu H*, *Nucl. Phys.* **B660** (2003) 289–321, [hep-ph/0302198].

[132] J. Kublbeck, M. Bohm, and A. Denner, *Feyn Arts: Computer Algebraic Generation of Feynman Graphs and Amplitudes*, *Comput. Phys. Commun.* **60** (1990) 165–180.

T. Hahn, *Generating Feynman Diagrams and Amplitudes with FeynArts 3*, *Comput. Phys. Commun.* **140** (2001) 418–431, [hep-ph/0012260].

J. Kublbeck, H. Eck, and R. Mertig, *Computeralgebraic Generation and Calculation of Feynman Graphs Using FeynArts and FeynCalc*, *Nucl. Phys. Proc. Suppl.* **29A** (1992) 204–208.

[133] T. Hahn and C. Schappacher, *The Implementation of the Minimal Supersymmetric Standard Model in FeynArts and FormCalc*, *Comput. Phys. Commun.* **143** (2002) 54–68, [hep-ph/0105349].

T. Hahn and M. Rauch, *News from FormCalc and LoopTools*, *Nucl. Phys. Proc. Suppl.* **157** (2006) 236–240, [hep-ph/0601248].

T. Hahn and J. I. Illana, *Extensions in FormCalc 5.3*, 0708.3652.

[134] T. Hahn, *Generating and Calculating One-loop Feynman Diagrams with FeynArts, FormCalc, and LoopTools*, hep-ph/9905354.

[135] T. Hahn, S. Heinemeyer, and G. Weiglein, *MSSM Higgs-boson Production at the Linear Collider: Dominant Corrections to the W W Fusion Channel*, *Nucl. Phys.* **B652** (2003) 229–258, [hep-ph/0211204].

[136] A. Denner, S. Dittmaier, and M. Roth, *Non-factorizable Photonic Corrections to e+ e- → W W → 4 fermions*, *Nucl. Phys.* **B519** (1998) 39–84, [hep-ph/9710521].

A. Denner and S. Dittmaier, *Reduction of One-loop Tensor 5-point Integrals*, *Nucl. Phys.* **B658** (2003) 175–202, [hep-ph/0212259].

[137] W. Beenakker and A. Denner, *Infrared Divergent Scalar Box Integrals with Applications in the Electroweak Standard Model*, *Nucl. Phys.* **B338** (1990) 349–370.

[138] A. Denner and S. Dittmaier, *Reduction Schemes for One-loop Tensor Integrals*, *Nucl. Phys.* **B734** (2006) 62–115, [hep-ph/0509141].

[139] G. 't Hooft and M. J. G. Veltman, *Scalar One Loop Integrals*, *Nucl. Phys.* **B153** (1979) 365–401.

[140] G. Passarino and M. J. G. Veltman, *One Loop Corrections for e+ e- Annihilation into mu+ mu- in the Weinberg Model*, *Nucl. Phys.* **B160** (1979) 151.

[141] A. Denner, U. Nierste, and R. Scharf, *A Compact Expression for the Scalar One Loop Four Point Function*, *Nucl. Phys.* **B367** (1991) 637–656.

[142] T. Kinoshita, *Mass Singularities of Feynman Amplitudes*, *J. Math. Phys.* **3** (1962) 650–677.

T. D. Lee and M. Nauenberg, *Degenerate Systems and Mass Singularities*, *Phys. Rev.* **133** (1964) B1549–B1562.

[143] S. Catani and M. H. Seymour, *The Dipole Formalism for the Calculation of QCD Jet Cross Sections at Next-to-Leading Order*, *Phys. Lett.* **B378** (1996) 287–301, [hep-ph/9602277].

S. Catani and M. H. Seymour, *A General Algorithm for Calculating Jet Cross Sections in NLO QCD*, *Nucl. Phys.* **B485** (1997) 291–419, [hep-ph/9605323].

[144] S. Dittmaier, *A General Approach to Photon Radiation off Fermions*, *Nucl. Phys.* **B565** (2000) 69–122, [hep-ph/9904440].

[145] M. Roth, *Precise Predictions for Four-fermion Production in Electron Positron Annihilation*, hep-ph/0008033.

[146] A. Denner, S. Dittmaier, M. Roth, and D. Wackeroth, *Electroweak Radiative Corrections to e+ e- → W W → 4 fermions in Double-pole Approximation: The RACOONWW Approach*, *Nucl. Phys.* **B587** (2000) 67–117, [hep-ph/0006307].

[147] D. R. Yennie, S. C. Frautschi, and H. Suura, *The Infrared Divergence Phenomena and High-energy Processes*, *Ann. Phys.* **13** (1961) 379–452.

[148] E. A. Kuraev and V. S. Fadin, *On Radiative Corrections to e+ e- Single Photon Annihilation at High-Energy*, *Sov. J. Nucl. Phys.* **41** (1985) 466–472.

G. Altarelli and G. Martinelli, *Radiative Corrections to the Z0 Line Shape at LEP*, . In *Ellis, J. (Ed.), Peccei, R.d. (Ed.): Physics At LEP, Vol. 1*, 47-57.

O. Nicrosini and L. Trentadue, *Soft Photons and Second Order Radiative Corrections to e+ e- → Z0*, *Phys. Lett.* **B196** (1987) 551.

O. Nicrosini and L. Trentadue, *Second Order Electromagnetic Radiative Corrections to e+ e- → gamma*, Z0 → mu+ mu-*, *Z. Phys.* **C39** (1988) 479.

F. A. Berends, W. L. van Neerven, and G. J. H. Burgers, *Higher Order Radiative Corrections at LEP Energies*, *Nucl. Phys.* **B297** (1988) 429.

A. B. Arbuzov, *Non-singlet Splitting Functions in QED*, *Phys. Lett.* **B470** (1999) 252–258, [hep-ph/9908361].

[149] **CDF** Collaboration, J. F. Arguin *et al.*, *Combination of CDF and D0 Results on the Top-quark Mass*, hep-ex/0507091.

[150] M. S. Carena, S. Heinemeyer, C. E. M. Wagner, and G. Weiglein, *Suggestions for Improved Benchmark Scenarios for Higgs- boson Searches at LEP2*, hep-ph/9912223.

[151] O. Brein and W. Hollik, *Distributions for MSSM Higgs Boson + Jet Production at Hadron Colliders*, *Phys. Rev.* **D76** (2007) 035002, [0705.2744].

[152] **ALEPH** Collaboration, S. Schael *et al.*, *Search for Neutral MSSM Higgs Bosons at LEP*, *Eur. Phys. J.* **C47** (2006) 547–587, [hep-ex/0602042].

[153] J. Fleischer and F. Jegerlehner, *Radiative Corrections to Higgs Decays in the Extended Weinberg-Salam Model*, *Phys. Rev.* **D23** (1981) 2001–2026.

[154] B. A. Kniehl, *Radiative Corrections for $H \to Z\ Z$ in the Standard Model*, *Nucl. Phys.* **B352** (1991) 1–26.

[155] B. A. Kniehl, *Radiative Corrections for $H \to W+\ W-$ (gamma) in the Standard Model*, *Nucl. Phys.* **B357** (1991) 439–466.

[156] F. Gliozzi, J. Scherk, and D. I. Olive, *Supersymmetry, Supergravity Theories and the Dual Spinor Model*, *Nucl. Phys.* **B122** (1977) 253–290.

[157] T. Kugo and P. K. Townsend, *Supersymmetry and the Division Algebras*, *Nucl. Phys.* **B221** (1983) 357.

[158] C. Wetterich, *Massless Spinors in More than Four-dimensions*, *Nucl. Phys.* **B211** (1983) 177.

[159] P. C. West, *Supergravity, Brane Dynamics and String Duality*, `hep-th/9811101`.

[160] A. Van Proeyen, *Tools for Supersymmetry*, `hep-th/9910030`.

[161] N. M. A. and S. A. I., *Theory of Group Representations*. Berlin, Germany: Springer (1982) 568 p.

B. Martin, *Representation Theory of Finite Groups*. New York, USA: Academic Press (1965) 185 p.

S. Barry, *Representations of Finite and Compact Groups*. Providence, RI: American Math. Soc. (1996) 266 p.

N. Morris, *Matrix Representations of Groups*. National Bureau of Standards, Wash., D.C.: Govt. Print. Off. (1968) 79 p.

[162] G. J. van Oldenborgh and J. A. M. Vermaseren, *New Algorithms for One Loop Integrals*, *Z. Phys.* **C46** (1990) 425–438.

[163] M. J. G. Veltman, *Unitarity and Causality in a Renormalizable Field Theory with Unstable Particles*, *Physica* **29** (1963) 186–207.

[164] A. Sirlin, *Theoretical Considerations Concerning the Z0 Mass*, *Phys. Rev. Lett.* **67** (1991) 2127–2130.

A. Sirlin, *Observations Concerning Mass Renormalization in the Electroweak Theory*, *Phys. Lett.* **B267** (1991) 240–242.

Acknowledgements

It is a pleasure to express my gratitude to all the people that supported me during the last three years of my PhD work.

First of all, I would like to thank my supervisor, Prof. Wolfgang Hollik for offering me the opportunity to work in his group, for his continuous support and encouragement, and for sharing with me his ideas and insights of physics. His detailed and constructive advice is always of great help throughout this work.

I also would like to thank all the people related to the IMPRS programme. Thanks to Mrs. R. Jurgeleit and Ms. F. Rudert for their kind help throughout these years.

I am indebted to Stefan Dittmaier for helpful discussions on the treatment of unstable particles and on the computation of loop integrals. Many thanks also go to Thomas Hahn, who always has the answer for my questions concerning his nice computer tools.

I wish to thank all the members of the theory group of the Max-Planck-Institut für Physik in München for the great working atmosphere. Many thanks to E. Mirabella, M. Trenkel, D. Lopez Val, S. Bejar Latonda and J. Germer for useful discussions, and for reading parts of the manuscript and giving valuable feedback. Special thanks to J. Germer for translating the abstract of this thesis into German. I would like to thank also my office mates, E. Mirabella and M. Stahlhofen for a pleasant office atmosphere and for lively discussions on physics and "unphysics".

I am very grateful to all my friends from inside and outside the institute, especially to my house mates during my stay in Munich, Chen Xun and Yuan Jianming, who made life so enjoyable. I wish them all the best in their future endeavors.

Thanks are not enough for my family. Without their unwavering and unconditional love and support, this work is simply not possible.